



Technische Universität
München Fakultät für Chemie
Institut für Wasserchemie und Chemische Balneologie
Lehrstuhl für Analytische Chemie und Wasserchemie

**The automation and validation of a morphological and chemical quantification
procedure for microplastic fragments using Raman microspectroscopy**

Elisabeth von der Esch

Vollständiger Abdruck der von der Fakultät für Chemie der Technischen
Universität München zu Erlangung des akademischen Grades eines

Doktors der Naturwissenschaften (Dr. rer. nat.)

genehmigten Dissertation.

Vorsitzender: Priv.-Doz. Dr. Natalia P. Ivleva
Prüfer der Dissertation: 1. Prof. Dr. Martin Elsner
2. Prof. Dr. Jürgen Geist
3. Prof. Dr. Eric Achterberg

Die Dissertation wurde am 26.10.2020 bei der Technischen Universität
München eingereicht und durch die Fakultät für Chemie am 05.01.2021
angenommen.

„Einfach machen“

Danksagung

Zu aller erst möchte ich mich bei PD Dr. Natalia Ivleva und Prof. Dr Martin Elsner für die Betreuung während meiner Doktorarbeit bedanken. Ihr habt mir so viele Möglichkeiten geben, meine Ideen frei zu entfalten. Sogar bei den sehr ambitionierten Ideen, wie der Entwicklung des Seminars „Automatisierung und Visualisierung von Laborprozessen und Daten“ konnte ich mich immer auf eure Unterstützung verlassen. Dank euch konnte ich in diesen drei Jahren so viel erreichen, von dem ich nie gedacht hätte, dass ich das alles schaffen kann.

Ein riesiges Dankeschön geht auch an alle meine Co-Autoren, insbesondere aber an Alexander Kohles und Philipp Anger! Mit euch war Forschen und Paper schreiben immer am schönsten.

Lieber Philipp, bei dir möchte ich mich auch insbesondere dafür bedanken, dass du von Tag eins meiner Promotion an immer für mich da warst, so dass ich wirklich schnell in das Thema reingefunden hab. Dabei war es total egal, wie viel wir zu tun hatten und wie viele Deadlines, Konferenzen oder exzessive Mengen an Proben gemessen werden mussten, mit dir war das alles immer auf eine spaßige Art und Weise zu schaffen.

Lieber Alex, du warst für unfassbare zwei Jahre mein Hiwi und wir haben zusammen wirklich viel erreicht. Gemeinsam haben wir zwei Paper, die Software TUM-ParticleTyper, 10 Chemometrie Projekte, 7 h Videolehrmaterialien für eine komplette Python und Statistik Einführung und 5 Konferenzbeiträge erstellt, unzählige Studentenmails beantwortet und bei der Public Climate School mitgemacht. Das wäre mit niemand anderem möglich gewesen. Vor allem war nichts davon einfach oder schnell mal eben gemacht. Wir haben uns da wirklich jedes Mal komplett reingekniet und es war trotzdem jedes Mal ein schönes Abenteuer. Als bei unserem Paper zum TUM-ParticleTyper unsere äquivalenten Beiträge mit einem 🍷 ausgewiesen wurden habe ich gedacht - ja, genau so würde ich unsere Zusammenarbeit in einem Symbol ausdrücken.

Liebe Institutsangehörige, vielen Dank für eure Unterstützung bei absolut allen verrückten Ideen. Gemeinsam haben wir so viele schöne Mittagspausen, Feste und Ausflüge gemacht und ich habe mich immer wie Zuhause gefühlt. Damit ihr nicht vergesst, wie man in der Kaffeedusche Wraps zubereitet, habe ich euch das Rezept hier aufgeschrieben:

https://wwwt3.ch.tum.de/fileadmin/tuchfak/www/my_direct_uploads/20200709_Kochbuch.pdf

Durch die Instituts Seminare konnte ich von dem Wissen aller Gruppenleiter am IWC profitieren und dafür danke ich euch. Im Besonderen möchte ich mich jedoch bei Prof. Dr. Nießner bedanken für die reichlichen Diskussionen und Ratschläge. Außerdem geht bei uns am Institut gar nichts ohne Christine Beese, Cornelia Popp, Roland Hoppe und Sebastian Wiesemann. Vielen Dank, dass ihr alles am Laufen haltet!

Besonders möchte ich mich bei Christian Schwaferts, Carolin Hartmann, Ruben Weiß, Oleksii Morgaienko, Irina Beer, Lisa Göpfert, Julia Klüpfel, Julia Neumair, Katharina Sollweck, David Bauer, Klemens Thaler, Sebastian Wiesemann und Jessica Beyerl bedanken. Mit euch konnte man die interessantesten wissenschaftlichen Diskussionen führen und anschließend in einer Bar versumpfen.

Lieber Chrisitan, liebe Lisa, liebe Jessi, Ihr seid während unserer Zeit am IWC mit mir durch dick und dünn gegangen. Selbst zu Corona Homeoffice Zeiten haben wir unsere Kaffeepausen virtuell durchgezogen und ohne unseren Zusammenhalt hätte ich es nicht geschafft. Und auch unsere gemeinsamen Projekte haben mir immer sehr viel Spaß gemacht.

Bei meinen Studierenden möchte ich mich auch sehr herzlich bedanken. Es hat mir immer Spaß gemacht euch zu betreuen und zu sehen wie ihr euch entwickelt. Ich hoffe, ich konnte euch viel beibringen und euch für die Analytische Chemie sowie Automatisierung in der Chemie begeistern.

Lieber Oliver Jacob, liebe Rosalie Koros, lieber Merlin Junk, liebe Maria Lanzinger und lieber Patrick Schlachta mit euren Forschungsarbeiten habt ihr alle zum Erfolg dieser

Dissertation beigetragen. Dafür und für unsere gemeinsamen Lernerfolge danke ich euch.

Liebe Studierende des Kurses „Automatisierung und Visualisierung von Laborprozessen und Daten“ bei euch möchte ich mich im Namen aller Dozenten und Tutoren dafür bedanken, dass ihr trotz Online-Lehre wegen Corona mit Begeisterung an unserem Seminar teilgenommen habt. Der ganze Aufwand und die zahllosen Stunden, die Alexander Kohles, Beatriz von der Esch und ich in die Lehrmaterialien gesteckt haben, haben sich mehr als bezahlt gemacht. Uns hat es wirklich beeindruckt, wie schnell ihr Fortschritte beim Programmieren gemacht habt, wie ihr die Chemometrie Projekte gemeistert habt und wie ihr eure Laborlegoroboter von der Idee bis zum Prototypen entwickelt habt. Außerdem möchte ich mich bei Alexander Kohles, Beatriz von der Esch, Dr. Miriam Voß, Mike Kramler, PD Dr. Natalia Ivleva, Prof. Dr. Martin Elsner und den Fonds der Chemischen Industrie für die Unterstützung bedanken.

Da das Beste zum Schluss kommt, möchte ich mich bei meiner Familie und bei Jonas und seiner Familie für die Unterstützung über mein gesamtes Studium hinweg bedanken. Ich hab euch lieb und ohne euch wäre ich nie so weit gekommen.

LIST OF PUBLICATIONS

Lead author publications

Philipp M. Anger[☉] and **Elisabeth von der Esch**[☉], Thomas Baumann, Martin Elsner, Reinhard Niessner, Natalia P. Ivleva, *RAMAN microspectroscopy as a tool for microplastic particle analysis*, Trends in Analytical Chemistry, (109) **2018**, 214-226, DOI: 10.1016/j.trac.2018.10.010

Elisabeth von der Esch, Maria Lanzinger, Alexander J. Kohles, Christian Schwaferts, Jana Weisser, Thomas Hofmann, Karl Glas, Martin Elsner and Natalia P. Ivleva, *Simple Generation of Suspensible Secondary Microplastic Reference Particles via Ultrasound Treatment*. Front. Chem. **2020**, 8:169. DOI: 10.3389/fchem.2020.00169

Elisabeth von der Esch[☉] and Alexander J. Kohles[☉], Philipp M. Anger, Reinhard Niessner, Martin Elsner, Natalia P. Ivleva, *TUM-ParticleTyper: A Detection and Quantification Tool for Auto-mated Analysis of (Microplastic) Particles and Fibers*, PLoS ONE 15(6): e0234766. <https://doi.org/10.1371/journal.pone.0234766>

The according software and documentation was published in the following repository:

Alexander J. Kohles[☉] and **Elisabeth von der Esch**[☉], Philipp M. Anger, Reinhard Niessner, *Martin Elsner, Natalia P. Ivleva, TUM-ParticleTyper: Software and Documentation*, <https://mediatum.ub.tum.de/1547636>, doi:10.14459/2020mp1547636, 2020

[☉]shared first authorship

Coauthor publications:

Darena Schymanski, Nizar Benismail, Kada Boukerma, Gerald Dallmann, Dieter Fischer, Franziska Fischer, Douglas Gilliland, Karl Glas, Sílvia Lacorte, Julie Marco, Barbara Oßmann, Maria Rakwe, Jana Weisser, Cordula Witzig, **Elisabeth von der Esch**, Nicole Zumbülte, Thomas Hofmann, Natalia P. Ivleva, *Analysis of microplastics in freshwater and drinking water: Minimum requirements and best practice guidelines, submitted to Water research, 2020*

Science communications to a broader audience:

Hannes K. Imhof, Mohammed Al-Azzawi, Astrid Bartonitz, Sebastian Beggel, Joerg E. Drewes, Martin Elsner, **Elisabeth von der Esch**, Karl Glas, Natalia P. Ivleva, Simone Kefer, Oliver Knoop, Horst-Christian Langowski, Oliver Miesbauer, Julia Reichel, Christian Schwaferts, Jana Weisser, Juergen P. Geist, *Der Eintrag von Mikroplastik in Lebensmittel und die Aquatischen Umwelt und seine Folgen – aktuelle Fragen und Antworten.*, Mitt Umweltchem Ökotox, **2020**

Elisabeth von der Esch, Alexander J. Kohles, Martin Elsner, Natalia P. Ivleva, *„Wie viele Mikroplastik-Partikel haben wir in unserer Probe?“ Wie können wir diese Frage in einem akzeptablen Zeitrahmen beantworten?*, Vom Wasser, **2020**

TABLE OF CONTENTS

List of publications	8
Summary	16
Zusammenfassung.....	20
General Introduction.....	24
What is Microplastic?	24
Microplastic analysis, state of the art prior to 2018.....	26
What is the goal of this thesis?	28
How many particles need to be analyzed to ensure a representative sample?	29
The selection of particles for Raman microspectroscopic analysis - state of the art	29
Target: statistically meaningful subsampling	31
How can reference materials be produced that mimic the properties of secondary microplastic, to advance method development?	32
Reference materials - state of the art.....	32
Target: suitable reference material for microplastic.....	34
How can the morphological and chemical quantification of particles and fibers be automated?.....	34
The automated morphological and chemical quantification of particles and fibers - state of the art.	35
Target: automated morphological and chemical quantification of particles and fibers for Raman microspectroscopy that can be validated	37
References	39
Declaration of scientific contribution and summary of summary of Raman microspectroscopy as a tool for microplastic particle analysis	46
Chapter : 1	48
Raman Microspectroscopy as a Tool for Microplastic Particle Analysis	48
Abstract	50
1.1 Introduction.....	52
Small and very small microplastic particles – the niche for Raman microspectroscopy.	52
1.2. Discussion	55

How small can RM analyze?.....	55
Theoretical considerations.....	55
Findings from literature	57
How fast can RM be?.....	61
Time effort for single measurement.....	61
Time effort for overall process	65
Potential of Raman microspectroscopy	66
Identification of MP polymer types	66
Influence of particle shape on the detection.....	69
Exploration of MP to non-MP ratio.....	71
Challenge of representativeness	72
Trade-off between measurement time and representativeness	76
Number of particles or filter area?	78
How to circumvent contaminations and fluorescence interference	79
1.3. Conclusion.....	81
1.4. References.....	82
Declaration of scientific contribution and summary for Simple Generation of Suspensible Secondary Microplastic Reference Particles via Ultrasound Treatment.	89
Chapter 2:.....	90
Simple Generation of Suspensible Secondary Microplastic Reference Particles via Ultrasound Treatment	90
Abstract	92
2.1 Introduction.....	93
2.2. Material and Methods	95
Equipment Preparation and Avoidance of Contamination	95
Fragmentation through Sonication	96
Characterization of the produced MP particles	98
2.3 Results and Discussion	102
Morphological Changes in Polymer Surface Due to Ultrasonic Degradation	102
Yield and Reproducibility of the Fragmentation.....	105

Size Distribution Comparison to Environmental MP Particles and other Reference Materials.....	109
Mechanistic Implications for the Degradation of Solid Polymers by Sonication ..	110
Analysis of Suspensibility and Sedimentation Rates by UV-VIS Spectroscopy	111
Comparison of Reference Particles with Environmental Microplastic by FTIR Spectroscopy.....	113
2.4 Conclusion.....	118
2.5 Outlook.....	119
2.6 References.....	121
Declaration of scientific contribution and summary of TUM-ParticleTyper: A Detection and Quantification Tool for Automated Analysis of (Microplastic) Particles and Fibers	126
Chapter 3:.....	128
<i>TUM-ParticleTyper</i> : A Detection and Quantification Tool for Automated Analysis of (Microplastic) Particles and Fibers	128
Abstract.....	130
3.1 Introduction.....	131
3.2 Material and Methods	134
Roughness testing for the development of filter holders.....	134
Production of reference materials for the development of the image processing program and optimization of image acquisition procedures	134
Acquisition of chemical information via Raman microspectroscopy.....	135
Fiber detection in washing machine water	135
3.3 Results and Discussion	135
Morphological and chemical analysis of MP reference materials via <i>TUM-ParticleTyper</i>	135
Flat filter surfaces as a prerequisite for optimal focus	135
Localization and morphological characterization of particles with <i>TUM-ParticleTyper</i>	136
Parametrization	144
Validation	149
Method comparison of the single point approach vs. imaging.....	152
How complex may images be to allow for successful analysis?	156

Application to a real sample for fiber detection in washing machine water.....	156
Challenges in the Analysis.....	157
3.4 Conclusion and Outlook.....	158
3.5 References.....	161
General Conclusion and Outlook.....	166
References	177
Appendix	178
Appendix A1 Supporting information for Chapter 2	179
Appendix A2 Supporting information for Chapter 3.....	198

SUMMARY

Microplastic contamination of a growing number of environmental compartments and food items is currently the focus of many news stories. But do we even have appropriate methods to detect microplastic? The overreaching goal of this dissertation was to create and validate automated measurement procedures for the quantification of particles larger than 10 μm and up to 1 mm via Raman microspectroscopy. To this end, (i) a procedure was developed for the production of reference materials, (ii) a method to determine the minimal sample size for a representative measurement, (iii) as well as the necessary tools to enable automated morphological and chemical analysis.

The reference materials were produced by sonication of solid polymers in alkaline solution, based on the rationale that many microplastic publications cautioned about the alteration of samples by sonication, but none had tried to harness this mechanism. Polylactide, polyethylene terephthalate, and polystyrene were chosen to cover various polymer materials with potentially different fragmentation behavior. We could produce particles in the range of 100 nm – 1 mm in aqueous solution in large numbers. In contrast to polymer reference materials that are produced by grinding, these particles were suspendable in water and did not adhere to glass walls. Hence, our procedure yields a fast and economic approach to generate reference materials using a simple ultrasonic bath accessible to any laboratory. Such reference materials may serve as standards to improve and validate workflows during method development and may even serve as spikes that mimic environmentally relevant particles for toxicological testing.

Subsequently, to provide a basis for quantitative analysis of microplastics, theory of sampling was applied to determine the minimal number of particles that a representative measurement requires. The calculation of the error induced by random sampling of single fragments yields a minimum sample size, which corresponds to the point at which the effort to measure additional fragments exceeds the improvement in the error margin. For samples containing 10 000 – 100 000

fragments and a microplastic content equal to or above 1%, a subsample of 7 000 will deliver a margin of error of ~20%.

Finally, automated processing is crucial when applying this theoretical consideration to samples. To determine the total number of fragments and to select a random subsample for measurement, a microscopy image of the entire sample needs to be acquired. This image may contain the morphological information of up to 100 000 particles which needs to be extracted quantitatively. Therefore, an automated image segmentation routine - *TUM-ParticleTyper* - was developed, which morphologically characterizes and localizes all fragments with an area exceeding 51 pixels. After the localization, the center coordinates of each particle are estimated and the subsample is automatically selected. All particles in the subsample are measured (in our case a by Raman microscope with an automated stage). The Raman measurements produce a single spectrum for each particle and can be interpreted by a database match. The optimal parameters of the matching procedure were determined by comparing the outcome of the database match with a manual evaluation of the spectra. Since only a single point is measured for each particle, the representativeness of this measurement was evaluated by a comparison with Raman mapping, a high-speed measurement of points separated by a small step size to create a chemical image. The single point approach was found to be faster and more accurate. By focusing on each step of the analysis individually, we were able to create an overall robust procedure, starting from the point that all particles are deposited on the filter, however excluding additional uncertainties from primary sampling or sample preparation.

Together, these advances enable the spectroscopic measurement of microplastic samples. The quantification range was validated and a comparative study showed that by using an adaptive threshold the common global thresholding for particle detection could be outperformed. Furthermore, a minimal quantifiable particle size and microplastic content of a sample was determined. Different reference materials, as well as genuine samples, were used to test the adaptability of this method. Samples can now be processed within 3 workdays. This includes 48 h for unsupervised automated localization of all particles/fibers larger than 10 μm and the measurement

of a subsample consisting of 7 000 fragments using a Raman microscope. Furthermore, about 6 h of operator time for sample preparation prior to the measurement and data verification after the measurement are required. As the analysis time and operator effort has been minimized systematic investigations of microplastic contaminations in e.g. production lines for bottled water or wastewater treatment plants become feasible.

ZUSAMMENFASSUNG

Die Kontamination einer steigenden Zahl von Ökosystemen und Nahrungsmitteln durch Mikroplastik steht derzeit im Fokus des medialen Interesses. Aber haben wir geeignete Methoden zum Nachweis von Mikroplastik? Das übergeordnete Ziel dieser Dissertation war die Entwicklung und Validierung eines automatisierten Messverfahrens für die Quantifizierung von Partikeln (10 µm – 1 mm) mittels Raman-Mikrospektroskopie. Dazu wurde (i) ein Verfahren zur Herstellung von Referenzmaterialien, (ii) ein Verfahren zur Ermittlung der minimalen Probenmenge, (iii) sowie die notwendigen Werkzeuge für eine automatisierte Quantifizierung entwickelt.

Die Referenzmaterialien wurden durch Ultraschallfragmentierung fester Polymere im Alkalischen hergestellt. Der Grundgedanke war, dass viele Mikroplastik-Publikationen vor der Veränderung von Proben durch die Aufbereitung mittels Ultraschall warnten, dieser Prozess jedoch bisher nicht zur Herstellung von sekundärem Mikroplastik verwendet wurde. Um verschiedene Strukturen abzudecken, die den Fragmentierungsmechanismus möglicherweise beeinflussen, wurden Polylactid, Polyethylenterephthalat und Polystyrol für die Methodenentwicklung ausgewählt. Mit dieser Methode können Partikel im Größenbereich von 100 nm – 1 mm in wässriger Lösung hergestellt werden. Dabei werden Probleme gelöst, die häufig bei gemahlten Referenzmaterialien im Gegensatz zu in der Umwelt entstandenen Mikroplastikfragmenten auftreten, wie etwa störendes Anhaften der Partikel an Glas oder ungünstiges Suspensionsverhalten in Wasser. Die wichtigste Errungenschaft unserer Methode besteht jedoch darin, dass Referenzmaterialien nun in einem schnellen und wirtschaftlichen Verfahren mit einem einfachen, für jedes Labor zugänglichen Ultraschallbad hergestellt werden können. Die Referenzmaterialien könnten somit anderen Laboren als Standard zur Verbesserung und Validierung eigener Methoden der Mikroplastikanalyse dienen, sowie toxikologische Studien mit umweltrelevanten Partikeln oder auch Wiederfindungsexperimente ermöglichen.

Um die minimale Anzahl von Partikeln zu bestimmen, die eine repräsentative Messung erfordert wurde Stichprobentheorie angewendet. Die Berechnung des Fehlers, der durch die Selektion einer Zufälligen Stichprobe entsteht, liefert die minimale zu messende Partikelzahl. Diese ist erreicht sobald der Zeitaufwand für die Messung weiterer Partikel, die Verbesserung des Fehlerbereichs übersteigt. Für Proben, die insgesamt zwischen Fragmenten 10 000 – 100 000 enthalten, der Mikroplastikgehalt bei mindestens 1 % liegt und ein relativer Fehler von 20% akzeptabel ist, ist der Berechnung zufolge eine Mindestprobengröße von 7 000 Fragmenten je Stichprobe erforderlich.

Diese theoretische Überlegung muss nun auf die Probe angewendet werden. Um die Gesamtzahl der Fragmente zu bestimmen und eine zufällige Teilprobe für die Messung auszuwählen, muss ein Mikroskopiebild der gesamten Probe aufgenommen werden. Dieses Bild kann die morphologischen Informationen für bis zu 100 000 Partikel enthalten, die quantitativ extrahiert werden müssen. Deshalb wurde eine automatisierte Bildsegmentierungsroutine - *TUM-ParticleTyper* - entwickelt, die alle Fragmente mit einer Fläche von mehr als 51 Pixeln morphologisch charakterisiert und lokalisiert. Nach der Lokalisierung werden die Mittelpunktswerte jedes Partikels bestimmt und die Teilprobe automatisch ausgewählt. Alle Partikel in der Teilprobe werden gemessen (in unserem Fall mit einem Raman-Mikroskop mit automatisiertem Tisch). Die Raman-Messungen erzeugen ein einziges Spektrum für jedes Partikel, welches durch einen Datenbankabgleich interpretiert werden kann. Die optimalen Parameter des Korrelationsabgleichs wurden durch den Vergleich der Ergebnisse des Datenbankabgleichs mit einer manuellen Auswertung der Spektren ermittelt. Da für jedes Partikel nur ein einziger Punkt gemessen wird, wurde darüber hinaus die Repräsentativität dieser Einzelmessung durch einen Vergleich mit einem „Raman-Mapping“ ermittelt. Diese Alternative zur Einzelpunktmessung ist eine Hochgeschwindigkeitsmessung von Punkten, die durch eine kleine Schrittweite getrennt sind, um ein chemisches Bild zu erzeugen. Der Einzel-Partikel-Ansatz erwies sich sowohl als schneller als auch als genauer.

Indem jeder Analysenschritt einzeln betrachtet und validiert wurde, konnte ein robustes Verfahren zur Mikroplastikanalyse erstellt werden. Ausgangspunkt ist eine Mikroplastikprobe, die bereits auf einem Filter fixiert ist, diese Fehlerberechnung vernachlässigt daher die vorhergehenden Schritte der Probennahme und Probenaufbereitung.

Insgesamt wurde ein Verfahren entwickelt und validiert, welches die Quantifizierung von Mikroplastik in diversen Matrices mittels Raman-Mikrospektroskopie ermöglicht. Für diese neue Methode wurde erstmals validiert, in welchem Messbereich eine Quantifizierung von Mikroplastik möglich ist und gezeigt, dass die Verwendung eines adaptiven Schwellwerts die herkömmlichen globalen Methoden für die Partikelerkennung übertrifft. Es wurde getestet, in welchem Größenbereich und bei welchem Mikroplastikgehalt eine Quantifizierung repräsentative Ergebnisse liefert. Zudem wurden sowohl Referenzmaterialien als auch Umweltproben verwendet, um die Vielseitigkeit dieser Methode zu demonstrieren. Die Methode ermöglicht die Quantifizierung von Mikroplastik in einem Zeitrahmen von 3 Arbeitstagen. Dies beinhaltet 48 h für automatisierte Lokalisierung aller Partikel/Fasern größer 10 μm , die Messung von 7000 Fragmenten mit dem Raman-Mikroskop, sowie etwa 6 h Arbeitsaufwand des Experimentators für vorbereitende Maßnahmen und die abschließende Datenverifizierung. Da der Arbeitsaufwand des Experimentators somit minimiert werden konnte, kann diese Methode zur systematischen Analyse von Mikroplastikkontamination in Beispielsweise Produktionsketten von Trinkwasserabfüllanlagen oder Klärwerken dienen.

GENERAL INTRODUCTION

WHAT IS MICROPLASTIC?

Microplastic is the topic of many recent news articles and is of growing concern among the general public. A search on Google trends reveals the relevance of this topic in our society by comparing the topics “Microplastics” with globally important topics such as “Global warming”, “Antibiotic resistance” and “Pandemic”. The search frequencies of these topics in Germany during the last twelve months are displayed in *Figure 1*. On average searches for “Microplastics” exceed the searches for “Global warming” and “Antibiotic resistance” and “Pandemic” until the outbreak of SARS-CoV-2 in the beginning of 2020.

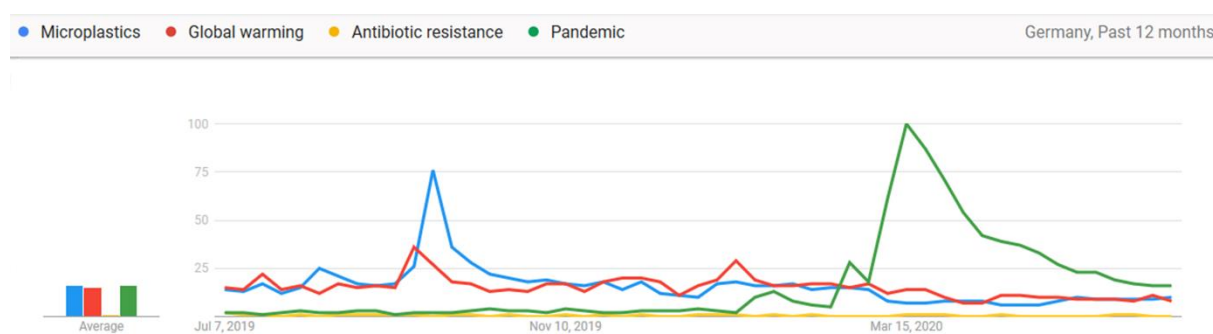


FIGURE 1: FREQUENCY OF SEARCHES FOR THE GLOBALLY RELEVANT CHALLENGES, MICROPLASTICS (BLUE), GLOBAL WARMING (RED), ANTIBIOTIC RESISTANCE (YELLOW) AND PANDEMIC (GREEN). THIS GRAPH CAN BE REPRODUCED, UPDATED, INVESTIGATED FURTHER, AND INTERACTED WITH ON GOOGLE TRENDS. [1]

Microplastic in general refers to microscopic synthetic polymer particles. Despite numerous efforts to unify all characterization, the term is defined very loosely. The debate is mainly centered among the material (e.g. are rubbers microplastic?), size range (1 μm – 5 mm, or should there be further subdivisions?) and the physical state (are gels also microplastic?). Throughout this thesis, we adhere to the definition given by Hartmann et al. 2018 [2]. Microplastic therefore includes all solid particles including fragments, fibers, films, and spheres composed of synthetic polymers in the size range of 1 μm – 1 mm. Among microplastic, two types can be distinguished:

primary and secondary microplastic. While both derive from anthropogenic polymers, primary microplastic is intentionally manufactured, as granulate [3] (precursor for plastic production) or as industrial cleaners and personal care products (toothpaste, facial and body scrubs, etc.). [4, 5] In contrast, secondary microplastic is formed when plastic debris enters the environment and is exposed to environmental conditions resulting in fragmentation to microparticles. [6]

The problem with microplastic is its ubiquitous presence in various environmental compartments and even in food, raising health concerns. Even though plastic is very resistant and is often used as a safe material for food packaging, it changes through weathering and may release potentially toxic components, such as polymer stabilizers, plasticizers, or heavy metals from incorporated pigments. In this context it is important to always consider the toxicological effect of microplastic - and potential adsorbed persistent organic pollutants - in comparison to naturally occurring particles, which can just as easily adsorb and transport pollutants. [7] It is also important to recall that the impact may be linked to the dose, similar to the issues experienced with road salt. Road salt (sodium chloride) is in principle a safe material but excessive amounts cause the deterioration of water quality and salinification of soils. [8] This is especially true, when physical processes such as ocean currents and winds lead to an accumulation, as has been observed for microplastics potentially changing the physical and chemical composition of sites, such as gyres and sediments. [9-13] Therefore, the question arises if degradable polymers would alleviate the problems associated with microplastic accumulation, as they decompose in months or years in the environment as opposed to decades and centuries for conventional polymers.[14, 15]

Metadata analyses of recent microplastic studies suggest that the most commonly found types of microplastic are polypropylene (PP) and polyethylene (PE). [16, 17] This is likely linked to their production rates, as they have the highest market shares [18] among the currently produced polymers. Additionally they are often utilized in single use plastic products, which are likely to end up in the environment due to improper disposal or by deposition in landfills. [19] Recent studies suggest that also

tire abrasion is one of the largest sources for microplastic. [3, 20, 21] So far, there are many datasets available on microplastic abundance, but the accounts vary by several orders of magnitude [17] within the same matrix and polymer type pointing to inadequate characterization.

MICROPLASTIC ANALYSIS, STATE OF THE ART PRIOR TO 2018

Numerous analytical techniques are currently being tested and refined for the quantification of microplastic. In principle, two complementary approaches are being pursued: 1) A mass-based determination of microplastic contamination, which focuses on the total microplastic concentration disregarding particle size. 2) A single particle approach, which delivers morphological and chemical information on individual particles of a sample but is currently a very cumbersome process. [22]

The first approach is mainly implemented through thermoextraction desorption gas chromatography mass spectrometry (TED-GC-MS) [23-26] and pyrolysis gas chromatography mass spectrometry (Pyr-GC-MS) [27, 28]. These methods provide data on polymer mass by analyzing their pyrolysis products. Additionally, the information on contained additives can be obtained, by their desorption prior to pyrolysis. TED-GC-MS is especially well suited to determine the concentration of tire wear particles in the environment provided that they are present in sufficient quantity to exceed the limit of detection of 0.23 µg in 10 - 50 mg sample. [25] Other polymers such as polystyrene (PS), polyvinyl chloride (PVC) etc. can also be detected up to a detection limit (0.5 - 2.5 µg) with this method, as they form very specific pyrolysis compounds. [29] The most abundant microplastic particles PE and PP are much more difficult to analyze with this type of setup, however, as they do not release oligomers that are specific to either of these polymers, but rather generate fragments that are easily confused with other hydrocarbon structures. [24]

For the second approach – single particle analysis – focal plane array Fourier-transform infrared spectroscopy (FPA-FT-IR) [22, 30-33] and Raman microspectroscopy [22, 31, 33, 34] are the most common techniques. FPA-FT-IR and

Raman microspectroscopy identify microplastic particles by means of vibrational spectra (“fingerprints”), which are unique for every polymer type, and can be allocated to specific particles resulting in morphological information in the form of chemical maps and optical images, respectively. A recent comparison by Cabernard et al. 2019 [33] showed that both FPA-FT-IR and Raman microspectroscopy deliver good results for single particle analysis of microplastic < 500 μm , Raman microspectroscopy being more successful (+23% more detected particles) especially in the size range below 20 μm . This is due to the higher spatial resolution of Raman microspectroscopy, as theoretically even targets as small as 300 nm can be detected with this technique. [16, 35] Indeed, the smallest particle identified in a sample was a 1 μm Polyamide particle reported by Ossmann et al. 2018 in drinking water. [36] When analyzing microplastic via Raman microspectroscopy, commonly also information on other contaminants, such as pigments, becomes available. [22, 36-38]

One of the key challenges in reducing the required time for measurements and data processing is to locate microplastic fibers and particles so that spectra acquisition can be dedicated to the relevant target as opposed to imaging the entire filter, as it is done for FPA-FT-IR. Once it is possible to locate both fibers and particles, this information enables an appropriate choice for subsampling by only measuring spectra in particle centers and allows the morphological characterization of the located particles. However, reducing the measurement targets to only located particles is not enough. For Raman microspectroscopy, the analysis of all particles on a filter is typically unrealistic, as the measurement of a single particle may take up to 20 s while there may be 10^6 particles on a filter, which would result in a net measurement time of 232 days per sample. Therefore, it is essential to estimate the number of particles that are required for a representative analysis of each sample (chapter 1). Furthermore, the procedure needs to be tested with appropriate reference materials, which need to be developed and characterized (chapter 2). With the insights gained from chapter 1 and 2 the automated detection, measurement, and evaluation procedure can be developed to reduce the total analysis time, as well as the time requirement for a human operator (chapter 3).

WHAT IS THE GOAL OF THIS THESIS?



This PhD thesis is part of the project MiPAq (Microparticles in the aquatic environment and in foodstuffs – are biodegradable polymers a conceivable solution to the "microplastic problem"?). [39] Therein, the focus of my thesis is on the detection of anthropogenic polymer fragments in the size range 1 μm – 1 mm, called microplastic.

The main goal is to develop methods for the quantification of biodegradable and conventional plastic along with naturally occurring particles in various matrices. This is challenging, since microplastic can be found in diverse matrices such as those of fresh water environments [12, 38, 40, 41], oceans [17, 42-44], sediments [45-48], soils [49], and living organisms [50, 51], as well as food [52-54] and beverages [36, 37]. Furthermore, the heterogeneity in size, shape, chemical composition, and the sheer number of particles that need to be analyzed makes the advancement and automation of current methods essential. [16, 22]

Even though the analytical tools to quantify microplastic in the environment already exist, methods for a quantitative analysis still need to be improved significantly to yield a statistically sound and therefore meaningful result in a reasonable timeframe. While this can be achieved in many ways, the focus of this thesis will be to refine the procedure for Raman microspectroscopy:

In chapter 1 the state of the art for the analysis of microplastic via Raman microspectroscopy is reviewed and a metadata analysis of the reported microplastic contents, composition and size range was performed. A trend towards finding ever smaller microplastic fragments could be identified as well as a trend towards larger sample sizes. An unanswered question however remained: How many fragments need to be analyzed to yield a reliable result? Therefore, a statistically sound approach to select an adequate number of particles to ensure that the measurement reflects the

composition of the original lot was developed and simulated for varying microplastic contents within the sample to assess the feasibility of the subsampling. This alone, however, was not enough to develop an automated microplastic quantification procedure: a reference material was still lacking. Therefore, as described in chapter 2, reference materials that mimic the properties of microplastic found in the environment were developed and characterized. After the theoretical basis for the procedure (chapter 1) and appropriate testing materials (chapter 2) had been developed, it was then possible to join the individual steps for a microplastic quantification procedure and assess its performance, which is detailed in chapter 3. In the following, a state of the art and target is defined for each chapter.

HOW MANY PARTICLES NEED TO BE ANALYZED TO ENSURE A REPRESENTATIVE SAMPLE?

THE SELECTION OF PARTICLES FOR RAMAN MICROSPECTROSCOPIC analysis - state of the art

As Pierre Gy explains in his book on *“Sampling of particulate materials, theory and practice”*: “the value of a sample is representativity, which leaves no material trace”. Meaning that the only way to differentiate a specimen (usually found at the museum) from sample (a correctly extracted representation) is to inspect the conditions under which it was obtained from the original quantity meant to be represented. [55] The goal remains to measure all microplastic fragments, as any subsampling will introduce an error. However, with a rising number of fragments in the sample this becomes increasingly time consuming and therefore uneconomical. The limiting number of fragments that can be measured in a reasonable timeframe (i.e. over the weekend) also depends on the measurement conditions (e.g. integration time, laser power, grating, etc.) and degree of automation of the procedure. The average sample size in 2018 (start of the thesis) was 300 fragments per sample [16] or 1.8% - 15.5% [32, 51] of the filter area. Therefore, a subsampling was and still is in many cases

unavoidable. Different subsampling strategies were applied, most of which are based on the selection of areas or windows on a filter, with subsequent extrapolation onto the entire filter area. [32] The focus of these patterns is to reflect the particle distribution on the filter, where particles are deposited for the measurement. Examples for these patterns can be seen in *Figure 2*.

Patterns for sampling on a filter

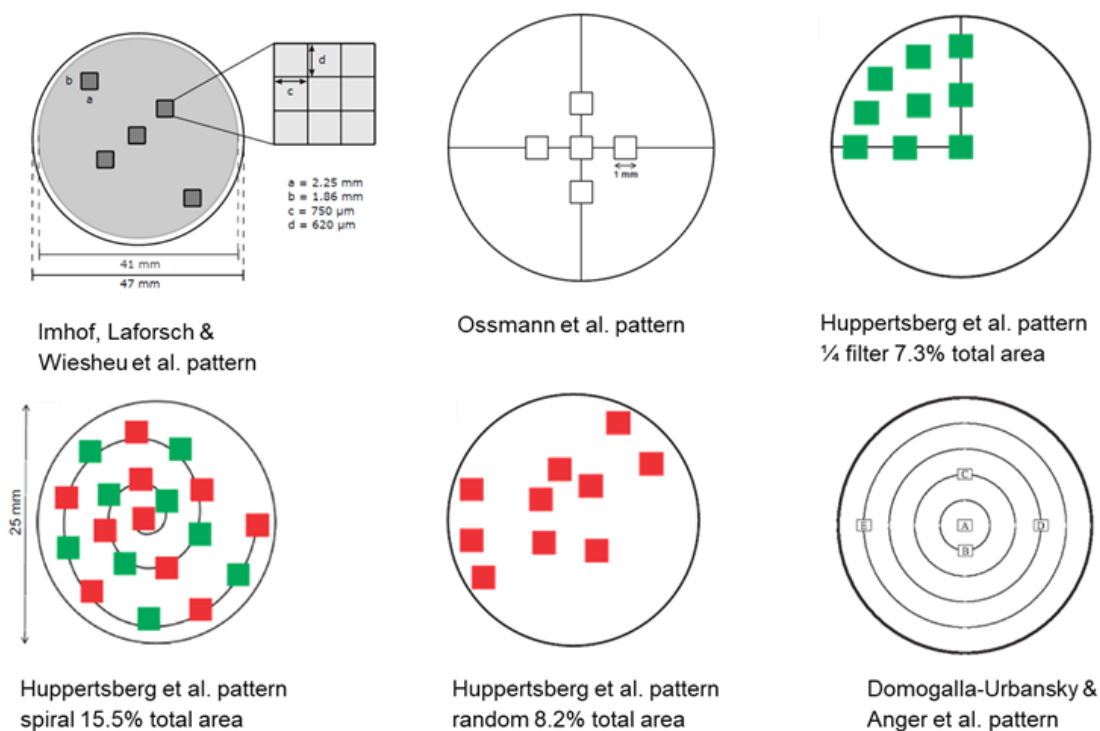


FIGURE 2: PATTERNS FOR THE SAMPLING OF MICROPLASTIC ON FILTER SURFACES UP TO 2019. [32, 36, 38, 51]

However, the success of the analysis is not only determined by the sampling pattern of the analysis with respect to the heterogeneity of the sample. It is also influenced by the detectability of microplastic in real life conditions (e.g. coating with humic substances, aggregation state, etc.). [56] Furthermore, the conditions of the Raman measurement (e.g. integration time, laser power, grating, etc.) influence the length and success of the procedure. [34]

TARGET: STATISTICALLY MEANINGFUL SUBSAMPLING

A statistically meaningful subsampling must account for the heterogeneity of the sample and must provide a mathematical model to estimate the error.

First, the concept of spatial heterogeneity must be examined. In the case of microplastic measurement, spatial heterogeneity refers to the distribution of single fragments on the filter surface. Since the goal is to measure mixtures of plastic fragments found in environmental and food samples, it is prudent to assume that the lot consists of many different components in varying concentrations, which may group according to their physical properties. The error that this composition (mixture of analyte and matrix particles) and spatial distribution inflicts on sampling can be mathematically described by the grouping and segregation error. [55] It boils down to the realization that the distribution of fragments is tied to the location on the filter. Therefore, a window-based approach will always introduce a bias in the selection, which cannot be quantified and leads to a systematic error. This error will become smaller with decreasing window size and increasing window number. [57] The error for this subsampling step theoretically approaches zero if all fragments belonging to the sample have an identical non zero probability of being selected for measurement. [58]

Second, a sampling model is only a model if the error it induces can be computed. This is something that presently all studies struggle with, as none can provide an error approximation for a subsampling on a filter. To solve this challenge, we were inspired by election forecasts, which are very accurate without actually asking the entire population. Which is why the same methodology was applied to microplastic sampling on a filter.

The resulting sampling model is described in Anger and von der Esch et al. 2018 [16] (Chapter 1), along with a comprehensive review of the state of the art of microplastic analysis and a metadata analysis of current microplastic reports. A further development of this method introducing a stratified model, was published in cooperation with Symanski and Ossmann (Analysis of microplastics in freshwater and

drinking water: Minimum requirements and best practice guidelines, *submitted*). The random model and stratified model were implemented in TUM-ParticleTyper in von der Esch and Kohles et al. 2020 [59, 60] and used by von der Esch et al. 2020 [61] for the characterization of microplastic fragments.

HOW CAN REFERENCE MATERIALS BE PRODUCED THAT MIMIC THE PROPERTIES OF SECONDARY MICROPLASTIC, TO ADVANCE METHOD DEVELOPMENT?

REFERENCE MATERIALS - STATE OF THE ART

To produce a suitable reference material, two requirements need to be fulfilled. Firstly, the reference material must display the same characteristics as the material that it is a reference for. Secondly, it must be produced with a robust procedure. [62]

The first concept is especially important for method development. An example of a mismatch between reference and target would be to choose and parametrize a fragment recognition algorithm based on reference images, which only contain evenly colored spheres, when the target is an image containing a multitude of shapes in different sizes and shadings. Therefore, the characteristics of the target must be known before any analysis procedure can be developed. This can be achieved by reviewing the descriptions of the target from already available data and the formation process itself.

Microplastic found in environmental samples is mostly derived from fragmentation processes induced by UV breakdown of the polymer due to the degradation of its stabilizers, as well as mechanical strain or biofouling. [63-67] This leads to an extremely heterogeneous particulate analyte.

The main characteristics are:

1. Microplastic in the environment usually consists of fragments from various polymers. [2, 5, 16]
2. Those fragments are usually in the size range 1 μm – 1 mm. [2]
3. The fragmentation process yields fragments of all shapes, irregular, spheres, fibers and films. [2, 68]
4. Since the fragmentation is a result of ageing, the particles usually show signs of ageing, such as carboxylic groups at the surfaces. [64, 67]
5. The ageing process in the environment leads to suspensibility of the fragments in water.

Therefore, the detection of microplastic is fundamentally limited by the fact that according to current practice, primary microplastic of defined shape is used to develop methods for the analysis of a very different type of material: environmentally aged microplastic.

The second requirement is robustness of production and characterization of a reference material. In our case this is defined as a procedure yielding reproducible size distributions, total particle number, and purity, within a defined margin of error. So far, it is common to characterize microplastic reference particles on size distribution and total particle number while ignoring the material purity. [69] For development of reference particles, we therefore integrate a validation by automated particle quantification with Raman microspectroscopy to determine both morphological and chemical composition of the replicates and analyze their variance to estimate the margin of error.

TARGET: SUITABLE REFERENCE MATERIAL FOR MICROPLASTIC

To achieve better methods for microplastic quantification, it is necessary to employ reference materials, which are as close as possible to microplastic found in the environment. The goal therefore is to develop an easy, repeatable, robust production procedure, without the need for special equipment, which delivers microplastic from various polymers in the typical size range (1 μm – 5 mm), yielding fragments of all shapes, which are ideally already aged and suspensible in water, along with characterization methods for all of these properties.

The production procedure and corresponding characterization methods for suitable microplastic reference materials is described in chapter 2, which corresponds to von der Esch et al. 2020 [61], including a comparison to state of the art of microplastic materials and fragments produced in weathering experiments.

HOW CAN THE MORPHOLOGICAL AND CHEMICAL QUANTIFICATION OF PARTICLES AND FIBERS BE AUTOMATED?

Although microplastic is the target analyte for the Raman microspectroscopy analysis, data on all measured Raman-active particles is gathered through the analysis. The first step is to define the actual research question and to determine whether morphological, chemical or either data on the single particle level is necessary to answer this specific question. If this is the desired information, Raman microspectroscopy is a particularly good choice, since also very small particles ($\sim 1 \mu\text{m}$) can be detected. [36] A prerequisite for the following analysis steps is that the sample needs to be filtrated onto a smooth substrate. Many options for optimizations have already been documented, most notably the use of silicon wafers [70] and gold-coated polycarbonate filters [71], which are smoothed through filter holders. [60]

THE AUTOMATED MORPHOLOGICAL AND CHEMICAL QUANTIFICATION OF PARTICLES AND FIBERS - STATE OF THE ART.

The automated morphological and chemical quantification of particles and fibers via Raman microscopy is important, since each sample contains thousands of particles that need to be chemically identified. In the context of Raman microscopy one approach is to localize particles deposited on a filter (the analyzed area may vary) and then measure a single spectrum at the particle center. This procedure, however, still lacks efficient algorithms for the localization of particles and fibers. Current approaches are only able to detect these shapes exclusively, as often segmentation algorithms are implemented to enable the particle detection, but these impede the detection of fibers (e.g. Otsu-Thresholding and Watershed [72]). If only global thresholding methods are implemented, fibers will be detected but individual particles may be combined into a larger particle due to improper segregation (e.g. only Otsu). [73]

Furthermore, the currently applied automatic global thresholding methods fail, when too many or too few particles are on the filter as the resulting image histogram will not have a clearly discernable peak for the white particles. Regardless of the particle number present on the filter, inhomogeneous lighting can have a detrimental impact on the segmentation, leading to an

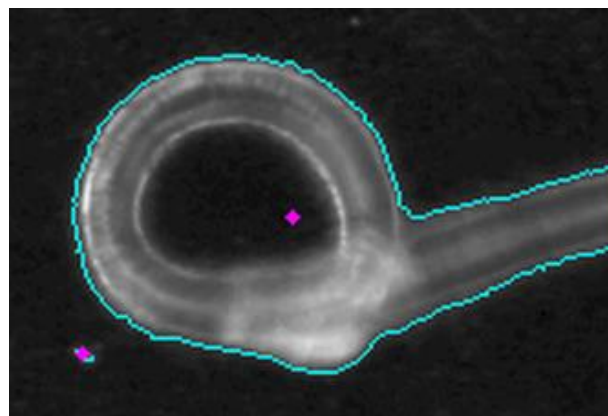


FIGURE 3 : CURLED FIBER LEADS TO MEASUREMENT AT GEOMETRIC PARTICLE CENTER, WHICH IS OUTSIDE OF THE PARTICLE.

under-segmentation in darker areas and over segmentation in lighter areas. Another issue that needs to be solved is to check if the calculated particle center is in fact located on the particle. An example, where the center (purple) is not located on the particle is shown in *Figure 3*. In addition to these parametrization and conceptual challenges, there is no clear procedure for the validation of the particle localization.

This in turn leads to the common practice that image segmentation tools often include options for the user to modify the segmentation threshold found by the applied algorithm to make the segmentation look better. While this may seem like a good way to improve the segmentation on each individual image, it leads to a biased and non-reproducible procedure. This can be expressed by comparing the segmentation proposed by two experts for the same image. As can be seen in *Figure 4* the segmentation of the two experts is similar but not identical, which is in accordance with the findings of Prata et al. [74]

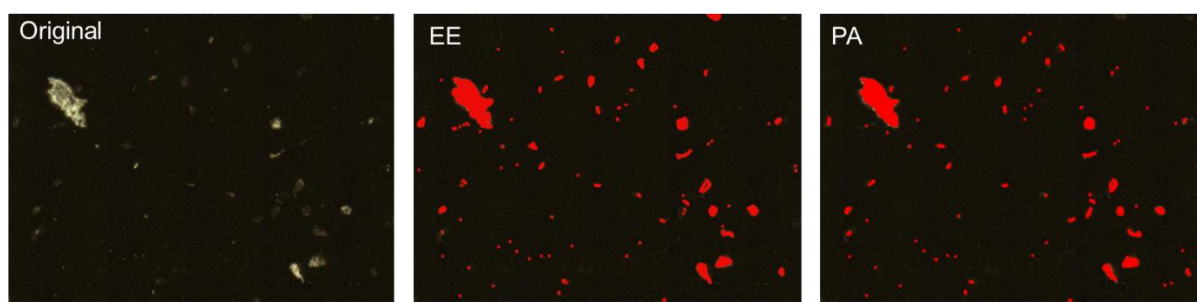


FIGURE 4: LEFT THE ORIGINAL IMAGE OF REFERENCE MATERIALS ON A FILTER, MIDDLE THE SEGMENTATION BY ELISABETH VON DER ESCH, RIGHT THE SEGMENTATION BY PHILIPP ANGER. RED INDICATES THE ASSIGNED PARTICLE AREA BY THE RESPECTIVE EXPERT

Therefore, creating a reference for optimization is already a difficult task, as no definitive ground truth can be established. Nonetheless, the accuracy, robustness, sensitivity, adaptability, reliability and efficiency must be determined for the image segmentation as is usual for any analytical procedure, which is precisely the target of chapter three.

TARGET: AUTOMATED MORPHOLOGICAL AND CHEMICAL QUANTIFICATION OF PARTICLES AND FIBERS FOR RAMAN MICROSPECTROSCOPY THAT CAN BE VALIDATED

In chapters one and two the foundation of such an automated morphological and chemical quantification of particles and fibers that can be validated was laid for Raman microspectroscopy. In chapter one an optimal measurement scheme was proposed and a random sampling approach was simulated to determine if subsampling is feasible. This was achieved by computing the estimated error for different microplastic contents and sample sizes. The maximum sample sizes in this approach were tied to measurement times, as the time spent on chemical identification via Raman microspectroscopy should not exceed two days. Consequently, the strategy applied for the analysis of microplastic is that all particles should be localized by the image processing tool and that subsequently a subset for chemical identification should be randomly selected from the original set containing the morphological information for all particles in the sample.

In chapter two a procedure to produce reference materials was designed and tested. These materials in turn were used to create sample images to parametrize and test different image segmentation algorithms in order to arrive at a suitable particle localization and characterization process.

In chapter three we therefore brought our advancements together to develop a tool with a corresponding measurement and validation procedure that allows the automated analysis of microplastic in a variety of samples e.g. washing machine samples. The accuracy, robustness, sensitivity, adaptability, reliability and efficiency was determined according to the criteria proposed by Wirth et al and Udupa et al. [75, 76] using the ground truth assigned by one expert with the criterion that the segmentation is accurate if the tool yields true positive results within the range of the assignments of expert one vs expert two.

Since the image processing is similar for all images, regardless of their origin, extending our image processing to scanning electron microscopy and fluorescence microscopy images will enable users of many techniques to apply the software. These techniques are often also used to characterize the morphology of microplastic [61, 77] and for a staining-based preselection of microplastic within a sample [74, 78, 79], respectively.

The development, the recommended measurement procedure and validation is described in full detail in chapter 3, which corresponds to von der Esch and Kohles et al. 2020. [60] Further information such as the software and documentation can be downloaded from the repository. [59]

REFERENCES

1. Google trend analysis for queries in Germany comparing the popularity of the terms "Microplastics", "Climate change", "Antibiotic resistance", "Pandemic". *Google Trends*. 2020 [cited 28.08.]. Available from: <https://trends.google.com/trends/explore?geo=DE&q=%2Fm%2F0bwh63b,%2Fm%2F0d063v,Antibiotic%20resistance,Pandemic>.
2. Hartmann NB, Huffer T, Thompson RC, Hasselov M, Verschoor A, Daugaard AE, et al. Are We Speaking the Same Language? Recommendations for a Definition and Categorization Framework for Plastic Debris. *Environ Sci Technol*. 2019;53(3):1039-47.
3. Jürgen Bertling RB, Leandra Hamann. Kunststoffe in der Umwelt: mikro- und makroplastik. *Fraunhofer-institut für Umwelt-, Sicherheits- und Energietechnik UMSICHT*. 2018.
4. Leslie HA. Review of Microplastics in Cosmetics. Institute for Environmental Studies VU University Amsterdam; 2014.
5. Ivleva NP, Wiesheu AC, Niessner R. Microplastic in Aquatic Ecosystems. *Angew Chem Int Ed Engl*. 2017;56(7):1720-39.
6. Gewert B, Plassmann MM, MacLeod M. Pathways for degradation of plastic polymers floating in the marine environment. *Environ Sci Process Impacts*. 2015;17(9):1513-21.
7. Koelmans AA, Besseling E, Foekema E, Kooi M, Mintenig S, Ossendorp BC, et al. Risks of Plastic Debris: Unravelling Fact, Opinion, Perception, and Belief. *Environ Sci Technol*. 2017;51(20):11513-9.
8. Tiwari A, Rachlin JW. A Review of Road Salt Ecological Impacts. *Northeastern Naturalist*. 2018;25(1):123-42.
9. Song YK, Hong SH, Jang M, Kang JH, Kwon OY, Han GM, et al. Large accumulation of micro-sized synthetic polymer particles in the sea surface microlayer. *Environ Sci Technol*. 2014;48(16):9014-21.
10. Van Cauwenberghe L, Vanreusel A, Mees J, Janssen CR. Microplastic pollution in deep-sea sediments. *Environ Pollut*. 2013;182:495-9.
11. Cole M, Lindeque P, Halsband C, Galloway TS. Microplastics as contaminants in the marine environment: a review. *Mar Pollut Bull*. 2011;62(12):2588-97.
12. Eerkes-Medrano D, Thompson RC, Aldridge DC. Microplastics in freshwater systems: A review of the emerging threats, identification of knowledge gaps and prioritisation of research needs. *Water Res*. 2015;75:63-82.
13. Everaert G, Van Cauwenberghe L, De Rijcke M, Koelmans AA, Mees J, Vandegehuchte M, et al. Risk assessment of microplastics in the ocean: Modelling approach and first conclusions. *Environ Pollut*. 2018;242(Pt B):1930-8.
14. Sintim HY, Flury M. Is Biodegradable Plastic Mulch the Solution to Agriculture's Plastic Problem? *Environ Sci Technol*. 2017;51(3):1068-9.

15. Tosin M, Weber M, Siotto M, Lott C, Degli Innocenti F. Laboratory test methods to determine the degradation of plastics in marine environmental conditions. *Front Microbiol.* **2012**;3:225.
16. Anger PM, von der Esch E, Baumann T, Elsner M, Niessner R, Ivleva NP. Raman microspectroscopy as a tool for microplastic particle analysis. *Trends Anal Chem.* **2018**;109:214-26.
17. Erni-Cassola G, Zadjelovic V, Gibson MI, Christie-Oleza JA. Distribution of plastic polymer types in the marine environment; A meta-analysis. *J Hazard Mater.* **2019**;369:691-8.
18. PlasticsEurope. Plastics – the Facts 2017 An analysis of European plastics production, demand and waste data [https://www.plasticseurope.org/application/files/5715/1717/4180/Plastics the facts 2017 FINAL for website one page.pdf](https://www.plasticseurope.org/application/files/5715/1717/4180/Plastics_the_facts_2017_FINAL_for_website_one_page.pdf) [
19. Hopewell J, Dvorak R, Kosior E. Plastics recycling: challenges and opportunities. *Philos Trans R Soc Lond B Biol Sci.* **2009**;364(1526):2115-26.
20. Stephan Wagner TH, Philipp Klöckner, Maren Wehrhahn, Thilo Hofmann, Thorsten Reemtsma. Tire wear particles in the aquatic environment - a review on generation, analysis, occurrence, fate and effect. *Water Res.* **2018**.
21. Dall'Osto M, Beddows DCS, Gietl JK, Olatunbosun OA, Yang X, Harrison RM. Characteristics of tyre dust in polluted air: Studies by single particle mass spectrometry (ATOFMS). *Atmos Environ.* **2014**;94:224-30.
22. Ivleva NP, Wiesheu AC, Niessner R. Mikroplastik in aquatischen Ökosystemen. *Angew Chem.* **2017**;129(7):1744-64.
23. Dumichen E, Eisentraut P, Bannick CG, Barthel AK, Senz R, Braun U. Fast identification of microplastics in complex environmental samples by a thermal degradation method. *Chemosphere.* **2017**;174:572-84.
24. Dumichen E, Barthel AK, Braun U, Bannick CG, Brand K, Jekel M, et al. Analysis of polyethylene microplastics in environmental samples, using a thermal decomposition method. *Water Res.* **2015**;85:451-7.
25. Eisentraut P, Dümichen E, Ruhl AS, Jekel M, Albrecht M, Gehde M, et al. Two Birds with One Stone—Fast and Simultaneous Analysis of Microplastics: Microparticles Derived from Thermoplastics and Tire Wear. *Environ Sci Technol Lett.* **2018**;5(10):608-13.
26. Duemichen E, Braun U, Senz R, Fabian G, Sturm H. Assessment of a new method for the analysis of decomposition gases of polymers by a combining thermogravimetric solid-phase extraction and thermal desorption gas chromatography mass spectrometry. *J Chromatogr A.* **2014**;1354:117-28.
27. Fischer M, Scholz-Bottcher BM. Simultaneous Trace Identification and Quantification of Common Types of Microplastics in Environmental Samples by Pyrolysis-Gas Chromatography-Mass Spectrometry. *Environ Sci Technol.* **2017**;51(9):5052-60.

28. Mintenig SM, Bäuerlein PS, Koelmans AA, Dekker SC, van Wezel AP. Closing the gap between small and smaller: towards a framework to analyse nano- and microplastics in aqueous environmental samples. *Environ Sci Nano*. **2018**;5(7):1640-9.
29. U. Braun MJ, G. Gerdtts, N.P. Ivleva, J. Reiber. Diskussionspapier Mikroplastik-Analytik. BMBF2018.
30. Löder MGJ, Gerdtts G. Methodology Used for the Detection and Identification of Microplastics—A Critical Appraisal. *Marine Anthropogenic Litter*2015. p. 201-27.
31. Käßler A, Fischer D, Oberbeckmann S, Schernewski G, Labrenz M, Eichhorn KJ, et al. Analysis of environmental microplastics by vibrational microspectroscopy: FTIR, Raman or both? *Anal Bioanal Chem*. **2016**;408(29):8377-91.
32. Huppertsberg S, Knepper TP. Instrumental analysis of microplastics-benefits and challenges. *Anal Bioanal Chem*. **2018**;410(25):6343-52.
33. Cabernard L, Roscher L, Lorenz C, Gerdtts G, Primpke S. Comparison of Raman and Fourier Transform Infrared Spectroscopy for the Quantification of Microplastics in the Aquatic Environment. *Environ Sci Technol*. **2018**;52(22):13279-88.
34. Araujo CF, Nolasco MM, Ribeiro AMP, Ribeiro-Claro PJA. Identification of microplastics using Raman spectroscopy: Latest developments and future prospects. *Water Res*. **2018**;142:426-40.
35. Schwaferts C, Niessner R, Elsner M, Ivleva NP. Methods for the analysis of submicrometer- and nanoplastic particles in the environment. *TrAC, Trends Anal Chem*. **2019**;112:52-65.
36. Ossmann BE, Sarau G, Holtmannspotter H, Pischetsrieder M, Christiansen SH, Dicke W. Small-sized microplastics and pigmented particles in bottled mineral water. *Water Res*. **2018**;141:307-16.
37. Schymanski D, Goldbeck C, Humpf HU, Furst P. Analysis of microplastics in water by micro-Raman spectroscopy: Release of plastic particles from different packaging into mineral water. *Water Res*. **2018**;129:154-62.
38. Imhof HK, Laforsch C, Wiesheu AC, Schmid J, Anger PM, Niessner R, et al. Pigments and plastic in limnetic ecosystems: A qualitative and quantitative study on microparticles of different size classes. *Water Res*. **2016**;98:64-74.
39. MiPAq Project - Microparticles in the aquatic environment and in foodstuffs, Water Research at TUM, Technical University of Munich. *Technical University of Munich*. **2020** [cited 28.08]. Available from: <https://www.wasser.tum.de/en/mipaq/home/>.
40. Dris R, Imhof H, Sanchez W, Gasperi J, Galgani F, Tassin B, et al. Beyond the ocean: contamination of freshwater ecosystems with (micro-)plastic particles. *Environ Chem*. **2015**;12(5):539-50.

41. Eriksen M, Mason S, Wilson S, Box C, Zellers A, Edwards W, et al. Microplastic pollution in the surface waters of the Laurentian Great Lakes. *Mar Pollut Bull.* **2013**;77(1-2):177-82.
42. Enders K, Lenz R, Stedmon CA, Nielsen TG. Abundance, size and polymer composition of marine microplastics $\geq 10 \mu\text{m}$ in the Atlantic Ocean and their modelled vertical distribution. *Mar Pollut Bull.* **2015**;100(1):70-81.
43. Frere L, Paul-Pont I, Rinnert E, Petton S, Jaffre J, Bihannic I, et al. Influence of environmental and anthropogenic factors on the composition, concentration and spatial distribution of microplastics: A case study of the Bay of Brest (Brittany, France). *Environ Pollut.* **2017**;225:211-22.
44. Hidalgo-Ruz V, Gutow L, Thompson RC, Thiel M. Microplastics in the marine environment: a review of the methods used for identification and quantification. *Environ Sci Technol.* **2012**;46(6):3060-75.
45. Hanvey JS, Lewis PJ, Lavers JL, Crosbie ND, Pozo K, Clarke BO. A review of analytical techniques for quantifying microplastics in sediments. *Anal Methods.* **2017**;9(9):1369-83.
46. Horton AA, Svendsen C, Williams RJ, Spurgeon DJ, Lahive E. Large microplastic particles in sediments of tributaries of the River Thames, UK - Abundance, sources and methods for effective quantification. *Mar Pollut Bull.* **2017**;114(1):218-26.
47. Imhof HK, Ivleva NP, Schmid J, Niessner R, Laforsch C. Contamination of beach sediments of a subalpine lake with microplastic particles. *Curr Biol.* **2013**;23(19):R867-R8.
48. Lots FAE, Behrens P, Vijver MG, Horton AA, Bosker T. A large-scale investigation of microplastic contamination: Abundance and characteristics of microplastics in European beach sediment. *Mar Pollut Bull.* **2017**;123(1-2):219-26.
49. Rillig MC. Microplastic in terrestrial ecosystems and the soil? *Environ Sci Technol.* **2012**;46(12):6453-4.
50. Collard F, Gilbert B, Eppe G, Parmentier E, Das K. Detection of Anthropogenic Particles in Fish Stomachs: An Isolation Method Adapted to Identification by Raman Spectroscopy. *Arch Environ Contam Toxicol.* **2015**;69(3):331-9.
51. Domogalla-Urbansky J, Anger PM, Ferling H, Rager F, Wiesheu AC, Niessner R, et al. Raman microspectroscopic identification of microplastic particles in freshwater bivalves (*Unio pictorum*) exposed to sewage treatment plant effluents under different exposure scenarios. *Environ Sci Pollut Res Int.* **2018**.
52. Dehaut A, Cassone AL, Frere L, Hermabessiere L, Himber C, Rinnert E, et al. Microplastics in seafood: Benchmark protocol for their extraction and characterization. *Environ Pollut.* **2016**;215:223-33.
53. Gundogdu S. Contamination of table salts from Turkey with microplastics. *Food Addit Contam Part A Chem Anal Control Expo Risk Assess.* **2018**;35(5):1006-14.

54. Karami A, Golieskardi A, Keong Choo C, Larat V, Galloway TS, Salamatinia B. The presence of microplastics in commercial salts from different countries. *Sci Rep.* **2017**;7:46173.
55. Gy PM. Sampling of Particulate Materials, Theory and Practice. Amsterdam 1979: Elsevier Scientific Publishing Company; 1979.
56. Chen W, Ouyang ZY, Qian C, Yu HQ. Induced structural changes of humic acid by exposure of polystyrene microplastics: A spectroscopic insight. *Environ Pollut.* **2018**;233:1-7.
57. Minkkinen PO, Esbensen KH. Sampling of particulate materials with significant spatial heterogeneity - Theoretical modification of grouping and segregation factors involved with correct sampling errors: Fundamental Sampling Error and Grouping and Segregation Error. *Anal Chim Acta.* **2019**;1049:47-64.
58. Petersen L, Minkkinen P, Esbensen KH. Representative sampling for reliable data analysis: Theory of Sampling. *Chemometrics and Intelligent Laboratory Systems.* **2005**;77(1-2):261-77.
59. Kohles AJ, von der Esch E, Anger PM, Hoppe R, Niessner R, Elsner M, et al. TUM-ParticleTyper: Software and Documentation. <https://mediatum.ub.tum.de/1547636>: TUM 2020.
60. von der Esch E, Kohles AJ, Anger PM, Hoppe R, Niessner R, Elsner M, et al. TUM-ParticleTyper: A detection and quantification tool for automated analysis of (Microplastic) particles and fibers. *PLoS One.* **2020**;15(6):e0234766.
61. von der Esch E, Lanzinger M, Kohles AJ, Schwaferts C, Weisser J, Hofmann T, et al. Simple Generation of Suspensible Secondary Microplastic Reference Particles via Ultrasound Treatment. *Front Chem.* **2020**;8(169).
62. NIST. SRM Definitions <https://www.nist.gov/srm/srm-definitions> [27.09.2019]. Available from: <https://www.nist.gov/srm/srm-definitions>.
63. Astner AF, Hayes DG, O'Neill H, Evans BR, Pingali SV, Urban VS, et al. Mechanical formation of micro- and nano-plastic materials for environmental studies in agricultural ecosystems. *Sci Total Environ.* **2019**;685:1097-106.
64. Brandon J, Goldstein M, Ohman MD. Long-term aging and degradation of microplastic particles: Comparing in situ oceanic and experimental weathering patterns. *Mar Pollut Bull.* **2016**;110(1):299-308.
65. Cai L, Wang J, Peng J, Wu Z, Tan X. Observation of the degradation of three types of plastic pellets exposed to UV irradiation in three different environments. *Sci Total Environ.* **2018**;628-629:740-7.
66. Cocca M, De Falco F, Gentile G, Avolio R, Errico ME, Di Pace E, et al. Degradation of Biodegradable Plastic Buried in Sand. Proceedings of the International Conference on Microplastic Pollution in the Mediterranean Sea. Springer Water2018. p. 205-9.
67. Lambert S, Wagner M. Formation of microscopic particles during the degradation of different polymers. *Chemosphere.* **2016**;161:510-7.

68. Koelmans AA, Mohamed Nor NH, Hermsen E, Kooi M, Mintenig SM, De France J. Microplastics in freshwaters and drinking water: Critical review and assessment of data quality. *Water Res.* **2019**;155:410-22.
69. Eitzen L, Paul S, Braun U, Altmann K, Jekel M, Ruhl AS. The challenge in preparing particle suspensions for aquatic microplastic research. *Environ Res.* **2018**:490-5.
70. Käppler A, Windrich F, Loder MG, Malanin M, Fischer D, Labrenz M, et al. Identification of microplastics by FTIR and Raman microscopy: a novel silicon filter substrate opens the important spectral range below 1300 cm(-1) for FTIR transmission measurements. *Anal Bioanal Chem.* **2015**;407(22):6791-801.
71. Ossmann BE, Sarau G, Schmitt SW, Holtmannspotter H, Christiansen SH, Dicke W. Development of an optimal filter substrate for the identification of small microplastic particles in food by micro-Raman spectroscopy. *Anal Bioanal Chem.* **2017**;409(16):4099-109.
72. Anger PM, Prechtel L, Elsner M, Niessner R, Ivleva N. Implementation of an Open Source Algorithm for Particle Recognition and Morphological Characterisation for Microplastic Analysis by Means of Raman Microspectroscopy. *Anal Methods.* **2019**.
73. Brandt J, Bittrich L, Fischer F, Kanaki E, Tagg A, Lenz R, et al. High-Throughput Analyses of Microplastic Samples Using Fourier Transform Infrared and Raman Spectrometry. *Appl Spectrosc.* **2020**:3702820932926.
74. Prata JC, Reis V, Matos JTV, da Costa JP, Duarte AC, Rocha-Santos T. A new approach for routine quantification of microplastics using Nile Red and automated software (MP-VAT). *Sci Total Environ.* **2019**;690:1277-83.
75. Wirth M, Fraschini M, Masek M, Bruynooghe M. Performance Evaluation in Image Processing. *EURASIP J ADV SIG PR.* **2006**;2006(1).
76. Udupa JK, Leblanc VR, Zhuge Y, Imielinska C, Schmidt H, Currie LM, et al. A framework for evaluating image segmentation algorithms. *Comput Med Imaging Graph.* **2006**;30(2):75-87.
77. Fries E, Dekiff JH, Willmeyer J, Nuelle MT, Ebert M, Remy D. Identification of polymer types and additives in marine microplastic particles using pyrolysis-GC/MS and scanning electron microscopy. *Environ Sci Process Impacts.* **2013**;15(10):1949-56.
78. Erni-Cassola G, Gibson MI, Thompson RC, Christie-Oleza JA. Lost, but Found with Nile Red: A Novel Method for Detecting and Quantifying Small Microplastics (1 mm to 20 µm) in Environmental Samples. *Environ Sci Technol.* **2017**;51(23):13641-8.
79. Maes T, Jessop R, Wellner N, Haupt K, Mayes AG. A rapid-screening approach to detect and quantify microplastics based on fluorescent tagging with Nile Red. *Sci Rep.* **2017**;7:44501.

DECLARATION OF SCIENTIFIC CONTRIBUTION AND SUMMARY OF SUMMARY OF RAMAN MICROSPECTROSCOPY AS A TOOL FOR MICROPLASTIC PARTICLE ANALYSIS

Philipp M. Anger[✉] and Elisabeth von der Esch[✉],

Thomas Baumann, Martin Elsner, Reinhard Niessner, Natalia P. Ivleva

Trends in Analytical Chemistry, (109) 2018, 214-226, DOI:
10.1016/j.trac.2018.10.010

[✉]shared first authorship

In this publication, the goal was to provide an overview of the current advances in the quantification of microplastics using Raman microspectroscopy. Therefore, PA and EE reviewed the available literature. EE focused on highlighting the niche for Raman microspectroscopy by assessing its strengths and weaknesses in comparison to alternative quantification methods such as infrared spectroscopy and thermoanalytical methods. After PA set the stage by explaining the Raman microspectroscopy theory and its implications on the measurement of polymer fragments, EE evaluated if these concepts are mirrored in the way Raman microspectroscopy is applied to microplastic samples. The synthesis of both chapters delivers the optimal measurement parameters for the quantification of microplastic using Raman microspectroscopy, taking into account the effort (time) and the output (accuracy). EE then compared the reports of microplastic in different matrices, finding that the most commonly produced polymers are also the most commonly found polymers, which is unsurprising but provides tentative evidence that the quantification is done correctly.

All findings together with the consideration of effort vs. output lead to the central question: How many particles need to be measured to provide a correct quantification?

The simple random sampling approach on a filter, which is the key novelty of this publication, was developed as a joint effort of PA, EE and TB and was thoroughly

reviewed by all authors for plausibility. With this approach, it is possible to estimate the uncertainty of a subsampling on the filter, without introducing a bias from the spatial distribution of the fragments and the measurement time reduction becomes more effective for growing total particle numbers. PA closes this chapter by discussing the relevance of filter area in light of our approach, which selects a subsample from the total number of particles determined by image analysis of the entire filter. Since our theoretical sample selection scheme is based on several assumptions, idealizing the Raman microspectroscopy measurement, EE explains these in detail and highlights how they may be achieved. The manuscript in its entirety was revised by all authors.

CHAPTER : 1

RAMAN MICROSPECTROSCOPY AS A TOOL FOR MICROPLASTIC PARTICLE ANALYSIS

Philipp M. Anger[☉], Elisabeth von der Esch[☉],

Thomas Baumann, Martin Elsner, Reinhard Niessner, Natalia P. Ivleva*

Trends in Analytical Chemistry, (109) 2018, 214-226, DOI:

10.1016/j.trac.2018.10.010

[☉] shared first authorship

Please note that, as the author of this Elsevier article, you retain the right to include it in a thesis or dissertation, provided it is not published commercially. Permission is not required, but please ensure that you reference the journal as the original source. For more information on this and on your other retained rights, please visit: <https://www.elsevier.com/about/our-business/policies/copyright#Author-rights>

ABSTRACT

This review discusses the identification and quantification of microplastic (MP) using Raman microspectroscopy (RM). It addresses scientists investigating MP in environmental and food samples. We show the benefits and limitations of RM from a technical point of view (sensitivity, smallest particle sizes, speed optimizations, analysis artefacts and background effects) and provide an assessment of the relevance of lab analyses and their interpretation (sample sizes for the analysis, uncertainty of the analysis). All parts are complimented by extensive literature data and a theoretical derivation of the concepts. We conclude with suggestions for a feasible and meaningful RM analysis of MP samples.

Highlights:

- Niche for Raman microspectroscopy in microplastic research
- Benefits and limitations of Raman microspectroscopy
- Suggestion for feasible and statistically meaningful analysis at single particle level

Keywords: Raman microspectroscopy (RM); Microplastic; Analysis; Statistical certainty; Contamination; Image processing; Simple random sampling

Nomenclature

NA - Numerical aperture

\ll MP - Smallest MP particle

Obj. - Objective

FPA-FT-IR - Focal plane array Fourier-
transform infrared spectroscopy

PA - Polyamide

PC - Polycarbonate

l/mm - Lines/mm

PCL - Polycaprolactone

LOD - Limit of detection

PE - Polyethylene

LWD - Long working distance

Meas. T. - Measurement time

PET - Polyethylene terephthalate

MP - Microplastic

PLA - Polylactic acid

PMMA - Poly(methyl methacrylate)

PP - Polypropylene

PS - Polystyrene

PTFE - Polytetrafluorethylene

PVC - Polyvinylchloride

Pyr-GC-MS - Pyrolysis gas
chromatography

RM - Raman microspectroscopy

SNR - Signal to noise ratio

Sp. Rn - Spectral range

TED-GC-MS - Thermo extraction
desorption-gas chromatography-mass
spectrometry

1.1 INTRODUCTION

SMALL AND VERY SMALL MICROPLASTIC PARTICLES – THE NICHE FOR RAMAN MICROSPECTROSCOPY.

Plastic particles in the size range of 1 μm to 5 mm are called microplastic (MP) [1]. Primary MP is mainly produced for personal care products (cosmetics, toiletries) or as scrubbing agents [2]. Primary particles can enter the environment mostly through waste waters, but they are not commonly found in the environment [3]. The origin of secondary MP is any plastic material, from improperly disposed plastic to car tires [4], as all anthropogenic polymers fragment due to UV radiation, weathering, abrasion, as well as chemical and (micro)biological degradation [5]. At the moment, sampling, sample preparation as well as identification and quantification techniques are mostly still under development and in testing phases [6]. Consequently, the extent of MP contamination in the environment is still difficult to quantify and reported concentrations and particle sizes vary by several orders of magnitude [1]. Different analytical techniques are being applied to environmental samples to detect, identify and quantify MP particles, most prominently focal plane array Fourier-transform infrared spectroscopy (FPA-FT-IR) [1, 7-9], Raman microspectroscopy alias Raman microscopy (RM) [1, 9-11], thermoextraction desorption-gas chromatography-mass spectrometry (TED-GC-MS) [12-15] and pyrolysis gas chromatography (Pyr-GC-MS) [16, 17] are utilized. According to Renner et al. [18] the spectroscopic methods (FT-IR and RM) are the most popular techniques for unambiguous chemical identification as they were applied in 90% of studies. FT-IR and RM identify MP particles via vibrational *fingerprint*, which is unique for every polymer type, whereas the other methods rely on MS information of monomers / oligomers or additives and provide information on polymer mass. FT-IR and RM are in principle non-destructive, whereas the MS-based methods rely on thermal extraction / decomposition, coupled to chromatographic separation and subsequent MS detection of volatile products [1, 12, 15, 16]. The MS-based methods need to be developed for each polymer and adapted for different matrices individually [15]. However, the methods are complementary in analyzing single particles (FT-IR, RM) or masses (TED-GC-MS, Pyr-

GC-MS) and the target sizes of single particles or minimal masses they can reach. The limit for the spectroscopic techniques for spatially resolved detection is the Abbe limit. In principle (non-linear) spectroscopic techniques can detect structures below the Abbe limit. However, spatially resolved detection, which includes chemical and morphological characterization of particles, is able to reach the lower limit of MP (1 μm) as it is currently defined. [1] We therefore focused on linear Raman techniques. For the MS methods the limit is set by the mass available for analysis, the mass portion of MP in the sample and the individual detection limit for each polymer. [12, 15, 18] *Figure 5* gives a graphical representation of the smallest detectable single particle for each method and the smallest particles found by means of RM. Detailed information about microplastic analysis with TED-GC-MS [12-15], Pyr-GC-MS [16, 19] and FPA-FT-IR [7, 8, 20, 21] can be found elsewhere.

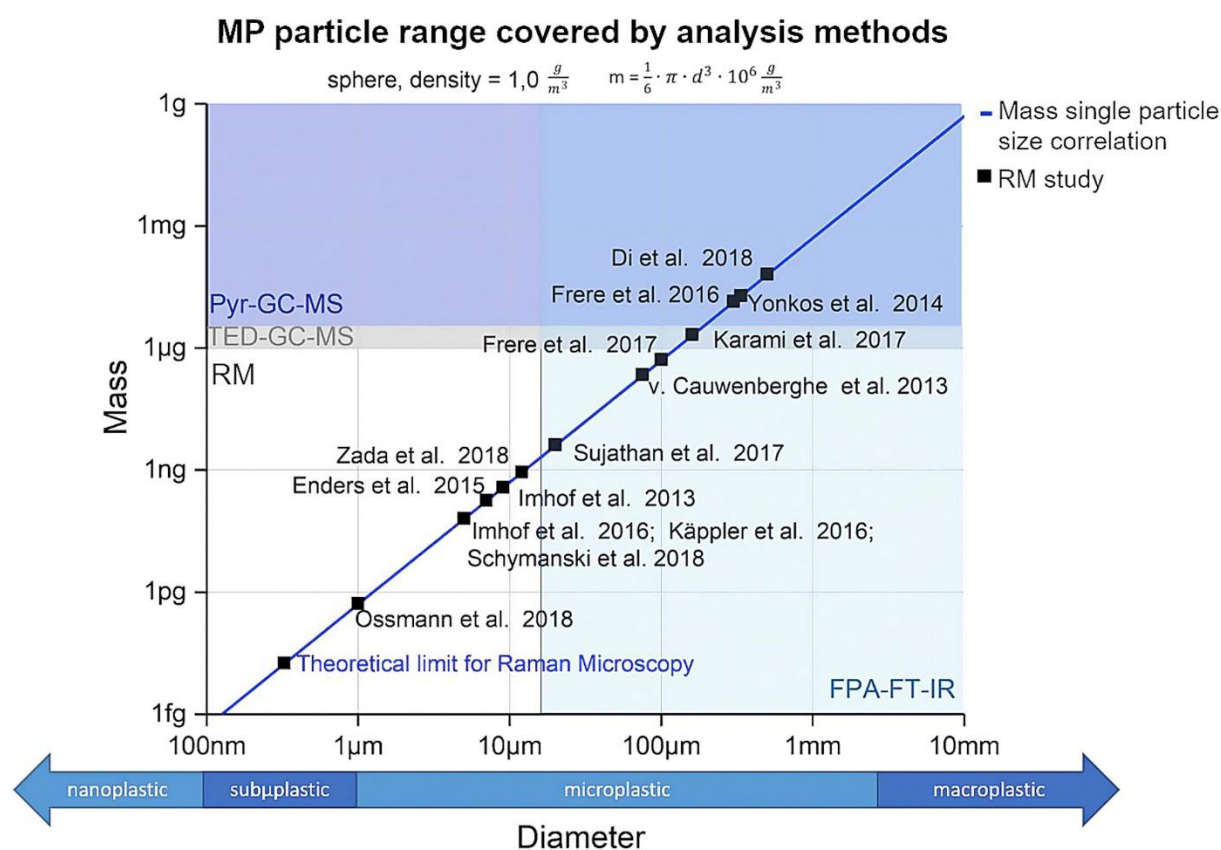


FIGURE 5: MASS TO DIAMETER CORRELATION OF SPHERICAL MP PARTICLES WITH A DENSITY OF 1 G/CM³ (DARK BLUE LINE). ANALYTICAL RANGE OF TED-GC-MS (GRAY) [15] AND PYR-GC-MS (DARK BLUE) [16,

17] FOR PE, AS THE MOST COMMONLY FOUND MP. AS WELL, THE LIMIT FOR FPA-FT-IR (LIGHT BLUE) [7] LEAVING THE NICHE FOR RAMAN MICROSPECTROSCOPY (WHITE). POINTS INDICATE SMALLEST REPORTED MP PARTICLE IN ENVIRONMENTAL [9, 22-34] AND FOOD [35-38] SAMPLES FOR EACH RM STUDY, RESPECTIVELY.

The mass to diameter ratio was calculated for a spherical polymer particle with a density of 1 g/cm^3 , as the most common polymers have densities ranging from 0.90 g/cm^3 (PP) and 1.6 g/cm^3 (PVC) and the polymers with the highest production rate have the lower densities [1, 39]. This visualization was chosen to compare mass and spectrometric analysis techniques, as they deliver different yet correlated information on the sample. For TED-GC-MS, the limit of detection (LOD) is $1,6 \mu\text{g}$ for PE [15]. Pyr-GC-MS has a limit of $4 \mu\text{g}$ for PE [16, 17]. Using automated MP detection FPA-FT-IR is limited to particles larger than $20 \mu\text{m}$ [7]. The theoretical limit of about 300 nm for RM is defined by the Abbe limit and calculated and explained in section 2.1. Furthermore, recent RM studies of environmental [9, 22-34] and food [35-38] samples are marked by the smallest detected MP particle reported. This visualization shows a niche for RM in the small MP range with decreasing practical particle size limitations. As illustrated in *Figure 5*, the theoretical limit has not yet been reached for environmental samples, leaving room for improvement.

The unique feature of the single particle approach with RM is its possibility to chemically and morphologically characterize MP particles even if they constitute only a small percentage of the total number of particles in a sample. This is very important, as MP analysis is a four-dimensional challenge composed of: (i) chemical composition, (ii) size and (iii) shape of the individual particle, as well as (iv) abundance of each polymer particle type within a sample [40]. RM is especially suited for small MP particles, which are plentiful in numbers, but not in mass and potentially exhibit the largest environmental threat [1, 41].

Furthermore, such an analysis allows the investigation of all Raman active particles in a sample, thus making it widely applicable throughout particle research, and enabling the investigation of a ratio of anthropogenic to natural substances in environmental samples.

For the analysis of MP particles in the environment, a method for the quick detection of the entire size range is desired. With the necessary automation and effective measures for minimizing the fluorescence background, RM provides all the prerequisites for the development of such a method. RM bears the potential to representatively measure the required number of particles from 1 μm up to 5 mm, deliver a size correlated compound distribution and morphological as well as chemical characterization on the single particle level. Current applications, however, are still exceedingly time-consuming, require skilled operators and currently do not yet follow harmonized protocols. This review therefore, aims to summarize current ongoing efforts to achieve such a transition towards routine RM analysis of MP. In the following sections, we will give a critical overview of the RM technique applied for MP analysis and will discuss trends for the future RM based MP analysis.

1.2. DISCUSSION

HOW SMALL CAN RM ANALYZE?

In chapter 1.1, the niche for RM was established to be the spatially resolved detection of the smallest MP particles and for analyzing samples with a low mass of MP. The question is: What is the smallest particle analyzable by RM? or How small can RM analyze? The second question refers to spatially resolved detection, which enables chemical and morphological characterization. We first give an answer from a theoretical point of view and in the second part compare them to findings from the literature. It should be mentioned that RM is capable of analyzing larger particles as well. In fact, as long as the particle fits under the microscope a spectrum can be acquired.

THEORETICAL CONSIDERATIONS

RM, is the combination of a Raman spectrometer and an optical microscope. This setup enables excitation of a defined volume with laser light, which is embraced by the lateral and the depth resolution. The theoretical basis has already been discussed

in various books [42, 43]. In this chapter we will give a short summary on the most important aspects relevant for the analysis of MP.

In microscopy, the lateral resolution (d) is confined by the Abbe or diffraction limit, which is dependent on the numerical aperture (NA) and the observed wavelength (λ): $d_{(\text{Abbe})} = \lambda / 2 \text{ NA}$. The Abbe resolution is only accessible with coherent light. Light guided through a circular aperture diffracts and forms a so-called Airy pattern. The resolution is calculated using the diameter of the Airy disk, limited by the first minimum of the Airy pattern, via the following equation: $d_{(\text{Airy})} = 1.22 \lambda / \text{NA}$. The Rayleigh criterion can be applied to describe the distance between two objects that can be resolved, which is, in this case defined by the distance between the two maxima of the Airy pattern of two objects, while the maximum of the Airy pattern of object one is located on the first minimum of object two: $d_{(\text{Rayleigh})} = 0.61 \lambda / \text{NA}$ [44].

The achievable resolution for the Raman part of the Raman microscope is in a first approximation described by the laser spot size, which is calculated using the Airy pattern, also used for calculating the lateral resolution of the microscope. In a second approximation the aforementioned Rayleigh criterion is utilized to calculate the difference between two objects that can be resolved. For laser sources with 532 nm, 633 nm and 785 nm wavelength, applying an objective with NA of 0.5 (e.g., a technical specification of 50 \times long working distance objectives) spatial resolutions of 649 nm, 772 nm and 958 nm are obtained, respectively. An even better resolution is achievable with objectives with NA = 1.0 (325 nm resolution with a 532 nm laser) [45].

These considerations show that the lower limit of 1 μm currently discussed for MP is easily accessible by the optical microscope as well as the Raman part. It also shows that the resolution needed for submicroplastic (< 1 μm) particles is achievable [Schwaferts et al. submitted]. Even smaller structures are analyzable by non-linear Raman techniques, which are able to overcome the Abbe limit. For further information, the reader is referred to Araujo et al. [10, 11] dealing especially with MP and non-linear techniques and to the works of Opilik et al. [46] and Stewart et al. [47] for a more general overview.

Axial or depth resolution is highly dependent on the sample itself. However, for the analysis of MP it is sufficient to approximate an excited volume of a few microns in depth [48]. Therefore, a sample containing particle sizes differing from a few millimeters to a few micrometers needs an approach that ensures focusing of the laser on every particle. This can be realized in two different ways: through auto-focusing software, which is often available by the manufacturer or by group-wise analysis of particles with defined depths for every group. The latter requires a method to determine the height of the particles.

FINDINGS FROM LITERATURE

RM enables the characterization of single particles. Together with an automated procedure for the recognition of particles and automated measurements, the number of analyzed particles has increased, as well as the size range *Figure 6*. A clear trend towards the detection of smaller and smaller particles, which is the niche of RM can be seen.

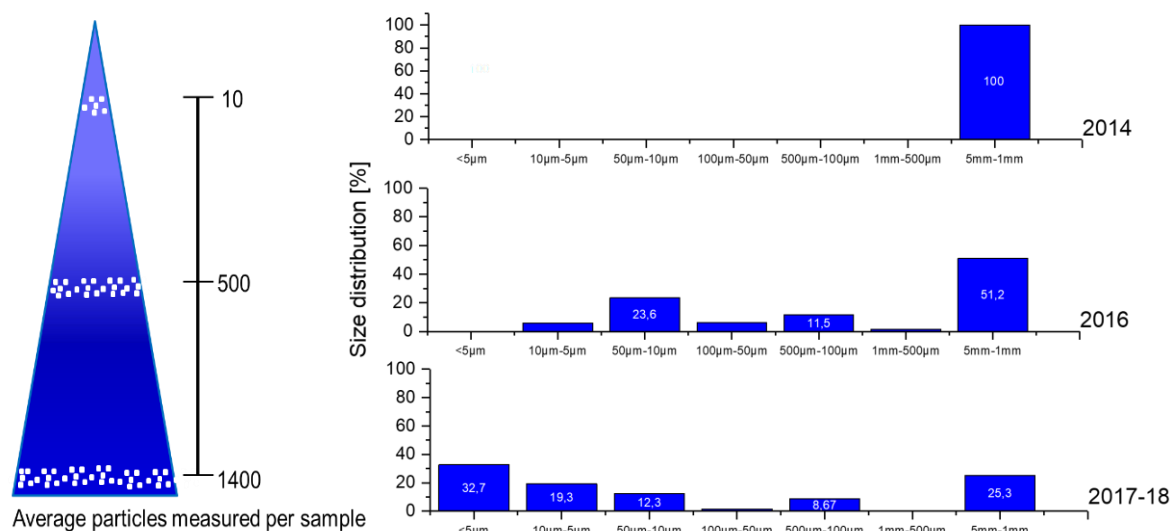


FIGURE 6: DEVELOPMENT OF REPORTED SIZE DISTRIBUTIONS IN LIQUID SAMPLES AS A FUNCTION OF TIME. FOR THE PERIOD BETWEEN 2014 [49], 2016 [9, 25, 30] AND 2017-18 [27, 35, 36] AS AUTOMATION ADVANCES, THE MEASUREMENT OF INCREASINGLY MORE AND SMALLER PARTICLES IS ENABLED.

The smallest reported MP particle found in a real sample (bottled mineral water) and confirmed by RM so far is a 1 μm polyamide (PA) particle published by Ossmann et al. [35]. They used a 532 nm laser and an objective with 50 \times magnification (NA = 0.75).

In addition, five other groups have reported on MP particles below 10 μm by now (entries 1 – 4 and 9 in *Table 1*). To shed light on the measurement conditions that are critical for measurements in this low size range, in the following we review the setup details employed in these studies. In particular, we address the choice of wavelengths and numerical aperture as critical parameters and discuss aspects of sample treatment that are crucial for measurements of very small particles.

TABLE 1: COMPARISON OF MEASUREMENT PARAMETERS FOR MP FOUND IN ENVIRONMENTAL AND FOOD SAMPLES WITH RM. Obj. = OBJECTIVE, MEAS. T. = MEASUREMENT TIME, SP. RN = SPECTRAL RANGE, L/MM = LINES/MM, LWD = LONG WORKING DISTANCE, << MP = SMALLEST MP PARTICLE

Study	Laser excitation	Power	Objective	Measurement Time.	Grating	Spectral Range	<< MP
Imhof et al. 2013 [31]	633 nm	0.4 – 4 mW	50 \times (NA = 0.75)	5 – 500 s	600 l/mm	50 – 4000 cm^{-1}	9 μm
Enders et al. 2015 [23]	455 nm	-	50 \times (NA = 0.75)	20 s	-	100 – 3500 cm^{-1}	7 μm
Imhof et al. 2016 [30]	633 nm	0.4 – 4 mW	50 \times LWD (NA = 0.5)	5 – 500 s	600 l/mm	50 – 4000 cm^{-1}	5 μm
Käppler et al. 2016 [9]	532 nm	5 mW	20 \times (NA = 0.5)	20 \times 500 ms	600 l/mm	160 – 3600 cm^{-1}	5 – 10 μm
Frère et al. 2016 [25]	785 nm	-	10 \times (NA = 0.25)	2 \times 10 s	300 l/mm	200 – 1700 cm^{-1}	279 μm
Sujathan et al. 2017 [32]	532 nm	10.8 mW	50 \times (NA = 0.55)	0.5 – 2 s / 4 h	600 l/mm	-120 – 3500 cm^{-1}	20 μm
Erni-Cassola et al. 2017 [24]	442 nm	-	-	20 \times 10 s + 5 min bleaching	-	100 – 3500 cm^{-1}	20 μm

Ossmann et al. 2018 [35]	532 nm	3.2 mW	50× (NA = 0.75)	2×1 s	600 l/mm	150 – 3500 cm ⁻¹	1.3 μm
Schymanski et al. 2018 [36]	532 nm	12%	20×	5 s	1040 l/mm	200 – 3200 cm ⁻¹	5 – 10 μm
Ghosal et al. 2018 [50]	785 nm	1 – 100 mW	20× - 100 ×	10 – 60 s	-	200 – 3200 cm ⁻¹	1 mm

In a study published in 2013 [31] we found a PA particle of 9 μm in size in sediment samples using a 633 nm laser and an objective with 50× magnification (NA = 0.75). The smallest particle Enders et al. [23] found in ocean water had a size of 7 μm. They applied a 455 nm laser and an objective with 50× magnification (NA = 0.75). In another study [30] we confirmed in sediment samples PA particles with a size of 5 μm. A 633 nm laser and an objective with 50× magnification and long working distance (NA = 0.5) was used. K appler et al. [9] did not state the size of the smallest particle, but found 9 particles in the size range of 5 – 10 μm in sediment samples. They used a 532 nm laser and an objective with 20× magnification (NA = 0.5). In contrast to the other papers, K appler et al. [9] used mapping to find smaller MP particles present in the sample. They applied a point distance of 10 μm for mapping. Schymanski et al. [36] did not report a smallest MP particle but found e.g. that 39% of MP particles in mineral water from beverage cartons were in the size range of 5 – 10 μm. They also analyzed mineral waters in other container materials and found similar MP particles portions for the lower size class. They used a 532 nm laser and an objective with 20× magnification.

The studies used either a 455 nm, a 532 nm or 633 nm laser, but no 785 nm laser was applied for analysis of particles smaller than 10 μm. This may be due to the better spatial resolution achieved with these lasers, but is also owed to the fact that measuring spectra with a 785 nm laser takes a lot more time. The intensity of the Raman signal declines with the fourth power of the laser wavelength. Furthermore, the efficiency of conventional CCD cameras applied for the entire visible region is

relatively low [51]. Therefore, a 785 nm laser takes a lot more time to acquire a spectrum with the same signal to noise ratio (SNR) a 633 nm laser would take.

The used objective of course has a great influence on spatial resolution. The studies that reported on very small MP particles, all applied objectives with at least a NA of 0.5. Ossmann et al. [35], who found the smallest particle, used the objective with the biggest NA (50×, NA = 0.75). The easiest solution would be to use objectives with 100× magnification which have a NA of ca. 0.9. However, a high NA results in a very small working distance of the objective. Objectives with 100× magnification normally have working distances around 300 µm. They can only be used for very smooth filter samples, bigger particles need to be excluded prior to analyses by sample preparation. For practical applications objectives with a NA of at least 0.5 and a long working distance are most recommendable.

From a theoretical point of view, the lower size limit of MP of 1 µm is easily reachable. However, only in one study the smallest particle reported has a size of 1 µm [35] and the second smallest particle found was 5 µm in diameter [30]. The reason why other groups did not find such small particles are various. Imhof et al. [30] utilized a quartz filter that consists of interwoven fibers. Particles smaller than 5 µm may have gotten into the woven fabric, which may have hindered optical detection. They also analyzed sediment samples, which means a highly complex matrix that hampers analyses of smaller particles. Käßler et al. [9] used mapping with a point distance of 10 µm for analysis of particles deposited on a Si filter with 10 µm pore size. Applying this pore size and distance for mapping means that particles smaller than 10 µm may be filtered out by sample preparation or be overlooked in subsequent RM analysis. However, this is of course a compromise to enable reasonable sample preparation and measurement times. Schymanski et al. [36] used gold coated polycarbonate filters with a pore size of 3 µm, which may have also hindered the analyses of particles smaller than 3 µm. In conclusion, although theoretically 1 µm MP particles should not be a problem for RM, their identification still is highly dependent on various other parameters such as complexity of sample, applied filter type and measurement parameters.

HOW FAST CAN RM BE?

An essential question for the overall performance of RM measurements is the needed time to get enough spectral information for a reliable evaluation. This splits into two aspects. On the one hand, the time for an evaluable single measurement and on the other hand the time needed for the overall process of measuring a sufficient number of particles. The latter is also discussed in chapter *Trade-off between measurement time and representativeness*, which is a deduction of this chapter *Challenge of representativeness*.

TIME EFFORT FOR SINGLE MEASUREMENT

For a reliable evaluation of RM spectra of MP it is recommendable to detect all spectral features of the most common polymer types. According to PlasticsEurope [39] the 12 polymers with the highest annual production are polypropylene (PP), polyethylene low/very low density (PE-LD/LLD), polyethylene high/medium density (PE-HD/MD), polyvinylchloride (PVC), polyurethane (PUR), polyethylene terephthalate (PET), polystyrene (PS), expanded PS (PS-E), styrene-acrylonitrile resin/acrylonitrile butadiene styrene (SAN/ABS), polyamide (PA), polycarbonate (PC) and poly(methyl methacrylate) (PMMA). The spectral range of these polymers needed to cover all spectral features from 200 cm^{-1} – $3\,200\text{ cm}^{-1}$ (compare *Table 2*), which gives a spectral range of $3\,000\text{ cm}^{-1}$. This spectral range covers the *fingerprint* area (200 cm^{-1} – $1\,500\text{ cm}^{-1}$) and the C-H stretching modes of alkyls, alkenes and aromatic protons ($2\,800\text{ cm}^{-1}$ – $3\,200\text{ cm}^{-1}$) [52].

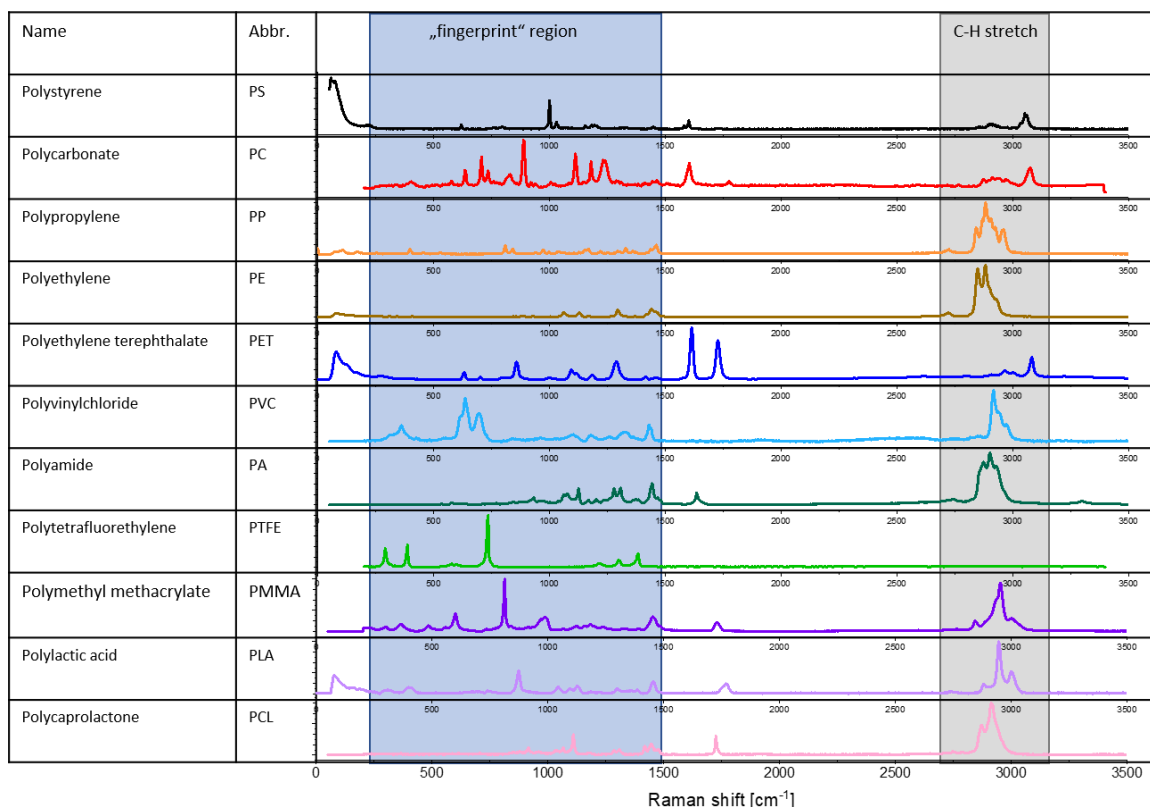


TABLE 2: RAMAN SPECTRA OF RELEVANT POLYMERS. “FINGERPRINT” REGION AND REGION FOR C-H STRETCHING MODES OF ALKYLs, ALKENES AND AROMATIC PROTONS ARE HIGHLIGHTED.

The time to cover the spectral range of 3 000 cm⁻¹ is determined by the excitation wavelength, the length of the beam path in the spectrometer, the number of lines in the grating and the width of the CCD camera. An optimal setting should cover the whole spectral range within one measurement using only one position for the grating. A shorter wavelength and a low number of lines in the grating results in a broad spectral range, which can be covered with one grating position. The trade-off is the decreasing spectral resolution for an increasing covered spectral range. However, this normally is not a problem as the analysis of MP spectra is accomplished by comparing several positions of spectral bands. Although a lower spectral resolution makes a spectrum less rich in information, for the comparison of spectral positions this is not a relevant factor. Therefore, normally the grating with lowest number of lines is

applicable. Frère et al. [25] are the only group we found applying a grating with 300 l/mm, which is also the lowest number of lines used in RM for analysis of MP to our knowledge. Most of the studies applied gratings with 600 l/mm (*Table 1*). Hence, it is possible to increase the time efficiency of the overall process. Commercially available Raman microscopes have a fixed beam path length in the spectrometer and normally one, sometimes two CCD cameras. The latter differ in response for different wavelength, which is important if lasers in broad wavelength range are used within one system [53].

Evaluation of Raman spectra is done either manually or via algorithms. For both approaches, the lowest possible measurement time should result in spectra where the SNR equals at least three for the weakest band that is needed for evaluation. To improve the SNR, the laser power can be increased to the point well below sample destruction at the given measurement time. Estimating an exact power is dependent on many different factors such as sample, matrix and instrument characteristics and often not worthwhile. The applied laser powers vary from 0.4 mW (633 nm) [30] to 10.8 mW (532 nm) [32]. It is recommendable to test the applicable laser power for every sample type. From ours and others experience (*Table 1*) a practical approach is to begin with a low laser power (e.g. 0.4 mW), than carefully increasing the laser power for small particles, since they can be easily destroyed. If the laser power should be the same for all particles, using less laser power and a longer measurement time are recommendable.

The estimation of the measurement time, which consists of the acquisition time and the number of accumulations, is also a critical task. The acquisition time is limited by the saturation of the CCD camera. The camera collects photons during the whole acquisition time but has a limited capacity. If saturation is reached, spectral features can be partially or completely lost [53]. Therefore, acquisition times are chosen where a single measurement does not reach saturation. To still achieve a good SNR, multiple measurements can be accumulated and averaged. The measurement time for pristine polymers is usually shorter than for weathered MP. In the following only studies where environmental samples were analyzed are taken into account. The shortest

measurement time was reported by Sujathan et al. [32] with 0.5 s, which is also the group that reported the highest applied laser power. In contrast, in Imhof et al. [30] we used a very low laser power and with 500 s one of the longest measurement times for a single particle. Both groups analyzed the particles in more than one step and did additional measurements with higher laser power and/or longer measurement times. Measurement times of other groups are found in between these two extrema. It is advisable to apply lowest possible measurement times tuned to the applicable laser power.

Furthermore, it is worth noting that both polymer and pigment of a MP particle can be analyzed simultaneously with RM, if appropriate measurement conditions are used. An unmonitored reduction of measurement time will lead to an incomplete analysis, where only the pigment is visible, as shown in *Figure 7* [30]. If an unambiguous spectrum of the polymer is not achievable through Raman, despite appropriate measurement conditions, it is advisable to apply complementary spectroscopic methods, such as IR spectroscopy (MP > 20 μm) [9] or possibly even nonlinear Raman spectroscopy (MP < 20 μm) [10, 11].

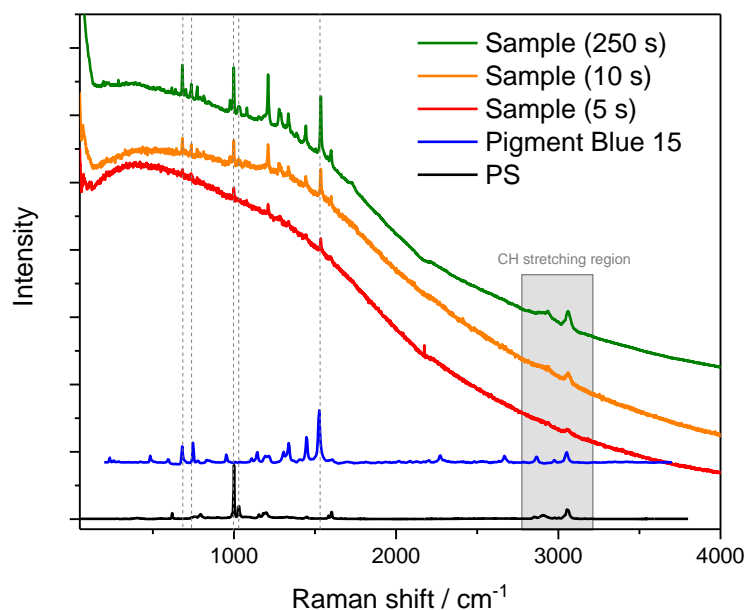


FIGURE 7: TIME DEPENDENCE OF SPECTRAL IDENTIFICATION, MODIFIED FROM [30] (SUPPORTING INFORMATION). SETTINGS FOR THE MEASUREMENT: 633 NM LASER, 4 MW AND OBJECTIVE WITH 50 \times MAGNIFICATION AND LONG WORKING DISTANCE ($NA = 0.5$).

TIME EFFORT FOR OVERALL PROCESS

The time for the total measurement consists of the threesome: (i) optical particle recognition, and selection of measurement locations (ii) actual Raman measurements at the selected locations (iii) evaluation of acquired spectra. In their article Araujo et al. [10] recently comprehensively reviewed the different approaches currently in use or under development. They also gave a comprehensive overview on total time consumption of studies applying RM for MP analysis. The fastest referenced RM method was applied by Frère et al. [25] with 20 s / mm², but they only analyzed particles down to 279 μm . The method by Erni-Cassola et al. [24] requires around 2 min / mm², analyzing particles down to 20 μm . Their approach starts with staining the particles with a fluorescent dye, which then enables particle identification by an ImageJ software tool. The next step is RM measurement of each stained particle. If,

and only if, the staining covers all plastic particles, the method is a smart way to reduce the number of particles which need to be characterized spectroscopically.

Although the selection of an optimized method is always depending on the objective of the study, we suggest a two step approach: (i) use image analysis software to determine particle coordinates (e.g. Schymanski et al. [36], Frère et al. [25]) and (ii) apply single point measurements of a statistically significant subset. In the following chapter, we will discuss what a significant subset of particles may be. Another possibility would be to expand the method of Erni-Cassola et al. [24] to particles smaller than 20 μm .

POTENTIAL OF RAMAN MICROSPECTROSCOPY

IDENTIFICATION OF MP POLYMER TYPES

The identification of the polymer type of the MP particles found in a sample is important, as different polymers can have varying impacts on the biosphere [54]. The detected MP by RM depends highly on the sample type, as shown in *Figure 8*. Additionally, the abundance of each polymer type was compared to the reported polymer market share (%) [39]. PE and PP have the highest market shares with 29% and 19%, respectively. They are also the most abundant polymers in environmental samples, with strikingly similar contents in the averaged sediment samples (PE 32.6%, PP 17.4%). The PP and PE percentage in the averaged water samples is much higher (74.3% and 40.4%) than the respective market shares. On the other hand, dense polymer types, such as PET (15%) and PS (26.2%) are enriched in sediments. This could be caused by a natural density separation in liquid matrices, where dense polymer types and heavily overgrown particles sink down leaving only the light plastic at the surface and burying the heavier polymers in the sediments. This hypothesis seems to fail for PS, which is also enriched in water samples. In the case of PS it is important to note that the density of PS can be tailored to specific applications by vaporizing the blowing agent pentane to introduce air bubbles rather than changing the chemical structure [55]. Based on the Raman spectrum of expanded PS

these particles will be assigned to PS as well. Contrary to PS, expanded PS would be expected to accumulate in water. Furthermore, PS in all its variations is a popular packaging material [56] which can easily be introduced into the environment through littering, which could help to further explain its enrichment in water and sediment samples. Overall, a greater polymer variety can be seen in sediment and salt samples, which also fits with the density separation hypothesis. PVC was only found in solid samples as it is the densest of the mentioned polymers. However, it is much less abundant than suggested by its market share. This is reasonable, as PVC is used less for packaging purposes than the other polymers limiting its exposure to the environment [56]. As expected, exceptionally high PET abundances were found in samples from PET bottles.

So far, there are no accounts of biodegradable MP, such as polylactic acid (PLA) or polycaprolactone (PCL) in the environment, although aging studies suggest that also biodegradable plastic form secondary MP through weathering [57]. The absence of these polymers in environmental samples may result from the relatively low production rates and also from the novelty of these materials as they have only recently entered the plastic market [39].

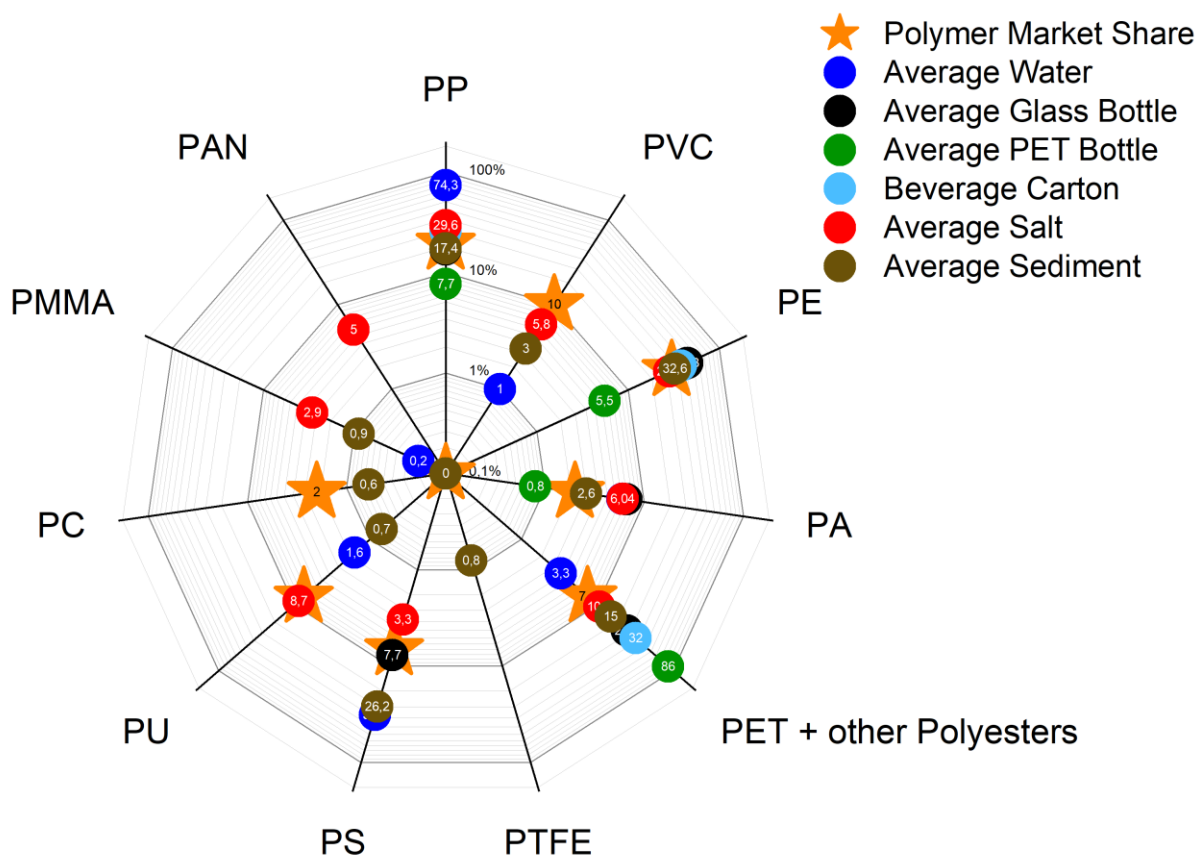


FIGURE 8: DISTRIBUTION OF POLYMERS FOR DIFFERENT MP SAMPLE TYPES ANALYZED BY MEANS OF RM AND CORRELATED TO THE POLYMER MARKET SHARE TO PLASTICSEUROPE [39] (STAR). THE POLYMER ABUNDANCE WAS AVERAGED FOR EACH SAMPLE TYPE: WATER (OCEAN [23, 24], RIVER [27] AND ESTUARY [25], DARK BLUE), GLASS BOTTLE [35, 36] (BLACK), PET BOTTLE [35, 36] (GREEN), BEVERAGE CARTON [36] (LIGHT BLUE), SALT [37, 38] (RED), SEDIMENT [9, 22, 25-31, 33] (BROWN).

For our analysis we evaluated papers where MP was analyzed by RM and matched the findings to the respective polymer market share. In another study by Fraunhofer the sources of MP were investigated through a top down approach where polymer consumption was extrapolated to potential MP formation. As the top ten contributors to MP in the environment they propose: abrasion of tires, emissions from waste disposal, abrasion of polymers and bitumen in asphalt, pellet losses, wind drift of materials from sports and play grounds, emissions from construction sites, packaging materials, road markings and fibers from textiles. Many of these sources have yet to be investigated. Due to the high carbon black content (22-40%) of tires it is very

difficult to apply single particle based spectroscopic methods. [58] For these tire wear particles a single particle analysis by means of EDX has been proposed, as sulfur and zinc are characteristic components of tires and can give an indication if the particle stems from a tire [4]. If the total tire wear particle mass exceeds 0.23 μg in a sample of 10-50 mg for styrene butadiene rubbers TED-GC-MS is the method of choice [15].

INFLUENCE OF PARTICLE SHAPE ON THE DETECTION

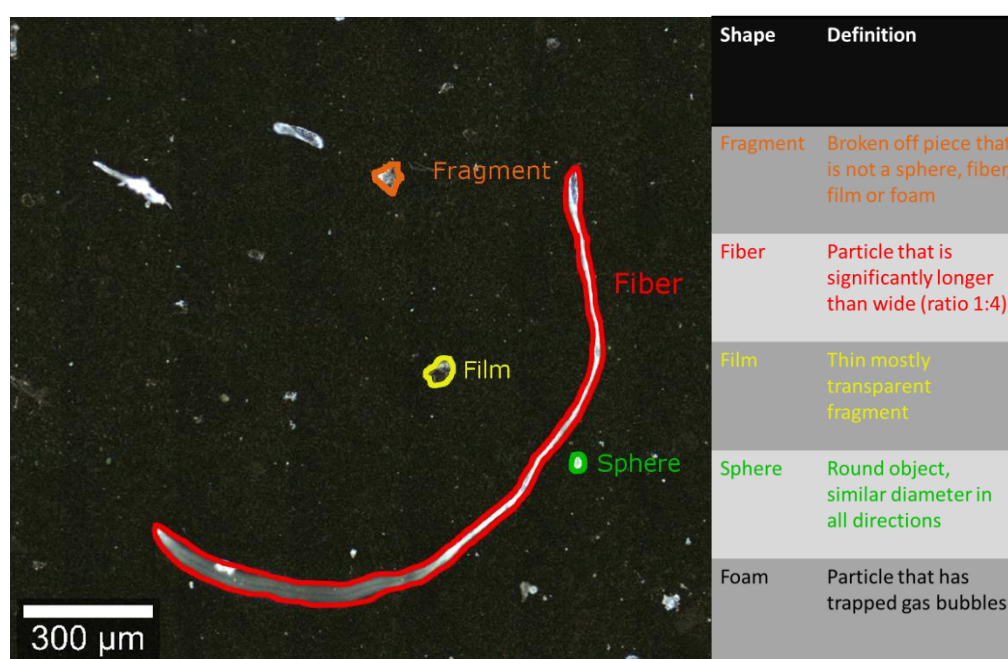


FIGURE 9: SECONDARY MP REFERENCE PARTICLES DESIGNED FOR PARTICLE DETECTION TESTING [E. VON DER ESCH ET. AL. IN PREPARATION]. SHAPE CLASSIFICATIONS ARISE FROM IMAGE PROCESSING REQUIREMENTS AND ARE IN ACCORDANCE WITH [59, 60].

One of the challenges in single particle analysis is the variety of different shapes that are encountered and require specific detection settings (*Figure 9*). Hence, finding a suitable detection algorithm for all particles on a filter is a rather difficult task. The fidelity of the source image that is used for particle detection is of key importance for the success of any particle detection algorithm. Acquiring high-resolution images with low depth-of-field is an essential prerequisite. In the case of the simultaneous

detection of very small and very large particles, image acquisition with subsequent focus stacking is required in order to minimize depth-of-field.

Modern particle recognition software packages, such as ParticleFinder (Horiba) [25], Single Particle Explorer (RapID) [36], Gepard Enabled PARTicle Detection GEPARD [IPF repository tba.] and Munich Microparticle Recognizer Raman Analyzer, MipRAN [Anger et al. in prep.] lead to very good results for the recognition of spherical particles, but lack reliability when it comes to other shapes. Fragments and films are likely to be detected correctly by these software packages, as they are similar to spherical particles in shape, but partly or completely translucent particles may introduce errors. Inconsistencies in color are a challenge for any particle recognition algorithm that exploits high contrast differences in brightness or color between background and particle, which is why dark field images were preferred over bright field in recent studies [35, 36]. Dark field is a microscopic visualization mode that collects stray light, which highlights edges and corners and thereby facilitates optical recognition via contrast. Blurred particle edges may lead to over- or underestimation of the particle size, or incorrect boundaries.

Fibers display the highest level of difficulty for recognition, if they should be detected in their entirety. At higher magnification the fiber might not fit into one single field-of-view, therefore, the image processing has to work on the entire montage of the individual images with all border and segmentation effects. Due to their high aspect ratio in combination with irregular contours, algorithms designed to separate overlapping agglomerated particles are likely to lead to unwanted fragmentation along the fiber. Different translucency of the particles has to be accounted for with an adaptive segmentation algorithm. The detection of fibers is especially important, as studies [61, 62] found that most fibers in a sample originate from laboratory contamination and must therefore be excluded from final results.

To improve the detection of particles, programs must be tailored to all MP shapes. Therefore, it is very important to work with MP reference materials, which contain MP particles similar to MP found in environmental samples for development and testing. [E. von der Esch et. al. in preparation]

Since traditionally MP particles are categorized by size we propose to keep the widely accepted categories (1 μm – 5 μm , 5 μm – 10 μm , 10 μm – 50 μm , 50 μm – 100 μm , 100 μm – 500 μm , 500 μm – 1 mm, 1 mm – 5 mm) [63] and additionally report the shape. Therefore, it is important to find a common shape and size classification for fibers. As longest and shortest dimension must be determined for each particle for automatic shape characterization, we propose to only classify a fiber as MP-fiber if both diameters are below 5 mm and the aspect ratio is at least 1:4. Further, fibers should be listed separately reporting both length and width together with the chemical identity.

EXPLORATION OF MP TO NON-MP RATIO

Through (semi-) automated RM, a (high) number of particles can be analyzed regardless of their origin so that a ratio between anthropogenic substances such as MP particles and native particles can be investigated. This ratio will strongly depend on the sample as well as the preparation procedure. Valuable information from the MP distribution in water samples could be gained as less preparation is necessary for those samples [64], Finding out this ratio could also help improve toxicological studies as environmental MP concentrations have yet to be determined [65]. Unfortunately, only very few studies provide information on this highly interesting matter. This could be because measurement automation is still in the development stages for single particle RM analysis. Hence, only very recent studies could have acquired enough data for such a comparison [35, 36]. Another factor is the interference of fluorescence which disrupts the classification of some particles [66, 67]. These are not always mentioned even though they make up a significant portion of the particles found in the sample.

Available insight suggests it is recommendable to report all analyzed particles by chemical identity, as well as the unidentified particles. This should show which procedures significantly reduce or induce fluorescence. Thus, a correlation between

measurement parameters such as acquisition time, number of accumulations and laser wavelength can be achieved. The same applies to sample preparation, where any information about steps that effectuate fluorescence quenching will be extremely helpful for operators.

CHALLENGE OF REPRESENTATIVENESS

Applying RM for the analysis of MP usually means analyzing single particles on a filter sequentially. The obvious question is: How many particles need to be analyzed to get a statistically meaningful result? The answer to this question strongly depends on sample matrix and success of sample preparation. Only for special cases if the total number of particles in the sample is low, as in, e.g., bottled water, it seems feasible to analyze all particles [35, 36]. In this chapter we want to give a suggestion for analysis of filters with a number of particles which cannot be measured in a reasonable time. For this assessment we assume a filter covered with 10^6 particles which is the magnitude we found in previous studies from samples of surface water. This is also the magnitude of particles calculated from a filter with 11 mm diameter covered with a single layer of 5 μm particles (area of filter divided by area of one particle). We emphasize that the following calculations apply to for the final filter sample. Sampling and sample processing are excluded at this point.

We will calculate the minimal required number of particles based on the following assumptions: (i) all particles on the filter can be divided into the two groups: MP and non-MP; (ii) all particles on the filter are separated from each other'; (iii) all particles are randomly distributed on the filter, meaning the MP to non-MP ratio is constant over all parts of the filter (no clustering of particles according to their properties); (iv) heterogeneous spatial distribution of the particles is allowed; (v) all particles are identified by image processing; (vi) independent of their size, all particles are treated equally as single measurement points; (vii) identification of particles by means of RM is flawless. We strongly emphasize that these assumptions reflect an idealized system.

Determining the sample size n (number of particles which need to be analyzed) is possible by applying a random sampling approach [68] called simple random sample of units selected without replacement (*srswor*) [69]. The sample size n is calculated using Equation 1 based on the normal distribution [70]. The precision is given by the symmetrical margin of error.

$$n \geq \frac{P(1 - P)}{\frac{e^2}{\sigma^2} + \frac{P(1 - P)}{N}} \quad \text{EQUATION 1}$$

with:

Sigma value for prediction interval	$\sigma = 1.65$ for 90% prediction interval [68]
Total number of particles found on the filter through image processing	N
Estimate of the MP fraction	P / decimals
Margin of error	e / decimals
Sample size / number of particles required	N

In *Table 3* the number of particles that need to be analyzed for a filter with 10^6 particles, $\sigma = 1.65$ (90%) and a tolerated margin of error $e = 10\%$ for the MP fraction is calculated. We varied the estimate of the MP fraction to show the correlation between the sample size and the analyte fraction.

TABLE 3: NUMBER OF PARTICLES THAT NEED TO BE ANALYZED FOR A FILTER WITH $N = 10^6$ PARTICLES, $\sigma = 1.65$ (90%) AND A TOLERATED MARGIN OF ERROR $E = 10\%$, P VARIED FROM 0.05% TO 5% MP FRACTION.

Variables	$P = 5\%$ MP	$P = 0.5\%$ MP	$P = 0.05\%$ MP
$e^* =$	0.005	0.0005	0.00005
$n \geq$	5 147	51 394	352 428

* e is always 10% of the estimated MP fraction P , i.e. the decimal number decreases with decreasing estimate of the MP fraction P .

We increased the tolerated margin of error e to 20% for the MP fraction $P = 5\%$ and to $e = 30\%$ for the MP fractions $P = 0.5\%$ and $P = 0.05\%$ in Table 4 leading to a non-linear decrease of the required particle number.

TABLE 4: NUMBER OF PARTICLES THAT NEED TO BE ANALYZED FOR A FILTER WITH $N = 10^6$ PARTICLES, $\Sigma = 1.65$ (90%) AND VARIED TOLERATED MARGINS OF ERROR $E = 20\%$ ($P = 5\%$) AND $E = 30\%$, $P = 0.05\%$ AND $P = 5\%$.

Variables	$P = 5\%$ MP	$P = 0.5\%$ MP	$P = 0.05\%$ MP
$e =$	0.01	0.0015	0.00015
$n \geq$	1 292	5 984	57 022

Table 3 and *Table 4* show that the number of particles that need to be analyzed strongly increases with decreasing fraction of MP among the total number of particles. On page 72, we will discuss to what extent these absolute minimal sample sizes n can be achieved under idealized conditions with state-of-the-art measurement techniques.

After estimating n , the subsequent RM measurement reveals the MP fraction p in the sample n . To extrapolate n to the total number of particles N the confidence interval has to be recalculated, as it is very unlikely, that the measured MP fraction p will match the estimated MP fraction P . The fraction of MP p is then reported by stating the recalculated margin of error. The lower limit is calculated by $MP_{(fraction\ lower\ limit)} = p - \sigma \sqrt{[p(1-p)/n]}$ and the upper limit is calculated by $MP_{(fraction\ upper\ limit)} = p + \sigma \sqrt{[p(1-p)/n]}$. Alternatively, the required number of particles can be adjusted during the measurement according to p .

Assuming 5% MP particles and having found 10^6 particles on the filter, according to Equation 1 we would have analyzed 5 147 particles ($e = 0.005$). After analysis a possible outcome would be 103 MP particles ($\sim 2\%$ of 5 147). Thus, the confidence interval is now from 1.6% to 2.4% MP particles in the sample, meaning that the MP fraction is $2 \pm 0.4\%$ (new $e = 0.004$ equaling a tolerated margin of error of 20%, which is twice as much as set prior to the analysis). In *Figure 10*, the development of the margin of error e for 2% MP fraction is displayed with increasing sample size. For the illustrated case 13 000 particles would have had to be analyzed to fulfill the original precision criterion $e = 10\%$.

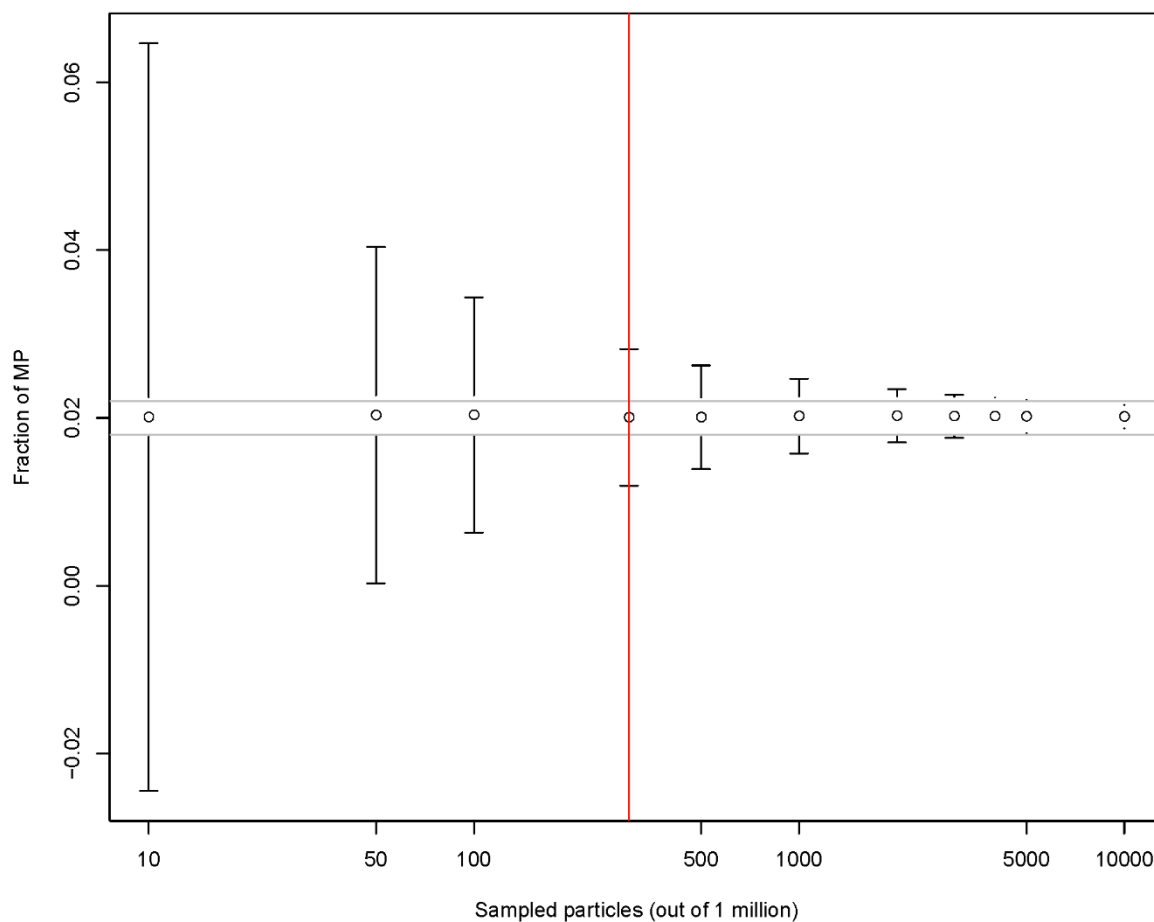


FIGURE 10: CORRELATION OF SAMPLE SIZE N AND MARGIN OF ERROR E FOR AN ASSUMED FRACTION OF MP PARTICLES OF 2%. THE PRECISION CRITERION MARGIN OF ERROR $E = 10\%$ IS DISPLAYED AS GRAY HORIZONTAL LINES. THE RED LINE MARKS A TYPICAL SAMPLE SIZE OF 300 PARTICLES.

TRADE-OFF BETWEEN MEASUREMENT TIME AND REPRESENTATIVENESS

On page 61 the settings for the shortest possible measurement time were considered. We also stated that the fastest method at the moment is not the most preferable as it dismisses the big advantage of RM to analyze particles smaller than 20 μm .

In Table 5, we calculated the possible number of particles from the absolute measurement time for RM approaches that found particles between 1 μm and 5 μm in environmental samples and also for the fastest RM approach. These numbers should work as points of reference. For practical measurements, the numbers of analyzable particles within these time spans will decrease due to several issues (e.g. movement of motorized table), nevertheless they can serve as a first approximation.

TABLE 5: COMPARISON OF ANALYZABLE NUMBER OF PARTICLES FOR GIVEN TIME SPANS FOR DIFFERENT RM APPROACHES.

Study	s/ particle	5 h total Meas. time	15 h total Meas. time	24 h total Meas. time	48 h total Meas. time
Imhof et al. 2016 [30]*	500 s	36 particles	108 particles	173 particles	346 particles
Käppler et al. 2017 [9]	10 s	1 800 particles	5 400 particles	8 640 particles	17 280 particles
Schymanski et al. 2018 [36], Imhof et al. 2016 [30]*	5 s	3 600 particles	10 800 particles	17 280 particles	34 560 particles
Ossmann et al. 2018 [36]	2 s	9 000 particles	27 000 particles	43 200 particles	86 400 particles

Sujathan et al. 2017 [32]	0.5 s	36 000 particles	108 000 particles	172 800 particles	345 600 particles
---------------------------	-------	------------------	-------------------	-------------------	-------------------

s/particle = Single measurement time per particle, Meas. time = Measurement time.

*Imhof et al. 2016 [30] reported times varying from 5 s to 500 s, the analyzable number of particles was calculated for both time spans.

In our assessment we chose 5 h, as it is the net measurement time available on a typical working day, leaving time for particle recognition and data evaluation. For unattended overnight runs, we assumed 15 h (5 p.m. to 8 a.m). Additionally, we calculated the number of analyzable particles for 1 and 2 days of uninterrupted measurement.

Comparing the numbers from *Table 5* with the calculated numbers of 10^6 particles on a typical filter from surface water even the very short measurement time of Sujathan et al. [32] would not allow measuring all particles within less than a few days. It is therefore obvious that some trade-off must be made. For a sample with 5% MP particles, $\sigma = 1.65$ (90%) and a tolerated margin of error $e = 10\%$ for the MP fraction 5 147 particles need to be analyzed which is possible in less than 5 h by using the approach of Ossmann et al. [35] or in 15 h with the approach of Schymanski et al. [36] or Imhof et al. [30]. For a sample with 0.5% MP, $\sigma = 1.65$ (90%) and a margin of error $e = 20\%$, 5 984 particles need to be analyzed. In this case the margin of error e is increased from 10% to 20%, making the same approaches feasible in the same time span. For MP fractions lower than 0.05% the number of particles that need to be analyzed is only reasonable if the tolerated margin of error e is expanded to 30%. In this case the method of Ossmann et al. [35] would need almost two days of total measurement time.

We emphasize again that the numbers calculated in pages 72 and following only account for an idealized measurement, which is of course not possible to fulfill and only mark the absolute minimum of required particles for a statistically meaningful

result. However, *Figure 10* shows that the required number of particles approaches a certain point above which additional measurements do not substantially improve the margin of error. This means that although the calculated required number of particles in pages 72 and following, will increase for cases with more realistic assumptions, the final value is limited nonetheless and will always be smaller than the total number of particles N . A more accurate estimation will require a more elaborate statistical model to account for systematic errors.

NUMBER OF PARTICLES OR FILTER AREA?

In the literature, the analyzed part is often expressed in percentage of the filter area [1, 71], which has two major drawbacks when comparing performance of RM analyses. The first drawback comes with the application of filters with different diameters, which makes the given numbers for filter area incomparable. The latter is of course only true if number densities on the two filters are the same. For differing number densities giving a percentage becomes even more confusing. It is therefore recommendable not to use percentages of filter areas or at least not use them in abstracts or prominently in conclusions.

The second major drawback is the indication of filter area itself. RM usually is used as a single particle analysis tool. Therefore, no real area is actually analyzed in the first place, but it is instead the particles – their number and nature – which matters. The same area may contain particles varying in orders of magnitude. To compare performance one needs the number of analyzed particles because this is the true analytical outcome of RM single particle analyses.

These two drawbacks led us to the conclusion not to use the indication of (the percentage of) analyzed filter area any further. The better approach is to estimate the overall number of particles on the filter N by image processing of the whole filter and therefore estimate the number of required particles n for a statistically meaningful

measurement. This in combination with an error margin e would give more insight into the quality of the measurement.

HOW TO CIRCUMVENT CONTAMINATIONS AND FLUORESCENCE INTERFERENCE

Contamination is a critical issue in MP research. We have compiled best practice approaches from various sources [9, 35, 36, 63] and our own experience to create general guidelines for contamination reduction (*Figure 11*). A special focus lies on the measurement of process blanks to quantify contamination from sample handling.

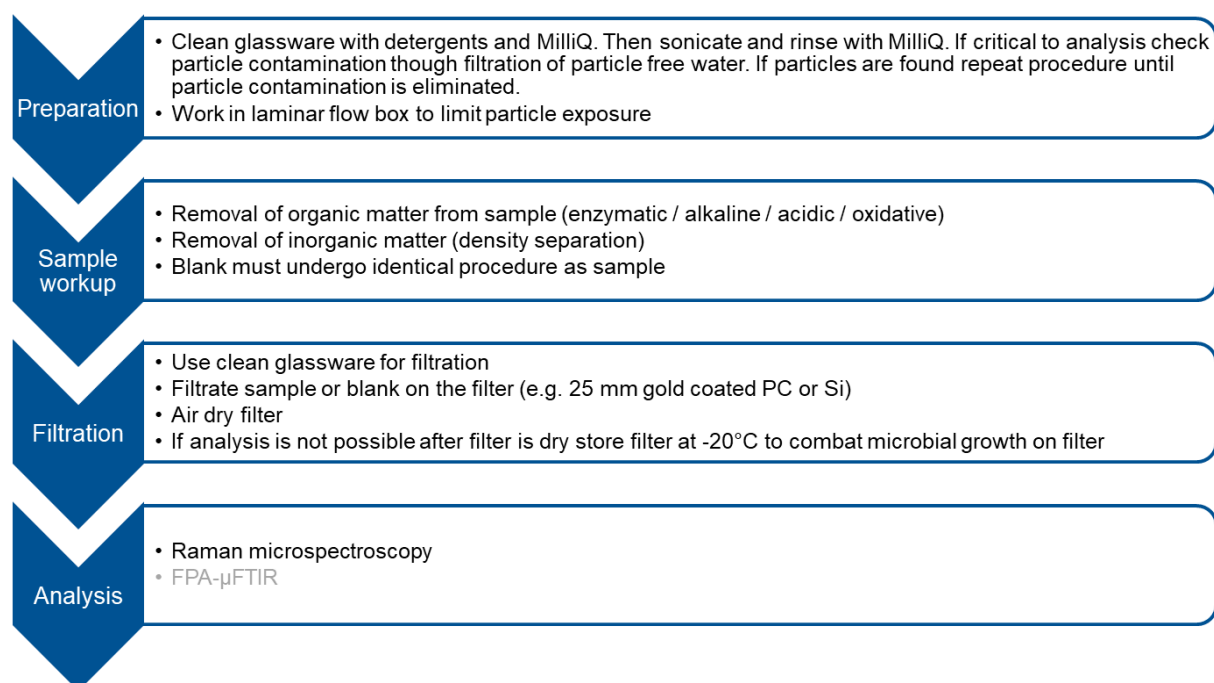


FIGURE 11: SCHEME FOR CONTAMINATION PREVENTION AND CONTROL.

Last but not least, the fluorescence background in Raman spectra of environmental samples needs to be addressed before the measurement, as the background signal interferes with the detectability of the particles. Inorganic materials (e.g., clay minerals) which are often found in sediment samples can exhibit strong fluorescence and therefore interfere with the detection of MP [66, 67]. These substances should be removed by density separation [72], centrifugation [30], or electrostatic charge [73]

before the measurement, if the MP to non-MP ratio is irrelevant to the desired analysis.

Another possible source for Raman background can be Mie scattering of stray light from the source or the Raman lines. The CCD camera collects this light and generates an additional Raman background. [74] Improving the effective morphology by e.g. compressing the sample to a pellet was shown to reduce this effect and hence the background. From our point of view this strategy is not applicable for the single particle RM analysis of (microplastic) particles on filter samples.

A significant fluorescence signal is derived from organic compounds that were adsorbed to the particle surface, therefore their removal is very important for the quality of the measurement. Currently there are enzymatic [75], alkaline [76], acidic and oxidative [76, 77] treatments that can be combined to free a particle from organic matter [1, 18].

A fluorescence background may also arise from pigments or additives, which should not be removed through pretreatment, as they give more insight into the composition and possible origin of MP particles. To overcome this issue, the fluorescence background still has to be reduced during the measurement. This can be achieved through laser- or photobleaching [78]. Laser induced bleaching of fluorophores may also be of interest in an automated analysis protocol as Ribeiro-Claro et al. pointed out. [11] An additional exposure time could be included prior to spectra recording thus improving the possibility to identify MP particles.

The most frequently mentioned possibility to circumvent fluorescence is detuning from fluorophores, which can be done by changing the laser source to longer wavelengths. [11] We discussed the use of different laser sources. From findings in the literature the most common laser with the longest wavelength applied for RM analysis of MP has 785 nm. However, this laser has several drawbacks discussed in this chapter, which is why it is not recommendable to detune the laser source to the technical extent, but rather use a maximum of e.g. 633 nm.

1.3. CONCLUSION

Even though RM has greatly advanced in recent years to become a useful tool for the detection of MP in the environment, there is still potential for significant further improvement and development of this technique. Especially the MP particles $<20\ \mu\text{m}$ and small total MP masses ($4\ \mu\text{g}$) provide a niche for RM. The most urgent challenges are to reach the theoretical size limit, to establish representative measurements, and to automate the procedure. Currently, the smallest MP particle found in a real sample (bottled mineral water) has a size of $1\ \mu\text{m}$. To find MP particles of this size, it is recommendable to use lasers with 532 nm or 633 nm and objectives with high NA and sufficiently high working distance, such as objectives with $50\times$ (or $100\times$) magnification. At this stage, RM methods can be accelerated by acquiring a spectral range of $200\ \text{cm}^{-1} - 3\ 200\ \text{cm}^{-1}$, using the least frames possible, e.g. a grating with 300 l/mm or 600 l/mm. Additionally, the highest non-destructive laser power with respect to acquisition time and accumulation should be applied. Possible settings can be found in section “*Findings from literature*”. As shown in this section the use of RM allows the distinction of polymer types and provides plausible MP abundances in the analyzed sample. To harness the full potential of RM, it is advisable to pay attention to, and to state the ratio of MP to non-MP particles, the overall number of particles, the size distribution and the shapes of the detected particles. Furthermore, the number of fluorescent and therefore not identifiable particles should also be given to catalyze an understanding of methodological challenges across laboratories. We also suggest the random sample of units selected without replacement (*srswor*) approach to calculate the minimum number of particles that need to be analyzed. In sections “*Challenge of representativeness*” and “*Trade-off between measurement time and representativeness*” we showed that the absolute minimum number of particles required can be reached with state of the art measurement techniques. However, the statistical model describes an idealized measurement system, and will need to be expanded to include procedural uncertainties to give a more realistic estimation of particles needed for a statistically meaningful analysis. Statistical certainty is especially relevant for MP as it is a topic of high public concern. Furthermore, the

automated particle detection will need to be advanced so that it is suited to all shapes of MP without miscalculations of particle sizes and size distributions. Automation and statistical sample size reduction results in an overall faster procedure and higher sample throughput, simultaneously providing high analytical accuracy. It has to be mentioned, that all these efforts are in vain if a contamination-free laboratory environment cannot be provided and controlled by procedural blanks. Therefore, to keep up with the increasing popularity of RM within MP research, major advances can be expected from bringing forward harmonized protocols of data acquisition and reporting, as well as intensified scientific exchange to avoid contaminations and interferences from fluorescence.

Declaration of interest: The authors have no competing interests to declare.

Acknowledgments: We like to thank Christoph Haisch, Christian Schwaferts, Dieter Fischer, Josef Brandt, Lisa Göpfert, Carolin Hartmann, Jonas Letica, Andreas Lichtenstern and Martin Jekel for helpful discussions. Furthermore, we would like to thank Allvac, Infiana and Huhtamaki for providing polymer samples. Funding by the German Federal Ministry of Education and Research (MiWa – Microplastic in the water cycle, 02WRS1378C) as well as funding by the Bayerische Forschungstiftung (MiPaq – Microparticles in the aquatic environment and in foodstuffs – are biodegradable polymers a conceivable solution to the “microplastic problem”?, AZ-1258-16) is gratefully acknowledged.

1.4 REFERENCES

1. Ivleva NP, Wiesheu AC, Niessner R. Microplastic in Aquatic Ecosystems. *Angew Chem Int Ed.* **2017**;56:1720-39.
2. Gregory MR. Plastic ‘Scrubbers’ in Hand Cleansers: A Further (and Minor) Source for Marine Pollution Identified. *Mar Pollut Bull.* **1996**;32(12):867-71.

3. Wheeler AF. Intentionally added microplastics in products. Environment Agency Austria; 2017.
4. Wagner S, Hüffer T, Klöckner P, Wehrhahn M, Hofmann T, Reemtsma T. Tire wear particles in the aquatic environment - A review on generation, analysis, occurrence, fate and effects. *Water Res.* **2018**;139:83-100.
5. Gewert B, Plassmann MM, MacLeod M. Pathways for Degradation of Plastic Polymers Floating in the Marine Environment. *Environ Sci Process Impact.* **2015**;17(9):1513-21.
6. Miller ME, Kroon FJ, Motti CA. Recovering microplastics from marine samples: A review of current practices. *Mar Pollut Bull.* **2017**;123(1-2):6-18.
7. Löder MGJ, Kuczera M, Mintenig S, Lorenz C, Gerdt G. Focal Plane Array Detector-Based Micro-Fourier-Transform Infrared Imaging for the Analysis of Microplastics in Environmental Samples. *Environ Chem.* **2015**;12(5):563-81.
8. Huppertsberg S, Knepper TP. Instrumental analysis of microplastics-benefits and challenges. *Anal Bioanal Chem.* **2018**.
9. Käßler A, Fischer D, Oberbeckmann S, Schernewski G, Labrenz M, Eichhorn KJ, et al. Analysis of environmental microplastics by vibrational microspectroscopy: FTIR, Raman or both? *Anal Bioanal Chem.* **2016**;408(29):8377-91.
10. Araujo CF, Nolasco MM, Ribeiro AMP, Ribeiro-Claro PJA. Identification of microplastics using Raman spectroscopy: Latest developments and future prospects. *Water Res.* **2018**;142:426-40.
11. Ribeiro-Claro PJA, Nolasco MM, Araujo CF. Characterization of Microplastics by Raman Spectroscopy. Characterization and Analysis of Microplastics. Comprehensive Analytical Chemistry. 752017.
12. Dümichen E, Eisentraut P, Bannick CG, Barthel AK, Senz R, Braun U. Fast identification of microplastics in complex environmental samples by a thermal degradation method. *Chemosphere.* **2017**;174:572-84.
13. Dümichen E, Braun U, Senz R, Fabian G, Sturm H. Assessment of a New Method for the Analysis of Decomposition Gases of Polymers by a Combining Thermogravimetric Solid-Phase Extraction and Thermal Desorption Gas Chromatography Mass Spectrometry. *J Chromatogr A.* **2014**;1354(0):117-28.
14. Dümichen E, Barthel AK, Braun U, Bannick CG, Brand K, Jekel M, et al. Analysis of Polyethylene Microplastics in Environmental Samples, Using a Thermal Decomposition Method. *Water Res.* **2015**;85:451-7.
15. Eisentraut P, Dümichen E, Ruhl AS, Jekel M, Albrecht M, Gehde M, et al. Two Birds with One Stone—Fast and Simultaneous Analysis of Microplastics: Microparticles Derived from Thermoplastics and Tire Wear. *Environmental Science & Technology Letters.* **2018**.
16. Fischer M, Scholz-Böttcher BM. Simultaneous Trace Identification and Quantification of Common Types of Microplastics in Environmental Samples by

Pyrolysis-Gas Chromatography-Mass Spectrometry. *Environ Sci Technol.* **2017**;51(9):5052-60.

17. Mintenig SM, Bäuerlein PS, Koelmans AA, Dekker SC, van Wezel AP. Closing the gap between small and smaller: towards a framework to analyse nano- and microplastics in aqueous environmental samples. *Environ Sci Nano.* **2018**;5(7):1640-9.
18. Renner G, Schmidt TC, Schram J. Analytical methodologies for monitoring micro(nano)plastics: Which are fit for purpose? *Current Opinion in Environmental Science & Health.* **2018**;1:55-61.
19. Kwon BG, Amamiya K, Sato H, Chung S-Y, Kodera Y, Kim S-K, et al. Monitoring of styrene oligomers as indicators of polystyrene plastic pollution in the North-West Pacific Ocean. *Chemosphere.* **2017**;180:500-5.
20. Simon M, van Alst N, Vollertsen J. Quantification of microplastic mass and removal rates at wastewater treatment plants applying Focal Plane Array (FPA)-based Fourier Transform Infrared (FT-IR) imaging. *Water Res.* **2018**;142:1-9.
21. Klein S, Worch E, Knepper TP. Occurrence and Spatial Distribution of Microplastics in River Shore Sediments of the Rhine-Main Area in Germany. *Environ Sci Technol.* **2015**;49(10):6070-6.
22. Zada L, Leslie HA, Vethaak AD, Tinnevelt GH, Jansen JJ, de Boer JF, et al. Fast microplastics identification with stimulated Raman scattering microscopy. *J Raman Spectrosc.* **2018**;49(7):1136-44.
23. Enders K, Lenz R, Stedmon CA, Nielsen TG. Abundance, Size and Polymer Composition of Marine Microplastics $\geq 10 \mu\text{m}$ in the Atlantic Ocean and Their Modelled Vertical Distribution. *Mar Pollut Bull.* **2015**;100(1):70-81.
24. Erni-Cassola G, Gibson MI, Thompson RC, Christie-Oleza JA. Lost, but Found with Nile Red: A Novel Method for Detecting and Quantifying Small Microplastics (1 mm to 20 μm) in Environmental Samples. *Environ Sci Technol.* **2017**;51(23):13641-8.
25. Frère L, Paul-Pont I, Moreau J, Soudant P, Lambert C, Huvet A, et al. A semi-automated Raman micro-spectroscopy method for morphological and chemical characterizations of microplastic litter. *Mar Pollut Bull.* **2016**;113(1):461-8.
26. Horton AA, Svendsen C, Williams RJ, Spurgeon DJ, Lahive E. Large microplastic particles in sediments of tributaries of the River Thames, UK - Abundance, sources and methods for effective quantification. *Mar Pollut Bull.* **2017**;114(1):218-26.
27. Di M, Wang J. Microplastics in surface waters and sediments of the Three Gorges Reservoir, China. *Sci Total Environ.* **2018**;616-617:1620-7.
28. Ballent A, Corcoran PL, Madden O, Helm PA, Longstaffe FJ. Sources and Sinks of Microplastics in Canadian Lake Ontario Nearshore, Tributary and Beach Sediments. *Mar Pollut Bull.* **2016**;110(1):383-95.

29. Clunies-Ross PJ, Smith GPS, Gordon KC, Gaw S. Synthetic shorelines in New Zealand? Quantification and characterisation of microplastic pollution on Canterbury's coastlines. *New Zeal J Mar Fresh.* **2016**;50(2):317-25.
30. Imhof HK, Laforsch C, Wiesheu AC, Schmid J, Anger PM, Niessner R, et al. Pigments and Plastic in Limnetic Ecosystems: A Qualitative and Quantitative Study on Microparticles of Different Size Classes. *Water Res.* **2016**;98:64-74.
31. Imhof HK, Ivleva NP, Schmid J, Niessner R, Laforsch C. Contamination of Beach Sediments of a Subalpine Lake with Microplastic Particles. *Curr Biol.* **2013**;23(19):R867-8.
32. Sujathan S, Kniggendorf AK, Kumar A, Roth B, Rosenwinkel KH, Nogueira R. Heat and Bleach: A Cost-Efficient Method for Extracting Microplastics from Return Activated Sludge. *Arch Environ Contam Toxicol.* **2017**;73(4):641-8.
33. Lots FAE, Behrens P, Vijver MG, Horton AA, Bosker T. A large-scale investigation of microplastic contamination: Abundance and characteristics of microplastics in European beach sediment. *Mar Pollut Bull.* **2017**;123(1-2):219-26.
34. Van Cauwenberghe L, Vanreusel A, Mees J, Janssen CR. Microplastic Pollution in Deep-Sea Sediments. *Environ Pollut.* **2013**;182:495-9.
35. Ossmann BE, Sarau G, Holtmannspotter H, Pischetsrieder M, Christiansen SH, Dicke W. Small-sized microplastics and pigmented particles in bottled mineral water. *Water Res.* **2018**;141:307-16.
36. Schymanski D, Goldbeck C, Humpf HU, Fürst P. Analysis of microplastics in water by micro-Raman spectroscopy: Release of plastic particles from different packaging into mineral water. *Water Res.* **2018**;129:154-62.
37. Karami A, Golieskardi A, Keong Choo C, Larat V, Galloway TS, Salamatinia B. The presence of microplastics in commercial salts from different countries. *Sci Rep.* **2017**;7(46173):1-9.
38. Gündogdu S. Contamination of table salts from Turkey with microplastics. *Food Addit Contam Part A-Chem.* **2018**;35(5):1006-14.
39. PlasticsEurope. <Plastics_the_facts_2017_FINAL_for_website_one_page.pdf>. **2017**.
40. Hale RC. Analytical challenges associated with the determination of microplastics in the environment. *Anal Methods.* **2017**;9(9):1326-7.
41. Waring RH, Harris RM, Mitchell SC. Plastic contamination of the food chain: A threat to human health? *Maturitas.* **2018**;115:64-8.
42. Turrell G, Corset J. Raman microscopy: developments and applications. London: Elsevier Academic Press; 1996.
43. Schrader B. Infrared and Raman Spectroscopy - Methods and Applications. 1 ed. Schrader B, editor. Weinheim, Germany: VCH Verlagsgesellschaft mbH; 1995.
44. Salzer R, Siesler HW. Infrared and Raman Spectroscopic Imaging. 2 ed. Weinheim, Germany: WILEY-VCH Verlag GmbH co. KGaA; 2014.

45. Lee E. Raman Imaging - Techniques and Applications. 1 ed. Berlin, Heidelberg: Springer; 2012.
46. Opilik L, Schmid T, Zenobi R. Modern Raman imaging: vibrational spectroscopy on the micrometer and nanometer scales. *Annu Rev Anal Chem (Palo Alto Calif)*. **2013**;6:379-98.
47. Stewart S, Priore RJ, Nelson MP, Treado PJ. Raman imaging. *Annu Rev Anal Chem (Palo Alto Calif)*. **2012**;5:337-60.
48. Overall NJ. Confocal Raman microscopy: common errors and artefacts. *Analyst*. **2010**;135(10):2512-22.
49. Yonkos LT, Friedel EA, Perez-Reyes AC, Ghosal S, Arthur CD. Microplastics in Four Estuarine Rivers in the Chesapeake Bay, U.S.A. *Environ Sci Technol*. **2014**;48(24):14195-202.
50. Ghosal S, Chen M, Wagner J, Wang Z-M, Wall S. Molecular identification of polymers and anthropogenic particles extracted from oceanic water and fish stomach – A Raman micro-spectroscopy study. *Environ Pollut*. **2018**;233:1113-24.
51. Smith E, Dent G. Modern Raman spectroscopy: a practical approach. 1 ed. Chichester, United Kingdom: John Wiley & Sons; 2013.
52. Bower DI, Maddams WF. The characterization of polymers. In: Davis EA, Ward IM, editors. The vibrational spectroscopy of polymers. 1 ed. Cambridge, United Kingdom: Cambridge University Press; 1989. p. 162-226.
53. Vandenabeele P. Raman Instrumentation. Practical Raman Spectroscopy - An Introduction. 1 ed. Chichester, United Kingdom: John Wiley & Sons, Ltd; 2013.
54. Green DS, Boots B, Sigwart J, Jiang S, Rocha C. Effects of Conventional and Biodegradable Microplastics on a Marine Ecosystem Engineer (*Arenicola Marina*) and Sediment Nutrient Cycling. *Environ Pollut*. **2016**;208(Pt B):426-34.
55. Horvarth JS. Expanded Polystyrene (EPS) Geofoam: An Introduction to Material Behavior. *Geotext Geomembranes*. **1994**;13(4):263-80.
56. Andradý AL, Neal MA. Applications and Societal Benefits of Plastics. *Philos T Roy Soc B*. **2009**;364(1526):1977-84.
57. Lambert S, Wagner M. Formation of microscopic particles during the degradation of different polymers. *Chemosphere*. **2016**;161:510-7.
58. Kole PJ, Lohr AJ, Van Belleghem F, Ragas AMJ. Wear and Tear of Tyres: A Stealthy Source of Microplastics in the Environment. *Int J Environ Res Public Health*. **2017**;14(10).
59. Hartmann NB, Verschoor A, Hüffer T, Daugaard AE, Thompson R, Rist S, et al. Towards definitions and categorisation of environmental plastic debris. **2018**.
60. Hong SH, Shim WJ, Hong L. Methods of analysing chemicals associated with microplastics: a review. *Anal Methods*. **2017**;9(9):1361-8.

61. Woodall LC, Gwinnett C, Packer M, Thompson RC, Robinson LF, Paterson GL. Using a Forensic Science Approach to Minimize Environmental Contamination and to Identify Microfibres in Marine Sediments. *Mar Pollut Bull.* **2015**;95(1):40-6.
62. Foekema EM, De Gruijter C, Mergia MT, van Franeker JA, Murk AJ, Koelmans AA. Plastic in north sea fish. *Environ Sci Technol.* **2013**;47(15):8818-24.
63. Braun U, Jekel M, Gerdts G, Ivleva NP, Reiber J. Mikroplastik-Analytik: Probenahme, Probenaufbereitung und Detektion. In: BMBF, editor. 2018.
64. Hidalgo-Ruz V, Gutow L, Thompson RC, Thiel M. Microplastics in the Marine Environment: A Review of the Methods Used for Identification and Quantification. *Environ Sci Technol.* **2012**;46(6):3060-75.
65. Wagner M, Scherer C, Alvarez-Munoz D, Brennholt N, Bourrain X, Buchinger S, et al. Microplastics in Freshwater Ecosystems: What We Know and What We Need to Know. *Environ Sci Eur.* **2014**;26(1):1-9.
66. Sobanska S, Hwang H, Choel M, Jung HJ, Eom HJ, Kim H, et al. Investigation of the chemical mixing state of individual Asian dust particles by the combined use of electron probe X-ray microanalysis and Raman microspectrometry. *Anal Chem.* **2012**;84(7):3145-54.
67. Iwata A, Matsuki A. Characterization of individual ice residual particles by the single droplet freezing method: a case study in the Asian dust outflow region. *Atmos Chem Phys.* **2018**;18(3):1785-804.
68. Myers JC. Normal Distribution Function. *Geostatistical Error Management* 1997. p. 134-51.
69. Valliant R, Dever JA, Kreuter F. Sample Design and Sample Size for Single-Stage Surveys. *Practical Tools for Designing and Weighting Survey Samples.* 1 ed. New York Heidelberg Dordrecht London: Springer; 2013. p. 37-9.
70. Kauermann G, Küchenhoff H. *Stichproben - Methoden und praktische Umsetzung mit R.* Berlin, Heidelberg: Springer; 2011.
71. Rocha-Santos T, Duarte AC. A Critical Overview of the Analytical Approaches to the Occurrence, the Fate and the Behavior of Microplastics in the Environment. *Trac-Trend Anal Chem.* **2015**;65:47-53.
72. Imhof HK, Schmid J, Niessner R, Ivleva NP, Laforsch C. A Novel, Highly Efficient Method for the Separation and Quantification of Plastic Particles in Sediments of Aquatic Environments. *Limnol Oceanogr-Meth.* **2012**;10:524-37.
73. Felsing S, Kochleus C, Buchinger S, Brennholt N, Stock F, Reifferscheid G. A new approach in separating microplastics from environmental samples based on their electrostatic behavior. *Environ Pollut.* **2017**;234:20-8.
74. Bonnier F, Mehmood A, Knief P, Meade AD, Hornebeck W, Lambkin H, et al. In vitro analysis of immersed human tissues by Raman microspectroscopy. *Journal of Raman Spectroscopy.* **2011**;42(5):888-96.

75. Loder MGJ, Imhof HK, Ladehoff M, Loschel LA, Lorenz C, Mintenig S, et al. Enzymatic Purification of Microplastics in Environmental Samples. *Environ Sci Technol.* **2017**;51(24):14283-92.
76. Hurley RR, Lusher AL, Olsen M, Nizzetto L. Validation of a Method for Extracting Microplastics from Complex, Organic-Rich, Environmental Matrices. *Environ Sci Technol.* **2018**;52(13):7409-17.
77. Tagg AS, Harrison JP, Ju-Nam Y, Sapp M, Bradley EL, Sinclair CJ, et al. Fenton's reagent for the rapid and efficient isolation of microplastics from wastewater. *Chem Commun.* **2016**;53(2):372-5.
78. Zięba-Palus J, Michalska A. Photobleaching as a useful technique in reducing of fluorescence in Raman spectra of blue automobile paint samples. *Vib Spectrosc.* **2014**;74:6-12.

DECLARATION OF SCIENTIFIC CONTRIBUTION AND SUMMARY FOR SIMPLE GENERATION OF SUSPENSIBLE SECONDARY MICROPLASTIC REFERENCE PARTICLES VIA ULTRASOUND TREATMENT.

Elisabeth von der Esch, Maria Lanzinger, Alexander J. Kohles, Christian Schwaferts,
Jana Weisser, Thomas Hofmann, Karl Glas, Martin Elsner and Natalia P. Ivleva,

Frontiers in Chemistry **2020**, 8:169. DOI: 10.3389/fchem.2020.00169

EE brought forward the idea that it might be possible to use ultrasonification of solid polymers to produce microplastic reference materials based on the rationale that several publications warn about the possibility of sample alteration due to the use of ultrasonification during sample preparation. EE, ME and NI designed the experiments to systematically investigate the potential of ultrasonification, with the goal to deliver a reproducible procedure to generate reference materials. EE implemented the idea for the production of secondary MP and carried out the fragmentation, as well as the analysis of the products using *TUM-ParticleTyper*, Raman microspectroscopy, ATR-FTIR and UV-VIS experiments and validated the procedures. Reproducibility was tested by ML, under the supervision of EE, ME and NI by replicating the fragmentation and *TUM-ParticleTyper* Raman microspectroscopy analysis. The *TUM-ParticleTyper* software was developed, optimized and validated by AK, EE and NI. The SEM and EDX analyses were carried out by CS. JW, KG and TH investigated ageing effects on the single particle level with μ -FTIR spectroscopy. All of these experiments and analyses culminated in a simple procedure to generate suspensible secondary reference particles via ultrasound treatment, enabling any laboratory with an ultrasonic bath to produce reference materials for method development. All authors discussed the results and contributed to the final manuscript.

CHAPTER 2:

SIMPLE GENERATION OF SUSPENSIBLE SECONDARY MICROPLASTIC REFERENCE PARTICLES VIA ULTRASOUND TREATMENT

Elisabeth von der Esch^a, Maria Lanzinger^a, Alexander J. Kohles^a, Christian Schwaferts^a,
Jana Weisser^b, Thomas Hofmann^b, Karl Glas^b, Martin Elsner^a, Natalia P. Ivleva^{a*}

Front. Chem. 8:169.doi: 10.3389/fchem.2020.00169

^aInstitute of Hydrochemistry, Chair of Analytical Chemistry and Water Chemistry,
Technical University of Munich, Munich, Germany

^bChair of Food Chemistry and Molecular Sensory Science, Technical University of
Munich, Freising, Germany

*** Correspondence:**

Natalia P. Ivleva

natalia.ivleva@tum.de

Copyright © 2020 von der Esch, Lanzinger, Kohles, Schwaferts, Weisser, Hofmann, Glas, Elsner and Ivleva. This is an open-access article distributed under the terms of the Creative Commons Attribution License (CC BY). The use, distribution or reproduction in other forums is permitted, provided the original author(s) and the copyright owner(s) are credited and that the original publication in this journal is cited, in accordance with accepted academic practice. No use, distribution or reproduction is permitted which does not comply with these terms.

ABSTRACT

In the environment the weathering of plastic debris is one of the main sources of secondary microplastic (MP). It is distinct from primary MP, as it is not intentionally engineered, and presents a highly heterogeneous analyte composed of plastic fragments in the size range of 1 μm – 1 mm. To detect secondary MP, methods must be developed with appropriate reference materials. These should share the characteristics of environmental MP which are a broad size range, multitude of shapes (fragments, spheres, films, fibers), suspensibility in water, and modified particle surfaces through ageing (additional OH, C=O, and COOH). To produce such a material, we bring forward a rapid sonication-based fragmentation method for polystyrene (PS), polyethylene terephthalate (PET), and polylactic acid (PLA), which yields up to $10^5/15$ mL dispersible, high purity MP particles in aqueous media. To satisfy the claim of a reference material, the key properties – composition and size distribution to ensure the homogeneity of the samples, as well as shape, suspensibility, and ageing – were analyzed in replicates ($N = 3$) to ensure a robust production procedure. The procedure yields fragments in the range of 100 nm – 1 mm ($< 20 \mu\text{m}$, $54.5\% \pm 11.3\%$ of all particles). Fragments in the size range 10 μm – 1 mm were quantitatively characterized via Raman microspectroscopy (particles = 500 – 1000) and reflectance micro Fourier transform infrared analysis (particles = 10). Smaller particles 100 nm – 20 μm were qualitatively characterized by scanning electron microscopy (SEM). The optical microscopy and SEM analysis showed that fragments are the predominant shape for all polymers, but fibers are also present. Furthermore, the suspensibility and sedimentation in pure MilliQ water was investigated using ultraviolet–visible spectroscopy and revealed that the produced fragments sediment according to their density and that the attachment to glass is avoided. Finally, a comparison of the infrared spectra from the fragments produced through sonication and naturally aged MP shows the addition of polar groups to the surface of the particles in the OH, C=O, and COOH region, making these particles suitable reference materials for secondary MP.

2.1 INTRODUCTION

The characterization of microplastics (MP) – i.e. of small synthetic polymer particles – is a four-dimensional challenge, consisting of (I) the broad size distribution of particles (and fibers) from 1 μm to 1 mm, (II) the variety of polymer types and natural particles, (III) the state of ageing, and (IV) the variety of forms (spheres, films, fragments, fibers) [1]. All four dimensions should ideally be detected and quantified simultaneously in one measurement [2-4]. The need to develop suitable analytical tools is accompanied by the need for effective methods to produce reference particles – reference materials that should be as similar as possible to the MP particles found in environmental and food samples.

Plastic undergoes ageing processes in the environment that cause fragmentation into secondary MP [5]. In contrast to primary MP, secondary MP is not produced in a targeted manner but originates from ageing and fragmentation of polymer materials and thus results in a heterogeneous mixture of particles. If Raman or infrared (IR) spectroscopy are used for analysis, the vibrational spectra of the particles may not match conventional databases since they may contain hydroxy, carbonyl, and carboxy groups in addition to the pure polymer spectrum, as an effect of environmental ageing [5-7]. Furthermore, environmental MP is suspended in bodies of water, such as fresh [8-13] and marine waters [14-17]. In the nanometer range the suspension of reference particles can be achieved by the addition of surfactants [18] or can result from the particle generation procedure, as shown by Magrì et al. 2018 for their nano polyethylene terephthalate (PET) generated by laser ablation [19] or by Pessoni et al. 2019 for their nano polystyrene (PS) particles from soap-free emulsion polymerization. These effects are much harder to achieve for MP reference particles (1 μm – 1 mm). The current state of the art to generate particles in this size regime is cryo milling [20]. These particles are not easily suspended and the difficulty arises that many sample preparation steps, such as filtration or fractionation require the MP reference particles to be suspended in order to accurately mimic environmental MP behavior [21], which renders them unsuitable as true reference materials for the

evaluation of these steps. Another difficulty while preparing MP reference materials is the multitude of shapes that needs to be covered. This is of special concern if the particles are used for the development of image-based methods. In order to develop appropriate morphological characterization tools, particles for all shapes (fragments, spheres, films, fibers) need to be available preferably in the same sample, as a genuine sample would also display all morphologies at once. On the other hand there are experiments, such as toxicological investigations that require tailored methods to achieve specific morphologies, such as Cole 2016 for the production of fibers [22] or Balakrishnan et al. 2019 for spheres [18]. To summarize, MP and nanoplastic reference materials each have their own challenges, but both are desperately needed for further method development. The described shortcomings of current MP reference particles can be overcome by using sonication of polymers in alkaline suspensions for *in situ* fragmentation. Ultrasonic treatment of various polymers has already been used to broaden the size distribution of polymer powders in water [23, 24]. Furthermore, Balakrishnan et al. 2019 used a combination of dissolution of polyethylene (PE) in toluene via sonication with subsequent emulsification in water to create PE spheres in the sub μ m range (200 nm – 800 nm) [18]. They suggest that the same methodology could potentially be used on other polymers, as long as they can be dissolved in a volatile solvent. Davranche et al. 2019 fragmented environmental MP in water through sonication to generate nanoplastic [24]. In this paper we propose, for the first time, the use of ultrasonication in alkaline conditions for the simple and controlled production of chemically aged MP particles from single use plastic items. To this end, we characterized morphological features such as size distribution, shape, and surface properties, as well as chemical properties such as purity and ageing effects as well as the suspensibility in water. Therefore, by characterizing the produced fragments in all important features of MP, including homogeneity and stability, we aimed to establish them as suitable reference materials. The overarching goal is to deliver an easy and reproducible protocol for the production of reference materials, as defined by NIST [25], from the solid target polymer of the analysis. The described procedure was validated for polylactic acid (PLA), PET, and PS. The underlying mechanism was researched to explain the

different degrees of reproducibility (PLA > PET > PS) of the method with respect to the polymer and to pinpoint possible pitfalls. This is important as the applied ultrasonic field plays a substantial role in the formation of the particles. This was one of the major challenges while performing reproducibility experiments, which required many fragmentation experiments and could only be overcome by testing the ultrasonic field (see *Supporting Information S1*) before starting the procedure. The final reproduction study was carried out by two different operators to ensure that the protocol is complete and comprehensible. Furthermore, the presented procedure was applied in proof of principle experiments to PE, polypropylene (PP), and polyvinylchloride (PVC) as well as polyamide (PA) to investigate if the method is generally applicable (see *S1*). Essentially any polymer that does not form a gel (like polyamides) in alkaline solutions can be fragmented through alkaline sonication but the hydrolyzability and mechanical properties of the polymer influence size and number of the fragments.

2.2. MATERIAL AND METHODS

EQUIPMENT PREPARATION AND AVOIDANCE OF CONTAMINATION

A 1 M KOH stock solution (22.2 g KOH, Chemsolute Batch No 25.101811 dissolved in 400 mL MilliQ) was used throughout the experiments to prepare the sonication medium. All equipment was cleaned multiple times with water, isopropanol, and MilliQ water to minimize contamination of the samples. The reaction vessels were additionally sonicated in alkaline solution (1 M KOH ultrasonic bath, 15 min). Before sonication, the polymer squares were submerged in KOH (1 M, 3.75 mL, 30 s) to clear any attached organic matter. The solution was then diluted with MilliQ for the fragmentation. After sonication the samples were handled and filtered in a laminar flow box (EN 1822, Spetec GmbH).

FRAGMENTATION THROUGH SONICATION

The idea to use sonication as the fragmentation method arose from many accounts that suggested that sonication might lead to MP fragmentation, and therefore should be avoided for sample preparation. Very recently nanometer-sized fragments from sonication (5 days, MilliQ) were employed to test the binding abilities of lead to nanoplastic [24]. As the goal of our research was to provide aged and dispersible particles, polymer squares (1 cm², approx. 30 mg) were sonicated (15 h at 35 kHz) under hydrolytic conditions (15 mL, 0.25 M KOH) to induce the formation of polar groups. Furthermore, the effect of the original fragment size on the produced size distribution was analyzed in a second experiment.

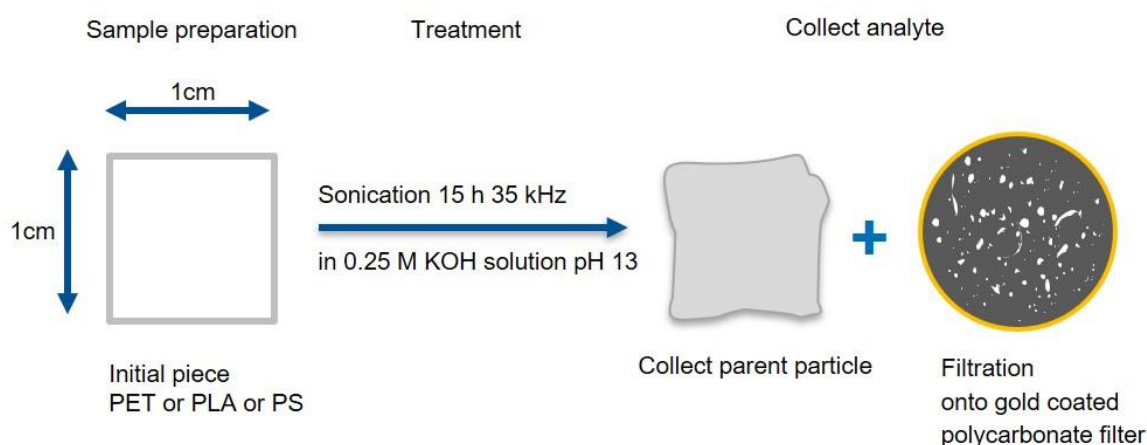


FIGURE 12: FRAGMENTATION AND WORK UP SCHEME A. PRODUCTION OF SMALL FRAGMENTS AND DEPOSITION ON A GOLD-COATED POLYCARBONATE FILTER AS WELL AS RECOVERY OF THE PARENT PARTICLE.

Fragmentation method A (*Figure 12*): Polymer squares (1 cm², approx. 30 mg, PLA and PS from Activia yogurt cups and PET from a “Ja” water bottle) were sonicated (15 h at 35 kHz) in hydrolytic conditions (15 mL, 0.25 M KOH). The parent particle was collected and the leftover suspension was filtrated (in a laminar flow box onto a 25 mm diameter, 0.8 μm pore size, gold-coated polycarbonate filter, APC). To ensure that the produced MP was quantitatively transferred from the reaction vessel to the filter, all glass parts, that were in contact with the particle suspension, were rinsed

with MilliQ water (about 30 mL) until no particles were visible under UV light ($\lambda = 285$ nm). Both the parent particle (before and after fragmentation) and the fragments on the filter were analyzed via Raman microspectroscopy and IR spectroscopy (detailed procedure in section “Characterization of the produced MP particles”). For each polymer the production and the subsequent measurements were repeated three times by two different operators ($N = 3$). A smaller proof of principle study (only one replicate) was applied to PVC (from wide neck containers Rotilabo), PE (pellets from Huhtamaki), PP (yogurt cup “Penny Vanilla desert”), and PA (foil from Huhtamaki) to check whether the fragmentation method is also transferrable to other polymers. PVC was chosen, as it contains chlorine, which can be detected by scanning electron microscopy coupled with energy dispersive X-ray spectroscopy (SEM/EDX) analysis to prove that the particles found in the nanometer range are indeed plastic particles produced by our method.

Fragmentation and work up method B (*Figure 13*): To generate particles in the entire MP size range (1 μm – 1 mm) randomly cut polymer pieces (approx. 30 mg) were sonicated (15 h at 35 kHz) in hydrolytic conditions (15 mL, 0.25 M KOH). Particles larger than the pipette opening (~ 1 mm) were collected for Raman and FTIR analysis, while the smaller fragments were collected from the alkaline suspension through centrifugation (3000 rpm, 20 °C, 30 min, Eppendorf 5804 R), removal of the supernatant and resuspension in MilliQ (pH = 7 was reached after 2 cycles).

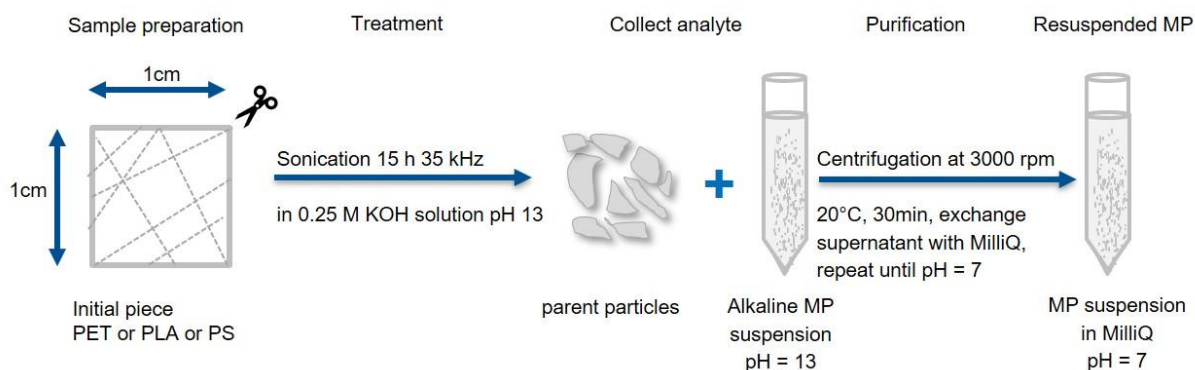


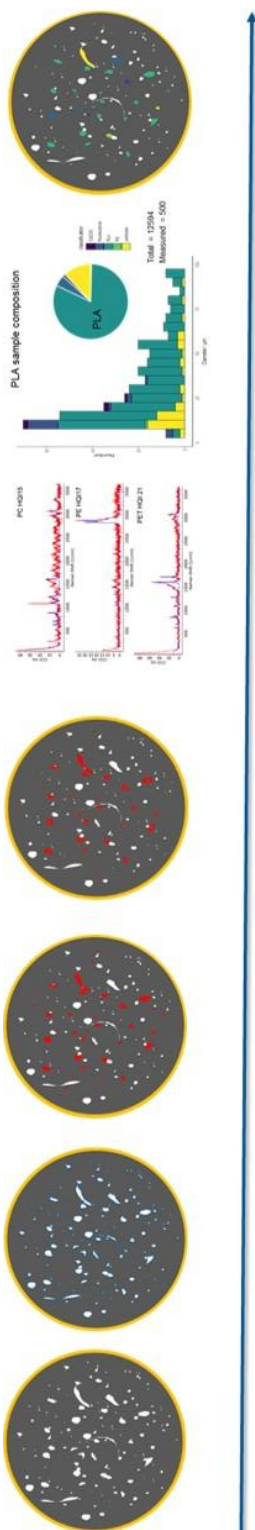
FIGURE 13: FRAGMENTATION AND WORK UP SCHEME B. PRODUCTION OF LARGE MP FRAGMENTS WITH RECOVERY OF THE PARENT PARTICLES. PARTICLES SMALLER THAN 1 MM ARE WASHED AND CONCENTRATED IN MILLIQ.

CHARACTERIZATION OF THE PRODUCED MP PARTICLES

The original polymer pieces were removed from the suspension and microscopically analyzed ($5\times$ and $20\times$ magnification with z stacking $30\ \mu\text{m}$, Raman microscope *alpha 300*, WITec, Germany).

The fragments were collected on the filter and analyzed with a Raman microscope *alpha 300* (using *TrueSurface*, *custom image stitching*, *z stacking*, *TruePower*, *PointViewer* and *TrueMatch*, WITec, Germany) applying the following steps. Firstly, the planarity of the filter was checked (optional *TrueSurface* measurement Δz should be $\leq 30\ \mu\text{m}$) and an image of the filter was acquired ($20\times$ objective, 3 [db] Gain, 3% top illumination, 1/10 fps, $16\ 000\ \mu\text{m} \times 16\ 000\ \mu\text{m}$, $8\ 000\ \text{pixel} \times 8\ 000\ \text{pixel}$, $30\ \mu\text{m}$ z-stacking, by custom image stitching). The particles were localized (calculation of centers for Raman measurement) and morphologically analyzed (Feret's diameter min and max, area, ratio of Feret's diameter and percentage of area covered by particle in Feret's box for shape analysis) via image processing using *TUM-ParticleTyper* (Gaussian window-based detection, E. von der Esch and A. J. Kohles et al., submitted [26], *preview in SI Figure 1*). Subsequent Raman microspectroscopy ($3\ \text{mW}$ using *TruePower*, $532\ \text{nm}$ laser, 2.5 – 20 s measurement time, $20\times$ objective,

inserting the determined coordinates by *TUM-ParticleTyper* via *PointViewer*) revealed the identity (database search with *TrueMatch*, for validation see *SI Figure 2*) of $n \sim 500$ randomly selected particles per filter as described by Anger and von der Esch et al. [2]. Combining these results, an overall compound distribution (desired MP vs. contamination) and a compound-correlated size distribution could be determined. The error of measurement was calculated through the number of detected particles, the portion of measured particles and the percentage of MP found. For a summary of the procedure and measurement effort, see *Table 6*. Furthermore, the morphological data enabled the discrimination of particle shapes to determine predominant shapes and sizes of the examined polymers. Fibers were identified by *TUM-ParticleTyper* if one of two conditions was fulfilled: 1) dividing the product of min and max Feret's diameter by the area yields a ratio larger than four or 2) max Feret's diameter divided by min Feret's diameter is larger than two and the overall area of the particle is larger than 400 pixels. Spheres are characterized by a Feret's diameter min/max ratio close to one (0.9 – 1). These conditions were empirically established by analyzing images and varying the selection thresholds. The reproducibility (homogeneity) of the fragmentation was accessed by comparing the replicates ($N = 3$) for each polymer according to composition, mean particle size, size distribution, and particle to fiber ratio. Fibers were further characterized by manual Raman measurements and the stability of the sample was checked after storage (particles deposited on the filter stored for 9 months in glass Petri dishes).



Steps	Take Image of Filter	Localize all Particles	Select Particles	Raman Measurement	Chemical Characterization	Data Visualisation	Overall Performance metrics
Tool	Image stitching + z stack	TUM-Particle Typer	TUM-Particle Typer	TruePower + PointViewer	TrueMatch	R-Script	-
Parameters	16 000 × 16 000 µm, 8000 × 8000 pixel, z stacking over 30 µm upwards starting from filter surface, Gain 3, Illumination 3%, exposure time 1/10, 20× magnification Darkfield mode	min pixel 2, resolution 0.5 Detection in Raman mode	Random sampling of 500 particles per filter	532 nm laser, 3 mW, 2.5 – 20 s, 600 L/mm grating, 20x magnification,	Correlation coefficient 2 components, HQI > 15, 600 – 1800 cm ⁻¹ Export as txt	Load TrueMatch and TUM-Particle Typer result sheet and run script	Localization, quantification, morphological and chemical characterization of Raman active particles 10 µm – 5 mm
Time	1 h	5 min – 20 min depending on particle loading	30 sec	~ 4 h	20 min	20 min	~ 6 h
Operator effort	20 min	2 min	-	1 h	20 min	5 min	~ 2 h
Goal	The entire filter surface should fit on the image	Particles and fibers of all sizes should be detected, verify by visual inspection	Minimize the amount of particles that need to be measured with reasonable margin of error	Minimize the time for a single measurement, but monitor the quality of spectra to get the best results in a reasonable time frame	Identification should be unambiguous, to ensure this, check low hitquality results 20 – 15 HQI	Merge morphological and chemical identification data to give a complete overview of the sample composition	Fast and easy detection of particulate matter on filter. Validation needs to be made for each type of sample individually

Table 6: Measurement scheme for the Raman microspectroscopic analysis of microplastic, featuring the tools, exact measurement parameters, time, operator effort and goal for each step.

The current detection limit of our automated Raman setup used for this study is limited to particles larger than 5 μm (based on the smallest particles that yield identifiable spectra *TUM-ParticleTyper* with a 20 \times magnification objective, N.A. = 0.4). Using this setup, a quantitative analysis can be performed for particles larger than 10 μm [26]. Particles in the low μm range and sub μm range were alternatively characterized by manual Raman analysis (100 \times magnification objective, N.A. = 0.9) and SEM. This technique also allowed a special focus on the surface morphology of the particles. The SEM images were recorded on a *Sigma 300 VP* (Carl Zeiss AG, Germany) using a HD secondary electron detector. For sample preparation, the suspensions (10 μL) were dried on silicon wafer slices and could be imaged without the need for coating with metals due to the use of a FE Schottky cathode and low acceleration voltages (2 – 3 kV). EDX analysis was performed on PVC to ensure that the particles visible in the SEM images are in fact nanoplastics (*Quantax XFlash 6/60* detector, Bruker Nano GmbH, Germany). All analyses that can be performed on particles deposited on filters such as automated Raman microspectroscopy and μ -FTIR were conducted on the same particles from one sample. SEM/EDX and manual Raman microspectroscopy for particles smaller than 5 μm requires an extremely smooth surface, therefore these were conducted on subsamples from the fragmentation, so that the same sample can be used but not the exact same particles.

To characterize the suspensibility of the produced particles (in 2.5 mL MilliQ) by UV-VIS (*Specord 250*, Analytik Jena, Germany) time series measurements were conducted (3 replicates for each polymer, 25 measurements in 25 min, $\lambda = 250 - 800$ nm, $\Delta\lambda = 1$ nm, slit 4 nm, speed 50.0 nm/s). A good signal could only be achieved by enriching the particle number in an aqueous suspension and then monitoring the transmission over time; therefore, fragmentation and work up method B was used.

The MP produced through fragmentation methods A and B by sonication should be similar, both chemically as well as morphologically to the MP present in the environment. To demonstrate this, attenuated total reflection Fourier transform infrared spectroscopy measurements (ATR-FTIR, *Nicolet 6700 FTIR*, 4 cm^{-1} spectral resolution) were conducted on the original polymer pieces before fragmentation

(themed reference / pristine in subsequent sections) and on fragments larger than 1 mm. Particles < 1 mm were measured by μ -FTIR spectroscopy on *Agilent Cary 620* coupled to *Agilent Cary 670*, equipped with a 128×128 pixel focal plane array (FPA) detector. Measurements were performed in reflectance mode, using a $15\times$ objective. Of each sample, 30 scans were recorded at a spectral resolution of 8 cm^{-1} within a spectral range from 3700 to 810 cm^{-1} .

2.3 RESULTS AND DISCUSSION

MORPHOLOGICAL CHANGES IN POLYMER SURFACE DUE TO ULTRASONIC DEGRADATION

The ultrasonic treatment of solid polymers leads to a changed morphology at the polymer surface, which is examined in the parent particles before and after sonication through optical microscopy (*SI, Figure 3a-c*). For PLA, the sonication in MilliQ increases the cloudiness, making the original plastic square opaque. Although the edges of the square remain intact, it shrinks during the sonication process (1 cm^2 to $0.57 \pm 0.07 \text{ cm}^2$). If sonication with KOH (0.25 M, pH = 13) is applied, the original square becomes cloudy and the edges are visibly eroded. Furthermore, holes in the surface appear. Changes in surface appearance that are observed for PET and PS are similar to PLA, but less intense (*SI, Figure 4*). Only PLA shows a slight increase in cloudiness after sonication in KOH, while PET and PS do not turn opaque. Instead they show less particles attached to the surface and smoothed edges after treatment (*SI, Figure 4*). Comparing the morphological changes induced by the fragmentation suggest different mechanisms. PLA as an ester might be strongly hydrolyzed, as well as mechanically worn, while PS and PET might be predominantly, but not exclusively mechanically fragmented, as subsequent ATR-IR analysis revealed through the appearance of OH, C=O, and COOH groups to all polymers (Section "Comparison of Reference Particles with Environmental Microplastic by FTIR Spectroscopy"). To

visualize the surface modification and to assess the shapes of the resulting particles, SEM was applied. Particle identity has been confirmed by SEM-EDX and Raman microspectroscopy (*SI, Figure 5*). All polymers produce fragments, in irregular and spherical shapes as well as films and fibers. Furthermore, the surface is visibly eroded. As with the parent particles, PLA fragments seem to be most affected by the sonication, producing extremely swollen and porous particles. PS and PET show eroded surfaces as well. The smallest particles that have been visualized for all polymers are around 100 nm (*Figure 14*).

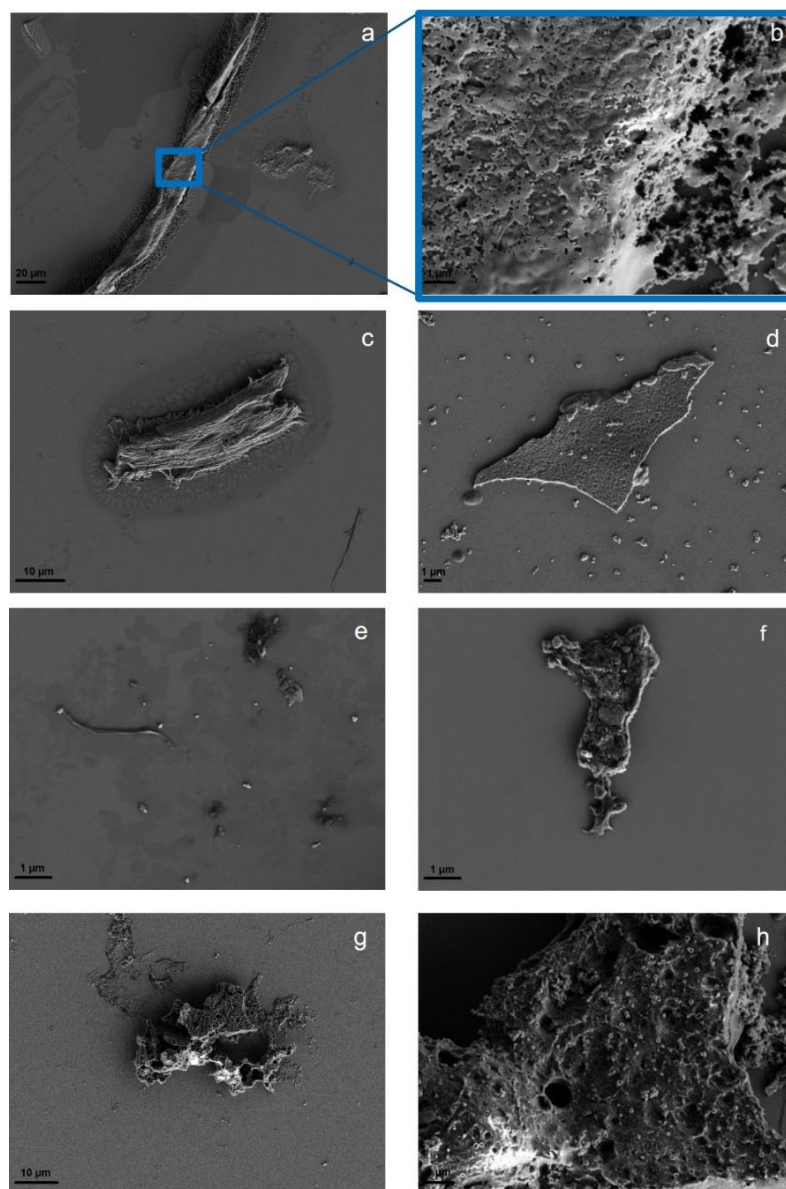


FIGURE 14: SURFACE MORPHOLOGY OF PS SHOWING A WIDE RANGE OF PARTICLE SHAPES: FIBER (A), WITH A CLOSE UP OF THE FIBER SURFACE (B), IRREGULAR FRAGMENT (C) AND SPHERES AND FILM (D). PET FRAGMENTS, FIBERS AND SPHERES ARE SHOWN IN (E) WITH A CLOSE UP OF THE SURFACE OF A FRAGMENT (F). TYPICAL PLA FRAGMENT (G) WITH A CLOSE UP OF THE SURFACE OF A FRAGMENT (H). MORE SEM IMAGES ARE AVAILABLE IN SI FIGURES 6 AND 7.

YIELD AND REPRODUCIBILITY OF THE FRAGMENTATION

As can be seen in *Figure 15* the polymer size (a, b and c) and shape (d, e and f) distribution is highly polymer-dependent. With the applicable microscopy set up, particles down to diameters of 5 μm could be analyzed, with the exception of PS – here, only particles larger than 10 μm could be analyzed through image processing, as there were too many particles to be processed below 10 μm (computation time exceeded 30 min).

PLA fragmented into $1.1 \times 10^4 - 2.1 \times 10^4$ comparatively large particles, which are mostly fringy irregular fragments. PET and PS yielded $1.8 \times 10^4 - 7.1 \times 10^4$ and $9.2 \times 10^3 - 2.1 \times 10^5$ smaller more jagged particles, respectively. The fragmentation of PLA and PET lead to reproducible results, as the number of fragments is within the same order of magnitude for all replicates. The fragmentation of PS is less reproducible, as we achieved fragment counts that are several orders of magnitude apart. This might be caused by the fragmentation mechanism through sonication in alkaline conditions, which relies on two parameters: Hydrolysis, which is systematic and controllable through pH and mechanical strain, which is systematic, but less controllable because it is dependent on the ultrasonic field. PLA is easily hydrolysable, while PET and PS are increasingly less hydrolysable and therefore the fragmentation mechanism must be more dependent on the less controllable mechanical strain and radical decay. (see section “Mechanistic Implications for the Degradation of Solid Polymers by Sonication”).

The sample composition, however, was very similar within the replicates and among the different polymers. In all samples also polycarbonate particles from the filter were found (~15 – 25%). These were removed from the compound distribution, as they are artefacts originating from the filtering material itself and are not present in the generated suspension. After removing these artefacts from the analysis, the composition of the samples created through sonication in alkaline solution were analyzed. The original polymer was the predominant component (~68.4 – 81.6% depending on the polymer). All samples also contained a portion of particles that

could not be classified, as the spectra were too noisy (HQI < 15 and manual identification failed), displayed only background signal or showed spectra for which no library match could be found (~12.2 – 26.8%). Only a very small number of particles (4.0 – 5.1%) showed too strong fluorescent backgrounds to be analyzed. Contamination with other polymers and CaCO₃ was negligible (0.6 – 1.2%). The Raman spectra of the polymers showed no signs of ageing in the form of additional bands, which is in accordance with prior ageing experiments [7, 27] (*see SI, Figures 8-10 for Raman spectra before and after fragmentation*).

Furthermore, 10 µl of sample were deposited on a CaF₂ substrate to measure selected particles ~ 2 µm (n = 30) to confirm the formation of small plastic particles through sonication, which was suggested but not chemically proven by Davranche et al. [24]. In *Figure 16* the smallest detectable particle through Raman microspectroscopy (100× magnification objective, N.A. = 0.9) for PS and PET is shown. This does not prove that all particles of this size originate from the plastic material but confirms the formation of small plastic particles through sonication.

The reproducibility of the size distribution and of the shape variation was tested by replication (N = 3). *Figure 17* shows that there is variation in between the replicates but overall the procedure leads to comparable results. The dominant size fraction is < 20 µm, which accounts for half of the particles of PLA (52.2% ± 9.0%), PET (56.55% ± 8.3%), and PS (54.7% ± 20.2%). We have, however, noted that there is a dip in the 5 µm – 10 µm size class, where we would have expected an increase in particle number. This suggests to us that although the measurement of particles in the size range 5 µm – 10 µm is possible as identifiable Raman spectra can be measured, this class may not be quantitatively represented by the method applied as indicated in von der Esch and Kohles et al. [26]. The second largest fraction is 20 µm – 50 µm for PLA (33.3% ± 4.7%), PET (33.4% ± 4.1%), and PS (33.0% ± 12.0%). Particles larger than 50 µm are present but make up only a small portion for PLA (14.5% ± 3.8%), PET (10.0% ± 3.5%), and PS (12.3% ± 7.3%). Although fragments in the shape of irregular fragments, fibers as well as spheres and films were found by optical microscopy and SEM, irregular fragments are the predominant shape

(66.4% – 72.1%) in all replicates across all polymers. The second major fragment shapes that occur are spheres (23.5% – 28.4%) followed by fibers (4.2% – 5.3%). Since our automated categorization is based on the comparison of diameter ratios and areas, we cannot further characterize into films with our current program. Fibers were additionally characterized via manual Raman microscopy to ensure that they truly originate from the fragmentation of the polymer parent particle (see *SI Figures 11 – 14*).

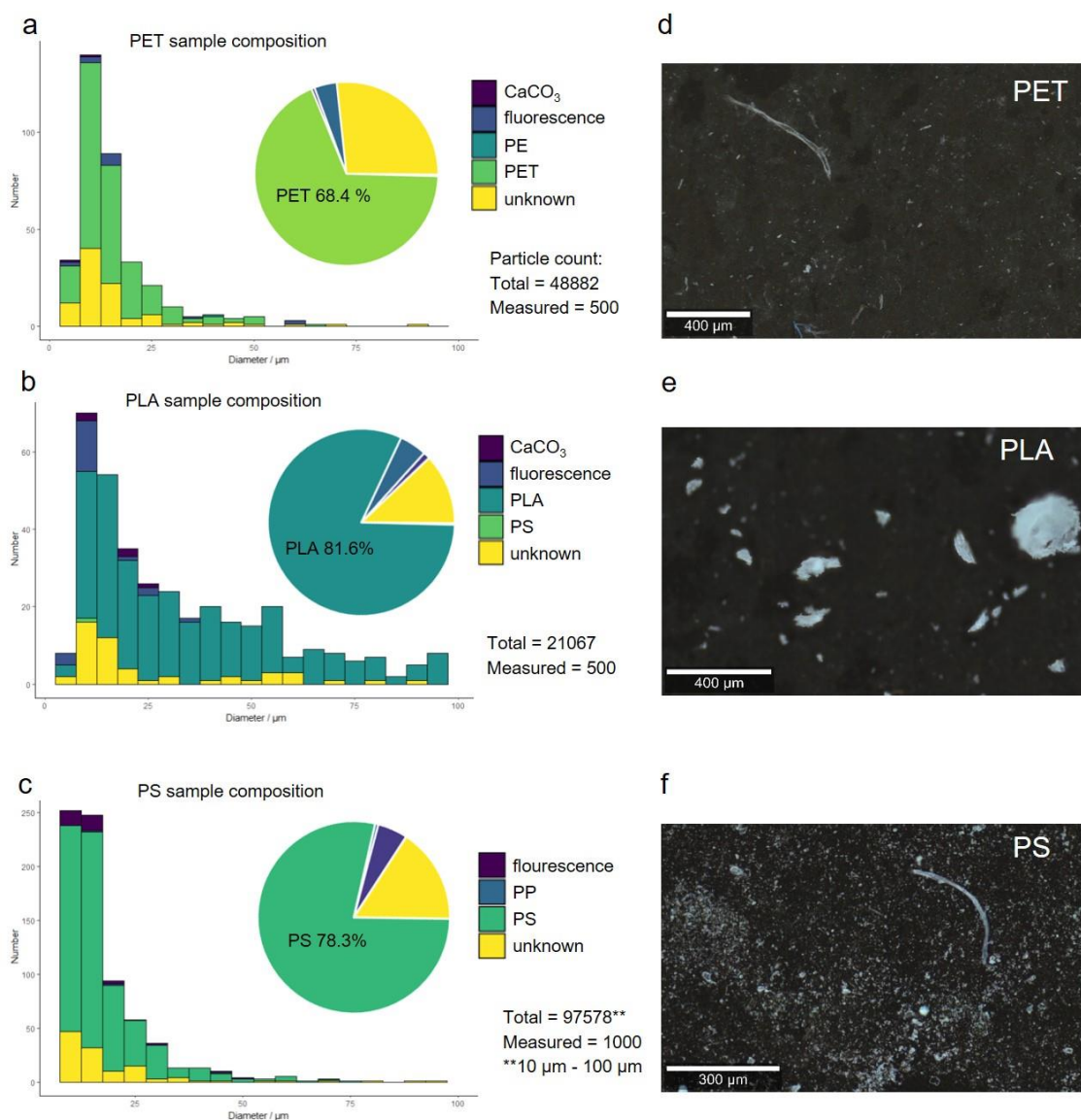


FIGURE 15: COMPOUND CORRELATED SIZE DISTRIBUTION OF REPLICATE 1 BY OPERATOR 1 FOR PET (A), PS (B), AND PLA (C). MICROSCOPY IMAGES OF POLYMER FRAGMENTS PRODUCED THROUGH SONICATION IN ALKALINE SOLUTION (REPLICATE 1) PET (D), PS (E), AND PLA (F).

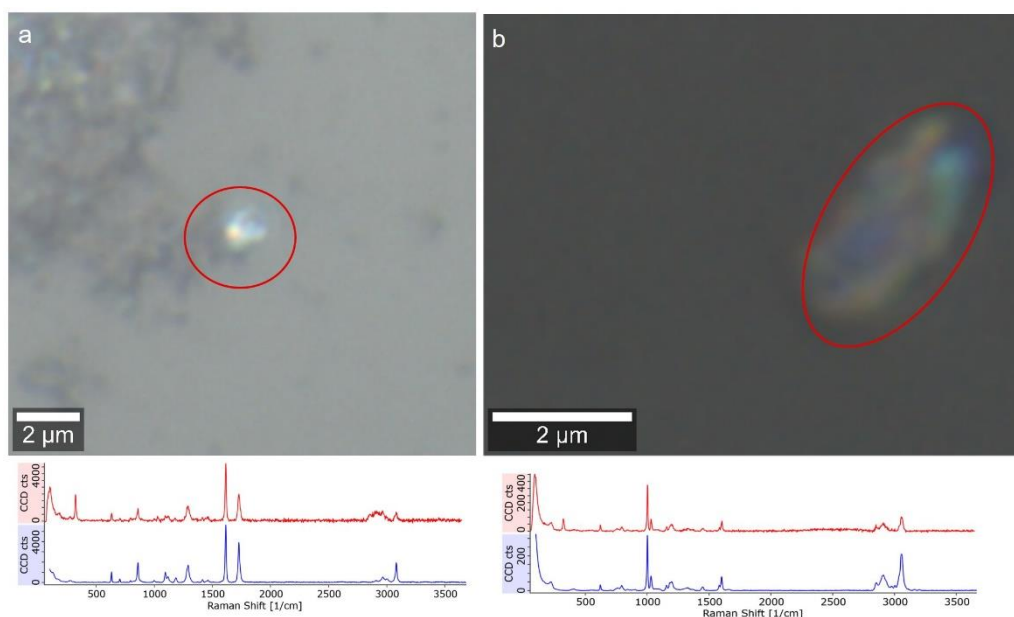


FIGURE 16: RAMAN MICROSCOPIC ANALYSIS OF PLASTIC FRAGMENTS, CONFIRMING THE FORMATION OF LOW μM RANGE PARTICLES THROUGH SONICATION. PET (A, REFERENCE BLUE, PARTICLE SPECTRUM RED), PS (B, REFERENCE BLUE, PARTICLE SPECTRUM RED).

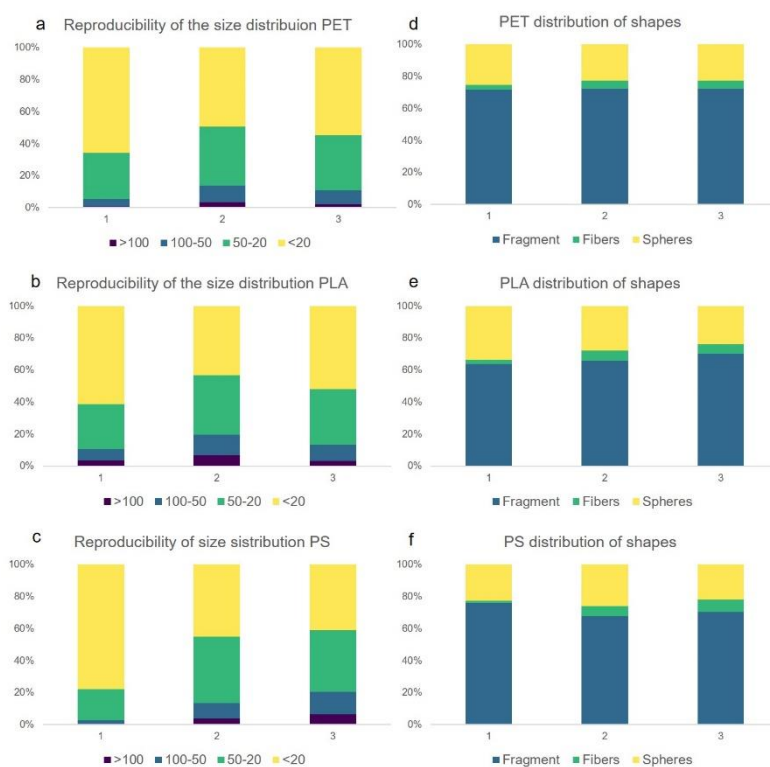


FIGURE 17: COMPARISON OF THE REPLICATES 1 – 3. REPLICATE 1 WAS PRODUCED BY OPERATOR 1 AND REPLICATES 2 AND 3 WERE PRODUCED BY OPERATOR 2. REPRODUCIBILITY OF THE SIZE DISTRIBUTION FOR PET (A), PLA (B), AND PS (C). DISTRIBUTION OF PARTICLE SHAPES FOR PET (D), PLA (E), PS (F). THE CORRESPONDING DATA CAN BE VIEWED IN SI, TABLE 1.

SIZE DISTRIBUTION COMPARISON TO ENVIRONMENTAL MP PARTICLES AND OTHER REFERENCE MATERIALS

A major challenge in MP production from both milling and sonication is control over particle size distribution. For the (cryo)milling, the size distribution seems to depend on the temperature, loading, and type of polymer [20, 28]. The major factors of influence on MP formation through sonication will be reviewed in detail in the following sections. Both preparation methods were compared to ageing experiments by Lambert et al. [6] and show that all MP production methods yield different size distributions. While milling produces large particles predominantly (50 μm – 100 μm [20] and 500 μm – 2 mm [28]) sonication rather leads to smaller particles (average Feret's diameter, $\mu = 30.23 \mu\text{m} \pm 12.14 \mu\text{m}$ for PS, $\mu = 32.04 \mu\text{m} \pm 6.53 \mu\text{m}$ for PLA and $\mu = 26.56 \mu\text{m} \pm 5.23 \mu\text{m}$ for PET). The average size of the particles produced through sonication is much closer to the average particle sizes relevant in the environment [2] and in weathering studies ($\sim 99\%$ of PLA, PS and PET particles are in the size range 0.6 – 18 μm) [6].

If extremely small particles are desired, some alternative procedures to the sonication method presented here are available. PS nanoparticles (125 nm – 437 nm) can be produced by blending in a food processor [29]. For PET, laser ablation delivers nanoplastic [19]. If specific shapes are the target of the production process, fibers (40 μm – 100 μm length) from nylon, PET, and PP can be produced by using a cryogenic microtom [22] and spheres in the nm range are commercially available for PS.

Our method provides an easy production of small MP fragments (1 μm – 1 mm) but is highly dependent on the ultrasonic field. While sub μ particles were also present in the suspensions produced through sonication as demonstrated by SEM/EDX analysis, additional analysis via asymmetric field flow fractionation or centrifugal field flow fractionation and possibly staining for chemical characterization is necessary to quantify the particles formed in this size range [30].

MECHANISTIC IMPLICATIONS FOR THE DEGRADATION OF SOLID POLYMERS BY SONICATION

The effect of sonication is usually tested on polymers in various organic solvents for molecular weight tuning [31]. The mechanistic picture is brought forward that sonication creates cavities in the liquid medium, which release energy during cavity collapse resulting in local pyrolytic conditions (about 5000 K, 2000 atm [32]) and the release of radicals. In water, OH^\cdot and H^\cdot radicals are formed, which create hydrogen peroxide (H_2O_2), thus providing oxidizing conditions. At the molecular level, in addition a rapid movement of solvent molecules is induced that cannot be followed at the same scale by the macromolecules in the solvent. Thus, friction is created which causes strain and ultimately bond breaking in the macromolecules. The chains are preferentially split at transitions between amorphous and crystalline regions [33]. In our case, these conditions are used to induce polymer scissions through physical breakage as well as radical polymer degradation. For the samples where KOH (0.25 M, pH = 13) was added, additional OH^- ions are available to provide strong hydrolysis/oxidation conditions for the newly split polymers, which lead to a strong increase in the number of detected fragments. The focus of our investigation was PLA, PET, and PS, where we conducted reproducibility analyses for the fragmentation. We also tested PE, PP, PVC, and PA to prove that the procedure is applicable to any polymer. The results are shown in the supporting information (*SI, Table 2*), as these were singular experiments and reproducibility can therefore not be accessed for PE, PP, PVC, and PA at this point in time.

It is important to note that all experiments were conducted in an ultrasonic bath which has the disadvantage that the fragmentation is not necessarily reproducible. Each ultrasonic bath produces its own inhomogeneous field [34]. To make this procedure reproducible, the field parameters, which are related to the cavitation effects, need to be investigated prior to particle fragmentation (for details see *SI Figure 15*). Alternatively, a more sophisticated reactor design may be resorted to, which could also lead to better results and higher reproducibility. We decided to

follow the first approach because we would like to enable anyone to repeat our fragmentation without the need for additional equipment.

Since not all laboratories will have the same ultrasonic bath at hand, the parameter-effect relationships are important to consider. For a conclusive review on current sonochemical research (reactor geometry, size, and solvent effects) we refer to [31, 34, 35].

ANALYSIS OF SUSPENSIBILITY AND SEDIMENTATION RATES BY UV-VIS SPECTROSCOPY

A common problem with (cryo)milled particles is their static charge, which prevents the suspension in water. Eitzen et al. even reported adhesion to glass walls for PS fragments from cryomilling, which increased with decreasing size [20]. However, due to their density (1.04 g/cm^3) PS fragments should sediment in water, as is observed, especially in non-stirred PS suspensions [21]. In order to alleviate the suspensibility issue usually one of two paths are chosen: (i) Suspension with a surfactant, which renders the sample unsuitable for toxicological testing, or (ii) oxidative treatment to modify the fragment surface, creating polar groups. For cryomilled particles both treatments require an additional processing step.

The fragments produced through sonication were suspended in pure MilliQ *Figure 18a*) to test the suspensibility and sedimentation rate. Particles were observed to remain suspended without visible adhesion to the walls of the centrifuge tube. All suspensions were examined with UV-VIS, as suspended particles will absorb light leading to a low transmission signal. With increasing sedimentation, the transmission signal should increase and level off at 100%, which is the transmission of MilliQ without suspended particles.

The UV-VIS analysis (*Figure 18 c-d*) shows that the fragments can be well suspended and that they sediment according to their density. PET particles had the

fastest sedimentation rate, while PLA particles sedimented slower and PS particles showed the slowest sedimentation rate. The suspensibility is likely a result of the *in situ* fragmentation in an alkaline solution, which introduces hydrophilic groups into the polymer surface while the fragments split off from the parent particle (see section below “Comparison of reference particles with environmental microplastic by FTIR spectroscopy”).

Thus, the produced fragments showed the desired sedimentation properties without the need for a surfactant, making them suitable for toxicological testing and validation of recovery rate experiments for sample preparation as well as for detection of MP.

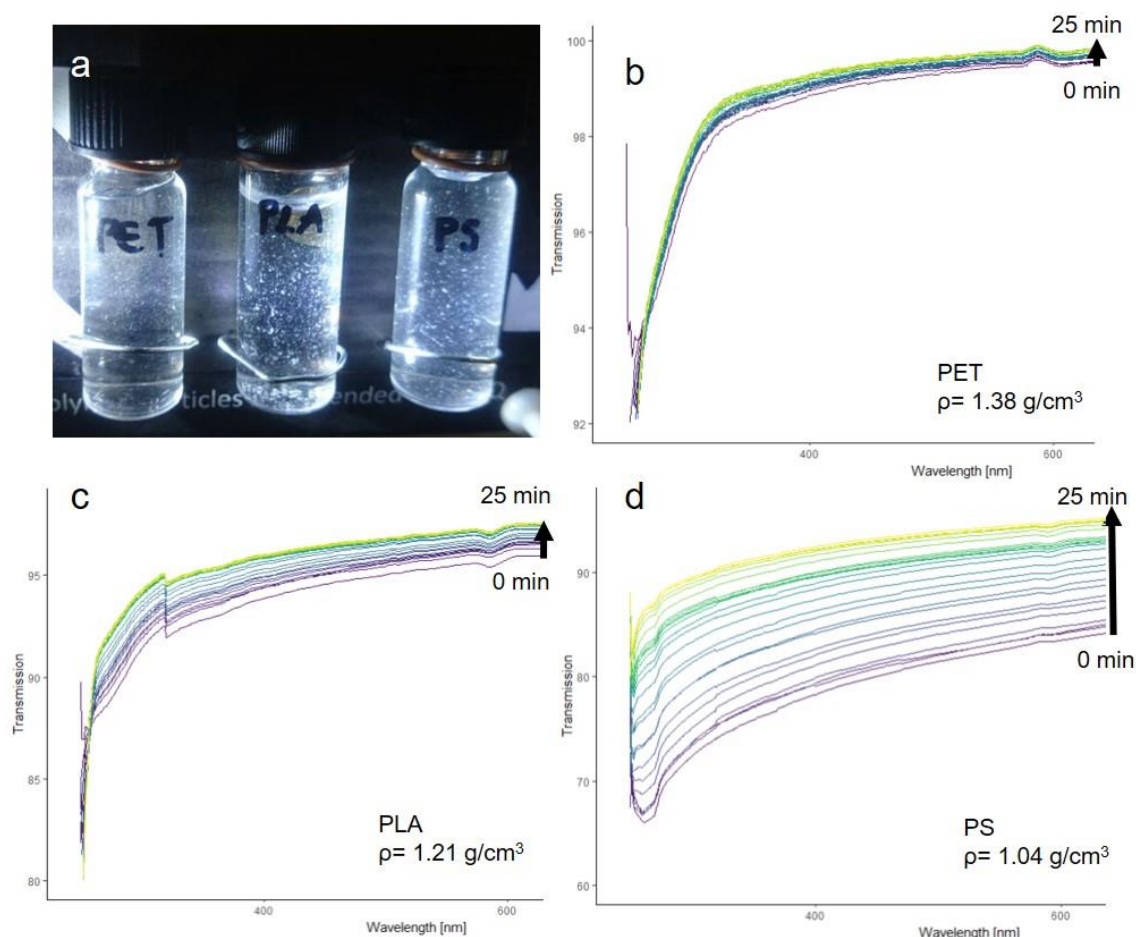


FIGURE 18: PET, PLA AND PS FRAGMENTS SUSPENDED IN PURE MILLIQ WATER (A).UV-VIS TRANSMISSION SPECTRA OF PET (B), PLA (C), PS (D).

COMPARISON OF REFERENCE PARTICLES WITH ENVIRONMENTAL MICROPLASTIC BY FTIR SPECTROSCOPY

The goal was to create reference particles, which mimic the properties of secondary MP formed in the environment through weathering. Therefore, we compared the spectra of our *in situ* aged fragments to reference polymer spectra and the spectra acquired by Scott Lambert and Martin Wagner in their 112 day weathering experiment [6].

Fragments larger than 1 mm of all three tested polymers (PLA, PS, and PET) showed significant changes in their FTIR spectra (*Figure 19a - c*).

The most pronounced changes are exhibited by PLA, which shows additional bands (3364 cm^{-1} , O-H and 1520 cm^{-1} , C=O) and shifting C-H stretching vibrations (blue shift, $2916\text{ cm}^{-1} \rightarrow 2993\text{ cm}^{-1}$ and $2848\text{ cm}^{-1} \rightarrow 2930\text{ cm}^{-1}$). Interactions of the C-H group with neighboring O-H groups cause the band shift of the C-H stretching vibration [36]. This and the emergence of a band at 3364 cm^{-1} shows either the formation of O-H groups through hydrolysis or the intercalation of water molecules into the polymer structure. Here, a combination of both is likely, as the appearance of COOH introduces electrostatic interactions which lead to stronger swelling of the polymer [37]. The overall shifts in intensity hint at a changed ratio of crystalline / amorphous structure within the polymer [38]. When comparing the spectra of the artificially and naturally aged PLA, we observe that the resulting spectra have similar new bands, leading to the conclusion that sonication under hydrolytic conditions is an effective method to artificially age polymers to produce reference materials.

PET shows changes in relative band intensity and additional bands (3250 cm^{-1} , O-H and 1639 cm^{-1} , C=O). The additional band at 3250 cm^{-1} is indicative of the formation of O-H groups [39], as PET does not absorb water well [40], but is known to hydrolyze at high temperatures ($T = 80 - 200^\circ\text{C}$) [41], which are easily reached through sonication as collapsing cavities create local pyrolytic conditions. In natural

environments photo-oxidation and hydrolysis are the driving forces for PET degradation [42] which should lead to similar results as the proposed sonication provides radicals and alkaline conditions. When comparing the spectra of the artificially and naturally aged polymers, we again see very similar modifications.

PS shows changes in band intensity and additional bands (3177 cm^{-1} , O-H; 1624 cm^{-1} , C=O as well as 1357 cm^{-1} , COOH and 1244 cm^{-1}), which are in accordance with the appearance of new bands found in naturally aged PS. The main degradation mechanism in a natural environment is photodegradation for PS, which in the presence of oxygen may introduce C-O bonds of various kinds leading to crosslinking and the formation of ketones [43].

For all additional bands it has to be said, that they cannot exactly correspond to the bands found in the naturally aged polymers, as the newly formed O-H, C=O, and COOH groups must have different interaction partners, which determine the exact position of the band within the group range.

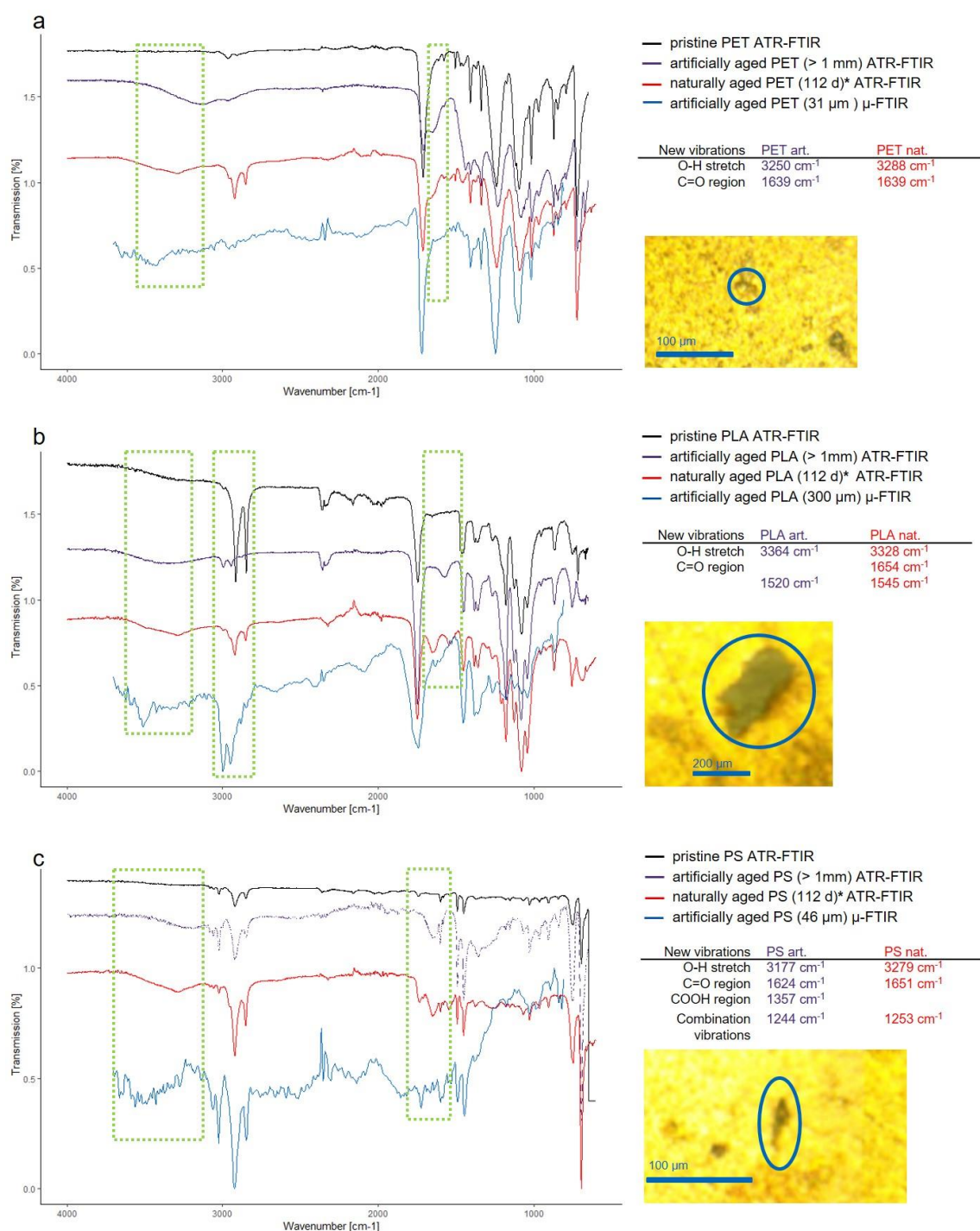


FIGURE 19: COMPARISON OF THE NEW VIBRATIONS IN ARTIFICIALLY AND NATURALLY AGED POLYMERS. THANKS TO SCOTT LAMBERT AND MARTIN WAGNER, WHO PROVIDED THE DATA FOR 112 DAY AGED MP [6] (MARKED WITH *), A COMPARISON BETWEEN NATURALLY AND ARTIFICIALLY AGED MP WAS POSSIBLE. THE ATR-FTIR SPECTRA FOR PRISTINE (BLACK) ARTIFICIALLY AGED (PURPLE) AND NATURALLY AGED (RED) AND REFLECTANCE μ-FTIR SPECTRA OF SMALL ARTIFICIALLY AGED MP (BLUE) ARE SHOWN FOR PET (A), PLA (B) AND PS (C), WHEREIN THE REGIONS OF INTEREST ARE MARKED (GREEN SQUARES). THE POSITIONS OF THE BANDS CORRESPONDING TO THE NEWLY FORMED FUNCTIONAL GROUPS OF THE ATR-

FTIR MEASUREMENTS ARE LISTED AND THE MICROSCOPY IMAGES OF THE PARTICLES ANALYZED ARE DISPLAYED TO THE RIGHT SIDE OF THE SPECTRA.

To investigate if smaller polymer fragments display the same ageing behavior as the large fragments, they were analyzed by μ -FTIR spectroscopy in reflectance mode. The number of measured particles was 10 for PLA and PET and 5 for PS (spectra available in *SI, Figure 17– 19*). Typical examples of MP spectra are given in *Figure 19a – c*. It is important to note that ATR and reflectance IR have different axial resolution, so that ATR will give spectra representing mostly the surface chemistry ($\sim 1 \mu\text{m} - 2 \mu\text{m}$, axial resolution, see calculation in *SI*) of the particle. Reflectance IR will pass through particles with rough surfaces ($\sim 2.6 \mu\text{m}$ at 3785 cm^{-1} to $20 \mu\text{m}$ at 500 cm^{-1} , axial resolution, see calculation in *SI, Figure 16*) and yield a spectrum describing the layer close to the surface of the particle at high wavenumbers but showing also the bulk properties of the particle at low wavenumbers.

Therefore, as it was the case in the ATR measurements, we can observe the C-H shift ($2916 \text{ cm}^{-1} \rightarrow 2997 \text{ cm}^{-1}$ and $2848 \text{ cm}^{-1} \rightarrow 2947 \text{ cm}^{-1}$) inherent to the surface modification for the PLA sample (see *Figure 19b*). In addition, the broad O-H stretch band at 3509 cm^{-1} is present. The C=O band of pristine PLA (1744 cm^{-1}) now shows a shouldering towards lower wavenumbers, resulting from the introduction of new C=O groups from the ultrasonic treatment. However, this is only visible as a shoulder, not as a free band as the light penetrates up to $6 \mu\text{m}$ deep and therefore gives more information on the bulk material than on the particle surface.

Regarding the PET sample (*Figure 19a*), the μ -FTIR measurements revealed the same spectra alterations as the ATR measurements. A C=O band shouldering at 1623 cm^{-1} appeared as well as a very broad O-H stretch band at 3420 cm^{-1} .

In the PS sample, only the O-H band (3501 cm^{-1}) appeared, whereas the other changes observed using ATR-FTIR do not show (*Figure 19c*).

The reflectance μ -FTIR measurements confirm that the surface modifications seen in the large particles also appear in the small fragments.

Therefore, our results suggest that if aged MP fragments are required for experimental work or validation, a simple 15 h sonication in alkaline conditions can provide materials that mimic not only the sedimentation properties, but also surface chemistry of aged MP.

2.4 CONCLUSION

Currently available MP reference particles (1 μm – 1 mm) are usually produced by grinding. To this end special cryomills are needed. This equipment is not accessible in every laboratory and thus decouples the manufacturers from the users, which makes fast method development difficult. In contrast, the ultrasonic-based method brought forward here makes it possible to produce reference particles in every chemical laboratory. These reference materials are already suspended during their formation process and can be resuspended in pure MilliQ (pH = 7). Furthermore, they have hydrophilic groups on the surface due to the production process, so that realistic environmental MP can be emulated. In addition, the different sizes and shapes help in the further development of image recognition methods used in Raman microspectroscopy and μ -FTIR spectroscopy to determine the measuring points.

The approach presented here delivers a mixture of particle shapes, which consists of predominantly irregular fragments. If the research question demands the investigation of a distinct shape, e.g. toxicological studies, monitoring the impact of fibers, an alternative method needs to be used. Furthermore, we would like to point out that the reproducibility was tested for PLA, PET, and PS and each laboratory employing the presented method will need to check the reproducibility with their equipment and with their polymers of choice. We have shown that it is possible to achieve reproducible results and have pinpointed the main influencing factors on the reproducibility namely the ultrasonic field, the mechanical properties of the polymer, as well as the hydrolyzability. In order to achieve the comprehensive characterization and quantification of MP reference materials a protocol including Raman microspectroscopy, ATR-IR, μ -FTIR, UV-VIS, SEM and EDX was presented, which can be applied to any MP sample. We have shown by qualitative analysis that sonication also produces particles in the sub μ plastic range. If these particles are to be used in future experiments, further quantitative analyses will be required.

2.5 OUTLOOK

Future experiments will include an upscaled procedure for the production of aged MP reference material. A possible path might include the (cryo)milling of polymers followed by the sonication (at alkaline conditions), thus enabling a high yield and the *in situ* generation of small, aged and suspensible particles. In addition to the fragmentation, the *in situ* coating of MP with humic substances could provide a helpful model to mimic the environmental adsorption of dissolved organic carbon and thus check the detectability of particles under environmental conditions. This is also a very important research gap so far, as it is often stated that Raman microspectroscopy is limited by the attachment of organic matter to the analyte inducing fluorescence and preventing the detection of particles. Even though it is extremely important to know the detection limits of a method, currently there is no systematic examination of this matter. With our optimized scheme for simple and reproducible generation of reference particles that can be adopted by laboratories around the world, using their polymers of interest, we hope to enable easier and more detailed method development and validation, as well as toxicological testing for future studies.

Conflict of Interest

The authors declare that the research was conducted in the absence of any commercial or financial relationships that could be construed as a potential conflict of interest.

Author Contributions

EE, ME and NI, designed the experiments. EE implemented the idea for the production of secondary MP, carried out the fragmentation, *TUM-ParticleTyper* Raman microspectroscopy, ATR-FTIR and UV-VIS experiments and validated the procedures. Reproducibility was tested by ML, under the supervision of EE, ME and NI, by replicating the fragmentation and *TUM-ParticleTyper* Raman microspectroscopy analysis. The *TUM-ParticleTyper* was developed, optimized and validated by AK, EE and NI. The SEM and EDX analyses were carried out by CS. JW, KG and TH investigated

ageing effects on the single particle level with μ -FTIR spectroscopy. All authors discussed the results and contributed to the final manuscript.

Funding

Bayerische Forschungsförderung (MiPaq “Microparticles in the aquatic environment and in foodstuffs” are biodegradable polymers a conceivable solution to the “microplastic problem”?, AZ-1258-16.

Furthermore, this work was supported by the German Research Foundation (DFG) and the Technical University of Munich, within the funding program Open Access Publishing.

Acknowledgments

The authors would like to thank Lisa Göpfert, Carolin Hartmann, Philipp Anger for helpful discussions. Furthermore, we thank Scott Lambert and Martin Wagner for granting us access to the original spectra of their publication “Formation of microscopic particles during the degradation of different polymers” [6].

Supplementary Material

Supplementary_Material_Simple_Generation_of_Suspensible_Secondary_Microplastic_Reference_Particles_via_Ultrasound_Treatment.docx

Data Availability Statement

The raw data supporting the conclusions of this manuscript will be made available by the authors, without undue reservation, to any qualified researcher.

We are delighted to respond to data requests as the full data set for all experiments for our reference particle study contains a total of 300 GB (including all experiments necessary to get to the point where the procedure is reproducible) mostly consisting of classified spectra (Raman, IR UV-VIS, EDX) and images (Optical microscopy, SEM).

2.6 REFERENCES

1. Hartmann NB, Huffer T, Thompson RC, Hasselov M, Verschoor A, Daugaard AE, et al. Are We Speaking the Same Language? Recommendations for a Definition and Categorization Framework for Plastic Debris. *Environ Sci Technol.* **2019**;53(3):1039-47.
2. Anger PM, von der Esch E, Baumann T, Elsner M, Niessner R, Ivleva NP. Raman microspectroscopy as a tool for microplastic particle analysis. *Trends Anal Chem.* **2018**;109:214-26.
3. Koelmans AA, Mohamed Nor NH, Hermsen E, Kooi M, Mintenig SM, De France J. Microplastics in freshwaters and drinking water: Critical review and assessment of data quality. *Water Res.* **2019**;155:410-22.
4. Ivleva NP, Wiesheu AC, Niessner R. Microplastic in Aquatic Ecosystems. *Angew Chem Int Ed Engl.* **2017**;56(7):1720-39.
5. Brandon J, Goldstein M, Ohman MD. Long-term aging and degradation of microplastic particles: Comparing in situ oceanic and experimental weathering patterns. *Mar Pollut Bull.* **2016**;110(1):299-308.
6. Lambert S, Wagner M. Formation of microscopic particles during the degradation of different polymers. *Chemosphere.* **2016**;161:510-7.
7. Cai L, Wang J, Peng J, Wu Z, Tan X. Observation of the degradation of three types of plastic pellets exposed to UV irradiation in three different environments. *Sci Total Environ.* **2018**;628-629:740-7.
8. Dris R, Imhof H, Sanchez W, Gasperi J, Galgani F, Tassin B, et al. Beyond the ocean: contamination of freshwater ecosystems with (micro-)plastic particles. *Environ Chem.* **2015**;12(5):539-50.
9. Eerkes-Medrano D, Thompson RC, Aldridge DC. Microplastics in freshwater systems: A review of the emerging threats, identification of knowledge gaps and prioritisation of research needs. *Water Res.* **2015**;75:63-82.
10. Eriksen M, Mason S, Wilson S, Box C, Zellers A, Edwards W, et al. Microplastic pollution in the surface waters of the Laurentian Great Lakes. *Mar Pollut Bull.* **2013**;77(1-2):177-82.
11. Free CM, Jensen OP, Mason SA, Eriksen M, Williamson NJ, Boldgiv B. High-levels of microplastic pollution in a large, remote, mountain lake. *Mar Pollut Bull.* **2014**;85(1):156-63.
12. Imhof HK, Ivleva NP, Schmid J, Niessner R, Laforsch C. Contamination of beach sediments of a subalpine lake with microplastic particles. *Curr Biol.* **2013**;23(19):R867-R8.
13. Imhof HK, Laforsch C, Wiesheu AC, Schmid J, Anger PM, Niessner R, et al. Pigments and plastic in limnetic ecosystems: A qualitative and quantitative study on microparticles of different size classes. *Water Res.* **2016**;98:64-74.

14. Enders K, Lenz R, Stedmon CA, Nielsen TG. Abundance, size and polymer composition of marine microplastics $\geq 10 \mu\text{m}$ in the Atlantic Ocean and their modelled vertical distribution. *Mar Pollut Bull.* **2015**;100(1):70-81.
15. Erni-Cassola G, Zadjelovic V, Gibson MI, Christie-Oleza JA. Distribution of plastic polymer types in the marine environment; A meta-analysis. *J Hazard Mater.* **2019**;369:691-8.
16. Frere L, Paul-Pont I, Rinnert E, Petton S, Jaffre J, Bihannic I, et al. Influence of environmental and anthropogenic factors on the composition, concentration and spatial distribution of microplastics: A case study of the Bay of Brest (Brittany, France). *Environ Pollut.* **2017**;225:211-22.
17. Hidalgo-Ruz V, Gutow L, Thompson RC, Thiel M. Microplastics in the marine environment: a review of the methods used for identification and quantification. *Environ Sci Technol.* **2012**;46(6):3060-75.
18. Balakrishnan G, Déniel M, Nicolai T, Chassenieux C, Lagarde F. Towards more realistic reference microplastics and nanoplastics: preparation of polyethylene micro/nanoparticles with a biosurfactant. *Environ Sci Nano.* **2019**;6(1):315-24.
19. Magri D, Sanchez-Moreno P, Caputo G, Gatto F, Veronesi M, Bardi G, et al. Laser Ablation as a Versatile Tool To Mimic Polyethylene Terephthalate Nanoplastic Pollutants: Characterization and Toxicology Assessment. *ACS Nano.* **2018**;12(8):7690-700.
20. Eitzen L, Paul S, Braun U, Altmann K, Jekel M, Ruhl AS. The challenge in preparing particle suspensions for aquatic microplastic research. *Environ Res.* **2018**:490-5.
21. Hüffer T, Praetorius A, Wagner S, von der Kammer F, Hofmann T. Microplastic Exposure Assessment in Aquatic Environments: Learning from Similarities and Differences to Engineered Nanoparticles. *Environ Sci Technol.* **2017**;51(5):2499-507.
22. Cole M. A novel method for preparing microplastic fibers. *Sci Rep.* **2016**;6:1-7.
23. G. J. Price, A. J. White, Clifton AA. The effect of high-intensity ultrasound on solid polymers. *Polymer.* **1995**;36(26):4919-25.
24. Davranche M, Veclin C, Pierson-Wickmann AC, El Hadri H, Grassl B, Rowenczyk L, et al. Are nanoplastics able to bind significant amount of metals? The lead example. *Environ Pollut.* **2019**;249:940-8.
25. NIST. SRM Definitions <https://www.nist.gov/srm/srm-definitions> [27.09.2019]. Available from: <https://www.nist.gov/srm/srm-definitions>.
26. E. von der Esch, A. J. Kohles, P. M. Anger, R. Hoppe, R. Niessner, M. Elsner, et al. TUM-ParticleTyper: A Detection and Quantification Tool for Automated Analysis of (Microplastic) Particles and Fibers. *PLOS ONE submitted*
27. Lenz R, Enders K, Stedmon CA, Mackenzie DMA, Nielsen TG. A critical assessment of visual identification of marine microplastic using Raman spectroscopy for analysis improvement. *Mar Pollut Bull.* **2015**;100(1):82-91.

28. Kuhn S, van Oyen A, Booth AM, Meijboom A, van Franeker JA. Marine microplastic: Preparation of relevant test materials for laboratory assessment of ecosystem impacts. *Chemosphere*. **2018**;213:103-13.
29. Ekvall MT, Lundqvist M, Kelpsiene E, Šileikis E, Gunnarsson SB, Cedervall T. Nanoplastics formed during the mechanical breakdown of daily-use polystyrene products. *Nanoscale Advances*. **2019**;1(3):1055-61.
30. Schwaferts C, Sogne V, Welz R, Meier F, Klein T, Niessner R, et al. Nanoplastic Analysis by On-line Coupling of Raman Microscopy and Field-Flow Fractionation Enabled by Optical Tweezers. *Anal Chem*. **2020**.
31. Gogate PR, Prajapat AL. Depolymerization using sonochemical reactors: A critical review. *Ultrason Sonochem*. **2015**;27:480-94.
32. Leonelli C, Mason TJ. Microwave and ultrasonic processing: Now a realistic option for industry. *Chemical Engineering and Processing: Process Intensification*. **2010**;49(9):885-900.
33. Price GJ, Smith PF. Ultrasonic Degradation of Polymer Solutions. I. Polystyrene Revisited*. *Polym Int*. **1991**;24:159- 64.
34. Jenderka KV, Koch C. Investigation of spatial distribution of sound field parameters in ultrasound cleaning baths under the influence of cavitation. *Ultrasonics*. **2006**;44 Suppl 1:e401–e6.
35. Liu B, Xia H, Fei G, Li G, Fan W. High-Intensity Focused Ultrasound-Induced Thermal Effect for Solid Polymer Materials. *Macromol Chem Phys*. **2013**;214(22):2519-27.
36. Schmidt P, Dybal J, Trchová M. Investigations of the hydrophobic and hydrophilic interactions in polymer–water systems by ATR FTIR and Raman spectroscopy. *Vib Spectrosc*. **2006**;42(2):278-83.
37. Proikakis CS, Mamouzelos NJ, Tarantili PA, Andreopoulos AG. Swelling and hydrolytic degradation of poly(d,l-lactic acid) in aqueous solutions. *Polym Degrad Stab*. **2006**;91(3):614-9.
38. Bower DI, Maddams WF. The characterization of polymers. In: Davis EA, Ward IM, editors. *The vibrational spectroscopy of polymers*. United States of America Cambridge University Press, New York: Cambridge University Press; 1989. p. 162 - 226.
39. H. Zhang, A Ranjin, Ward IM. Determination of the end-group concentration and molecular weight of poly(ethylene naphthalene-2,6dicarboxylate) using infra-red spectroscopy. *Polymer*. **1996**;37(7):1079-85.
40. S. Venkatachalam, S. G. Nayak, J. V. Labde, P. R. Gharal, K. Rao, Kelkar AK. Degradation and Recyclability of Poly (Ethylene Terephthalate). *Polyester2012*. p. 75 - 98.

41. D.S. Achilias, Karayannidis GP. The Chemical Recycling of PET in the Framework of Sustainable Development. *Water, Air, and Soil Pollution: Focus* **2004**:385-96.
42. Gewert B, Plassmann MM, MacLeod M. Pathways for degradation of plastic polymers floating in the marine environment. *Environ Sci Process Impacts*. **2015**;17(9):1513-21.
43. E. Yousif, R.Haddad. Photodegradation and photostabilization of polymers, especially polystyrene: review. *SpringerPlus*. **2013**;2(398):1 -32.

DECLARATION OF SCIENTIFIC CONTRIBUTION AND SUMMARY OF TUM-PARTICLETYPER: A DETECTION AND QUANTIFICATION TOOL FOR AUTOMATED ANALYSIS OF (MICROPLASTIC) PARTICLES AND FIBERS

Elisabeth von der Esch[☉] and Alexander J. Kohles[☉],

Philipp M. Anger, Reinhard Niessner, Martin Elsner, Natalia P. Ivleva

[☉]shared first authorship

PLoS ONE, 2020,15(6): e0234766 DOI: 10.1371/journal.pone.0234766

TUM-ParticleTyper is an open source software developed by EE, AK, ME and NI that detects particles in images and provides measurement coordinates for a subsequent measurement e.g. by Raman microspectroscopy. As other visualization methods such as fluorescence microscopy and scanning electron microscopy are also used for the characterization of microplastics, the program was adapted to handle these images as well by providing an optimized parametrization for the respective image, delivering a morphological characterization (Feret's diameters, area, classification of shape) for any image that is input. This enables the automated quantitative analysis of particles that contain a minimum of 51 pixels. By combining the image analysis with a statistical subsampling and a spectral analysis it is possible to quantify microplastic in various matrices. EE, AK, ME and NI designed the experiments and agreed upon the requirements for *TUM-ParticleTyper*. EE collected the Raman microspectroscopy data required for the program development by producing the reference materials and testing the parametrization of the Raman microscope as well as the particle detection program in an iterative process. AK implemented the image processing functions. EE, AK and PA did the validation of the particle localization and quantification in a joint effort. EE and PA provided the expert assessment of images delivering the "Ground truth" for the following evaluation of the automated analysis by AK. AK developed the grid search approach and evaluation of *TUM-ParticleTyper*. All findings were put into the literature context and compared to recent methods by EE. Furthermore, EE

applied this method to genuine samples. All authors reviewed the results and contributed to the final version of the manuscript.

The according software and documentation was published in the following repository:

Alexander J. Kohles[©] and **Elisabeth von der Esch[©]**, Philipp M. Anger, Reinhard Niessner, *Martin Elsner, Natalia P. Ivleva, TUM-ParticleTyper: Software and Documentation*, <https://mediatum.ub.tum.de/1547636>,
doi:10.14459/2020mp1547636, 2020

CHAPTER 3:

TUM-PARTICLETYPER: A DETECTION AND
QUANTIFICATION TOOL FOR AUTOMATED
ANALYSIS OF (MICROPLASTIC) PARTICLES AND
FIBERS

Elisabeth von der Esch [✉] 1, Alexander J. Kohles [✉] 1,

Philipp M. Anger¹, Roland Hoppe¹, Reinhard Niessner¹, Martin Elsner¹, Natalia P.
Ivleva^{1*} PLoS ONE 15(6): e0234766. <https://doi.org/10.1371/journal.pone.0234766>

¹Institute of Hydrochemistry, Chair of Analytical Chemistry and Water Chemistry,
Technical University of Munich, Munich, Germany

[✉] These authors contributed equally to this work.

Copyright: © 2020 von der Esch et al. This is an open access article distributed
under the terms of the Creative Commons Attribution License, which permits
unrestricted use, distribution, and reproduction in any medium, provided the
original author and source are credited.

ABSTRACT

TUM-ParticleTyper is a novel program for the automated detection, quantification and morphological characterization of fragments, including particles and fibers, in images from optical, fluorescence and electron microscopy (SEM). It can be used to automatically select targets for subsequent chemical analysis, e.g., Raman microscopy, or any other single particle identification method. The program was specifically developed and validated for the analysis of microplastic particles on gold coated polycarbonate filters. Our method development was supported by the design of a filter holder that minimizes filter roughness and facilitates enhanced focusing for better images and Raman measurements. The *TUM-ParticleTyper* software is tunable to the user's specific sample demands and can extract the morphological characteristics of detected objects (coordinates, Feret's diameter min/max, area and shape). Results are saved in csv-format and contours of detected objects are displayed as an overlay on the original image. Additionally, the program can stitch a set of images to create a full image out of several smaller ones. An additional useful feature is the inclusion of a statistical process to calculate the minimum number of particles that must be chemically identified to be representative of all particles localized on the substrate. The program performance was evaluated on genuine microplastic samples. The *TUM-ParticleTyper* software localizes particles using an adaptive threshold with results comparable to the "gold standard" method (manual localization by an expert) and surpasses the commonly used *Otsu* thresholding by doubling the rate of true positive localizations. This enables the analysis of a statistically significant number of particles on the filter selected by random sampling, measured via single point approach. This extreme reduction in measurement points was validated by comparison to chemical imaging, applying both procedures to the same area at comparable processing times. The single point approach was both faster and more accurate proving the applicability of the presented program.

3.1 INTRODUCTION

Microplastic (MP) may be formed from plastic over time by, fragmentations under the influence of UV light and mechanical abrasion, as well as oxidation and biological breakdown [1]. MP has been found in air [2-4], water [3, 5-7] and soil samples [8]. However, MP particles are very challenging to analyze, as the term “microplastic” describes a heterogeneous mixture of polymer types (at varying stages of degradation), sizes (1 μm -1 mm) and shapes (fragments, fibers, films, and spheres). Consequently, chemical and morphological heterogeneity is combined with low analyte concentrations in the respective samples and a high contamination potential from any plastic material used during sampling or processing [9]. Ideally, all chemical and morphological characteristics, such as polymer types, size distribution and number concentration, of MP should be analyzed and quantified for each sample to answer the question: “How many MP particles are in the sample?”

The general scheme for single particle analysis of MP is a workup step for the extraction and purification of MP [10] after which all remaining particles – microplastic as well as residual environmental colloids – are deposited on a smooth filter surface. The smoothness of the filter is of high importance, as any subsequent measurement, be it Fourier-transform infrared spectroscopy (FTIR) or confocal Raman microspectroscopy, will depend on a flat surface to enable optimal focus on the particles [11, 12]. This is especially true if automated routines are used, where particles are first identified by acquiring images for a morphological assessment, including the determination of the particle centers for the subsequent measurement. Programs enabling these automated routines are commercially available and open source alternatives exist [13-18]. However, almost all routines lack a calibration and validation tool. The problem with the validation of a particle localization program is that spheres are typically used to demonstrate segmentation efficiency. This is a valid procedure and has the benefit that a ground truth is easily accessible through computer generated images. Unfortunately, this does not accurately validate the procedure for the multitude of shapes and color inhomogeneities within the sample. Another possible validation procedure is to extract images from several publications,

representing several image capture devices and settings, and then analyzing those images with the processing routine in question [15]. This is a good routine to show the generalizability of the implemented functions but lacks the ground truth for each image. A third path is to apply an automatic thresholding routine, which can be overruled by the user to “make the segmentation look good”. This is also a valid approach, used in most commercial software, as the current gold standard for the identification of particles in images is still the human operator. The drawbacks of this approach are the missing reproducibility, its high dependency on the operator and the lack of validation possibilities. Therefore, we focused on building a particle detection program (*TUM-ParticleTyper*) that can be calibrated and assembled a manageable validation procedure in accordance with With et al. and Udupa et al. [19, 20]. It can be transferred to the output of the readers preferred software. The initial focus was on microscopy images taken with darkfield illumination, and it was subsequently adapted to the analysis of SEM and fluorescence images.

Merely detecting and morphologically characterizing the particles is not enough as so far, the results produced by any image processing routine do not include the chemical properties of the particles [21]. So, after this first step we are still unable to distinguish between microplastic and native particles and can therefore not yet answer the question: “How many microplastic particles do we have in our sample?” At this stage, results from the particle detection can be used, however, to substantially reduce the measurement time of the sample. By only targeting the particle centers the number of e.g. Raman spectra to be measured and classified via database matching is reduced to the number of particles found in the sample. Provided that the measurement of only one spectrum at the particle’s center is representative for the entire particle, this reduction is common practice [5, 6, 9] and was implemented into *TUM-ParticleTyper*. The reduction was nonetheless tested and validated through a comparison with a chemical image of the same area, analyzed in a comparable time frame. Area and time were chosen as fixed parameters, as the area of the filter, which is measured, is synonymous with representatively in the case of imaging, and time is the variable that

needs to be optimized. This means that the resolution and timeframe of the mapping process is set to match the “single point measurement at each particle” strategy.

Even so, assuming that a filter contains only 200 000 particles and one spectrum is acquired in the center of each particle, sample analysis would still take N (number of particles, i.e. 200 000) * t (acquisition time e.g. 20 s) = 47 days. Thus, a subsampling on the filter is a requirement for feasible MP analysis. There are currently many subsampling schemes [5, 6, 22]. However, it has not been determined, which strategy yields the most accurate extrapolation. A random sampling tool was implemented into the software to allow a sample reduction according to Anger and von der Esch et al. 2018 [9], the csv output file generated by *TUM-ParticleTyper* can be used to extract the particle coordinates for any selection scheme.

In this project, it was our objective to create a particle detection software that operates on Raman microscopy, fluorescence microscopy and scanning electron microscopy (SEM) images. Furthermore, the goal was to deliver calibration and validation tools for the particle detection within the images. The validation protocol should be generally applicable and transferrable to the output of any other particle detection software. For Raman microspectroscopy, an additional validation addressed the often-used single point measurement approach for chemical characterization. Further, to reduce the overall measurement time, it was our goal to implement a subsampling routine into the software. To show the prospects and limits of our automated morphological and chemical characterization routine, we subsequently applied it to a washing machine water sample.

The paper was split into three parts: 1) The main text, which informs on the general analysis routine and highlights the strengths and challenges of *TUM-ParticleTyper*. 2) The supplementary information, which gives details on the experiments conducted for the development, calibration, and validation of the program. 3) The software documentation, which gives details on the program itself and highlights the functions used for the particle detection. The program documentation, the *TUM-ParticleTyper* software and test images are available freely in our GIT repository [23]. This partitioning of the publication was necessary so that each target group can easily find

the necessary information for their purpose 1) general information 2) and 3) for the reproduction of our results and for the application of *TUM-ParticleTyper*. Furthermore, it enabled us to write an interactive documentation, where the functions of our program can easily be looked up, while coding.

3.2 MATERIAL AND METHODS

ROUGHNESS TESTING FOR THE DEVELOPMENT OF FILTER HOLDERS

To define a parameter to optimize the smoothness of filters as prerequisite for optimal focus in FTIR or Raman spectroscopy, the flattening potential of different filter fixation techniques was evaluated by measuring the maximum peak-to-peak distance. This is the distance of the highest to the lowest pixel on the surface: the smaller this distance is, the smoother is the surface and the better the fixation method. For details, we refer to the full procedure in the SI section 1.1.

PRODUCTION OF REFERENCE MATERIALS FOR THE DEVELOPMENT OF THE IMAGE PROCESSING PROGRAM AND OPTIMIZATION OF IMAGE ACQUISITION PROCEDURES

Reference materials were produced by ultrasonication of solid polymers and filtrated onto gold coated polycarbonate filters [24]. The filters carrying the reference materials were then used to optimize the camera settings of the Raman microscope (*alpha300R* Raman Microscope, WITec GmbH, Germany) and the scanning electron microscope (*Sigma 300 VP*, Carl Zeiss AG, Germany).

The most important parameters when producing images for the characterization of particles are 1) contrast, 2) definition, 3) resolution, and 4) color range of the image. The settings used for Raman microscopy, fluorescence microscopy and SEM can be found in the SI section 1.2.

ACQUISITION OF CHEMICAL INFORMATION VIA RAMAN MICROSPECTROSCOPY

Chemical information can be acquired by measuring Raman spectra and comparing the spectra with a database. For this study, spectra at a single position (particle centers determined by *TUM-ParticleTyper*) were measured as well as maps, which combine many short measurements at specified distances to create a chemical image according to the procedure developed by K  ppler et al. 2016 [25]. For details, we refer to the full procedure in the SI section 1.3.

FIBER DETECTION IN WASHING MACHINE WATER

To test the applicability of our particle localization and characterization program, a washing machine sample was deposited on a filter and processed with *TUM-ParticleTyper*. The goal was to determine how many textile microfibers were present in the sample and to characterize them chemically via Raman spectroscopy. For details, we refer to the full procedure in the SI section 1.4.

3.3 RESULTS AND DISCUSSION

MORPHOLOGICAL AND CHEMICAL ANALYSIS OF MP REFERENCE MATERIALS VIA *TUM-PARTICLETYPER*

FLAT FILTER SURFACES AS A PREREQUISITE FOR OPTIMAL FOCUS

A smooth surface is a prerequisite for optimal focus in a confocal measurement with Raman microspectroscopy [9]. One possibility to achieve this is to use inherently stiff filter materials like silicon wafers [12]. However, silicon wafers are expensive and show a very strong Raman signal, which may interfere with the identification of MP. Therefore, a subtraction of the silicon signal from all spectra before a database matching is required. Alternative filter materials were tested by Ossmann et al. 2017 [11], who found aluminum-coated polycarbonate filters to have the lowest interference in the recorded particle spectra. Furthermore, they found that the

particles are best visualized using darkfield illumination delivering highly defined and high contrast images of particles down to 1 μm [11]. As alternative gold coated polycarbonate filters can be used for Raman and infrared spectroscopy [6, 26]. To combine both a smooth surface and low signal interference, a series of filter holders was developed (Fig S1.) and tested with commercially available gold-coated polycarbonate filters. After optimization the roughness, which was expressed as the distance of the highest to the lowest part of the filter on 12 mm \times 12 mm area could be reduced from originally 63.1 μm to 5.8 μm , which is comparable to a silicon wafer (details in SI section 2.1).

LOCALIZATION AND MORPHOLOGICAL CHARACTERIZATION OF PARTICLES WITH *TUM-ParticleTyper*

Independent of the original image (fluorescence, optical, or SEM), the *TUM-ParticleTyper* delivers three outputs. First, an overlay of the original image with the extracted contours is created. Therefore, the user can see what particles were recognized and roughly assess the success of the automatic particle detection. This is not to be confused with a proper validation. Second, a black and white image with all detected particles is generated. This can be used to transfer the particle detection information into any other software using an automatic thresholding technique, as only black and white pixels exist. For example, the user can combine the *TUM-ParticleTyper* localization with the automated measurement of the *Witec ParticleScout* or any software that allows the import of images and the assignment of a space transformation. Third, should a graphical input not be possible the *TUM-ParticleTyper* delivers a csv file that contains the measurement coordinates and the morphological features of the detected particles (*Figure 20*). If the system (fluorescence microscope, Raman microscope, FTIR microscope or SEM) has a way of importing coordinates via csv, this is how coordinates can be assigned for subsequent Raman, FTIR, or EDX measurements. We decided to create this set of outputs rather than trying to control any measurement devices directly. This has the benefit that if

the measurement device can load images or csv files the particle locations can be transferred to it.

#	cx	cy	area	diameters_min	diameter_max	classification
1	-1662.6	-7995.5	122.5	10.0	21.0	Particle
2	-3947.9	-7994.6	128.5	10.0	16.0	Particle
3	3251.4	-7992.7	279.5	16.0	27.0	Particle
4	1118.1	-7993.4	191.0	17.0	18.0	Particle
5	-2074.1	-7991.2	381.0	18.0	27.0	Particle
6	4406.7	-7991.4	487.0	20.0	37.0	Particle
7	792.5	-7992.6	464.5	20.0	41.0	Fiber
8	3341.5	-7999.0	1402.5	21.0	135.0	Fiber
9	2128.4	-7989.4	320.0	21.0	21.0	Particle
10	-2991.3	-7991.1	1897.0	21.0	167.0	Fiber
11	-4613.4	-7989.4	148.0	13.6	22.9	Particle
12	-4093.1	-7988.9	319.0	24.0	25.0	Particle
13	1956.5	-7990.4	935.0	26.0	66.0	Fiber
14	1438.4	-7988.0	486.5	26.0	26.0	Particle

Parameter for Raman Measurement

Morphological data

Automated classification

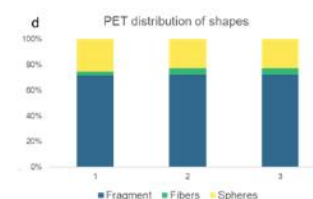
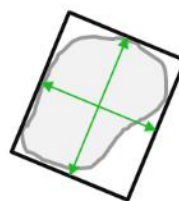
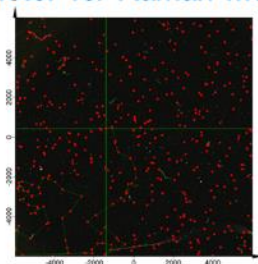


FIGURE 20: TUM-PARTICLE TYPER OUTPUT. PARAMETERS NEEDED FOR A SUBSEQUENT RAMAN MEASUREMENT (BLUE BOX); MORPHOLOGICAL DATA (GREEN BOX) REPRESENTED BY THE AREA (PIXEL THAT EXCEED THE BRIGHTNESS THRESHOLD WITHIN THE DETERMINED CONTOUR); DIAMETERS MIN/MAX (DETERMINED BY THE FERET'S METHOD, MEANING THAT THE WIDTH AND LENGTH OF THE SMALLEST POSSIBLE BOX THAT ENCLOSES THE CONTOUR YIELD THE DIAMETERS); THE CLASSIFICATION IN PARTICLES AND FIBERS (PURPLE BOX).

The challenge for any particle detection software is to automatically identify the contours of all particles and fibers depicted in the image that match the user's input specifications. To this end, the image is first transformed into gray scale. Thereafter often a global thresholding method (like *Otsu* [15, 27]) is applied to the image. This might lead to different results in different parts of the image if the lighting or the background is inhomogeneous. In addition, since not all particles share the same gray values (some appear darker, some appear lighter), global thresholding will not result in optimal outcome. Even though increasing contrast and brightness could separate the image strictly into black and white so that the use of a global threshold could work

in theory, the parametrization is difficult in practice. Enhancing the contrast and brightness too much also increases the noise in the image, which is then detected as particles leading to artefacts. Furthermore, the hard-coded parameters are not very well generalizable and different settings, in which the optical image was taken, might lead to different qualities of particle detection. This issue is illustrated by Anger and Prechtel et al. 2019 [15], who presented an open source software package based on *Otsu's* algorithm, which was built to enable detection and morphological characterization of particles. A common workaround for this problem is to implement features into the program where the user can adjust contrast, brightness or the threshold itself. However, as Prata et al. 2019 pointed out this approach, while sometimes effective, leads to non-reproducible results. An example image that challenges these adjustments is the following SEM image (Fig. 2).



FIGURE 21: WHEN IMAGE ENHANCEMENT FAILS. ORIGINAL SEM IMAGE OF PS SPHERES OF NOMINALLY $D=80$ NM (A); SEM IMAGE WITH SLIGHTLY ENHANCED CONTRAST AND BRIGHTNESS (B); SEM IMAGE WITH STRONGLY ENHANCED CONTRAST AND BRIGHTNESS (C).

As can be seen in *Figure 21* the particles at the bottom of the image become better visible when increasing the contrast and the brightness of the image slightly, whereas the particles at the top are still not recognizable. Only when enhancing them further do they become apparent, but at the price of a greater noise in the lower half of the image. This is the reason why a global-thresholding fails for these kinds of images. The logical consequence is to change the thresholding approach to suit the variable lighting conditions and the brightness range of the particles. Therefore, the global thresholding strategy was changed to an adaptive threshold, where only pixels in proximity influence the threshold in the *TUM-ParticleTyper* software. Our procedure

also starts with the transformation of the image into a gray scale image. Subsequently the contours are found by using an adaptive threshold with a Gaussian window [28]. The background interference problem is alleviated by blurring the image and then applying the adaptive threshold. The blurring is required to reduce the runtime of the particle detection and to prevent random noise from being falsely detected as particles. With this procedure, we were able to solve the problem, as can be seen in *Figure 22* (Further information on the program sequence can be viewed in the program documentation [23]).

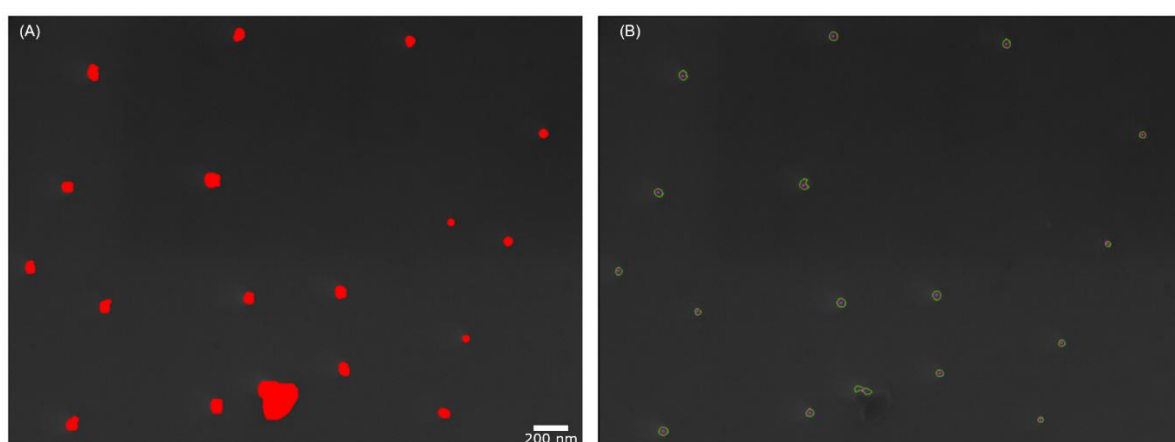


FIGURE 22: SUCCESSFUL PARTICLE DETECTION WITH TUM-PARTICLETYPER. SAMPLE SEM IMAGE WITH MARKED GROUND TRUTH IN RED (A) AND SEM IMAGE ANALYZED BY TUM PARTICLETYPYR (B).

Another challenge was that the area of the particles and the size of the Gaussian window influenced each other. A large Gaussian window resulted in excellent detection of large particles, but poor recognition of small particles. When the Gaussian window was small, the opposite effect was observed. For a more accurate detection, the image is analyzed twice, first with a large window to find the large particles only. The second run with the small Gaussian window focuses on the small objects only. This two-step process leads to 5 trainable hyperparameters: The neighborhood size and C-value (constant subtracted from the mean of the neighborhood) of each of the two thresholds and the size boundary between small and large objects. Their parametrization is described later. An overview is given in *Table 6*:

TABLE 6: TRAINABLE HYPERPARAMETER FOR THE ADAPTIVE THRESHOLD.

Name	Meaning	Effect	Typical Range
Neighbourhood Size small / large	The number of nearby pixels considered for the thresholding of each pixel.	Higher number of pixels: More accurate detection of larger particles. Worse detection of smaller particles. Smaller number of pixels: vice versa.	> 49 pixels for a large window > 9 pixels for a small window Scales with the resolution of the image
C-value small / large	A constant subtracted from the weighted mean of the neighbourhood pixels	Larger constant: smaller difference between brightness of object and brightness of background needed for a detection. Smaller constant: vice versa.	[-10; +10]
Size boundary	Decision boundary for which particles will be considered during the first run of the program and which in the second.	Higher number of pixels: Used when we expect the particles to be larger. Smaller number of pixels: Used when we expect the particles to be smaller.	> 50 pixels Scales with the resolution of the image.

The program generates and saves the input image in gray values, with contours of particles marked in green (particles detected by the first run with the large gaussian window) or yellow (particles detected by the second run small gaussian window) and contours of fibers marked in blue. Additionally, their centers are depicted. The analyzed example image can be seen in *Figure 23*.

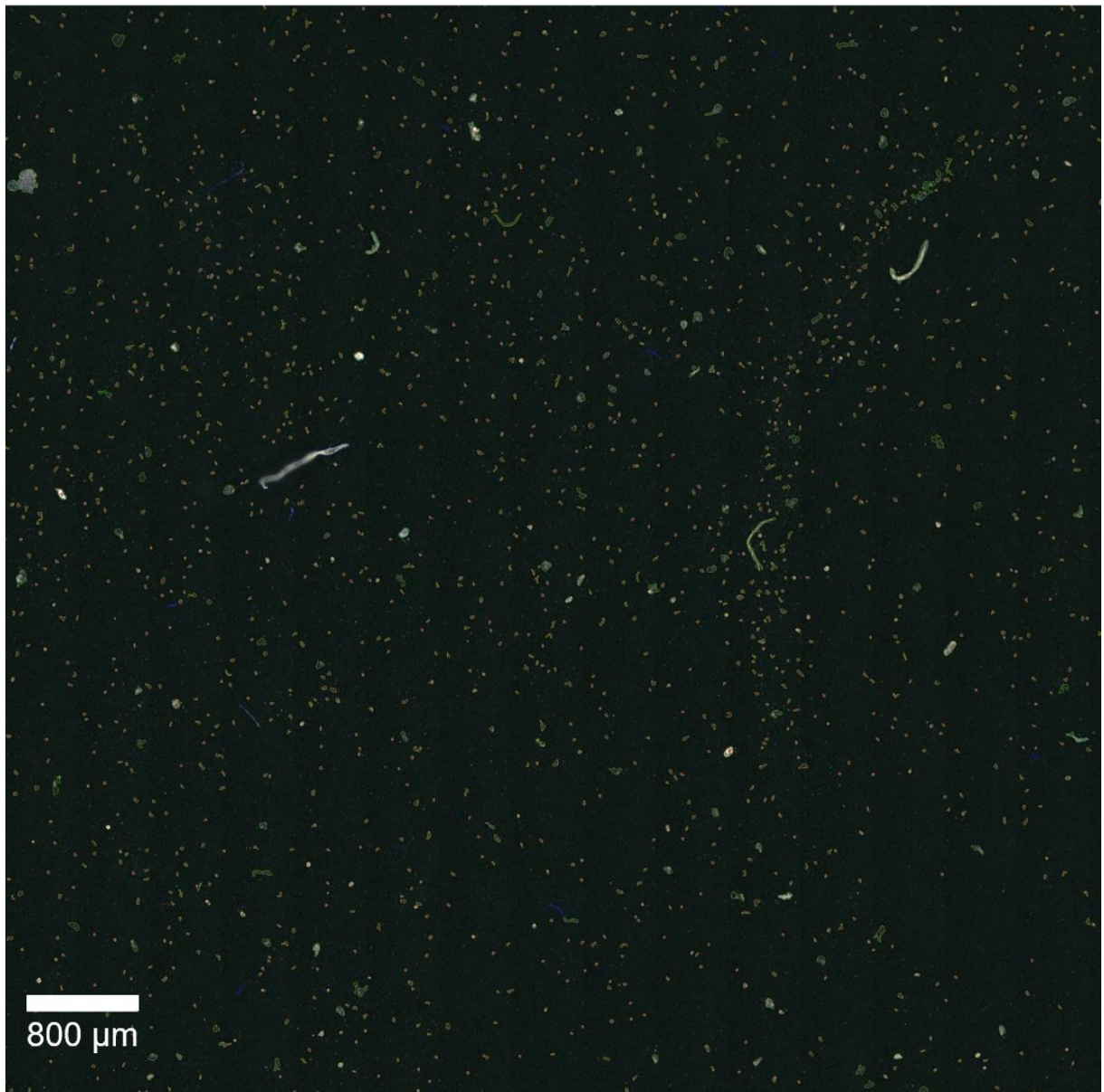


FIGURE 23: SAMPLE OPTICAL IMAGE FOR RAMAN ANALYZED BY TUM-PARTICLETYPER. FULL SCALE IMAGES CAN BE DOWNLOADED FROM OUR GIT REPOSITORY. [23]. THE SCALE BAR WAS ADDED AFTER PROCESSING, AS IT IS OTHERWISE RECOGNIZED AS AN OBJECT BY THE IMAGE PROCESSING SOFTWARE.

After all contours were extracted, the morphological characteristics for each particle could be calculated. For further characterization, the area, coordinates of the center, and Feret's diameters are required, as these yield the size distribution of the sample and enable us to classify the particle shape roughly in general categories (particle or fiber). This estimation was done by checking the ratio between the maximum and the minimum Feret's diameter to be larger than 2.0 and checking the ratio between the

product of minimum and maximum Feret's diameter and the area of the contour to be larger than 4.0. If either of these criteria is fulfilled, the object will be classified as a fiber, otherwise the object will be classified as a particle (further information in the documentation under challenges in the analysis). The centers of the particles are used for a subsequent Raman measurement in our case. One problem is however, that the center of a contour does not always lie within the contour (e.g. when the contour is bow-shaped) or lies inside of a hole within the contour (e.g. when the object is torus-shaped). An example can be seen in the following image (*Figure 24*).

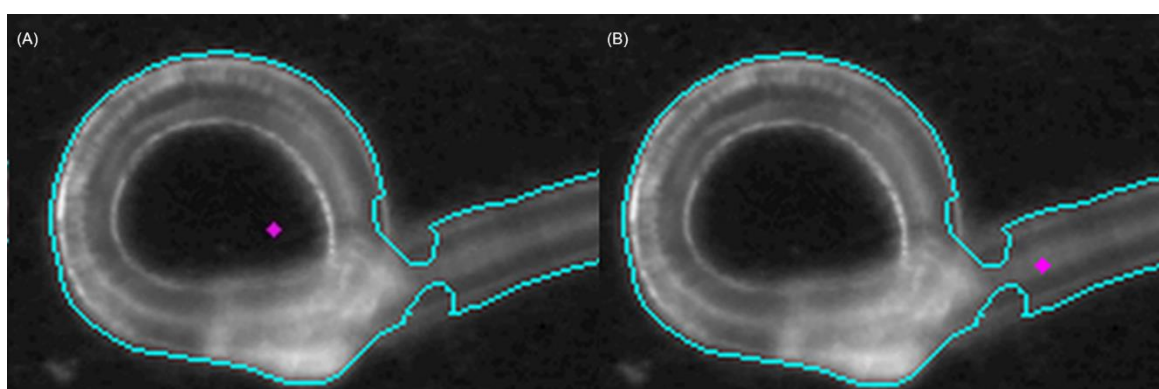


FIGURE 24: CENTER CORRECTION FOR CURVED FIBER. THE CONTOUR IS DRAWN IN TURQUOISE. ORIGINALLY CALCULATED CENTER (A). CORRECTED CENTER (B).

These cases can be detected firstly by checking the color of the pixel on which the center is positioned (a dark pixel indicates the background) and secondly by calculating the distance to the contour, which will be negative if the center lies outside of the contour and positive otherwise. Therefore, centers within holes, centers outside of contours or centers not far enough on the inside of a contour, will be drawn far inside of the contour by the program. This ensures that the laser does not miss the object or hits it just on its edge. Therefore, yielding a robust coordinate selection for the measurement of the particle's or fiber's spectrum.

Another challenge was the separation of particles that lie in proximity to each other or are agglomerated. An example of such situations is depicted in the following fluorescence image (*Figure 25*). The task was to selectively detect and quantify the dyed MP fragments, ideally by their respective color.

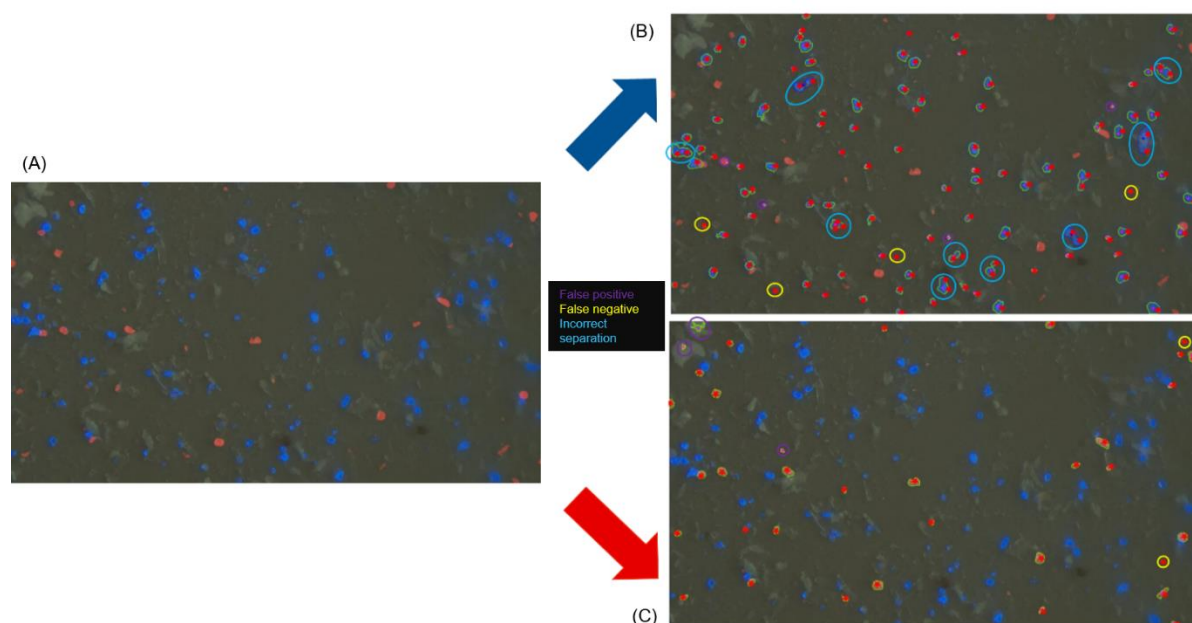


FIGURE 25: PARTICLE LOCALIZATION USING THE FLUORESCENCE CHANNELS. ORIGINAL FLUORESCENCE MICROSCOPY IMAGE BY HANNES IMHOF AND ASTRID BARTONITZ, TUM, AQUATIC SYSTEMS BIOLOGY UNIT (A). TUM-PARTICLETYPER OUTPUT FOR THE BLUE CHANNEL (B) AND FOR THE RED CHANNEL (C). ADDITIONAL PROCESSED IMAGES CAN BE FOUND IN THE REPOSITORY [23]. FALSE POSITIVES ARE MARKED IN PURPLE, FALSE NEGATIVES IN YELLOW AND INCORRECT SEPARATION IS MARKED IN BLUE. THE EXPERT PARTICLE ASSIGNMENT IS INDICATED THROUGH RED STARS. THE EVALUATION IS FURTHER DESCRIBED IN TABLE 7.

TABLE 7: EVALUATION OF THE PARTICLE LOCALIZATION USING THE FLUORESCENCE CHANNELS.

	Operator	TUM-ParticleTyper	False positive	False negative	Incorrect separation
Blue channel	106	96	4	4	20 in 9 inst.
Red channel	33	34	3	2	0

The filtering of colors is achieved through a preprocessing step. The analysis mode is used to select the RGB-color, all other color values are set to zero. Therefore, only particles with the fitting colors are distinguished from the black background. After the selection, the contrast and brightness are enhanced to ensure that the particles appear white after the transformation into gray values. For the fluorescence images automatic thresholding via *Otsu* was found to be suitable, so it was applied here while Raman and SEM images require the Gaussian window thresholding. Both the blue and

the red stained particles can be detected separately and a comparison between operator and *TUM-ParticleTyper* shows, that the program delivers reasonable results. In the processed images we see that the borders of the particles fit the contours of the particles very well and result in good size estimates. We could however not completely overcome the problem that grouped or agglomerated particles are detected as a large particle. In this instance 20 particles were detected as 9 particles, leading to a lower particle count by the *TUM-ParticleTyper*. Overall, we observe that the particle counts are similar but if we investigate the objects detected as particles, we do see differences between the operator and the software. Which is why not only the total particle number but also the false positives and false negatives should be considered during validation. As red and blue selective channels were already introduced into the software, a green selective channel was added to enable the preselection of microplastic through Nile red staining for subsequent Raman identification. Nile Red is a fluorescent dye that has been used to stain both pristine and aged microplastic [16, 29, 30]. While Shim et al. 2016 reported false positive and false negative staining of microplastic in the range of 100 μm – 300 μm , Erni-Cassola et al. 2017 found that all microplastics in the range of 20 μm – 1000 μm were stained by this dye ($n = 60$ overall, $n_{\text{polymer}} = 37$, negative control $n_{\text{nonpolymer}} = 23$). This makes fluorescent preselection for further IR or Raman analysis an attractive way to reduce the number of particles that need to be analyzed, if and only if, the method indeed provides an effective staining on environmental microplastic.

An alternative to reduce the sample size, by random sampling was also implemented. This feature selects an appropriately large subset of measurement targets according to the users specifications on the margin of error, confidence interval and estimated microplastic content of the sample [9]. The selection will then be exported into a separate file.

PARAMETRIZATION

A very important part of this project is the parametrization and validation of the program. To make sure that the program's output is as close as possible to a

predefined consensus value, it is necessary to tune the hyperparameters accordingly and to make sure that the program's error be as small as possible. To perform this parametrization, it was separated into different steps:

1. Creating the consensus value: To evaluate the program's performance and to adapt hyperparameters based on an error function, a consensus value is needed. Therefore, an expert manually analyzed seven images for each Raman and SEM and marked all particles and fibers in red. Using the "red_fluorescence" function of the program, it is easily possible to extract all needed information for each particle from the labeled images. The most important information hereby is the number and position of the particles.
2. Performing grid-search: A search over all five hyperparameters (neighborhood size small/large, C-value small/large and the size boundary) is performed. All combinations of hyperparameters within a certain range are tested using a predefined step size. A smaller step size results in a longer runtime of the search but ensures a thorough search. The result is the test of all possible combination of hyperparameters within the defined range. This range was not chosen arbitrarily but based on the experience of prior analysis using the program and in a way that analyses with useless results are omitted. Besides the program's usual output, the summed up area, summed up minimum *Feret's* diameters and the summed up maximum *Feret's* diameters of all particles of each image are saved.
3. Evaluating the grid-search results: After the grid-search, the best-performing hyperparameter sets are selected. This is done by comparing the mean of the relative errors of the number of found particles, the total size of all found particles and the sum of each particle's minimum and maximum *Feret's* diameter for each image. The mean of these four relative errors is used as a comparative value between all iterations of the grid search. A smaller value indicates a more accurate result.
4. Investigating the best results: The results of the elected hyperparameter sets are manually checked regarding the following classifications.

- a. True Positive: An object of the consensus value was detected at the same position as one object in the analysis
- b. False Negative: An object of the consensus value was not detected
- c. False Positive: An object was detected in the analysis with no corresponding object of the consensus value

Based on these steps the best performing hyperparameter set (neighborhood size small/large, C-value small/large and the size boundary) was chosen and implemented in the software. Since images of different use cases might vary, these values can be adjusted in the program code to fit the application. Additionally, the neighborhood sizes of the adaptive threshold scale with the resolution of the image, since the same particle occupies a different number of pixels in a low-resolution image and a high-resolution image, which means that also a different number of neighborhood pixels must be considered for the same result. Oftentimes the image's quality has a larger impact on the analysis than small variations within the parameters. As can be seen in *Figure 26*, with decreasing number of pixels to represent an image (hence decreasing resolution), the information contained in the image decreases and therefore the number of detectable particles decreases too, and the shapes of the detected objects are less detailed.

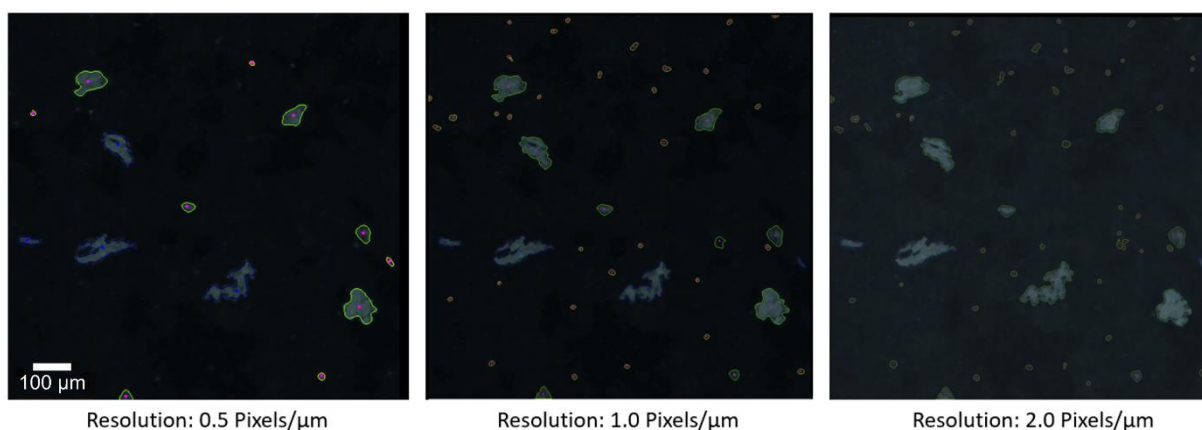


FIGURE 26: RESULTS OF THE ANALYSIS OF AN IMAGE WITH DIFFERENT RESOLUTIONS.

Furthermore, it is important to mention that there is no "perfect" parametrization. There are a lot of parameter sets that work well on the images and produce similar

results. But dependent on the image, the objects and the task, different parameters might lead to better results. During the evaluation of the particle assignment of two experts, we found that they produce deviant results, which is in accordance with Prata et al. 2019 [13]. Leading to the conclusion there is a margin in uncertainty / inaccuracy that can be tolerated when analyzing the optical images.

Example: For the first grid-search based on optical images for Raman, the results for the constraints we searched with (minPixels of 20, min Feret's diameter of 5 and resolution of 0.5 pixel/ μm) resulted in 171 false negatives (particles that were not detected) in all test images and showed that 62.6% occurred for object areas below 51 pixels, when using the best performing parametrization. The limit of a minimal area of 51 pixels for the successful detection is the limiting factor for the lowest detectable particle area but this area is relative to the resolution. Therefore, if smaller particles are to be detected a higher resolution is necessary. With our current setup we are limited to particles larger than 10 μm (*Figure 27*). By taking smaller images with the same objective we can distribute the maximal number of pixels (8000×8000) on a smaller area (e.g. $4000 \mu\text{m} \times 4000 \mu\text{m}$) creating a higher resolution (resolution = 2 pixel/ μm) image enabling the search for smaller particles.

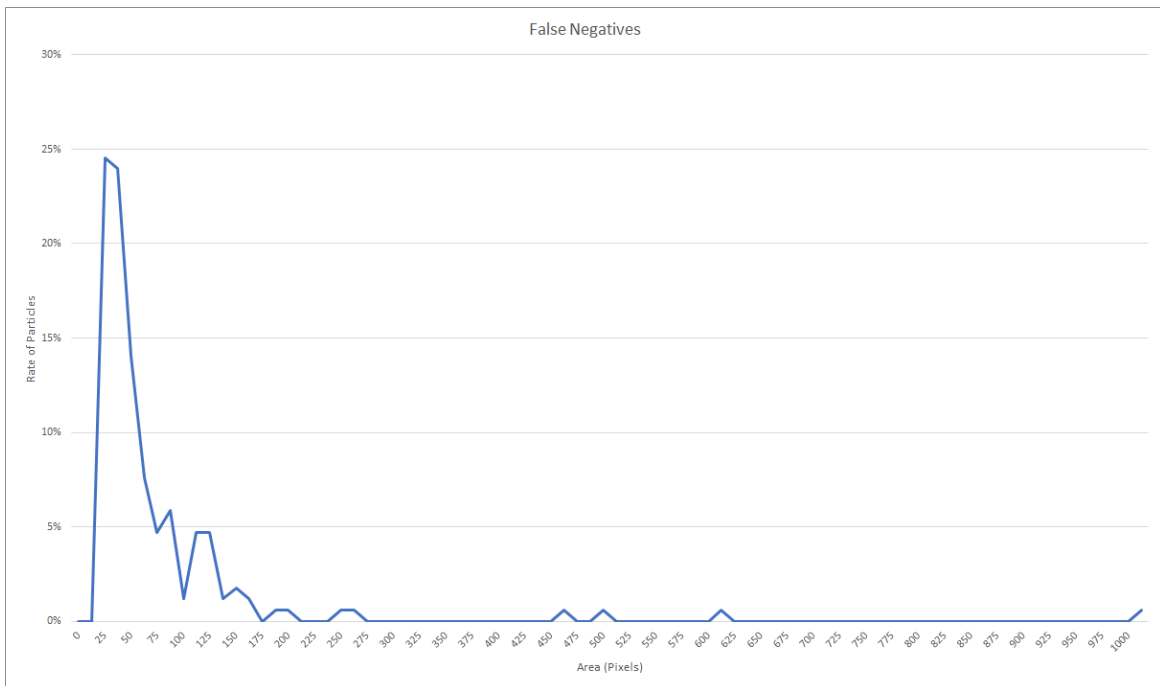


FIGURE 27: SIZE DISTRIBUTION OF PARTICLES NON DETECTED WITH TUM PARTICLETYPYER DURING PARAMETRIZATION OF OPTICAL IMAGES FOR RAMAN.

This implies that the *TUM-ParticleTyper* is limited regarding small particles. When reanalyzing the parametrization considering only objects larger than 50 pixels, the parametrization used above was still in the top 5 of best-performing parameters and the number of false positives decreased substantially. The other four top results had very similar parameters.

VALIDATION

For the validation of a program for image analysis and to ensure its functionality it is recommended to test its performance before the application. The performance was validated according to the following six factors for "performance evaluation in image processing" [19]:

- Accuracy: How well has the algorithm performed with respect to some reference?

The accuracy is covered during the parametrization step, when the program's performance is compared to the consensus value of the expert.

- Robustness: An algorithm's capacity for tolerating various conditions.

With the use of an adaptive threshold the algorithm can overcome inhomogeneous conditions in images (e.g. lighting). To test the algorithm's robustness, a real-life sample from a washing machine was analyzed. Even though the filter is overloaded with particles and dried foam, which built a cake on top of the filter, the *TUM-ParticleTyper* was able to detect fibers on this cluttered surface.

- Sensitivity: How responsive is the algorithm to small changes in features?

In general, the adaptive threshold works independent of the shape of the particle. It's size, however, is the most influential feature on the detection quality. When the user chooses the "minPixels" input-value too small, the algorithm might detect a high number of false positives and false negatives. It is therefore very sensitive to decreasing sizes of particles. However, this can be overcome by capturing high resolution images possibly also switching to higher magnification objectives and choosing values for "minPixels" accordingly.

- **Adaptability:** How well does the algorithm deal with variability in images?

The adaptability of the algorithm is demonstrated by the different modes (Raman, SEM and fluorescence) it can handle. Additionally, the program was tested for proper functioning not only with images taken in our own laboratory, but also with images from other publications and therefore from other cameras and camera setups. Since promising results were achieved, the program's ability to adapt to different images has been demonstrated.

- **Reliability:** The degree to which an algorithm, when repeated using the same stable data, yields the same result.

Since the algorithm is deterministic, every analysis of an image using the same parameters results in the same found contours. Additionally, tests with flipped, rotated and cropped images were performed. They all generated the same results. Deviations only occurred at the edges of the cropped images since objects were cut-off and therefore the area or diameters did not fit anymore.

- **Efficiency:** The practical viability of an algorithm.

Since the program needs to handle large-size images, blurring the image before the extraction of contours ensures that small particles (noise) will be reduced or removed. This is important to guarantee an acceptable runtime. Since the algorithm focuses on particles starting at a certain size, the neglect of smaller ones is not a problem. To show the enormous improvement regarding the time of analysis, a comparison between the expert's time on creating the consensus value and the program's runtime was made on the test images for SEM. While the expert needed approximately 16 seconds to find and mark a particle, the program requires approximately 1 millisecond for each particle (on the developer's machine. Results may vary). This results in a speedup of a factor over 1500.

To show the program's validity, its results were not only compared to the data created by a single expert, but also to the estimate of a second expert and the detection using *Otsu*-thresholding as in [15]. Hereby, each detected object was classified into true positive (if it corresponds to a particle also identified by the expert) or false positive (if it was not identified by the expert). Additionally, the particles identified by the expert that do not have a correspondence in the analyzed image are classified as false negative. For each classification the rate regarding the total number of particles in each test image was calculated and averaged over all seven test images to weight each test image equally. The results can be seen in *Figure 28*.

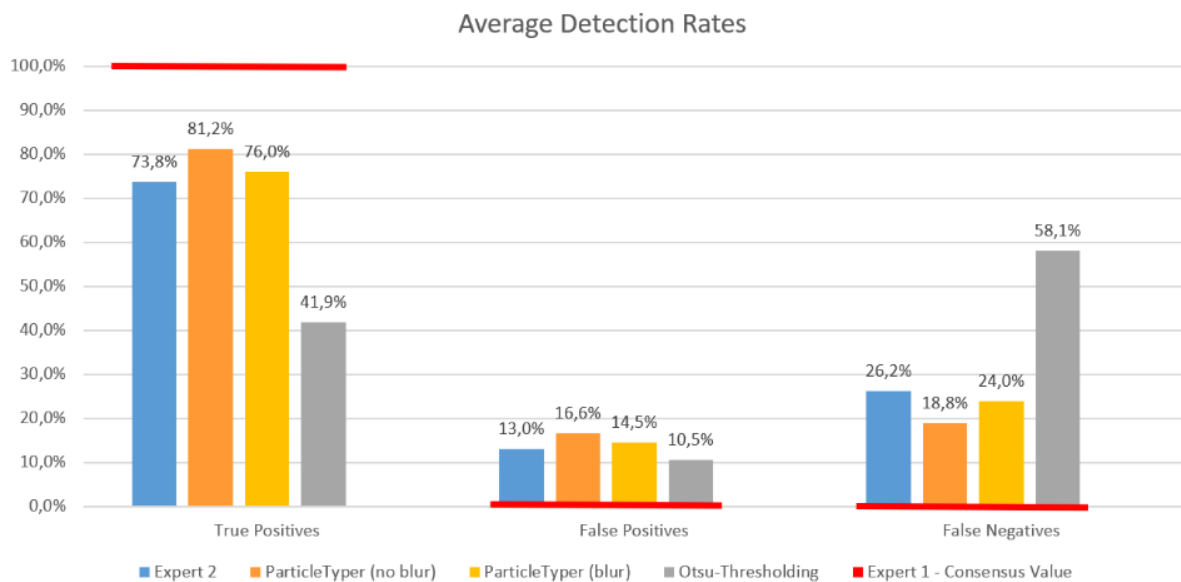


FIGURE 28: AVERAGE DETECTION RATES OF SECOND EXPERT, *TUM ParticleTyper* WITH AND WITHOUT BLUR AND A PROGRAM USING *Otsu*-THRESHOLDING COMPARED TO THE PARTICLES IDENTIFIED BY EXPERT ONE.

The *TUM-ParticleTyper* achieved detection rates that lie between the estimates of both experts for true positives and false negatives. With blurring the images, the accuracy is decreased, since the original data is altered beforehand and therefore information is lost. However, the impact is relatively minor, and it is necessary to guarantee an acceptable runtime. The software using *Otsu*-thresholding from [15] fails to detect many particles (58.1%) and is clearly outperformed. The rate of false positives for *TUM-ParticleTyper* is higher than the second expert and the *Otsu*-method. This has two reasons: First, the program is in general more sensitive than the

Otsu-method, which detected less objects in general. It has a smaller false positive rate, since it detects only the most characteristic parts of the image, which are clearly recognizable objects. The second reason is that oftentimes objects were indeed detected in a position where also expert one marked a particle but their areas oftentimes did not fulfill the criterium “minPixels” larger than 51 in expert one’s findings but did so in the analysis with *TUM-ParticleTyper* due to small inaccuracies in the exact extraction of the contour.

For the seven SEM test images (See Git repository [23]), outstanding detection rates were achieved: The best parameter set achieved a detection rate of 98.3% for the true positives, accordingly 1.7% for the false negatives and only a false positive rate of 2.9%. Compared to the results from the Raman images these rates are remarkably good. However, as mentioned above analyzing too complicated SEM images may result in worse rates, due to their more complex nature.

All in all, the analysis with *TUM-ParticleTyper* generates solid results within the margin of the error of the two experts and can therefore be considered as valid alternative. The validation protocol applied here can generally be used to evaluate the performance of an image processing program.

METHOD COMPARISON OF THE SINGLE POINT APPROACH VS. IMAGING

An alternative to the single point measurement of particles (localization and measurement of particles at their centers) is the imaging of filter areas to analyze all particles therein, by clustering the resulting spectra and calculating the size of the particles based on the spectral signature. This approach is prominently used for the automated μ -FTIR analysis [17, 18, 26, 31] of microplastics but can also be applied for Raman microspectroscopy as demonstrated by K appler et al. 2016 [25]. One of the drawbacks of the mapping approach is that large datasets (~ 30 GB) are created and need to be processed for spectral identification. The supposed advantage of the imaging procedure is that no particles are overlooked and that there are multiple

spectra for each particle, which can be averaged to yield a clean spectrum. The single point approach on the other hand only considers one measurement position per particle, but the integration time is longer for each measurement resulting in a higher signal to noise ratio for the specific point that is measured. In our approach, a maximum of 7000 particles is analyzed resulting in a much smaller dataset and faster analysis (~315 MB for 7000 spectra). The comparison of a mapping and a single point measurement for an area of 1 mm² is shown in *Figure 29*. In order to validate the extreme reduction of measurement points in the single particle approach, particles were localized with *TUM-ParticleTyper* and multiple measurements were performed for each particle to see if all measurement points on one particle yield equal results regardless of their position, thus proving that one point is sufficient. As can be seen in *Figure 29* most measurement points yield the same spectrum for each particle. The spectra acquired within the boundaries of the particle differ solely by the achieved hit quality indices (HQI) but would have led to the identification of the particle in an average of 82% of all cases, even when the points are close to the boundary. Comparing these findings to images from μ -FT-IR imaging, it becomes clear that the signal intensity of the spectrum is highest in the particle center and decreases towards the edges [18, 31]. Furthermore, refractive errors occur for irregularly shaped materials [32] which introduces artefacts to the spectra and may lead to an underestimation of particle size, as these spectra are difficult to classify. To determine the influence of the measurement position on the HQI we correlated it to the distance of the measurement position in reference to the point, where the highest HQI was determined. The result of this analysis is that the HQI decreases when the distance to the particle center increases, which is consistent with the observations for μ -FT-IR imaging [18, 31]. When comparing our results from Raman imaging and Raman single point measurements it becomes clear that this effect will be even more pronounced when short integration times are needed for the acquisition of spectra. In our Raman images we see that less particles (7 out of 13) were identified as poly lactide and that the particle size is severely underestimated, because the spectral quality of the boundary regions is so poor that it is not classified as PLA through clustering. Specifically, the combined total area of all particles from imaging yielded 35.47 mm²

for seven particles (incorrectly segmented particles were joined for this count) vs. 109.3 mm² for 13 particles that were chemically identified by single point measurements and morphologically characterized based on the evaluation of the optical microscopy image via *TUM-ParticleTyper*. This 82% difference in overall area could however be remedied by using a smaller step size and / or a longer integration time per scan, which would substantially increase the measurement time. With the parameters applied here a 1000 μm × 1000 μm area was measured in 2 h (3.3 times longer than the single point measurements referring to our Raman system). We conclude that neither imaging nor single point measurement is flawless but selecting single points based on particle recognition is a valid way to reduce the overall measurement time, In addition, the morphological characterization based on image processing of the microscopy image yields better results than the size estimation based on the spectral fingerprint.

Single point measurement more accurate and efficient than map for large areas

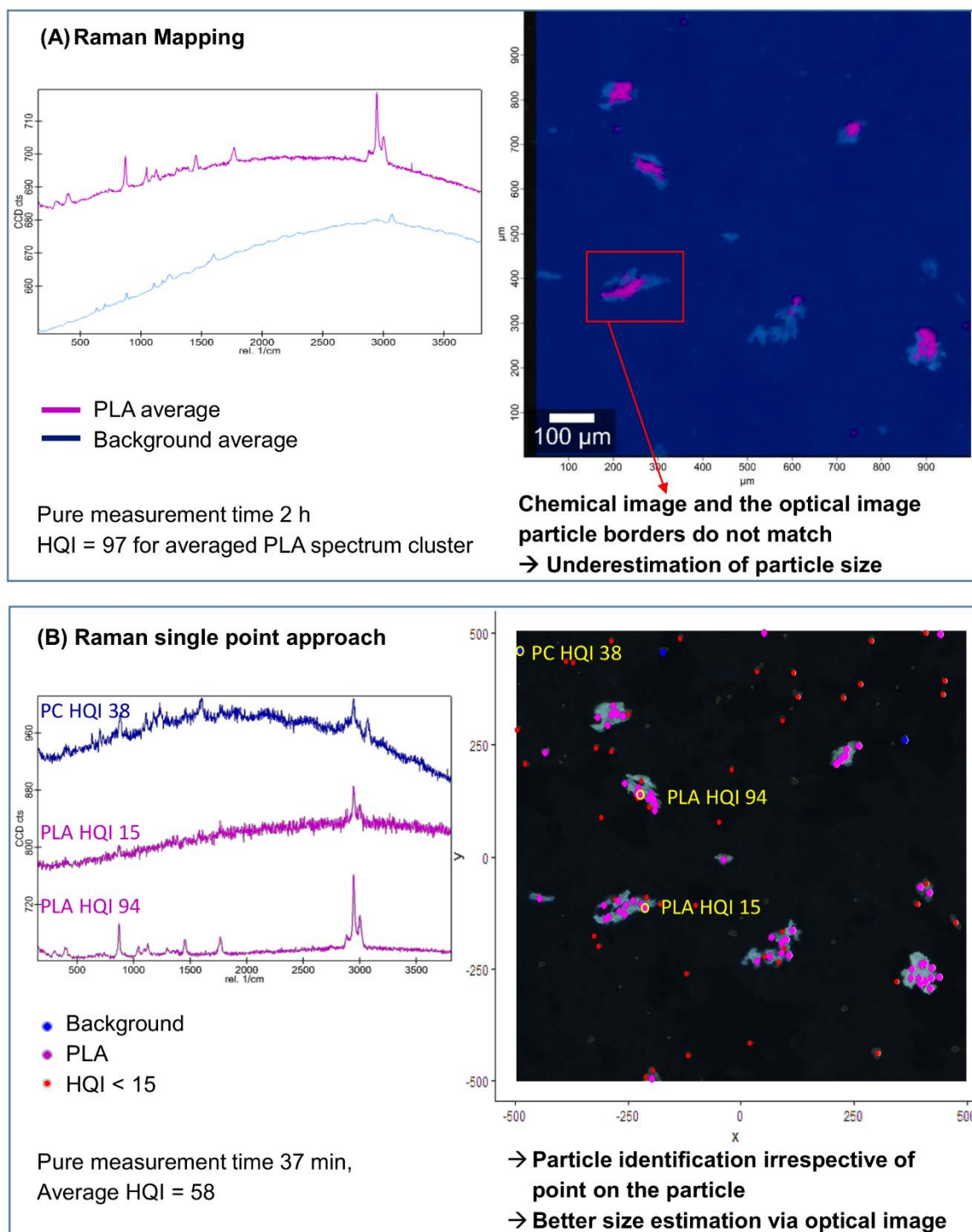


FIGURE 29: COMPARISON OF RAMAN MAPPING VS RAMAN SINGLE POINT MEASUREMENT IN THE SAME $1000 \times 1000 \mu\text{m}$ SQUARE OF A PLA REFERENCE SAMPLE, WITH THE GOAL TO ANALYZE THE AREA IN A SIMILAR PERIOD. MAPPING WITH, $10 \mu\text{m}$ STEPS 5 mW, 500ms/SCAN 532 NM LASER 20 \times MAGNIFICATION (A). MEASUREMENT OF MULTIPLE POINTS ON A PARTICLE TO DETERMINE IF ALL POINTS ON A PARTICLE ARE EQUALLY REPRESENTATIVE, WITH 3 mW, 4 \times 5s/SCAN 532 NM LASER, 20 \times MAGNIFICATION (B).

PURPLE INDICATES THE PRESENCE OF THE TARGET PLA, BLUE INDICATES THE PREVALENCE OF THE BACKGROUND POLYCARBONATE SIGNAL FROM THE FILTER. ALL SPECTRA THAT COULD NOT BE IDENTIFIED ARE MARKED RED. FOR LARGE AREAS, SINGLE POINT MEASUREMENTS ARE BOTH EFFICIENT AND REPRESENTATIVE.

HOW COMPLEX MAY IMAGES BE TO ALLOW FOR SUCCESSFUL ANALYSIS?

APPLICATION TO A REAL SAMPLE FOR FIBER DETECTION IN WASHING MACHINE WATER

To prove that *TUM-ParticleTyper* is also able to handle very complex images, microplastic analysis was conducted in a sample of washing machine water. The aim was to detect fibers originating from synthetic clothing treated in the washing step. After the localization and morphological characterization via *TUM-ParticleTyper* 2000 of 4000 found fibers were analyzed. Thereof 320 could be automatically assigned via *TrueMatch*, and additional 109 fibers could be identified via manual assignment. The segmentation of the particles is shown in *Figure 30*. Due to matrix interference from dried detergent on the filter surface it is difficult to manually locate fibers. In the processed image the particle counts may not be reliable anymore, as there are too many particles on the filter surface and they are therefore detected as aggregates. The fibers on the other hand can still be localized. This shows that also complex samples can be morphologically analyzed via *TUM-ParticleTyper*. However, since the success of the particle detection critically depends on the quality of sample treatment and of the image, it is recommended to validate the performance for each sample type, image acquisition setup and research question.

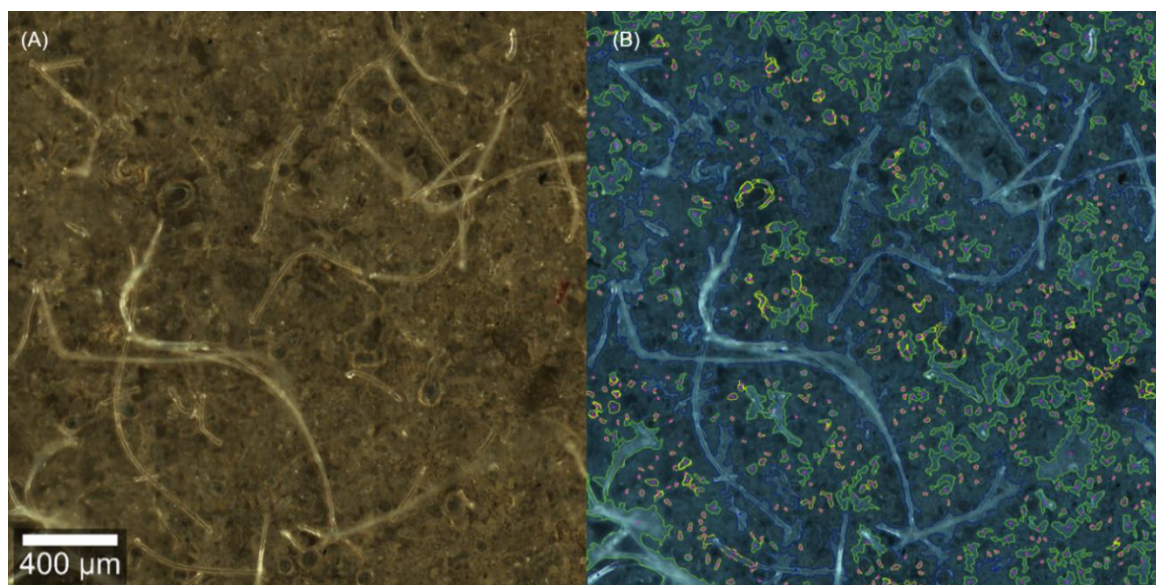


FIGURE 30 SEGMENTATION ACCURACY FOR SAMPLES WITH INTENSE MATRIX BACKGROUND. ORIGINAL IMAGE (A), PROCESSED IMAGE (B). FIBERS ARE MARKED IN BLUE, PARTICLES ARE MARKED IN GREEN, BUT WERE IGNORED FOR THE CHEMICAL IDENTIFICATION, AS HERE THE FOCUS WAS ON FIBERS.

CHALLENGES IN THE ANALYSIS

Despite the program's successful performance, a few challenges remain to be resolved in further improvements. The first are holes in contours. As mentioned earlier, the program has an algorithm to move the center away from such holes to the inside of a particle (e.g. for torus-shaped particles). Nevertheless, the hole affects the calculated area of the particle, since the hole's area cannot be calculated and subtracted easily.

A second challenge are long fibers that shape a ring. The contour might contain a huge area that is not part of the fiber, but which is nonetheless considered in the calculation of the area. Here Primpke et al. 2019 proposed the determination of fiber sizes using a skeletonize function which is superior to our fiber size estimation [33].

A third issue is the detection of agglomerated particles. Since the algorithm for contour detection cannot separate agglomerates, particles that overlap or adjoin to each other are detected as one contour and therefore as one particle. Usually an approach using a watershed algorithm allows the separation of agglomerates, but the

images also contain fibers. Watershed has a poor performance on fibers and separates them into several small fractions [15]. It is therefore not suitable and not implemented so that agglomerates remain a restriction in the program.

As fourth aspect, the *TUM-ParticleTyper* can have a weak performance when the minimum area is chosen too small. Even though blurring usually removes noise, false positive detections still occur more frequently for smaller minimum sizes. Finally, SEM images can contain bright and dark objects, but only the performance on images with only bright ones can be regarded as satisfactory. An approach to overcome this challenge is the inversion of the colors of the image. Dark objects then appear as bright objects and can be detected in a second analysis.

A general problem is the fact that the program's performance can only be validated in relative terms. There are no images with perfectly extracted particles available that would provide a defined true value. The only ways to assess the performance is to manually evaluate the image and assign a consensus value, considering that even the particle detection by two experts does not yield the same result. If the program's output is within an acceptable range of deviation from this consensus value, we can consider it as functioning properly.

3.4 CONCLUSION AND OUTLOOK

TUM-ParticleTyper is an open access image processing tool for the morphological characterization of particles in optical-, fluorescence and scanning electron microscopy images. It is the first such tool that can be calibrated to fit the camera system of the user, the requirements of the analysis, as well as the complexity of the sample. The essential part of the work presented here was not only the development of such a tool but also the development of validation protocols for the particle localization with *TUM-ParticleTyper* and the sample reduction from full filter imaging to single point measurements at the particle centres. It is recommended to prepare a test sample, to analyse it with the *TUM-ParticleTyper* and to parallelly do a manual particle identification, by marking all particles in red. The found particle number,

mean area and Feret's diameters should be compared to get a rough quality assessment, but it is important to assess the true positives, false positives and false negatives as described in the protocol presented here to assess the accuracy. As demonstrated a 100 % accuracy is not possible to achieve with complex samples as even the assessment of two experts deviates by ~30 %, which is why no ground truth can be found for the assessment only a consensus value. The protocol can be transferred to alternative systems and programs for quality control, enabling users to check their current or future analysis protocols. To enable such an analysis, the sample surface must be as flat as possible. Therefore, a filter holder was developed, produced and characterized. With the setup brought forward here, we advance Raman microspectroscopy analysis of microplastic particles to accomplish a routine, size-resolved chemical quantification of particles down to a size limit of 10 μm . Further efforts will need to concentrate on pushing this boundary towards the detection of even smaller particles.

Conflict of Interest

The authors declare that the research was conducted in the absence of any commercial or financial relationships that could be construed as a potential conflict of interest.

Author Contributions

EE, AK, ME and NI, designed the experiments and agreed upon the requirements for *TUM-ParticleTyper*. EE collected the Raman microspectroscopy data required for the program development by producing the reference materials and testing the parametrization of the Raman microscope, as well as the particle detection program in an iterative process. The implementation of the image processing functions was done by AK. The validation of the particle localization was done by AK (development of grid search approach and evaluation of the Results), EE and PA (expert image assessment). RH designed and built the filter holders. PA validated the filter holders. All authors discussed the results and contributed to the final manuscript.

Funding

Funding by the Bayerische Forschungsstiftung (<https://www.forschungsstiftung.de/>) for the Project MiPaq "Microparticles in the aquatic environment and in foodstuffs" are biodegradable polymers a conceivable solution to the "microplastic problem"?, AZ-1258-16 is gratefully acknowledged.

Funding by the German Federal Ministry of Education and Research <https://www.bmbf.de/> for the Project MiWa – Microplastic in the water cycle, 02WRS1378C is gratefully acknowledged.

Furthermore, this work was supported by the German Research Foundation (DFG, <https://www.dfg.de/>) and the Technical University of Munich, within the funding program Open Access Publishing.

Acknowledgments

We would like to thank Christian Schwaferts for providing SEM images, Hannes Imhof, Sebastian Beggel and Astrid Bartonitz for providing fluorescence microscopy images, Marco Sallat for providing the washing machine sample and Lisa Göpfert for helpful discussions.

Supplementary Material

Supplementary information for Materials and Methods

Roughness testing for the development of filter holders

Image acquisition procedures for optical, fluorescence and scanning electron microscopy

Acquisition of chemical information via Raman microspectroscopy

Fiber detection in washing machine water

Supplementary information for Results and discussion

Flat filter surfaces as a prerequisite for optimal focus

Figure 1: Exploded view of the filter holder a), massive filter holder for filters with diameters of around 25 mm b), schematic drawing of the filter holder c), filter holder with opening in

the center for filters with diameters of around 25 mm d), constructed at the Institute of Hydrochemistry

Table 1: Comparison of peak-peak distances for clean gold-coated polycarbonate filters with a diameter of 25 mm; mean and standard deviation were calculated from triplicate TrueSurface measurement of one filter.

Data Availability Statement

Data are in the TUMmedia repository: Kohles AJ, von der Esch E, Anger PM, Hoppe R, Niessner R, Elsner M, et al. TUM-ParticleTyper: Software and Documentation. (<https://mediatum.ub.tum.de/1547636>) TUM 2020. doi: 10.14459/2020mp1547636

3.5 REFERENCES

1. Ivleva NP, Wiesheu AC, Niessner R. Microplastic in Aquatic Ecosystems. *Angew Chem Int Ed Engl.* **2017**;56(7):1720-39.
2. Dris R, Gasperi J, Saad M, Mirande C, Tassin B. Synthetic fibers in atmospheric fallout: A source of microplastics in the environment? *Mar Pollut Bull.* **2016**;104(1-2):290-3.
3. Eerkes-Medrano D, Thompson RC, Aldridge DC. Microplastics in freshwater systems: A review of the emerging threats, identification of knowledge gaps and prioritisation of research needs. *Water Res.* **2015**;75:63-82.
4. Catarino AI, Macchia V, Sanderson WG, Thompson RC, Henry TB. Low levels of microplastics (MP) in wild mussels indicate that MP ingestion by humans is minimal compared to exposure via household fibres fallout during a meal. *Environ Pollut.* **2018**;237:675-84.
5. Ossmann BE, Sarau G, Holtmannspotter H, Pischetsrieder M, Christiansen SH, Dicke W. Small-sized microplastics and pigmented particles in bottled mineral water. *Water Res.* **2018**;141:307-16.
6. Schymanski D, Goldbeck C, Humpf HU, Furst P. Analysis of microplastics in water by micro-Raman spectroscopy: Release of plastic particles from different packaging into mineral water. *Water Res.* **2018**;129:154-62.
7. Imhof HK, Laforsch C, Wiesheu AC, Schmid J, Anger PM, Niessner R, et al. Pigments and plastic in limnetic ecosystems: A qualitative and quantitative study on microparticles of different size classes. *Water Res.* **2016**;98:64-74.
8. Chae Y, An YJ. Current research trends on plastic pollution and ecological impacts on the soil ecosystem: A review. *Environ Pollut.* **2018**;240:387-95.
9. Anger PM, von der Esch E, Baumann T, Elsner M, Niessner R, Ivleva NP. Raman microspectroscopy as a tool for microplastic particle analysis. *Trends Anal Chem.* **2018**;109:214-26.
10. Renner G, Schmidt TC, Schram J. Analytical methodologies for monitoring micro(nano)plastics: Which are fit for purpose? *Current Opinion in Environmental Science & Health.* **2018**;1:55-61.
11. Ossmann BE, Sarau G, Schmitt SW, Holtmannspotter H, Christiansen SH, Dicke W. Development of an optimal filter substrate for the identification of small microplastic particles in food by micro-Raman spectroscopy. *Anal Bioanal Chem.* **2017**;409(16):4099-109.
12. K ppler A, Windrich F, Loder MG, Malanin M, Fischer D, Labrenz M, et al. Identification of microplastics by FTIR and Raman microscopy: a novel silicon filter substrate opens the important spectral range below 1300 cm⁻¹ for FTIR transmission measurements. *Anal Bioanal Chem.* **2015**;407(22):6791-801.

13. Prata JC, Reis V, Matos JTV, da Costa JP, Duarte AC, Rocha-Santos T. A new approach for routine quantification of microplastics using Nile Red and automated software (MP-VAT). *Sci Total Environ.* **2019**;690:1277-83.
14. L. Bittrich, Brandt J. GEPARD - Gepard-Enabled PARticle Detection for Raman microscopes. <https://gitlab.ipfdd.de/GEPARD/gepard>: Leibniz-Institut für Polymerforschung Dresden e. V.; 2018.
15. Anger PM, Pechtl L, Elsner M, Niessner R, Ivleva N. Implementation of an Open Source Algorithm for Particle Recognition and Morphological Characterisation for Microplastic Analysis by Means of Raman Microspectroscopy. *Anal Methods.* **2019**.
16. Erni-Cassola G, Gibson MI, Thompson RC, Christie-Oleza JA. Lost, but Found with Nile Red: A Novel Method for Detecting and Quantifying Small Microplastics (1 mm to 20 µm) in Environmental Samples. *Environ Sci Technol.* **2017**;51(23):13641-8.
17. Simon M, van Alst N, Vollertsen J. Quantification of microplastic mass and removal rates at wastewater treatment plants applying Focal Plane Array (FPA)-based Fourier Transform Infrared (FT-IR) imaging. *Water Res.* **2018**;142:1-9.
18. Primpke S, Lorenz C, Rascher-Friesenhausen R, Gerdts G. An automated approach for microplastics analysis using focal plane array (FPA) FTIR microscopy and image analysis. *Anal Methods.* **2017**;9(9):1499-511.
19. Wirth M, Fraschini M, Masek M, Bruynooghe M. Performance Evaluation in Image Processing. *EURASIP J ADV SIG PR.* **2006**;2006(1).
20. Udupa JK, Leblanc VR, Zhuge Y, Imielinska C, Schmidt H, Currie LM, et al. A framework for evaluating image segmentation algorithms. *Comput Med Imaging Graph.* **2006**;30(2):75-87.
21. Ogunola OS, Tahavamani P. Microplastics in the Marine Environment: Current Status, Assessment Methodologies, Impacts and Solutions. *Journal of Pollution Effects & Control.* **2016**;04(02).
22. Huppertsberg S, Knepper TP. Instrumental analysis of microplastics-benefits and challenges. *Anal Bioanal Chem.* **2018**;410(25):6343-52.
23. Kohles AJ, von der Esch E, Anger PM, Hoppe R, Niessner R, Elsner M, et al. TUM-ParticleTyper: Software and Documentation. <https://mediatum.ub.tum.de/1547636>: TUM 2020.
24. von der Esch E, Lanzinger M, Kohles AJ, Schwaferts C, Weisser J, Hofmann T, et al. Simple Generation of Suspensible Secondary Microplastic Reference Particles via Ultrasound Treatment. *Front Chem.* **2020**;8(169).
25. Käßler A, Fischer D, Oberbeckmann S, Schernewski G, Labrenz M, Eichhorn KJ, et al. Analysis of environmental microplastics by vibrational microspectroscopy: FTIR, Raman or both? *Anal Bioanal Chem.* **2016**;408(29):8377-91.
26. Cabernard L, Roscher L, Lorenz C, Gerdts G, Primpke S. Comparison of Raman and Fourier Transform Infrared Spectroscopy for the Quantification of Microplastics in the Aquatic Environment. *Environ Sci Technol.* **2018**;52(22):13279-88.

27. Otsu N. A Threshold Selection Method from Gray-Level Histograms. *IEEE Transactions on Systems, Man, and Cybernetics*. **1979**;9(1):62-6.
28. Image Thresholding
https://docs.opencv.org/3.2.0/d7/d4d/tutorial_py_thresholding.html: Open Source
Computer Vision; **2016** [
29. Shim WJ, Song YK, Hong SH, Jang M. Identification and quantification of microplastics using Nile Red staining. *Mar Pollut Bull*. **2016**;113(1-2):469-76.
30. Maes T, Jessop R, Wellner N, Haupt K, Mayes AG. A rapid-screening approach to detect and quantify microplastics based on fluorescent tagging with Nile Red. *Sci Rep*. **2017**;7:44501.
31. Tagg AS, Sapp M, Harrison JP, Ojeda JJ. Identification and Quantification of Microplastics in Wastewater Using Focal Plane Array-Based Reflectance Micro-FT-IR Imaging. *Anal Chem*. **2015**;87(12):6032-40.
32. Bassan P, Kohler A, Martens H, Lee J, Byrne HJ, Dumas P, et al. Resonant Mie scattering (RMieS) correction of infrared spectra from highly scattering biological samples. *Analyst*. **2010**;135(2):268-77.
33. Primpke S, A. Dias P, Gerdt G. Automated identification and quantification of microfibrils and microplastics. *Anal Methods*. **2019**;11(16):2138-47.

GENERAL CONCLUSION AND OUTLOOK

Plastic is essential for modern life, especially in the packaging industry. However, when plastic gets into the environment and is exposed to UV light and mechanical stress, it can fragment into smaller particles. These are called microplastic particles and can be found in the environment and even in water from reusable polyethylene terephthalate (PET) bottles. [1, 2]

Before the start of this thesis, the automated measurement of microplastic was already possible. It was however, unclear how many measurements per sample are enough to ensure a representative result. Furthermore, a validation procedure for the chemical identification and morphological characterization of microplastic including the determination of a quantification limit wasn't established. [3]

To identify these important questions and to find a path towards answering them, the theoretical background of Raman microspectroscopy was summarized with respect to the microplastic field. From there a theoretical ideal procedure was laid out and planned (*Figure 31*). In the beginning, the focus was on how to produce a representative sample. A decisive, yet unresolved issue was: "How many particles must be analyzed to obtain a statistically significant result?" To answer this question a simple random sampling approach was adapted for the analysis of microplastic with Raman microspectroscopy. Thus, a minimum number of particles n required for an idealized measurement system can be calculated from the total number of particles N in the sample. This estimation only accounts for the error induced by the subsampling on the filter. Errors in the sample preparation that occurred before the fixation of particles on the filter cannot be estimated with this approach. However, it was possible to show that if small numbers of particles are present, measuring all particles is feasible and recommended. The subsampling approach only becomes a powerful tool if particle numbers are so high that measuring all particles becomes uneconomical. This is the case if 10 000 particles per sample are exceeded. The minimum subsample size is reached when the error stagnates and the further measurement of particles therefore does not notably reduce the error. Thus, it is no

longer necessary to measure each particle, since this consumes valuable time and the error does not improve much. Further, we exploit the law of large numbers, so the total number of particles becomes irrelevant for the minimum sample size, meaning, that 7 000 particles per sample is a good subsample size if the microplastic content is higher than 1% of total particles allowing an error of ± 0.1 irrespective of the total number of particles. It is however; of utmost importance to determine the total number of fragments to perform the selection of the subsample, as this process is only bias free if all particles within the sample have the same probability of being selected for the subsample. Should the determined microplastic content fall below 1% there are two options: The first is to randomly select additional particles for the measurement to ensure that the error interval can be upheld. The second would be to recalculate the error based on the known microplastic content.

In summary, this approach allows the required number of particles to be adjusted so that samples can be measured in feasible timeframes at the expense of the error margin e . Another advantage is that the e can be estimated without replication measurements. This provides robust criteria for future comparative studies to quantify microplastic in the environment.[4]

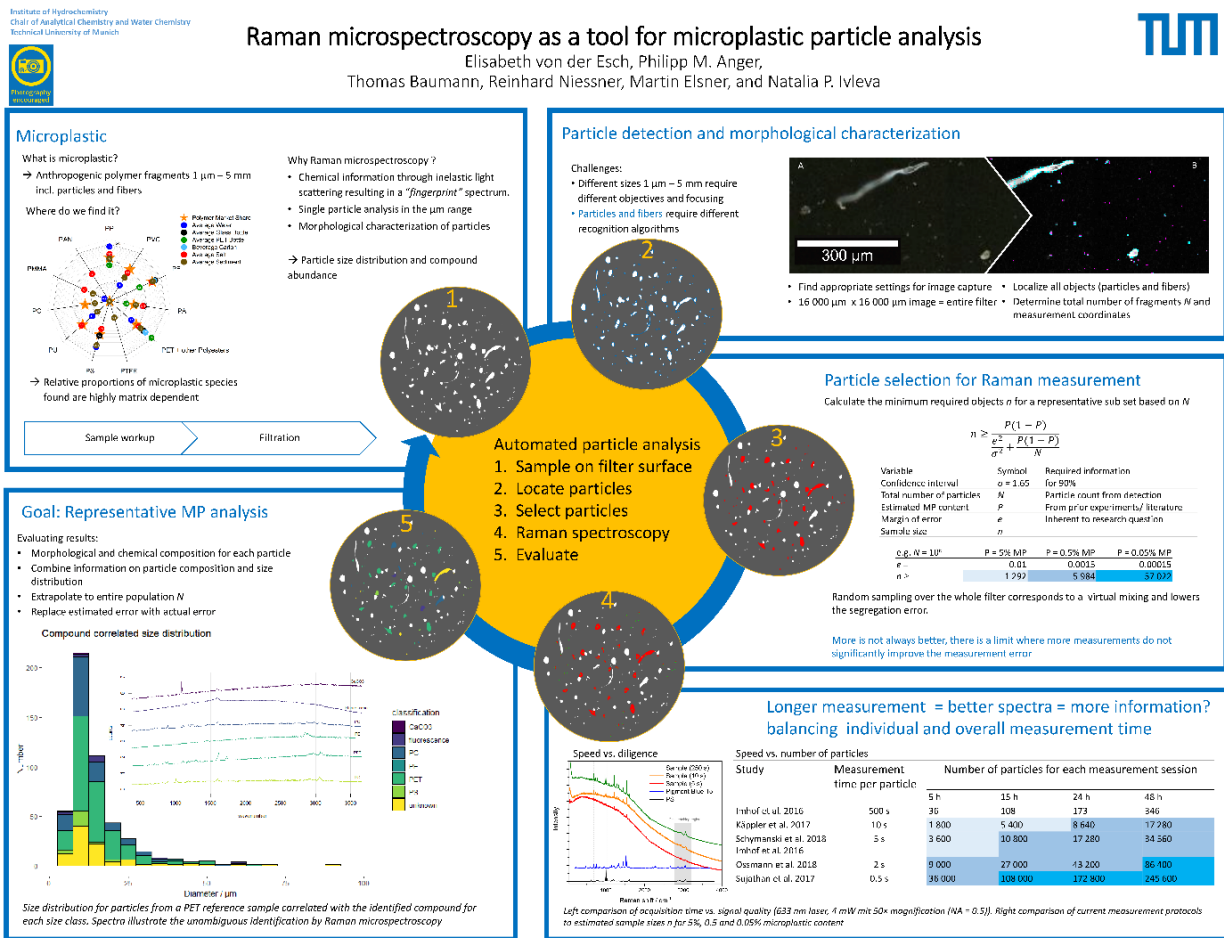


FIGURE 31: RAMAN MICROSCOPY AS A TOOL FOR MICROPLASTIC PARTICLE ANALYSIS. A LARGE VERSION CAN BE FOUND HERE [HTTPS://WWW.EGU.EU/AWARDS-MEDALS/OSPP-AWARD/2019/ELISABETH-VON-DER-ESCH/](https://www.egu.eu/awards-medals/ospp-award/2019/elisabeth-von-der-esch/)

One important criterion for the application of this procedure is that all particles within the sample need to have the same probability to be selected for chemical identification, therefore we require a tool with which we can quantitatively localize all particles deposited on the filter. In order to build such a tool, reference materials, that mimic the properties of the microplastic found in the environment (Figure 32), are required. [5]

The challenge here is that most of the microplastic detected in the environmental samples are caused by weathering and fragmentation of larger plastic waste. [6] This results in microplastic particles of a wide size range (1 μm – 1 mm) and a variety of shapes (fragments, spheres, fibers), which are suspended in water (sedimentation by density) and have particle surfaces modified by ageing (additional OH, C=O and COOH

groups on the particle surface). To produce such a material, we present a fast, ultrasonic-based fragmentation method for PS, PET and PLA, which produces dispersible, high-purity microplastic particles (up to 10^5 particles/15 mL) in aqueous solution. [7] To meet the requirements of a reference material, the key properties - composition and size distribution to ensure sample homogeneity, as well as shape, susceptibility and aging - were analyzed in triplicates to ensure a robust production process. In addition, the stability of the manufactured plastic particles was demonstrated over a period of nine months.

The presented method produces particles in the range of nano- and microplastic ($<20 \mu\text{m}$, $54.5\% \pm 11.3\%$ of all particles). To ensure that all properties were characterized, various methods were applied. Raman microspectroscopy was used for quantitative chemical identification and size distribution analysis for microplastic larger than $10 \mu\text{m}$. Attenuated total reflection Fourier Transform Infrared Spectroscopy and reflection micro-Fourier Transform Infrared Analysis were used on microplastic fragments to investigate surface modifications, showing the formation of polar groups on the surface of the particles in the OH, C=O and COOH range. Smaller particles from 100 nm to $20 \mu\text{m}$ were characterized qualitatively by scanning electron microscopy (SEM) in combination with energy dispersive X-ray spectroscopy showing that irregular fragments are the predominant form in all polymers, but fibers are also present. Furthermore, UV-VIS spectroscopy showed that like microplastic from environmental samples these particles sediment according to their density and that adhesion to glass is avoided.

The key achievement of this study is that reference materials can now be generated in a simple ultrasound procedure accessible to any laboratory, therefore eliminating the need for expensive instrumentation such as cryomills, while delivering particles resembling the ones found in environmental samples in all key characteristics, outlined in the target section. With these reference materials, the development of TUM-ParticleTyper was enabled. Furthermore, Christian Schwaferts also used these reference materials to test the applicability of Raman microspectroscopy for the chemical identification of submicrometer plastic fragments. [8] However, there are

many more applications for these materials as they could be used to facilitate toxicological studies by being suspensible in water so that no additional surfactants need to be used, which could potentially influence the results of the study. To enable such types of studies the procedure must be upscaled. Furthermore, these materials were already used in a small pilot study that aimed at understanding the biodegradation of PLA via bacteria. [9] Expanding this research may enable us to answer whether biodegradable plastic truly is a good alternative to conventional plastic, when it comes to microplastic formation and the release of additives. Herein the single particle analysis via Raman microspectroscopy might also help identify structural changes within the molecular structure of the microplastic particles and could provide insights into whether the fragments are actually degraded or only colonized by the bacteria. These insights might be particularly important for agricultural applications, where plastic mulch foils made up of biodegradable are already used in large scales. [10]

MiPAq Simple Generation of Suspensible Secondary Microplastic Reference Particles via Ultrasound Treatment TUM

Elisabeth von der Esch, Maria Lanzinger, Alexander J. Kohles, Christian Schwaferts, Jana Weisser, Thomas Hofmann, Karl Glas, Martin Elsner, Natalia P. Ivleva

Microplastic reference material requirements

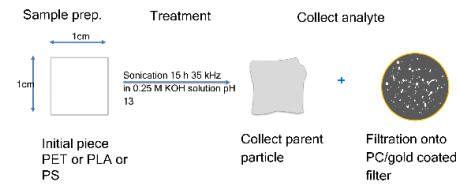
Key characteristics of microplastic:

- Size distribution 1 μm - 1 mm
- Multitude of polymer types are found
- Variety of shapes: spheres, films, fragments, fibers
- Ageing through UV-light, abrasion, interaction with environment
- Susceptibility, as it is found in the water column, sediment and surface water

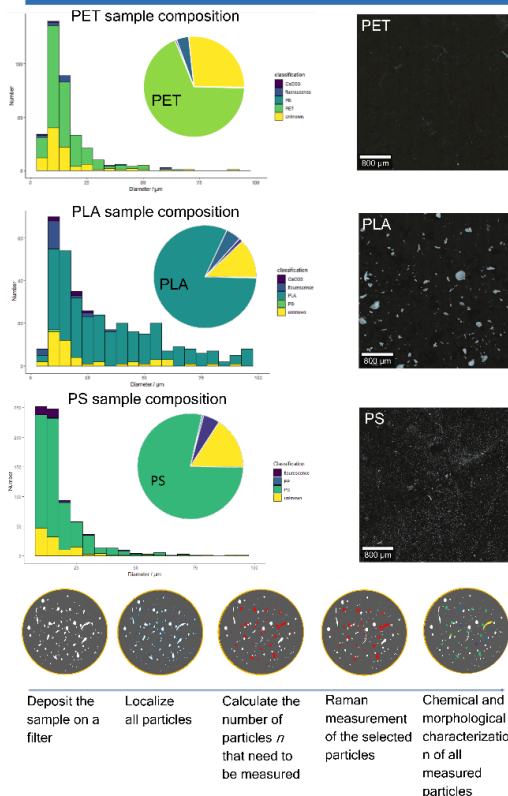
Reference materials should be:

- As similar as possible to the microplastic found in the environment
- Produced through a robust, reproducible procedure
- Characterized with a defined margin of error in the metrics that they are a reference for

Fragmentation through sonication



Size, polymer type & shape by Raman microscopy analysis



Summary

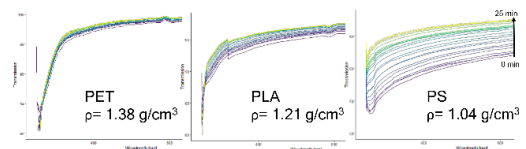
Characteristics of microplastic reference particles formed through sonication:

- Size \rightarrow 1 μm (detected) - depending on parent particle size
- Polymer type \rightarrow all tested polymers fragment in high purity and are detectable by Raman microscopy and IR spectroscopy
- Shapes \rightarrow each polymer yields specific shapes preferably but all shapes occur
- Ageing \rightarrow visual and chemical signs of oxidation/hydrolysis
- Suspensibility \rightarrow creeping effect could be avoided in all cases

Ideal for application in:

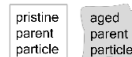
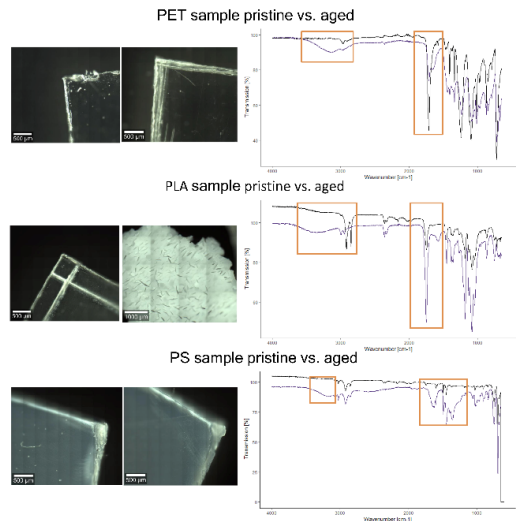
- Method development (image processing training, database search testing, automation, detectability assessment)
- Method validation (recovery rate determination, sample spiking with PLA)
- Experimental work (as behavior is similar to environmental microplastic)

Suspensibility by UV-Vis analysis



UV-VIS time series 0 - 25 min at pH = 7
 → Higher transmission = less particles are in the beam path
 → Particles are suspended but sediment slowly according to their density

Ageing by microscopy and ATR-IR analysis



Sonication under hydrolytic conditions:
 Parent particle \rightarrow visible surface changes
 Small fragments \rightarrow new OH and CO bands in IR Spectra

FIGURE 32: SUMMARY OF THE SIMPLE GENERATION OF SUSPENSIBLE SECONDARY MICROPLASTIC REFERENCE PARTICLES VIA ULTRASOUND TREATMENT

Returning to our objective of microplastic quantification via Raman microscopy, the single particle characterization of microplastic by means of a combined microscopy and spectroscopy technique offers the advantage that both morphological and chemical investigations can be performed. This is particularly useful in microplastic research, since a large number of polymers, sizes and shapes occur, which must be detected in presence of naturally occurring particles.

TUM-ParticleTyper [11, 12] is an open source software tool developed for effective particle and fiber quantification in different types of microscope images (optical, fluorescence, SEM). This tool allows an automated analysis of microplastic samples from deposition on a filter to chemical identification. The software performs particle detection on images (*Figure 33*) and provides a morphological classification of particles present in the sample, including size distribution and shape classification. A comparison of different thresholding methods showed that by using an adaptive

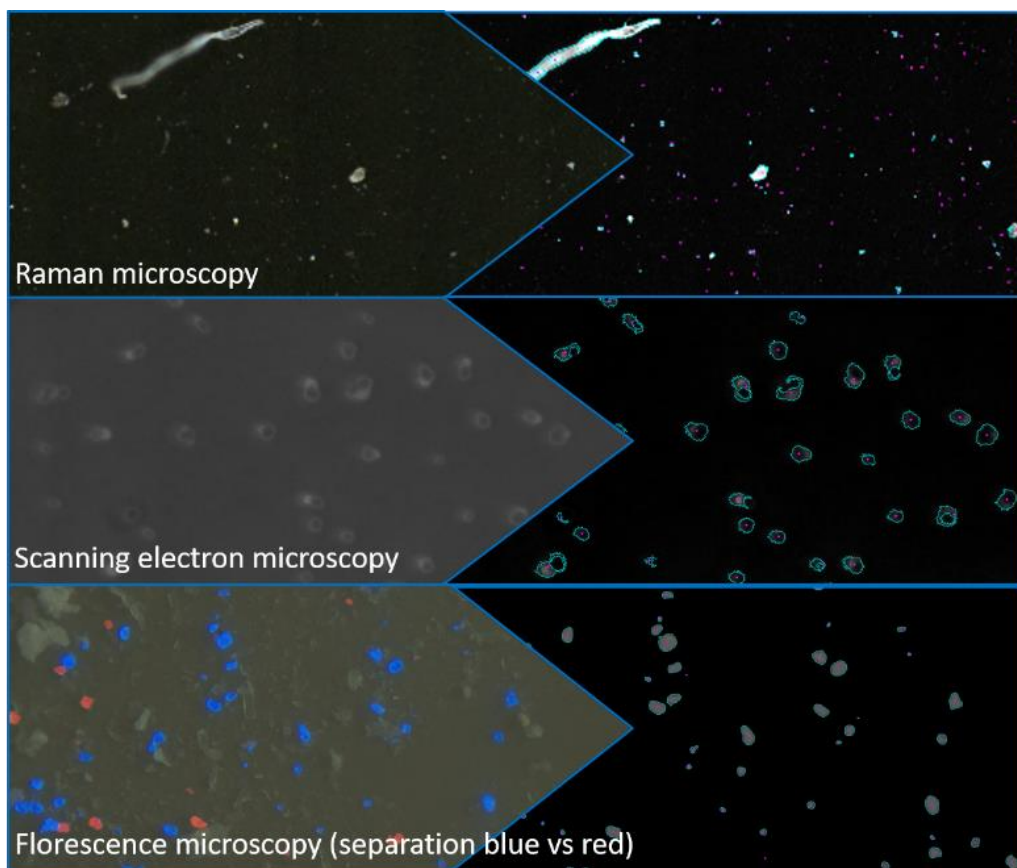


FIGURE 33: PARTICLE LOCALIZATION AND MORPHOLOGICAL CHARACTERIZATION OF PARTICLES THROUGH IMAGE

threshold, the number of true positive particle detections could almost be doubled compared to the common global thresholding. The information generated by the thresholding is used by the software to define the particle contours and optimal coordinates for subsequent chemical identification, by e.g. Raman microspectroscopy. For samples with a large number of particles, it is even possible to create a subsample to avoid disproportionately long measurement times without compromising statistical significance. Our user-friendly graphical interface allows the user to tailor the analysis to individual needs and research questions.

With this software we have taken a big step towards answering the question: "How many microplastic particles are in my sample?" (*Figure 34*)

Combining all efforts in sample size estimation and reduction (chapter 1), production of reference materials (chapter 2) and establishment of a morphological and chemical identification and validation procedure (chapter 3) we can now quantify microplastic down to 10 μm in environmental and food samples with microplastic contents as low as 1%. The 10 μm limit is due to the resolution of the image. With our microscope we have a maximum resolution of 8 000 \times 8 000 pixels at our disposal, for a 16 000 μm \times 16 000 μm area and 20 \times magnification objective. This means that if an image of the entire filter is taken, we achieve a maximum resolution of 2 μm / pixel. In order to achieve a higher resolution, the pixels must be distributed over a smaller area, and thus the image section must be smaller. There are two ways to adapt the method for particles < 10 μm . First, all particles < 10 μm can be measured on a section of the filter (window) and extrapolated to the total area. This path requires proof that such an extrapolation is permissible, i.e. that smaller particles are distributed sufficiently homogeneously on the filter. If this is not possible because even small particles are distributed inhomogeneously, another path must be considered. The second possibility is to measure the filter as a mosaic. For this purpose, a picture would be taken of a section of the filter and a sample of the particles would be measured. This procedure is repeated until the samples are distributed over the entire filter. From our metadata analysis it becomes apparent that Raman microspectroscopy holds the potential to detect microplastics as small as 1 μm . However, lowering the

quantification limit to this level while keeping the procedure at an economically sensible timespan will be a challenging but necessary task to reach the full potential of this method.

The key achievement of this dual publication [11, 12] is that the software *TUM-ParticleTyper* allows a reproducible and validatable particle localization for Raman microspectroscopy, Fluorescence microscopy and SEM images. Furthermore, for the quantification of microplastic via Raman microspectroscopy the image acquisition and measurement, parameters were validated and the protocol for the validation was generalized so that it is applicable for any image and spectroscopy-based quantification procedure. By automating the localization, subsampling and measurement of the particles, it is now possible to perform a representative microplastic analysis within 48 h of measurement time for a subset of 7 000 particles and / or fibers. This excludes ~ 6 additional hours of operator effort, to deposit the particles on the filter before the analysis and to check the results after the analysis. This in turn enables a reasonable sample throughput for the investigation of microplastic in environmental and food samples. It might even become feasible to monitor an entire production cycles, to investigate, at which stage microplastic enters our food.

A very important point in such investigations will be to analyze the mode of sampling, as the analytical error and parts of the sampling error, where characterized in this thesis but primary sampling and all potentially necessary sample preparation steps specific to the sampled lot still need to be investigated. An alternative to the theoretical calculation is the empirical determination of the error, which can be done by accessing the variance in results of replicate measurements ideally in a ring trial, where the performance can be benchmarked to alternative methods. The representativity of the sampling and analysis process could further be determined by the accordance of orthogonal methods (e.g. mass vs. particle number) by using a genuine sample. These further investigations of the entire experimental design will

lead to more reliable results and to harmonized methods for the quantification of microplastic in various matrices.

This thesis provides the basis for statistically correct sampling on a filter, reference materials for further method development and a robust and validated quantification method. All of the presented advances can still be expanded to smaller fragments, up scaled, pushed towards harmonization and even adapted to other particulate substances, thus unlocking the full potential of Raman microspectroscopy for the analysis of single particles.



“How many MP particles are in our sample?”
How can we answer the question accurately within two days?

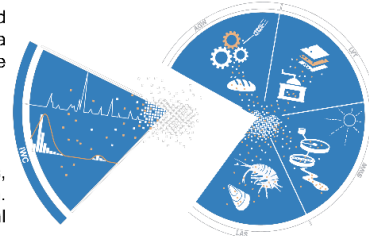


Elisabeth von der Esch, Alexander J. Kohles, Philipp M. Anger, Reinhard Niessner, Martin Elsner, Natalia P. Ivleva

Plastic is subject to environmental influences such as UV irradiation and mechanical strain and thus is broken down into microplastic (MP) a heterogeneous particulate impurity. The main characteristics of the analyte are:

- the variety of polymer types (at differing stages of degradation),
- shapes (fragments, fibers, films, and spheres)
- sizes (1 μm - 1 mm)

These already complex samples have notoriously low microplastic contents, in relation to the native particles and are famously prone to contamination. Consequently, to deliver a satisfactory answer, chemical and morphological characteristics of MP should be quantified for each sample.



The particle and fiber quantification procedure in detail

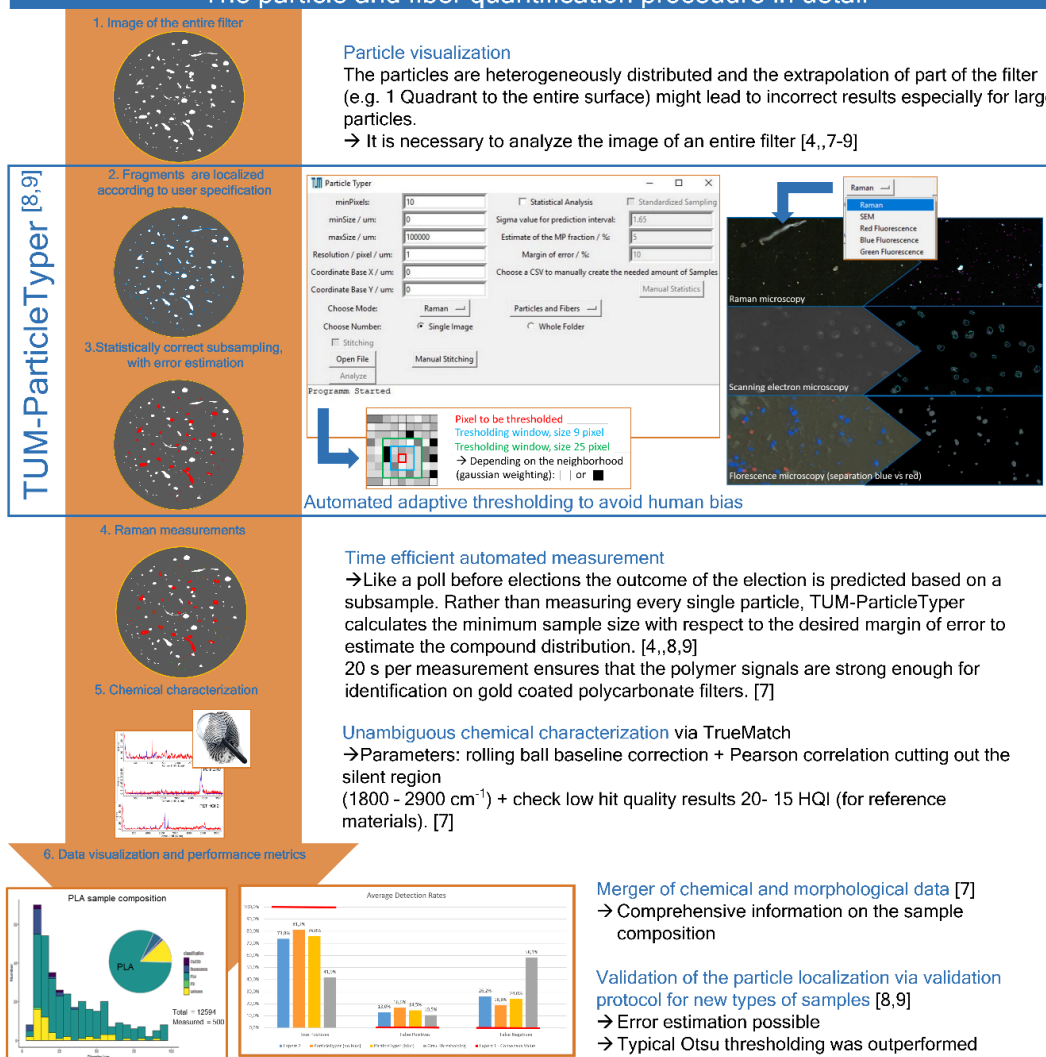


FIGURE 34: “HOW MANY MP PARTICLES ARE IN OUR SAMPLE?” HOW CAN WE ANSWER THE QUESTION ACCURATELY WITHIN TWO DAYS? BY USING OUR MP LOCALIZATION TOOL, TUM-PARTICLETYPER.

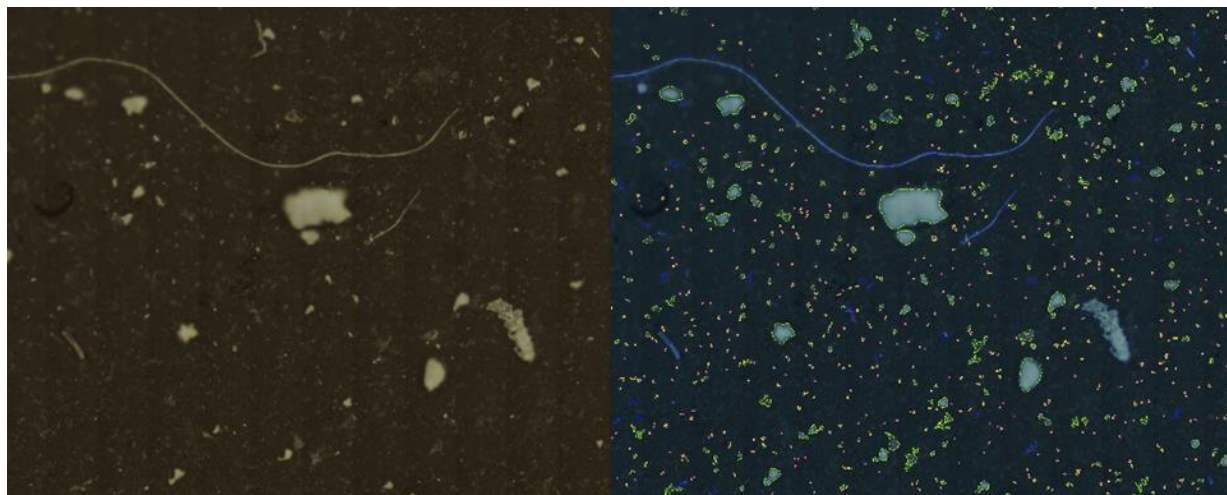
REFERENCES

1. Ossmann BE, Sarau G, Holtmannspotter H, Pischetsrieder M, Christiansen SH, Dicke W. Small-sized microplastics and pigmented particles in bottled mineral water. *Water Res.* **2018**;141:307-16.
2. Schymanski D, Goldbeck C, Humpf HU, Furst P. Analysis of microplastics in water by micro-Raman spectroscopy: Release of plastic particles from different packaging into mineral water. *Water Res.* **2018**;129:154-62.
3. Koelmans AA, Mohamed Nor NH, Hermsen E, Kooi M, Mintenig SM, De France J. Microplastics in freshwaters and drinking water: Critical review and assessment of data quality. *Water Res.* **2019**;155:410-22.
4. Anger PM, von der Esch E, Baumann T, Elsner M, Niessner R, Ivleva NP. Raman microspectroscopy as a tool for microplastic particle analysis. *Trends Anal Chem.* **2018**;109:214-26.
5. Hüffer T, Praetorius A, Wagner S, von der Kammer F, Hofmann T. Microplastic Exposure Assessment in Aquatic Environments: Learning from Similarities and Differences to Engineered Nanoparticles. *Environ Sci Technol.* **2017**;51(5):2499-507.
6. Lambert S, Wagner M. Formation of microscopic particles during the degradation of different polymers. *Chemosphere.* **2016**;161:510-7.
7. von der Esch E, Lanzinger M, Kohles AJ, Schwaferts C, Weisser J, Hofmann T, et al. Simple Generation of Suspensible Secondary Microplastic Reference Particles via Ultrasound Treatment. *Front Chem.* **2020**;8(169).
8. Schwaferts C. Detektion und Identifizierung von Submikrometer-Plastikpartikeln mittels Raman-Mikroskopie und Rasterelektronenmikroskopie **2019** [Available from: <https://www.gdch.de/netzwerk-strukturen/fachstrukturen/analytische-chemie/preise-ehrunen/weitere-preise.html>].
9. Göpfert L. Characterization of chemical and morphological changes in microplastics during bacterial degradation at environmentally relevant conditions SETAC Dublin2020 [Available from: https://dublin.setac.org/wp-content/uploads/2020/04/SETAC-SciCon-Programme-book_v3.pdf].
10. Sintim HY, Flury M. Is Biodegradable Plastic Mulch the Solution to Agriculture's Plastic Problem? *Environ Sci Technol.* **2017**;51(3):1068-9.
11. Kohles AJ, von der Esch E, Anger PM, Hoppe R, Niessner R, Elsner M, et al. TUM-ParticleTyper: Software and Documentation. <https://mediatum.ub.tum.de/1547636>: TUM 2020.
12. von der Esch E, Kohles AJ, Anger PM, Hoppe R, Niessner R, Elsner M, et al. TUM-ParticleTyper: A detection and quantification tool for automated analysis of (Microplastic) particles and fibers. *PLoS One.* **2020**;15(6):e0234766.

APPENDIX

APPENDIX A1 SUPPORTING INFORMATION FOR CHAPTER 2

PREVIEW TUM-PARTICLETYPER



#	cx	Cy	area	diameters_min	diameter_max	classification
1	-1662.6	-7995.5	122.5	10.0	21.0	Particle
2	-3947.9	-7994.6	128.5	10.0	16.0	Particle
3	3251.4	-7992.7	279.5	16.0	27.0	Particle
4	1118.1	-7993.4	191.0	17.0	18.0	Particle
5	-2074.1	-7991.2	381.0	18.0	27.0	Particle
6	4406.7	-7991.4	487.0	20.0	37.0	Particle
7	792.5	-7992.6	464.5	20.0	41.0	Fiber
8	3341.5	-7999.0	1402.5	21.0	135.0	Fiber
9	2128.4	-7989.4	320.0	21.0	21.0	Particle
10	-2991.3	-7991.1	1897.0	21.0	167.0	Fiber
11	-4613.4	-7989.4	148.0	13.6	22.9	Particle
12	-4093.1	-7988.9	319.0	24.0	25.0	Particle
13	1956.5	-7990.4	935.0	26.0	66.0	Fiber
14	1438.4	-7988.0	486.5	26.0	26.0	Particle

Figure 1: Example of particle and fiber detection using TUM-ParticleTyper, left original image, right processed image. Particles are marked in green, fibers in blue. The red and blue dots mark the center points calculated for each particle. An example of a morphological characterization for particle and fiber detection using the TUM-ParticleTyper can be seen at the bottom. Here the particle number (#), the center coordinates (cx, cy), the area (area), the Feret's diameters (diameters_min, diameters_max) and the classification into fiber or particle (classification) are

displayed. All data were reprocessed with the latest TUM-ParticleTyper version July 2019 to ensue best and consistent results (E. von der Esch, A. Kohles et al. submitted [1]).

Validation of Database Identification with TrueMatch

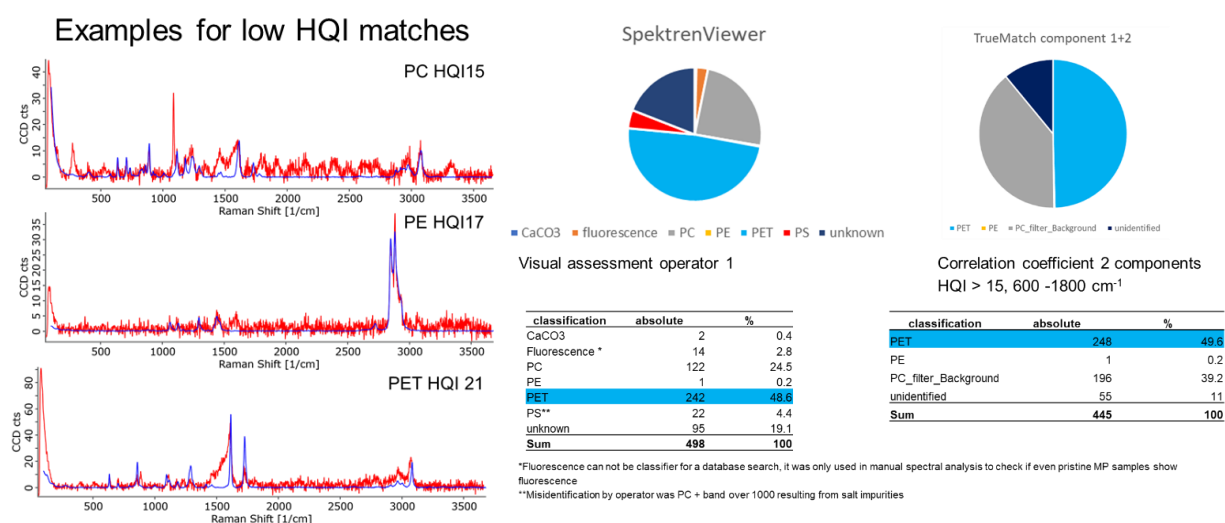


Figure 2: All spectra from Replicate 1 were manually classified by operator 1 and then reprocessed with TrueMatch using a custom database. On the left examples for low HQI matches are displayed. HQI > 15 was found to be the lowest acceptable value all classifications below this value were marked as unidentified. All TrueMatch identifications below HQI = 20 should be checked before continuing the analysis, which is why the TrueMatch analysis takes 20 min, the actual runtime of the program is ~ 30 sec for 1000 spectra. A comparison of the spectral identification of operator 1 (middle) vs. True match (right) shows that the identification with both methods leads to comparable results.

Morphological Changes in Polymer Surface Due to Ultrasonic Degradation

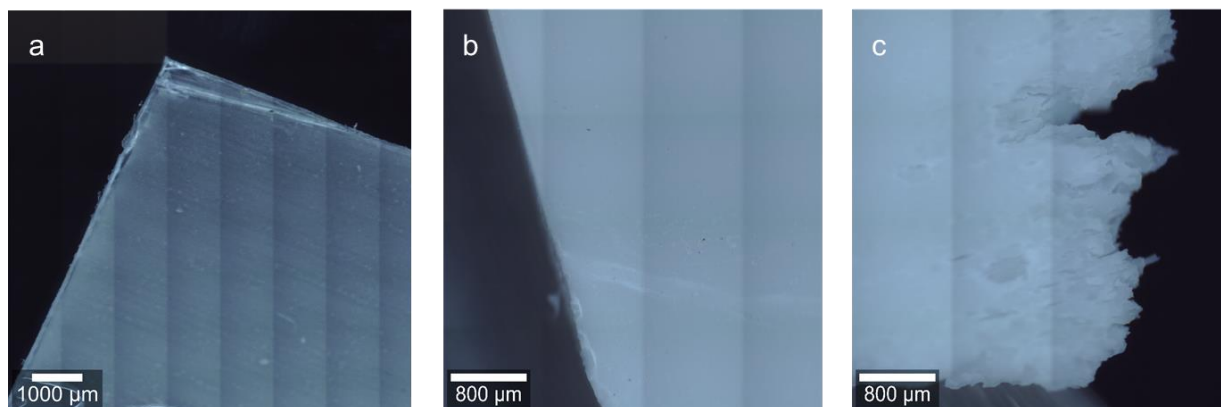


Figure 3: Surface of PLA square, before sonication (a), after sonication with MilliQ (b) and KOH (c) recorded on a Witec alpha 300 Raman microscope 20× magnification.

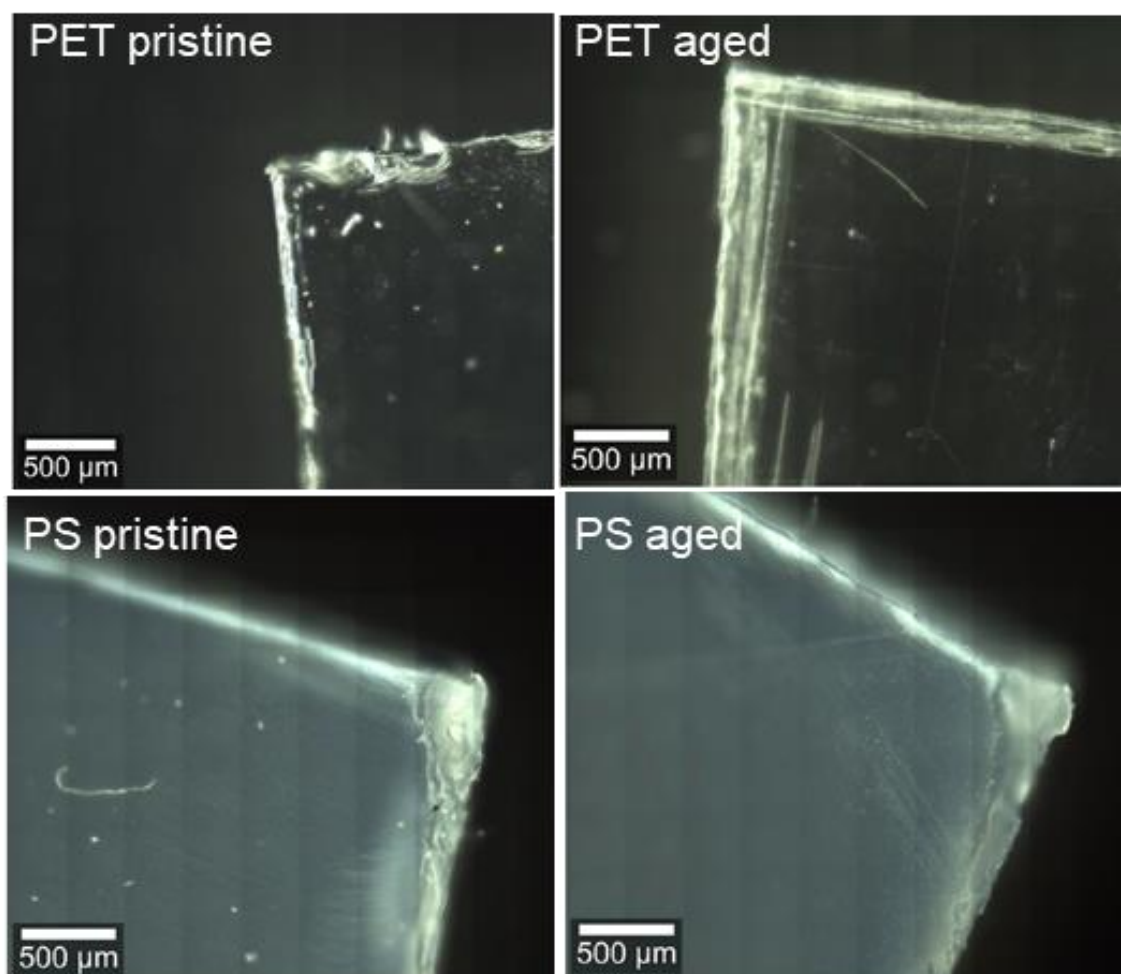


Figure 4: Surface of the polymer parent particle, before sonication and after sonication in alkaline solution recorded on a Witec alpha 300 Raman microscope 20× magnification.

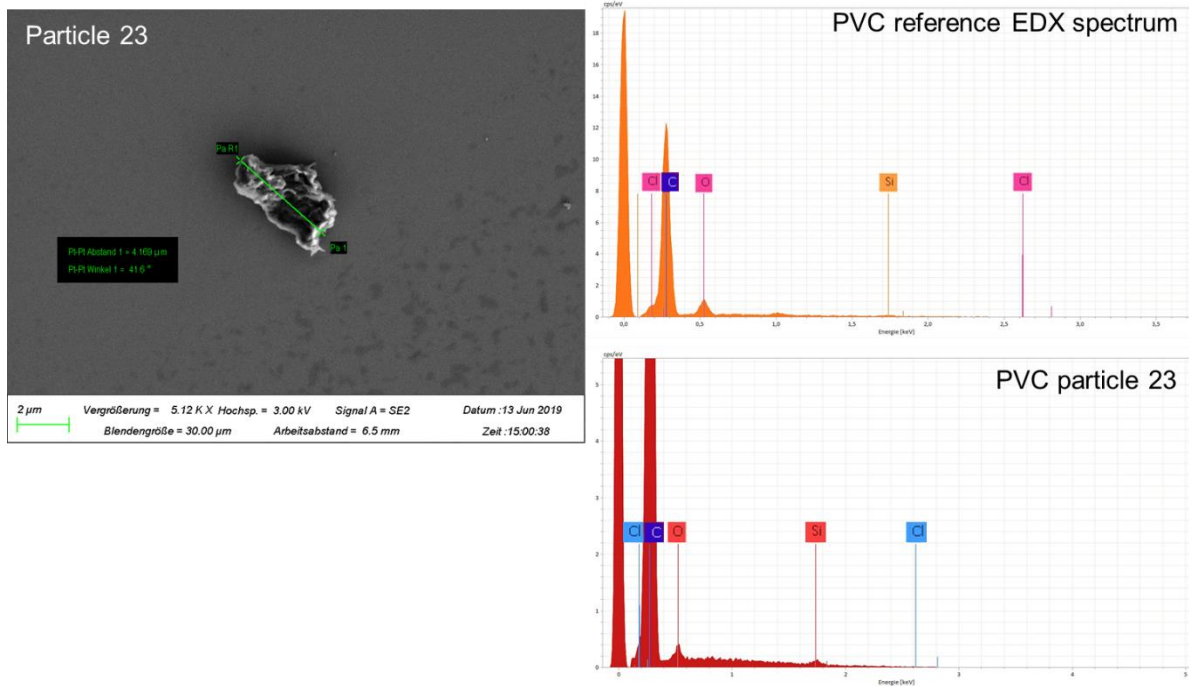


Figure 5: Example for a SEM/EDX analysis of PVC microplastic particles.

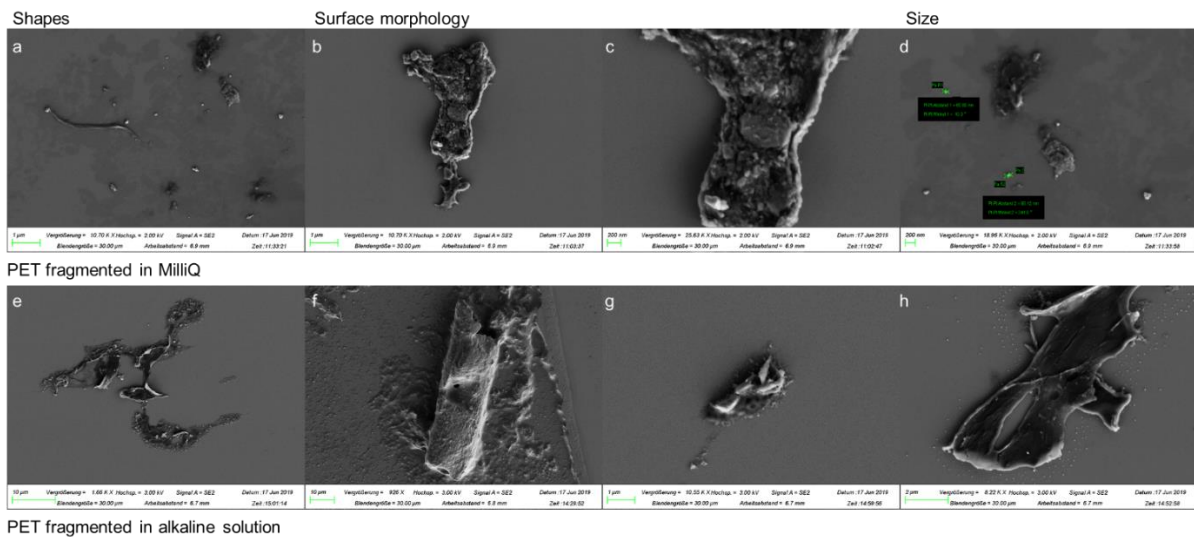


Figure 6: Surface morphology changes by fragmentation in pure MilliQ and KOH.

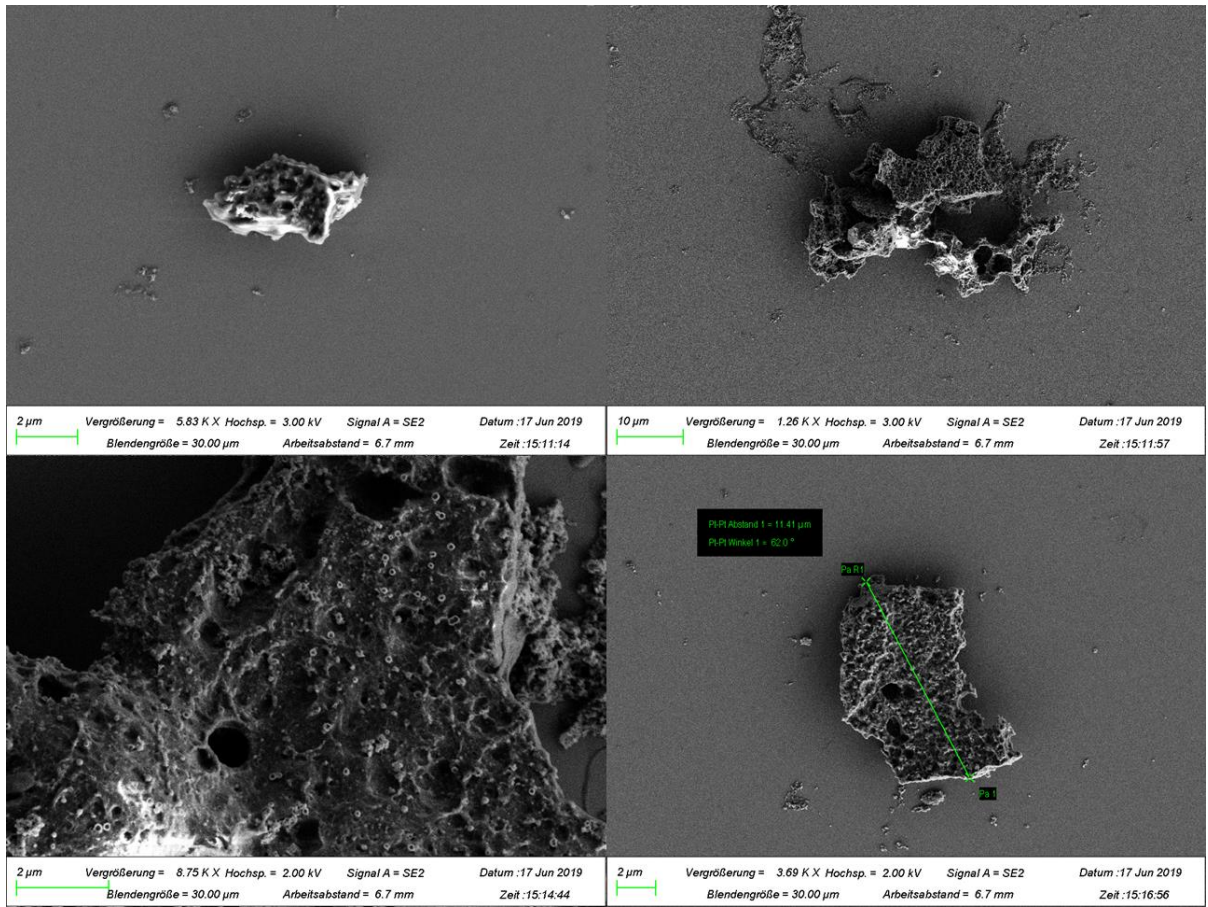


Figure 7: Surface modification of PLA.

Yield and Reproducibility of the Fragmentation

Characterization of the starting materials

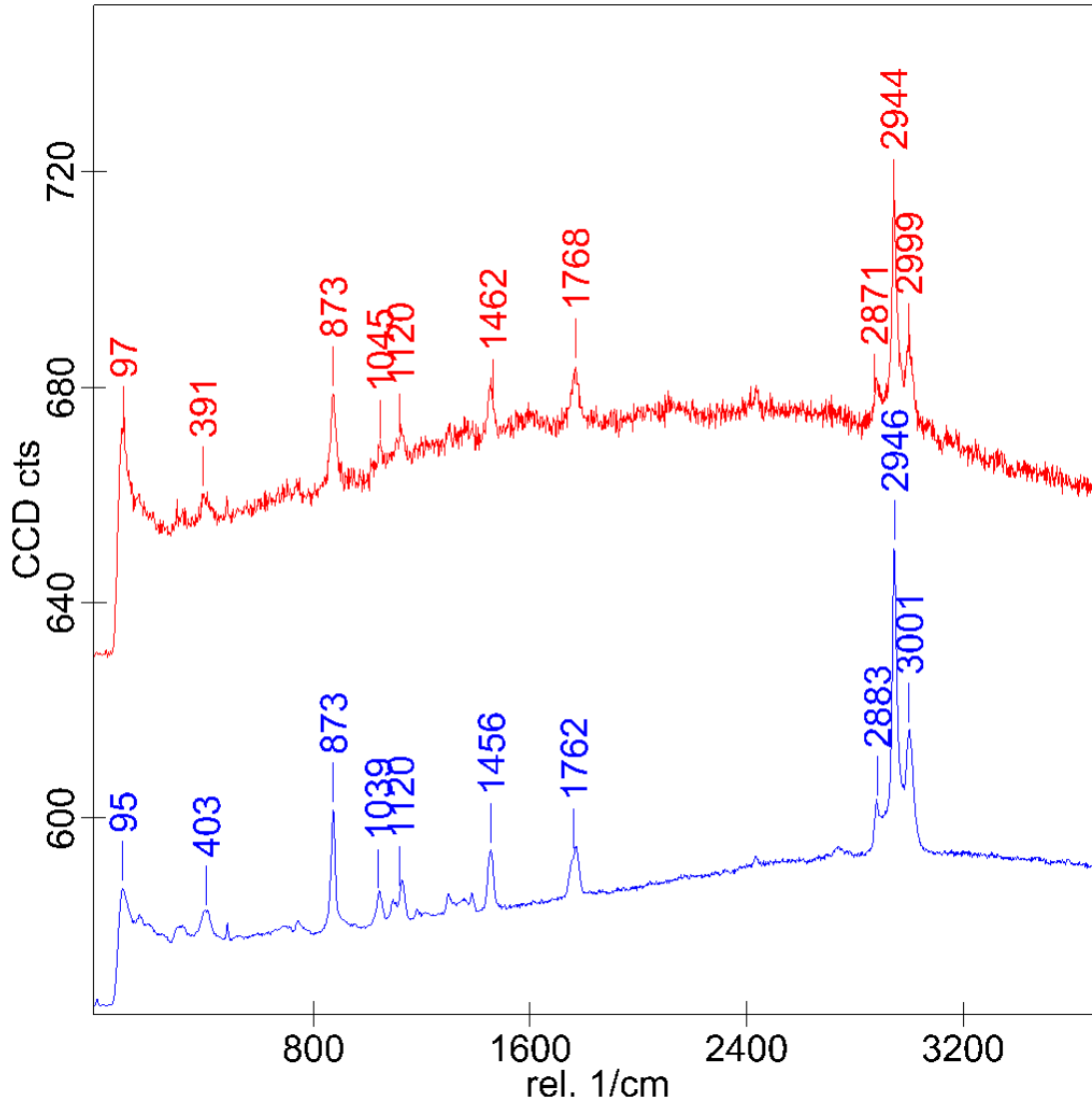


Figure 8: Exemplary spectrum of PLA starting material (blue) fragmented PLA (red).

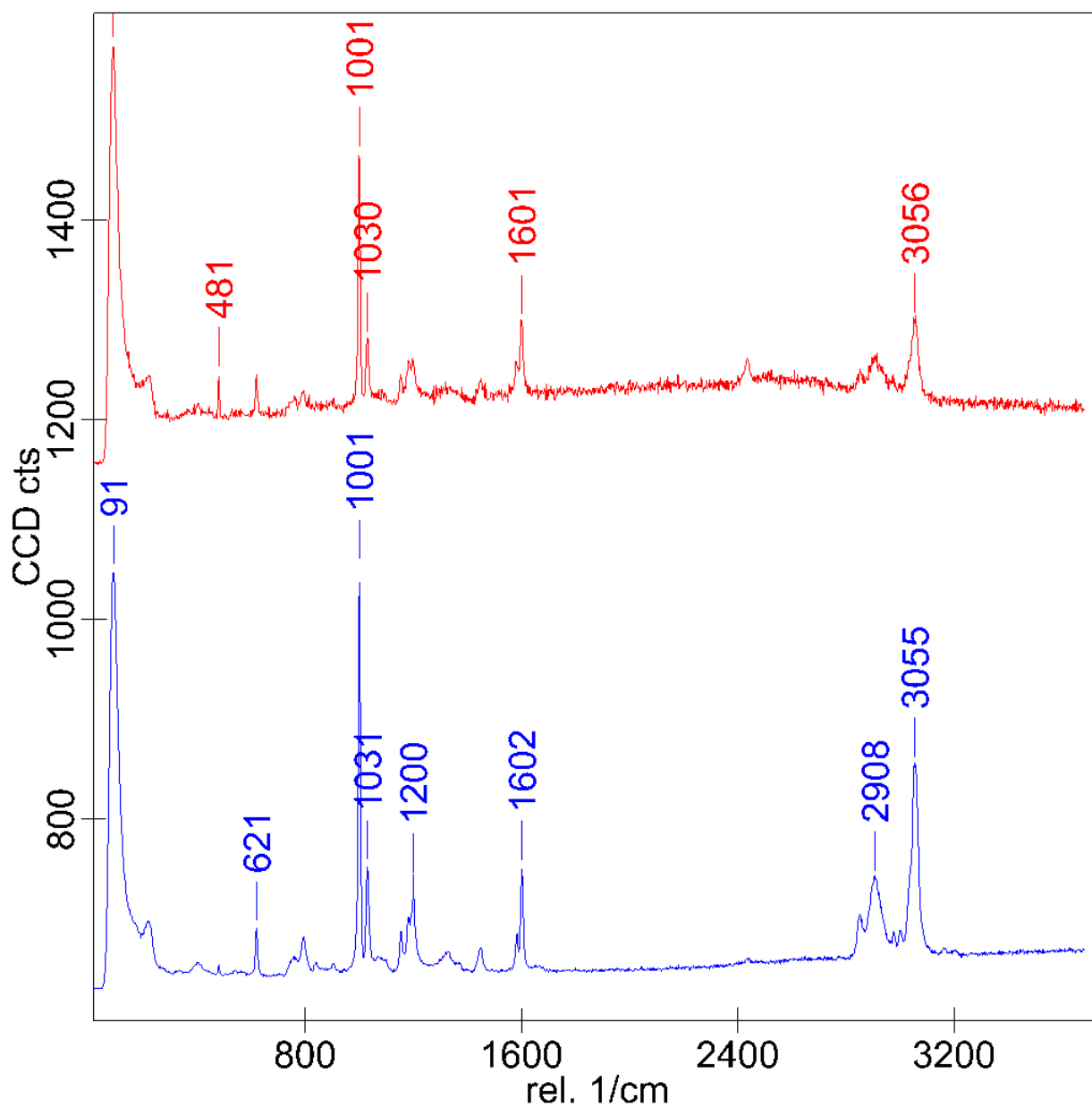


Figure 9: Exemplary spectrum of PS starting material (blue) fragmented PS (red).

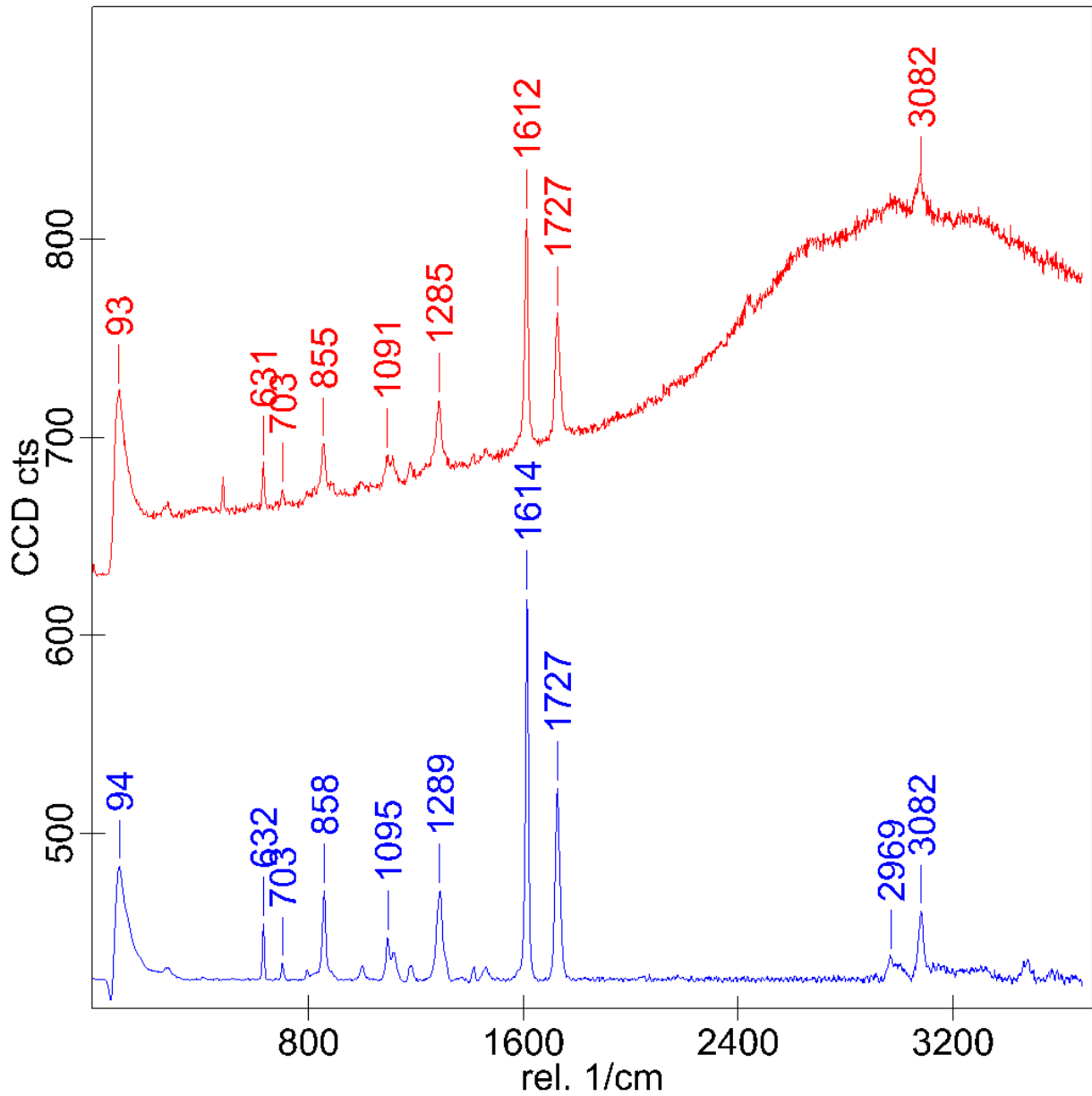


Figure 10: Exemplary spectrum of PET starting material (blue) fragmented PET (red).

Additional in-depth manual fiber analysis:

To confirm that the fibers detected in the automated analysis originate from the fragmentation of the original polymer piece additional manual measurements were performed. (Original automated analysis Jan. 2019, second manual analysis Sept 2019) We can confirm that PET, PLA and PS produce fragments in the shape of fibers. These fibers are typically shorter than 100 μm (for PET there was one exception see Figure 11) and could be identified through Raman microspectroscopy (Figure 11-14). We also found fibers from aerial contamination. These showed only a fluorescence signal and were typically larger than 100 μm . Examples for the recorded spectra and images of the fibers can be viewed in Figure 12. Since the samples could be remeasured after a 9-month storage (on gold coated polycarbonate filters in glass Petri dishes) we further conclude that the particles generated through sonication are stable for at least 9 months

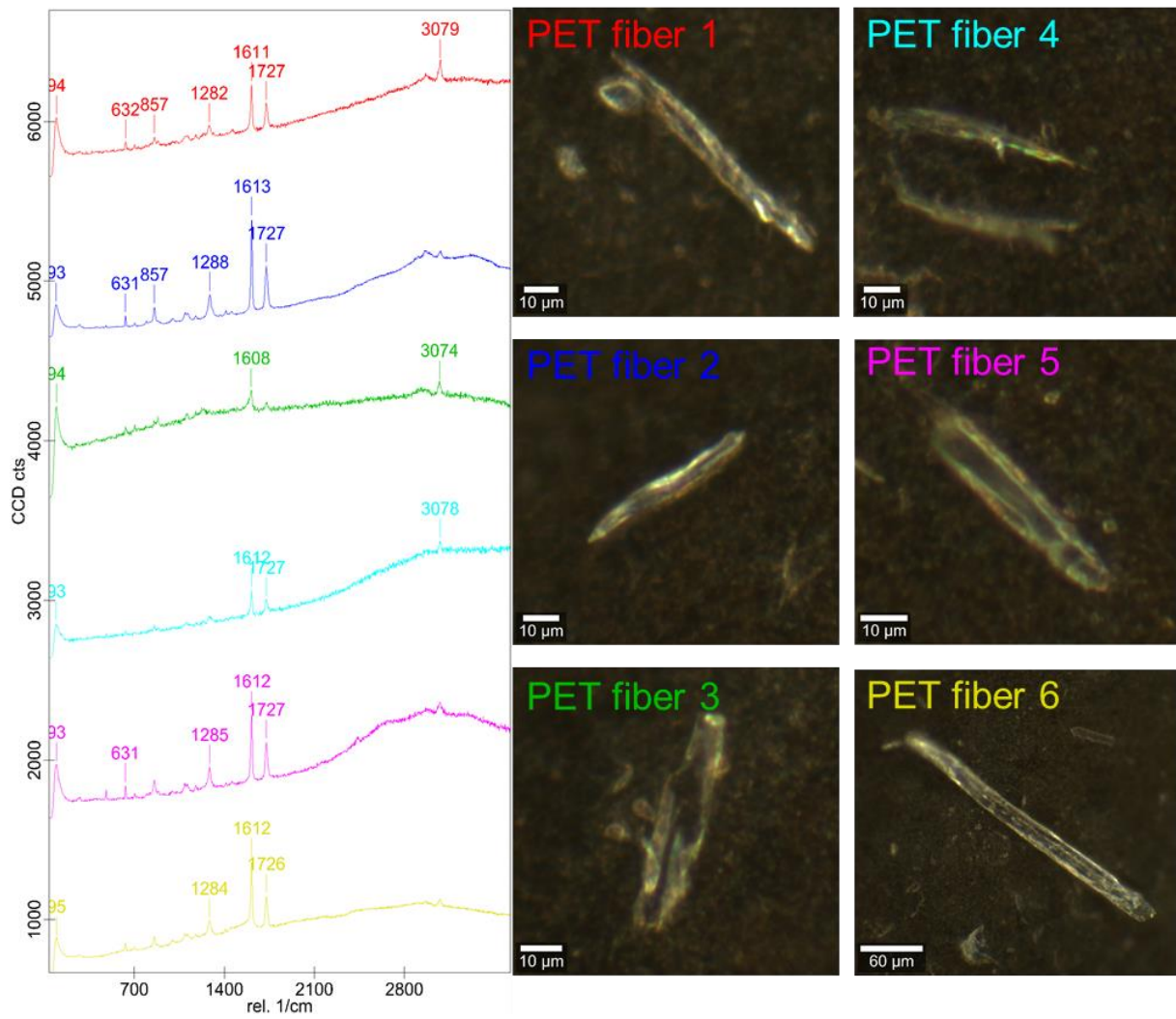


Figure 11: Fiber-like structures produced through sonication of PET.

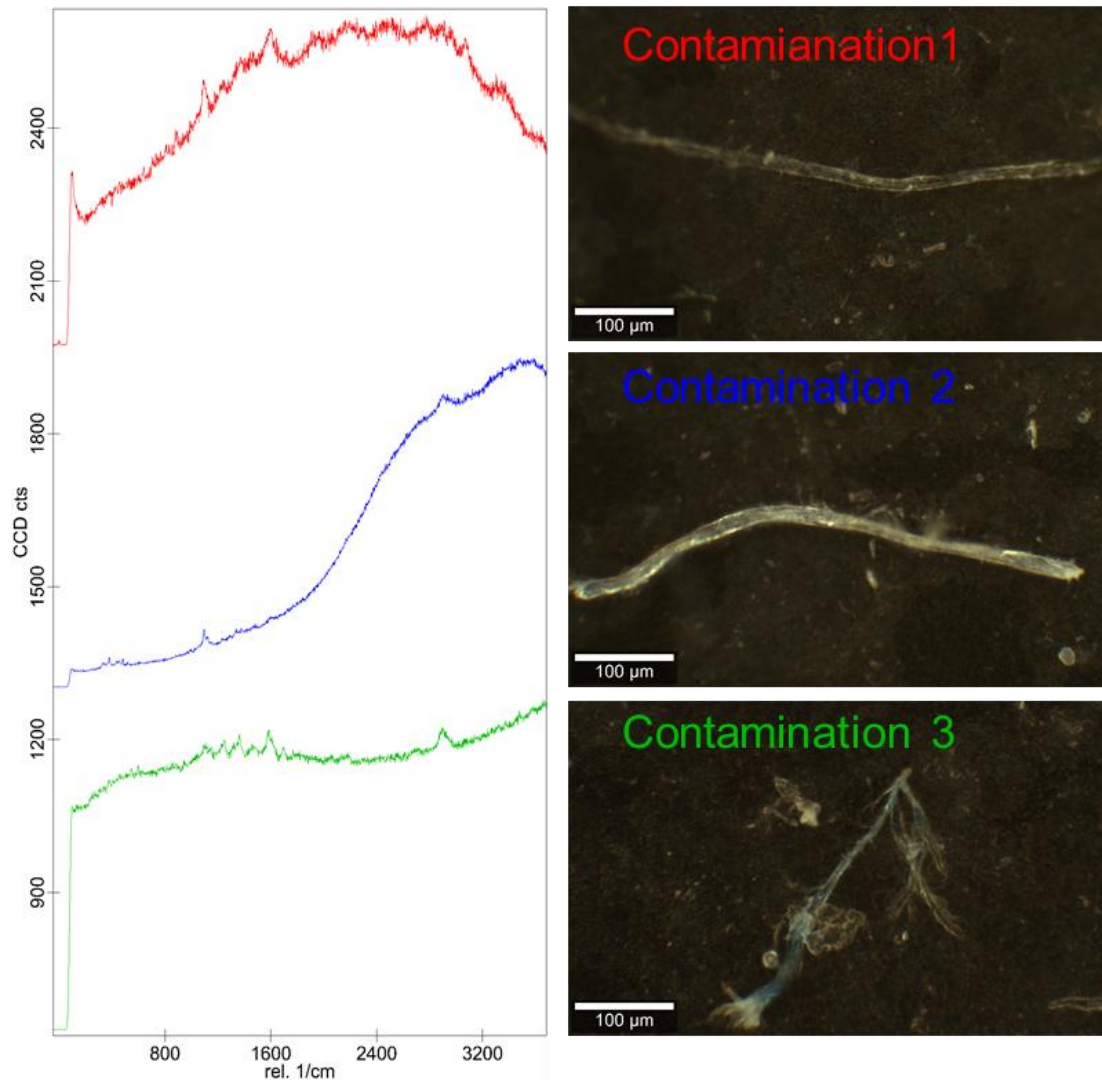


Figure 12: Fibers from aerial contamination.

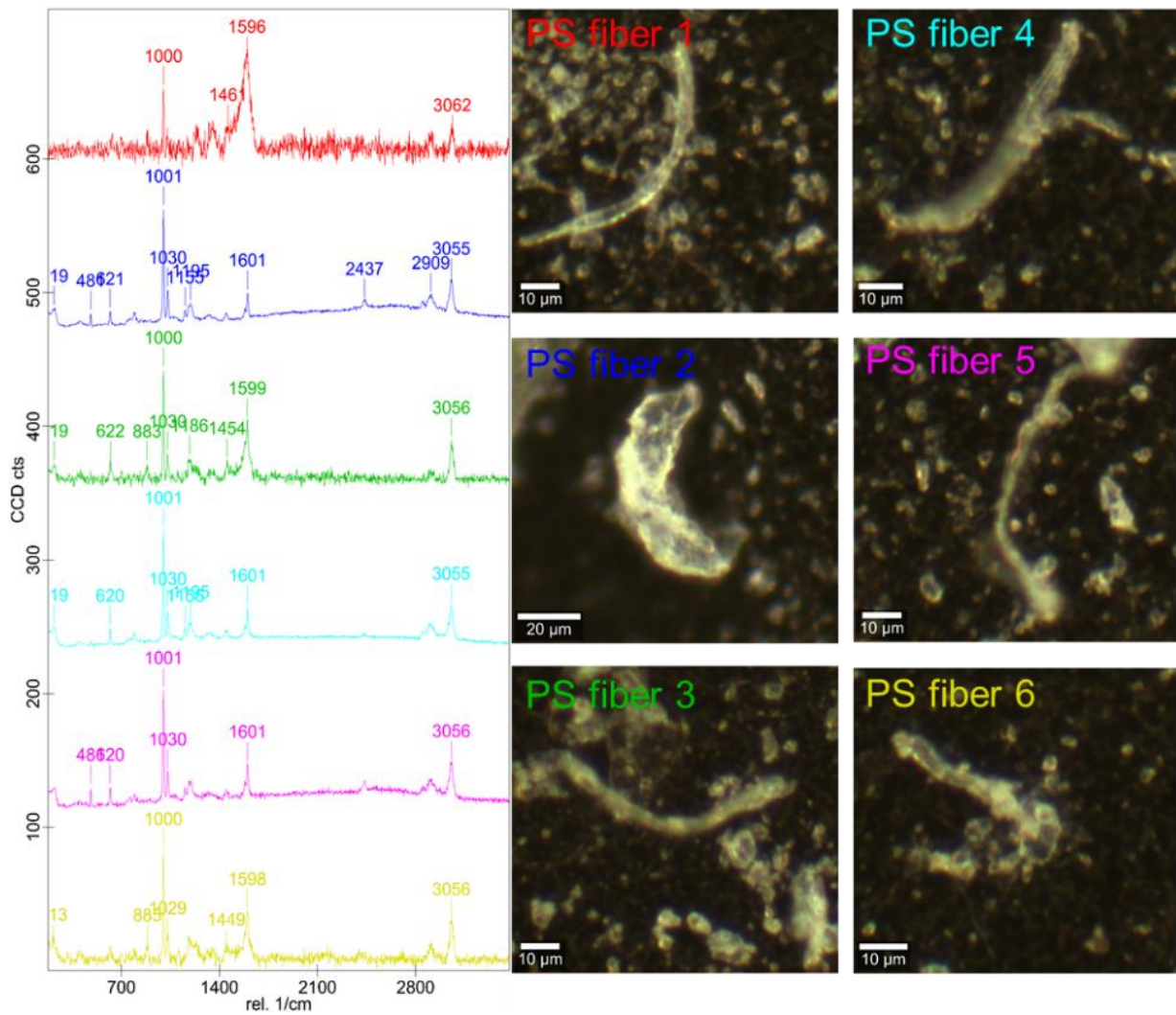


Figure 13: Fiber-like structures produced through sonication of PS.

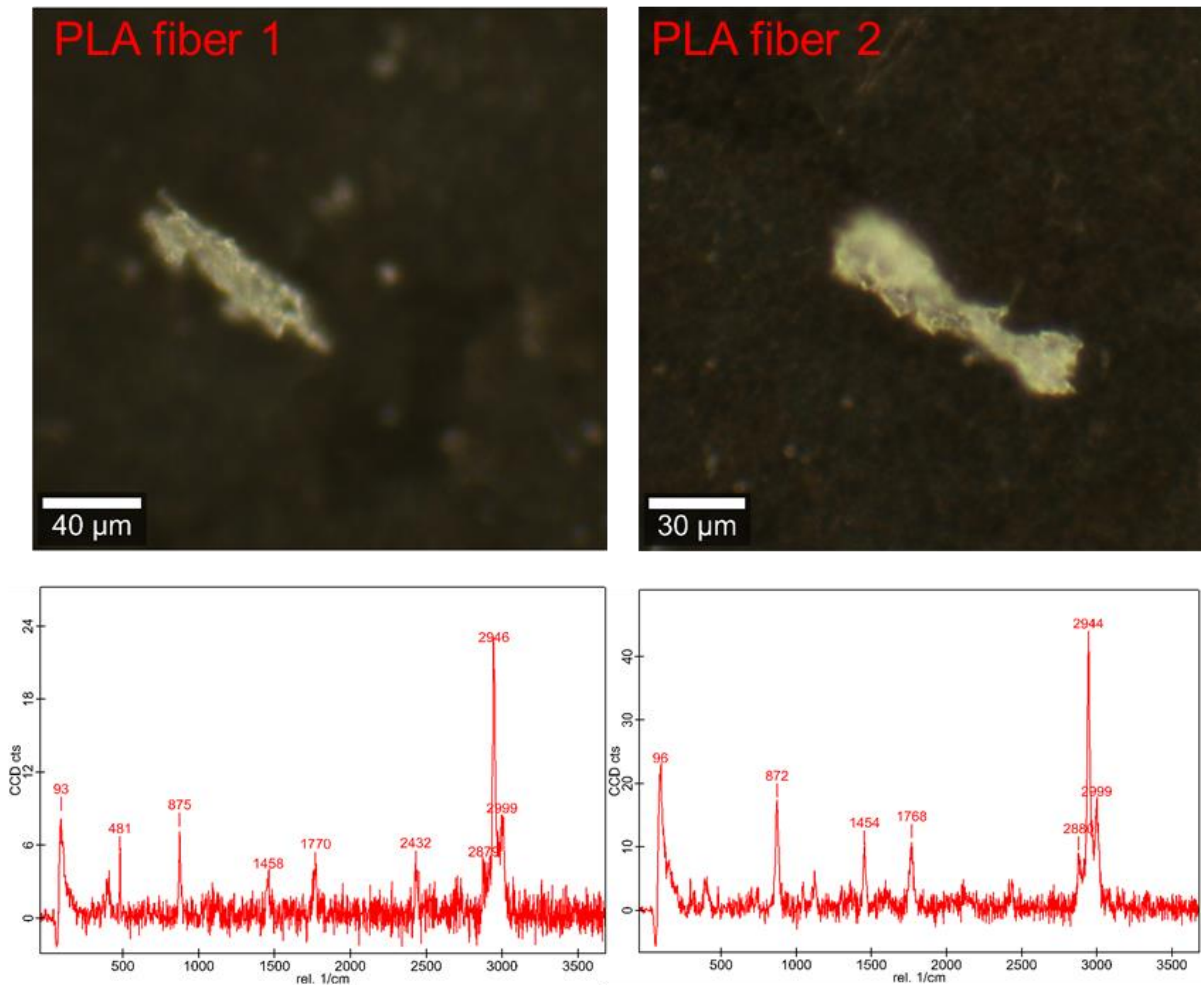


Figure 14: Fiber-like structures produced through sonication of PLA.

Size Distribution Statistics

Table 1: Size distribution statistics.

PS	Absolute Numbers			size distribution in %				descriptive statistics	
	Total	Particle s	Fiber s	>10 0	100- 50	50- 20	<20	Average size in μm	MAD in μm
	21732						77.9		
Replicate 1	8	214382	2946	0.36	2.37	19.33	4	16.47	8.45
							45.2		
Replicate 2	9227	8638	589	3.55	9.94	41.29	2	34.77	23.13
							40.9		
Replicate 3	61464	56613	4851	6.46	14.10	38.49	6	39.44	27.46
Mean R 1-							54.7		
3	96006	93211	2795	3.46	8.80	33.04	0	30.23	
SD	10826						20.2		
absolute	5	107644	2135	3.05	5.95	11.95	3	12.14	
SD percent	113	115	76						

PLA	Absolute Numbers			size distribution in %				descriptive statistics	
	Total	Particle s	Fiber s	>10 0	100- 50	50- 20	<20	Average size in μm	MAD in μm
							61.4		
Replicate 1	21067	20454	613	3.40	7.24	27.94	1	26.10	18.58
							43.3		
Replicate 2	10602	9924	678	6.92	12.76	36.95	7	39.03	28.07
							51.8		
Replicate 3	20757	19471	1286	3.16	10.06	34.96	2	30.99	20.17
Mean R 1-							52.2		
3	17475	16616	859	4.50	10.02	33.28	0	32.04	
SD									
absolute	5954	5817	371	2.11	2.76	4.73	9.03	6.53	
SD percent	34	35	43						

PET	Absolute Numbers			size distribution in %				descriptive statistics	
	Total	Particle s	Fiber s	>10 0	100- 50	50- 20	<20	Average size in μm	MAD in μm
							65.6		
Replicate 1	48882	47480	1402	0.70	4.76	28.89	5	20.97	11.62

							49.4		
Replicate 2	72075	68436	3639	3.53	10.30	36.76	1	31.34	19.85
							54.6		
Replicate 3	17586	16753	833	2.00	8.73	34.66	1	27.38	16.04
Mean R 1-							56.5		
3	46181	44223	1958	2.08	7.93	33.44	5	26.56	
SD									
absolute	27345	25995	1483	1.42	2.86	4.07	8.29	5.23	
SD percent	59	59	76						

Mechanistic Implications

Table 2: Preliminary data for PE, PP and PA for PVC see SI, Figure 5.

Polymer	Absolute Numbers			size distribution in %			
	Total	Particles	Fibers	>100	100-50	50-20	<20
PE	11795	11090	705	1.27	6.20	39.04	53.49
PP	83635	81617	2018	0.43	3.63	22.70	73.24
PA	could not be fragmented in alkaline solution and resulted in the formation of a gel						

Ultrasonic bath testing procedure

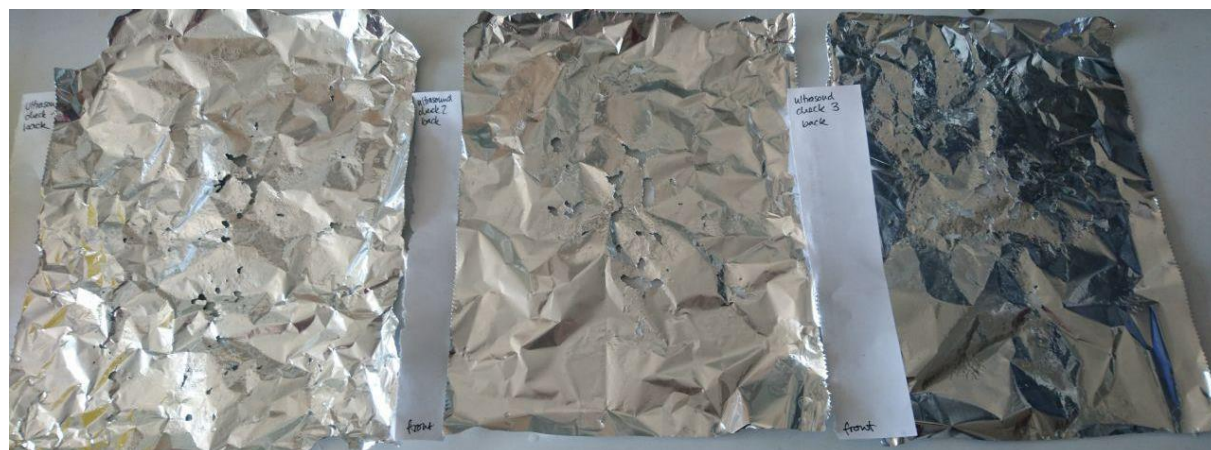
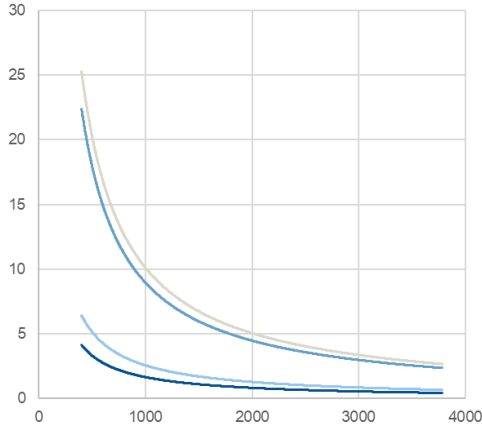


Figure 15: Identification of hotspots in ultrasonic bath with aluminum foil. Submerge the foil in the ultrasound bath and turn it on after a few seconds holes should appear in the surface. Leave the foil in for approximately one minute. The largest holes will indicate the strongest field. After finding these hotspots all samples should be placed in exactly this position to ensure identical fragmentation conditions.

Axial resolution of the Measurements

ATR and Reflectance IR Spectroscopy



pi 3.14159265
 n(ATR) 2.4
 sin2(45) 0.5
 1.4 PLA,
 1.58 PS
 n(Sample) 1.57 PET
 n(ratio) 0.58333333

$$d_p = \frac{\lambda}{2\pi n_1 \sqrt{\sin^2(\Theta) - (n_2/n_1)^2}}$$

Raman spectroscopy with a 532 Laser

Sample and instrumental properties			Sample	λ in cm	axial resolution in cm	axial resolution in μm
n(PS)	1.58	refractive	PS	5.32E-05	2.10E-03	2.1014
n(PET)	1.57	index in	PET	5.32E-05	2.09E-03	2.0881
n(PLA)	1.4	g/cm	PLA	5.32E-05	1.86E-03	1.862
N.A.	0.4	numerical aperture				

$$\Delta = \frac{4 \cdot n \cdot \lambda}{(N.A.)^2}$$

Figure 16: In order to perform a successful analysis and to interpret the results it is important to know what exactly you are measuring and at what depth. We have put together our penetration depths for ATR-FTIR, Reflectance FTIR and Raman microspectroscopy with a 532 nm laser.

μ -FTIR analysis

PET analysis

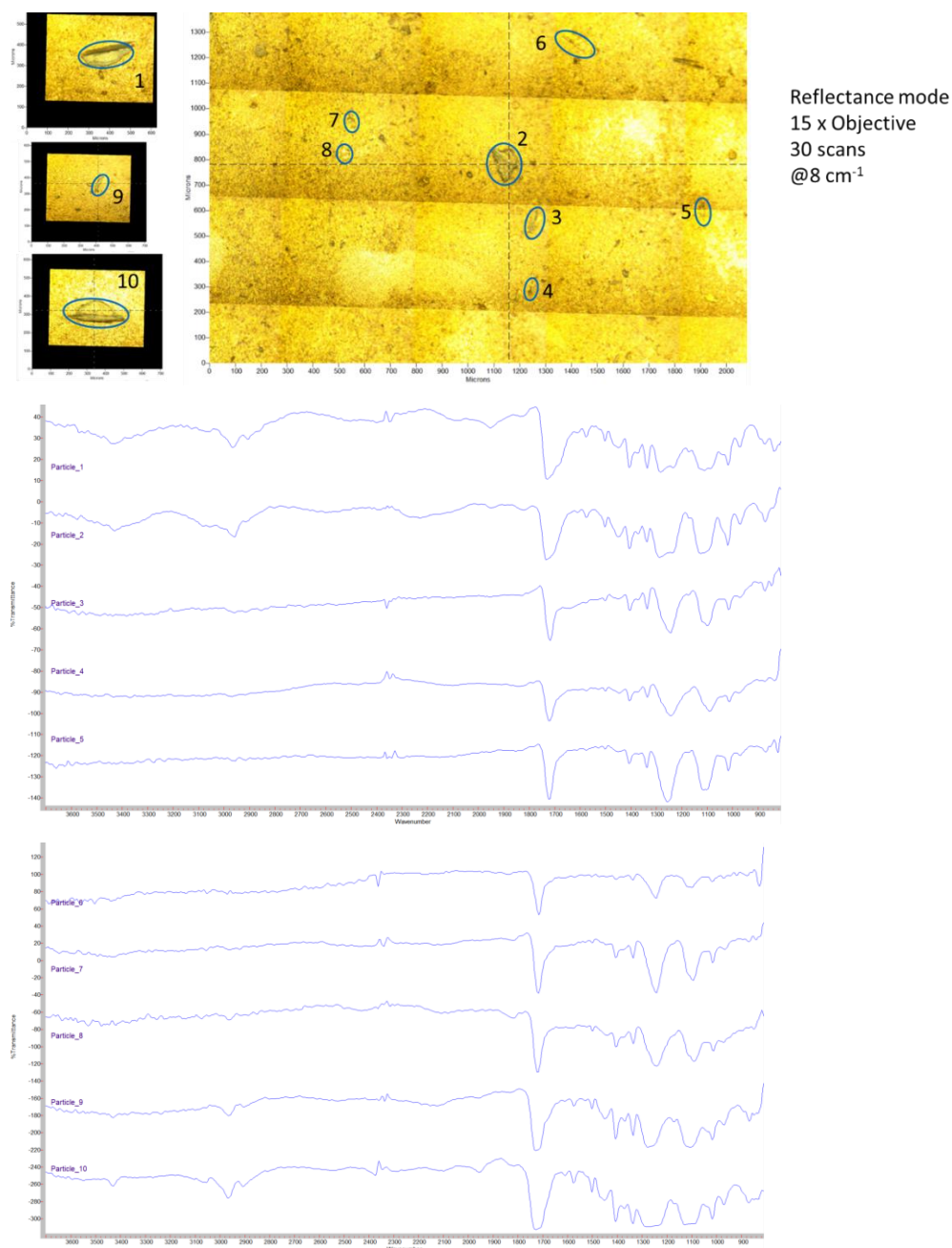


Figure 17: Image of the analyzed particles (top). The particle numbers correspond to the spectra below. All measurements were conducted on a μ -FTIR system by Agilent Cary 620.

PLA analysis

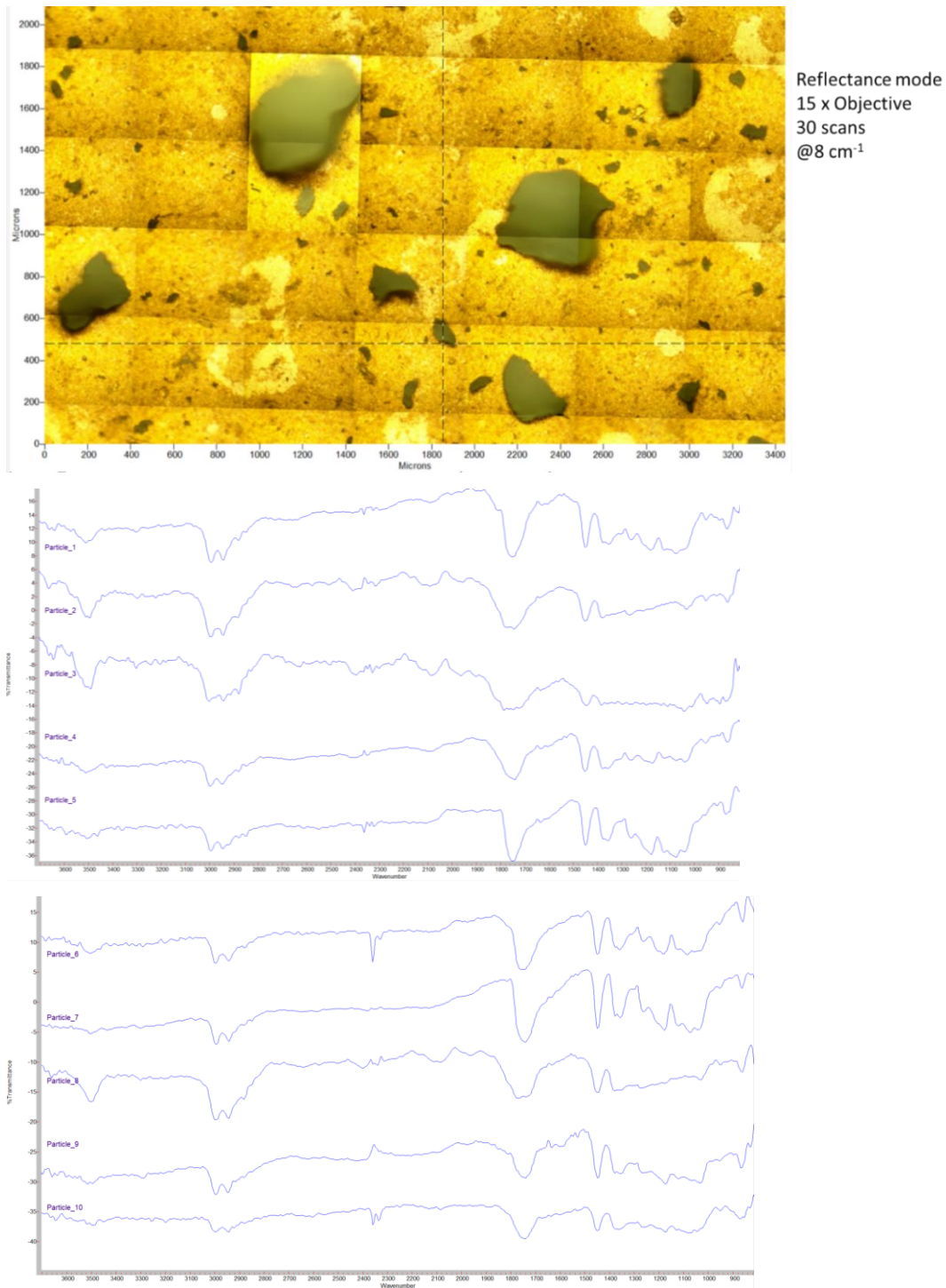


Figure 18: Image of the analyzed particles (top). The particle numbers correspond to the spectra below. All measurements were conducted on a μ -FTIR system by Agilent Cary 620.

PS analysis

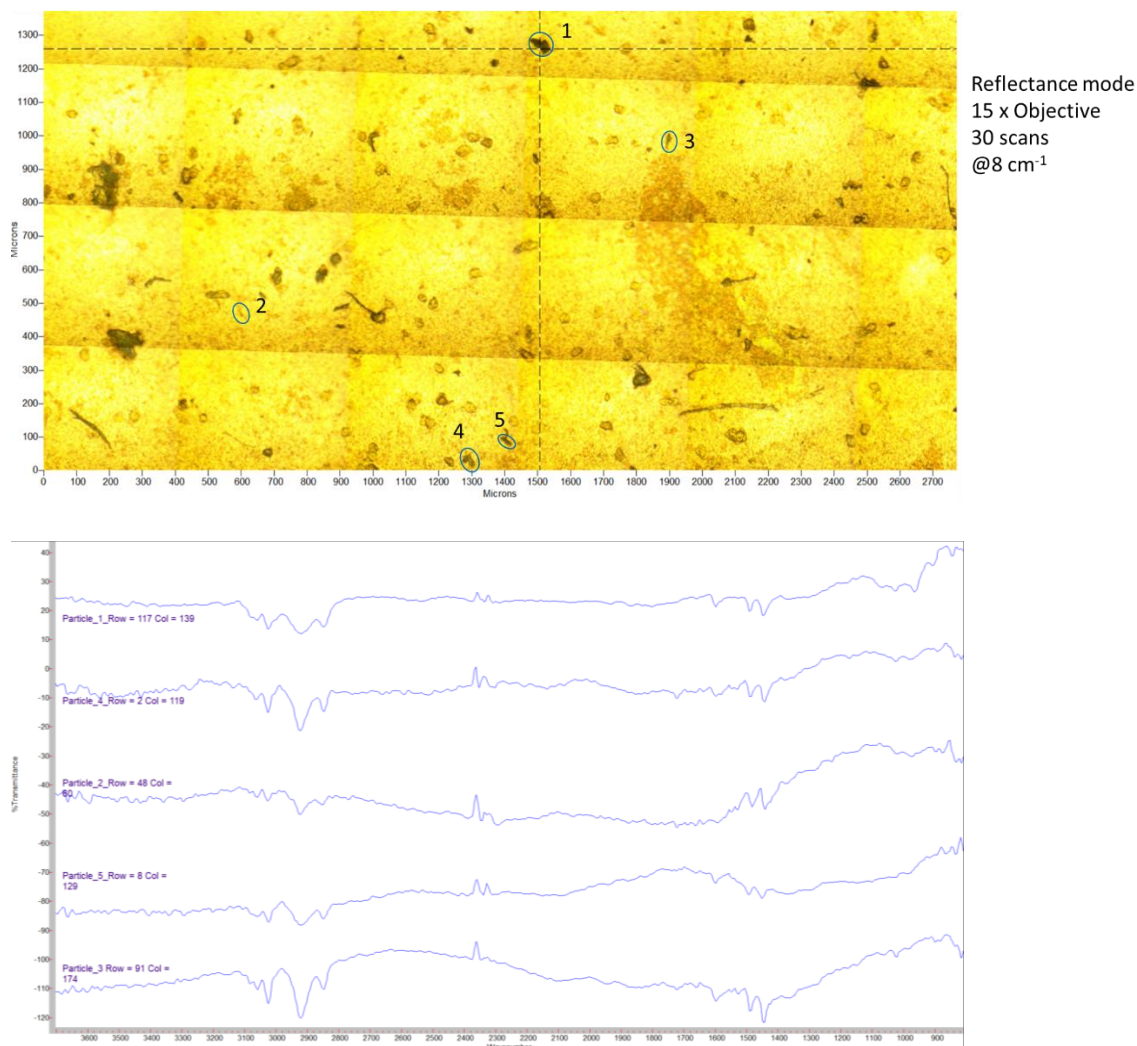


Figure 19: Image of the analyzed particles (top). The particle numbers correspond to the spectra below. All measurements were conducted on a μ -FTIR system by Agilent Cary 620.

1. Elisabeth von der Esch, Alexander J. Kohles, Philipp M. Anger, Roland Hoppe, Reinhard Niessner, Martin Elsner, and N.P. Ivleva, TUM-ParticleTyper: A Detection and Quantification Tool for Automated Analysis of (Microplastic) Particles and Fibers. PLOS ONE submitted

APPENDIX A2 SUPPORTING INFORMATION FOR CHAPTER 3

Supplements to the Material and Methods

Roughness testing for the development of filter holders

The suitability of the filter holder for the analysis of MP by means of RM was evaluated by measuring the surface roughness. Therefore, a gold-coated polycarbonate filter (diameters 25 mm and 50 mm, pore size 0.8 μm , Analytische Produktions-, Steuerungs- und Controllgeräte GmbH, Germany) was used. The roughness was evaluated by using clean and used filters. The used filters were in contact with an artificial matrix which was a suspension of humic acids (native, Carl Roth GmbH + Co. KG, Germany) and bentonite (Carl Roth GmbH + Co. KG, Germany) in ultrapure water (Milli-Q® Reference, Merck KGaA, Germany), which was filtered onto the filter (vacuum filtration, 25 mm, 30 mL, with glass frit, Sartorius Lab Instruments GmbH & Co. KG, Germany) and afterwards the filter was freed from the residue with ultrapure water (Milli-Q® Reference, Merck KGaA, Germany). The dried filter was clamped into the filter holder and analyzed with *TrueSurface* (WITec GmbH, DE). For comparison the same filters were laid onto a glass slide and fixed to a glass slide with a double sided tape (tesa® Doppelband TRANSPARENT, tesa SE, DE) and equally analyzed with *TrueSurface* (WITec GmbH, Germany) which measures the surface topography.

The roughness for filters with 50 mm diameter was evaluated on an area of 30 mm \times 30 mm and a size of 100 Pixel \times 100 Pixel. For filters with 25 mm diameter an area of 12 mm \times 12 mm and a size of 40 Pixel \times 40 Pixel was evaluated. This resulted in an equal resolution of 300 μm Pixel⁻¹. The roughness was evaluated by the maximum peak-peak distance which is the distance of the highest to the lowest pixel. The smaller this distance is, the smoother the surface and the better the fixation method.

Image acquisition procedures for optical, fluorescence and scanning electron microscopy

For the Raman microscopy analysis images of the reference particles and of particles from washing machine samples were acquired on an *alpha300R* Raman Microscope (20× objective, 3 [db] Gain, 3 % top illumination, 1/10 fps, WITtec GmbH, Germany)

The fluorescence images under a Leitz Laborlux S with a 4× objective in combination with an Olympus DP74 camera and the Olympus Software CellSense Standard (Olympus Europe SE & Co. KG, Germany). Blue channel was imaged using a filter cube A (Immission BP340-380, Emission LP430) and the red channel with a N2.1 (Immission BP515-560, Emission LP580) filter cube. Both were imaged in RGB mode and merged afterwards. The size of the particles is between 35 and 50 µm.

The SEM images were recorded on a *Sigma 300 VP* (Carl Zeiss AG, Germany) using a HD secondary electron detector. For sample preparation, the suspensions (10 µL) were dried on silicon wafer slices and were imaged without the need for coating with metals due to the use of a FE Schottky cathode and low acceleration voltages (2 – 3 kV).

Furthermore, images from publications were extracted and analyzed to show the generalizability of our approach. For the acquisition parameters we refer to the original publications.

Acquisition of chemical information via Raman microspectroscopy

Single point measurements:

The particles were localized (calculation of centers for Raman measurement) and morphologically analyzed (Feret's diameter min and max, area, ratio of Feret's diameter and percentage of area covered by particle in Feret's box for shape analysis) via image processing using *TUM-ParticleTyper*. Subsequent Raman microspectroscopy revealed the identity after an automated spectral assignment. Measurement parameters: 532 nm laser, 3 mW using *TruePower*, 20 s measurement time, 20× objective, inserting the determined coordinates by *TUM-ParticleTyper* via *PointViewer* on to the *alpha300R* Raman Microscope, WITtec GmbH, Germany. Spectral assignment: *2 component search via correlation coefficient [1]* in the region

of 600 – 1800 cm^{-1} up to a hit quality index of 15, using *TrueMatch*, Witec, Germany see validation of these parameters in von der Esch et al. 2020[2].

Imaging:

The Raman imaging experiments were performed according to the procedure by K ppler et al. 2016. [3] (Measurement parameters: 1000 $\mu\text{m} \times 1000 \mu\text{m}$ area, a 10 μm step size 5 mW 500 ms/scan 532 nm laser 20 \times magnification on an *alpha300R* Raman Microscope WITtec GmbH, Germany). The identification of the particles is done by k-means clustering of the acquired spectra. (k=20, yielded best results using *Project FIVE*, Witec, Germany) Only the target Cluster (of the searched polymer polylactic acid) was used to calculate the number and size of the respective particles and for the overlay with the original image.

Fiber detection in washing machine water

The sample was prepared at “S chsisches Textilforschungsinstitut” (*Saxonian institute of textile research*, STFI), by washing a fleece with ECE-2-detergent (4 g/L) and sodium percarbonate (0.66 g/L). The water from the washing procedure was collected yielding a suspension (35 mL). The suspension was shaken and filtrated (25 mm diameter, 0.8 μm pore size, Au-coated polycarbonate filter, APC GmbH) in a laminar flow box (EN 1822, Spetec GmbH). To reduce particle contamination all filtration equipment was sonicated (in MilliQ, 30 min) and dried with lint free cloth (Kimberly Clark Kimtech). The setup was then rinsed with MilliQ water (100 mL) until no particles were visible in direct white light (Chameleon, CU6, 400 lm). Then the entire sample was deposited on the filter and treated with KOH (1 M, 4 mL twice for 1 minute) to remove the organic matrix. The suction strainer was rinsed with MilliQ (100 mL) to deposit particles stuck to its walls onto the filter. After deposition a microscopy image of the filter was taken (see 2.3) and processed with the procedure presented in this work using the *TUM-ParticleTyper* software (min pixel 20, resolution 0.5 pixel/ μm , detection mode Raman only fibers). For the chemical identification 2000 fibers were selected by random sampling. The selected fibers were measured using the single point approach (see 2.4).

For the comparison of single point measurements and imaging the parameters were tweaked so that the same area was analyzed roughly in the same amount of time, without sample size reduction in the single point approach (no random sampling). The exact parameters for each comparison are stated next to the overlay images.

Results and Discussion

Flat filter surfaces as a prerequisite for optimal focus

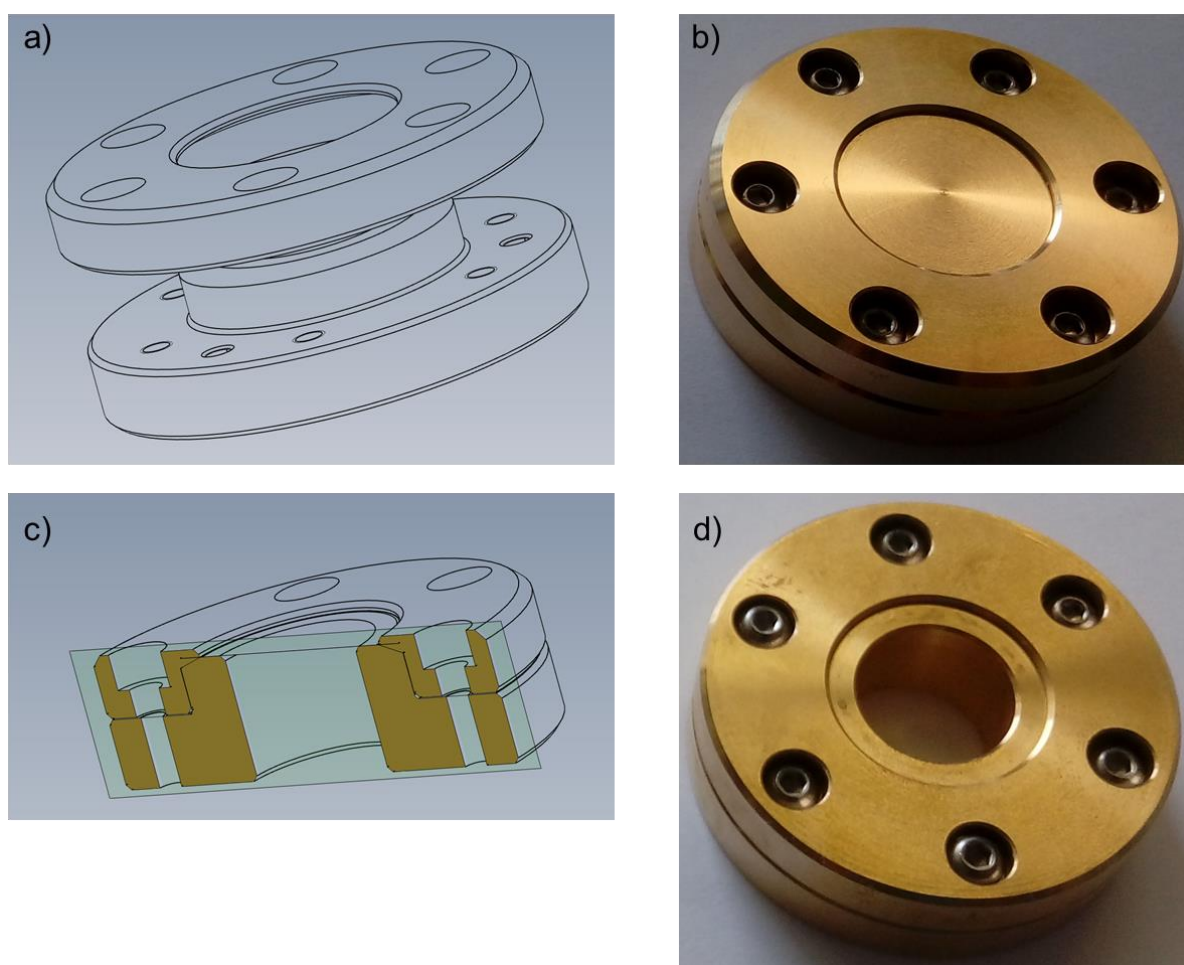


Figure 1: Exploded view of the filter holder a), massive filter holder for filters with diameters of around 25 mm b), schematic drawing of the filter holder c), filter holder with opening in the center for filters with diameters of around 25 mm d), constructed

at the Institute of Hydrochemistry, Chair of Analytical Chemistry and Water Chemistry, TUM.

Two sizes for filters with 50 mm diameter and for filters with around 25 mm (Figure 1) and two types of filter holders were constructed. The first type is a massive one (Figure 1b), the second type possesses an opening in the center that can be used for transmission measurements or illumination from the downside of the filter (Figure 1).

For fixation of a filter the upper part of the filter holder is lifted. The filter is placed onto the lower part and the upper part is laid down on the filter carefully. By tightening the screws in an alternating manner, the filter is smoothly fixated between the two parts of the filter holder.

In Table 8 the peak-peak distances for clean gold-coated polycarbonate filters with 50 mm and 25 mm diameter as well as the peak-peak distances for the same filters that were previously in contact with an artificial matrix are given. For the calculation of the mean and the standard deviation for the filters with an asterisk (*) three different filters were measured in triplicate. For every other fixation a sole triplicate measurement of the same filter was used for calculation.

Table 8: Comparison of peak-peak distances for clean gold-coated polycarbonate filters with a diameter of 25 mm; mean and standard deviation were calculated from triplicate TrueSurface measurement of one filter.

Fixation method	Peak-Peak
Clean gold-coated polycarbonate filter with 50 mm diameter	
Massive filter holder*	31.2 $\mu\text{m} \pm 7.8 \mu\text{m}$
Filter holder with opening in the center	24.0 $\mu\text{m} \pm 1.1 \mu\text{m}$
Glued to glass slide	589.2 $\mu\text{m} \pm 2.4 \mu\text{m}$
Laid on glass slide	99.2 $\mu\text{m} \pm 2.6 \mu\text{m}$
Gold-coated polycarbonate filter with 50 mm diameter; contact with artificial matrix	

Filter holder with opening in the center	34.8 $\mu\text{m} \pm 5.0 \mu\text{m}$
Glued to glass slide	466.3 $\mu\text{m} \pm 1.7 \mu\text{m}$
Laid on glass slide	871.4 $\mu\text{m} \pm 3.0 \mu\text{m}$
Clean gold-coated polycarbonate filter with 25 mm diameter	
Massive filter holder*	5.8 $\mu\text{m} \pm 2.1 \mu\text{m}$
Filter holder with opening in the center*	10.4 $\mu\text{m} \pm 2.3 \mu\text{m}$
Glued to glass slide	121.4 $\mu\text{m} \pm 2.5 \mu\text{m}$
Laid on glass slide	63.1 $\mu\text{m} \pm 11.8 \mu\text{m}$
Gold-coated polycarbonate filter with 25 mm diameter; contact with artificial matrix	
Filter holder with opening in the center	9.4 $\mu\text{m} \pm 0.3 \mu\text{m}$

*Mean and standard deviation were calculated out of three filters each measured in triplicate.

1. Kwiatkowski A, Gnyba M, Smulko J, Wierzba P. Algorithms of Chemicals Detection Using Raman Spectra. *Metrology and Measurement Systems*. 2010;17(4):549-59.
2. von der Esch E, Lanzinger M, Kohles AJ, Schwaferts C, Weisser J, Hofmann T, et al. Simple Generation of Suspensible Secondary Microplastic Reference Particles via Ultrasound Treatment. *Frontiers in Chemistry*. 2020;8(169).
3. K appler A, Fischer D, Oberbeckmann S, Schernewski G, Labrenz M, Eichhorn KJ, et al. Analysis of environmental microplastics by vibrational microspectroscopy: FTIR, Raman or both? *Anal Bioanal Chem*. 2016;408(29):8377-91.